TRIBOLOGICAL STUDY OF NANOPARTICLES ENRICHED BIO-BASED LUBRICANTS FOR ENGINE PISTON RING–CYLINDER INTERACTION

MUBASHIR GULZAR

FACULTY OF ENGINEERING
UNIVERSITY OF MALAYA
KUALA LUMPUR

2017

TRIBOLOGICAL STUDY OF NANOPARTICLES ENRICHED BIO-BASED LUBRICANTS FOR ENGINE PISTON RING–CYLINDER INTERACTION

MUBASHIR GULZAR

THESIS SUBMITTED IN FULFILMENT OF THE REQUIREMENTS FOR THE DEGREE OF DOCTOR OF PHILOSOPHY

FACULTY OF ENGINEERING
UNIVERSITY OF MALAYA
KUALA LUMPUR

2017

UNIVERSITY OF MALAYA

ORIGINAL LITERARY WORK DECLARATION

Name of Candidate: Mubashir Gulzar I.C/Passport No: AJ4716112

Registration/Matric No: KHA130090

Name of Degree: Doctor of Philosophy

Title of Thesis:

Tribological Study of Nanoparticles Enriched Bio-based Lubricants for Engine Piston Ring–Cylinder Interaction

Field of Study: Energy

I do solemnly and sincerely declare that:

(1) I am the sole author/writer of this Work;
(2) This Work is original;
(3) Any use of any work in which copyright exists was done by way of fair dealing and for permitted purposes and any excerpt or extract from, or reference to or reproduction of any copyright work has been disclosed expressly and sufficiently and the title of the Work and its authorship have been acknowledged in this Work;
(4) I do not have any actual knowledge nor do I ought reasonably to know that the making of this work constitutes an infringement of any copyright work;
(5) I hereby assign all and every rights in the copyright to this Work to the University of Malaya ("UM"), who henceforth shall be owner of the copyright in this Work and that any reproduction or use in any form or by any means whatsoever is prohibited without the written consent of UM having been first had and obtained;
(6) I am fully aware that if in the course of making this Work I have infringed any copyright whether intentionally or otherwise, I may be subject to legal action or any other action as may be determined by UM.

Candidate's Signature Date:

Subscribed and solemnly declared before,

Witness's Signature Date:

Name:

Designation:

ABSTRACT

Given continuous environmental legislation, the lubrication industry has been striving to produce environmentally suitable lubrication alternatives for internal combustion engines. Addressing this challenge requires the use of lubricants that conform to environmental standards while maintaining excellent lubrication performance. This thesis investigates the tribological viability of bio-based base stock to which different nanoparticles were incorporated for engine piston ring–cylinder liner interaction. The specific base stock examined was trimethylolpropane (TMP) ester derived from palm oil, and the nanoparticles were used as additives to obtain tribologically enhanced bio-based lubricants. Nano sized additives included copper oxide, molybdenum disulfide and titanium silicate nanoparticles as lubricant additives. The effects of lubricating oil conditions (new and engine-aged) on the friction and wear of the materials used for piston rings and cylinder liners were experimentally determined. The research began with investigation of wear protection and friction reduction behavior of palm oil-derived TMP ester for piston ring–cylinder liner interaction. It was followed by the investigation of lubrication behavior of variety of nanoparticles as additives to palm TMP ester. The friction and wear characteristics of the lubricant samples were examined in contact conditions that were simulated using a high-stroke reciprocating tribometer. Four-ball tribo-testing was conducted to evaluate the extreme pressure characteristics of the samples. Suitable nanoparticle types and concentrations were then evaluated to enhance wear protection and reduce friction. Finally, surface analyses were carried out to ascertain potential lubrication mechanisms contributed by nanolubricants. In the next stage of the research, bio-based nanolubricant degradation under actual engine conditions and its tribological effect on the piston ring–cylinder liner combination was examined. Long duration engine testing was carried out using a single-cylinder compression ignition engine. To control lubricant acidity, a chemically active filter technology was used during

engine bio-based lubrication. Engine sump oil samples were collected and analyzed for their physicochemical and tribological properties in comparison to a conventional diesel engine lubricant. The results have shown that friction reduction and antiwear behavior of palm TMP ester can be improved by addition of suitable concentrations of considered nanoparticles. The most significant improvement in the lubrication performance of palm TMP ester has been shown by 0.75 wt% of titanium silicate nanoparticles. A reduction of 68% in average friction coefficient was observed while wear volume was reduced to half for piston ring and cylinder liner specimen. The surface analysis results showed that the nanoparticles improved the lubrication performance by surface enhancement of interacting surfaces in terms of tribofilm formation, polishing and mending effects. Bio-based nanolubricant showed high degradation during long hours' engine tests resulting in 17% lower viscosity, 30% high acidity and 16.8% higher oxidation than that of conventional engine oil. However, the friction and wear behavior of corresponding engine-aged samples were comparable to that of engine-aged conventional engine lubricant samples. The overall analysis of results demonstrated the potential of nanoparticles to improve the tribological behavior of bio-based base stock for piston ring–cylinder liner interaction.

ABSTRAK

Disebabkan penguatkuasaan undang-undang alam sekitar dipertingkatkan secara berterusan, industri pelinciran telah berusaha untuk memperkenalkan pelincir yang mesra alam untuk enjin pembakaran dalam. Untuk menangani cabaran ini, pelincir mesra alam amat diperlukan dan pada masa yang sama tidak menjejaskan prestasi pelinciran. Tesis ini melihat daya maju tribologi bagi stok asas berasaskan bio ditambah dengan nanozarah yang berbeza untuk interaksi gelang omboh – bahan pelapik silinder enjin. Stok asas berasaskan bio yang dikaji adalah ester trimethylolpropane (TMP) berasal dari minyak sawit dan nanozarah digunakan sebagai bahan tambah untuk mendapatkan peningkatan tribologi bagi pelincir berasaskan bio. Bahan tambah nanozarah yang digunakan termasuk kuprum oksida, molibdenum disulfida dan titanium silikat. Kesan ke atas keadaan minyak pelincir (baru dan terpakai enjin) terhadap geseran dan kehausan gelang omboh dan bahan pelapik silinder telah disiasat melalui ujian eksperimen. Bahagian pertama kajian ini adalah untuk meningkatkan ciri – ciri perlindungan haus dan mengurangkan geseran ester TMP sawit untuk interaksi gelang omboh dan bahan pelapik silinder. Kemudian, kelakuan pelinciran bagi pelbagai nanozarah yang digunakan sebagai bahan tambah untuk ester TMP sawit telah diselidiki. Ciri-ciri geseran dan haus bagi sampel-sampel pelincir telah diuji dalam keadaan sentuhan menggunakan simulasi tribometer salingan lejang tinggi. Ujian tribo empat-bola telah digunakan untuk menilai ciri-ciri tekanan lampau bagi sampel-sampel pelincir. Jenis dan kepekatan nanozarah yang sesuai telah dinilai untuk perlindungan kehausan yang lebih baik dan pengurangan geseran. Akhir sekali, teknik analisa permukaan telah digunakan untuk menentukan mekanisme pelinciran yang boleh disebabkan oleh nano-pelincir. Dalam bahagian kedua kajian ini, degradasi pelincir berasaskan bio di bawah keadaan enjin sebenar dan kesan tribologi terhadap kombinasi gelang omboh – bahan pelapik silinder enjin telah diperiksa. Ujian enjin jangka masa panjang telah dijalankan dengan menggunakan enjin pencucuhan mampatan silinder

tunggal. Untuk mengawal keasidan pelincir, penapis alkali yang aktif secara kimia telah digunakan semasa pelincir berasaskan bio diuji. Sampel-sampel minyak enjin dari takungan telah dikumpulkan dan dianalisis untuk ciri-ciri kimia-fizik dan tribologi. Keputusan telah menunjukkan bahawa pengurangan geseran dan tingkah laku anti-haus oleh ester TMP sawit boleh ditingkatkan dengan penambahan nanozarah yang dipertimbangkan pada kepekatan yang sesuai. Peningkatan yang paling ketara pada prestasi pelincir ester TMP sawit telah ditunjukkan oleh nanozarah titanium silikat dengan 0.75 %berat. Pengurangan sebanyak 68% dalam purata pekali geseran telah diperhatikan. Manakala, isipadu haus berkurang kepada separuh pada segmen gelang omboh – bahan pelapik silinder. Analisa permukaan telah menunjukkan bahawa nanozarah telah meningkatkan prestasi pelinciran dengan memperbaiki permukaan saling tindak dari segi kesan pembentukan lapisan filem tribo, kesan penggilapan dan pembaikian. Nano-pelincir berasaskan bio telah menunjukkan degradasi yang tinggi sewaktu ujian enjin untuk jangka masa yang panjang dengan 17% kelikatan lebih rendah, 30% keasidan lebih tinggi dan 16.8% pengoksidaan lebih tinggi daripada minyak enjin konvensional. Namun demikian, kelakuan geseran dan kehausan sampel-sampel pelincir terpakai tersebut adalah setanding dengan sampel-sampel pelincir konvensional terpakai. Analisis keseluruhan hasil kajian menunjukkan potensi nanozarah untuk meningkatkan kelakuan tribologi stok asas berasaskan bio bagi interaksi gelang omboh – bahan pelapik silinder enjin.

ACKNOWLEDGEMENTS

First of all, I am thankful to ALMIGHTY ALLAH Who gave me all the strength I needed and Who gave me all the insight I was lacking. I am all in praise of my advisors Professor Dr. Masjuki Hj Hassan, Assoc. Professor Dr. Md. Abul Kalam, Dr. Mahendra Varman A/L Munusamy and Dr. Nurin Wahidah Mohd Zulkifli, who have been a source of motivation, guidance and affection for me during all this phase. Without their inspiration, it would have been a journey with full of difficulties. Therefore, I am extremely grateful to all of my supervisors who sacrificed so much of their precious time to enlighten my thoughts.

I am thankful to all the honorable members and graduate students of Centre for Energy Sciences, Faculty of Engineering, University of Malaya. I cannot forget the logistics and procurement support by research officer, Ms Mei Yee and research companionship of Mr. Rehan Zahid. I deeply admire the whole-hearted assistance of technical staff of the General Tribology Lab and Engine Lab.

I ought to acknowledge my parents who sacrificed a lot and always prayed for my success. I am extremely thankful to my caring wife and lovely son, Musa Mubashir who suffered hard times due to my research commitments and involvement in the long duration experimental work. I am really thankful to my friends Mr. Muhammad Sajjad Sabir Malik and Mr. Abdul Wahab Qureshi for the continuous moral support.

In the end, I would like to mention that I am highly indebted to University of Malaya for the sponsorship through High Impact Research Grant, Project title: "Development of Alternative and Renewable Energy Carrier" Grant Number: UM.C/HIR/MOHE/ENG/60.

TABLE OF CONTENTS

LIST OF FIGURES

LIST OF TABLES

LIST OF SYMBOLS AND ABBREVIATIONS

Al	:	Aluminum
Al/Sn	:	Aluminum-tin
Al_2O_3	:	Aluminum oxide
Al_2O_3/SiO_2	:	Alumina-Silica
AW	:	Antiwear
APS	:	Average particle size
B20	:	20% methyl ester and 80% DF
BN	:	Boron nitride
C	:	Carbon
Co	:	Cobalt
Cu	:	Copper
COF	:	Coefficient of friction
CuO	:	Copper (II) oxide
$CaCO_3$	:	Calcium carbonate
CATO302	:	Cationic starch
CMRO		Chemically modified rapeseed oil
DF	:	Diesel fuel
EP	:	Extreme pressure
EDS		Energy dispersive Spectrometer
EDX	:	Energy-dispersive X-ray spectroscopy
Fe	:	Iron
FM	:	Friction modifier
Fe_3O_4	:	Iron(II,III) oxide
FAME	:	Fatty acid methyl esters

FTIR	:	Fourier transform infrared
g	:	Gravity
hBN	:	Hexagonal boron nitride
IC	:	Internal combustion
IF	:	Inorganic fullerene
IR	:	Infrared
ISL	:	Initial seizure load
LNSL	:	Last non-seizure load
Mo	:	Molybdenum
MoS_2	:	Molybdenum disulfide
MoS_2/TiO_2	:	Molybdenum disulphide-titanium dioxide
Ni	:	Nickel
NPG	:	Neopentylglycol
NaOH	:	Sodium hydroxide
O	:	Oxygen
OA	:	Oleic acid
Pb	:	Lead
PE	:	Pentaerythritol ester
PB20	:	20% palm methyl ester and 80% DF
PAM	:	Polyacrylamide
PAO	:	Polyalphaolefin
PbS	:	Lead sulfide
PAGs	:	Polyalkylene glycols
PFPEs	:	Perfluoroalkylpolyethers
POME	:	Palm oil methyl ester
PTFE	:	Polytetrafluoroethylen

r	:	Radius of nanoparticle
Ra	:	Average roughness
Rq	:	Mean root mean square roughness
Rz	:	Mean roughness depth
S	:	Sulfur
Si	:	Silicon
SDS	:	Sodium dodecyl sulfate
SEM	:	Scanning electron microscope
SiO_2	:	Silicon dioxide, Silica
Ti	:	Titanium
TAG	:	Triacylglycerols
TAN	:	Total acid number
TBN	:	Total base number
TiO_2	:	Titanium dioxide
TME	:	Trimethyoloethane
TMH	:	Trimethylolhexane
TMP	:	Trimethylolpropane
TiO_2/SiO_2	:	Titanium silicon oxide, Titanium silicate, Silicon titanate
UV-vis	:	Ultraviolet–visible
ULSD	:	Ultra-low sulfur diesel
v_z	:	settling velocity
VI	:	Viscosity index
WL	:	Weld Load
WS_2	:	Tungsten disulfide
WSD	:	Wear scar diameter
XPS	:	X-ray photoelectron spectroscopy

ZnO	:	Zinc oxide
ZrO_2	:	Zirconium dioxide
$ZnAl_2O_4$	:	Zinc aluminate
ZrO_2/SiO_2	:	Zirconia-Silica
ZnDDP		Zinc dialkyl dithiophosphate
ρ_{NP}	:	Density of nanoparticles
ρ_F	:	Density of fluid
μ	:	Viscosity of the fluid

CHAPTER 1: INTRODUCTION

1.1 Research Background

Modern internal combustion (IC) engines require effective lubricant formulations to minimize friction and wear losses while satisfying environmental standards. In an IC engine, the piston assembly is the largest contributor to friction; within this engine component, the interactions between piston rings and the cylinder liner surface induce significant parasitic losses (Figure 1.1). For effective lubrication of IC engine parts, a number of high performance lubricant formulations have been developed. These engine oil formulations constitute the largest volume application for conventional lubricants (Figure 1.2), and thus pose environmental problems owing to their toxicity and low biodegradability. The use of conventional engine lubricants causes environmental pollution because of the evaporation and engine exhaust emissions that occur during engine operation. At the end of an engine's service life, wastes from conventional engine oils slowly degrade and are toxic to human health, fauna, and flora.

Because the hazardous effects associated with conventional engine lubricants have become a global concern, increasing interest has been directed toward bio-based base stocks for their suitability in various applications. Bio-based feedstocks enable performance that is identical to that achieved with conventional engine base oils under different lubricant applications (Fan, 2010). With a view to maintaining domestic energy security and addressing environmental concerns, researchers have recommended bio-based lubricants for their unique characteristics, including bio-degradability, renewability, and low toxicity classification. These properties qualify the aforementioned materials as the future of engine lubrication technology (M Nosonovsky & Bhushan) (Lovell, Higgs, Deshmukh, & Mobley, 2006) (Salih, Salimon, Yousif, & Abdullah, 2013) (W. Li et al., 2010).

The challenges that accompany the use of bio-based lubricants encompass minimum energy loss, effective engine lubrication, and enhanced engine life. Overcoming these challenges necessitates environmentally conformable engine lubrication that does not compromise the service life and efficient performance of engine parts. In this regard, recent advances in nanoparticle technology have opened new prospects for lubricant additivation, with such technology leveraging the interesting friction and wear-reducing properties of nanoparticles. Many reasons drive the adoption of nanoparticles as lubricant additives, the most important of which is their tiny size, which enables nanoparticles to enter a contact area and thereby achieve a positive lubrication effect (Demas, Timofeeva, Routbort, & Fenske, 2012; Ghaednia, 2014). They are also small enough to pass undisturbed through the filters used in oil systems (Ghaednia, 2014; Spikes, 2015). Five major potential advantages of using nanoparticles as lubricant additives have been mentioned by Spikes (2015): (1) insolubility in non-polar base oils; (2) low reactivity with other additives in the lubricant; (3) high possibility of film formation on many different types of surface; (4) more durability; and (5) high non-volatility to withstand high temperatures.

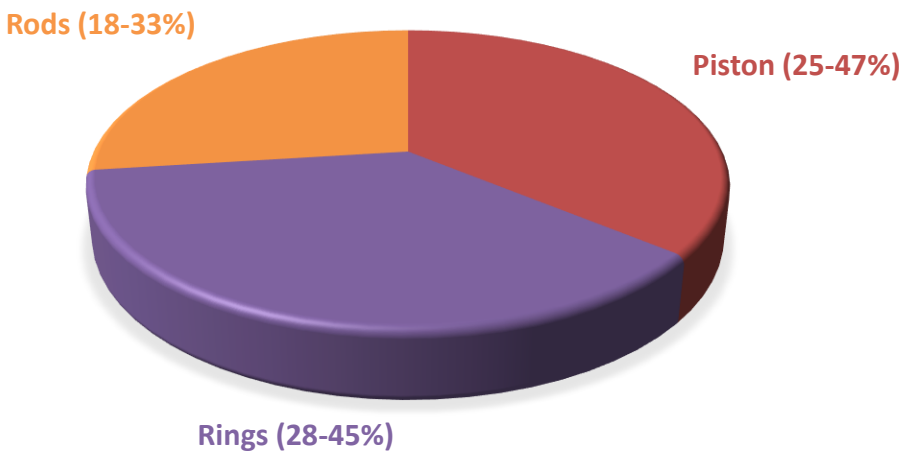

Figure 1.1: Frictional energy losses distribution of piston/ring/rod
Source: Richardson (2000)

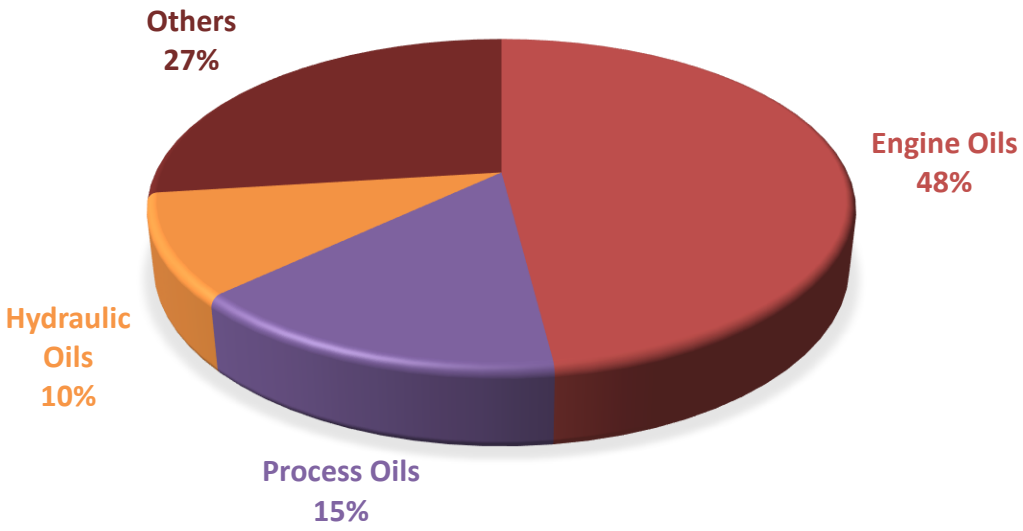

Figure 1.2: World market, the segmentation by application
Source: Mobarak et al. (2014)

1.2 Problem Statement

Chemically modified vegetable oils, as a class, have gained a reputation of thermo-oxidative stability with added environmental benefits. The major difficulty in their widespread use is the lack of suitable lubrication performance for certain applications. For such base stocks to use in IC engine application, suitable additive technology is required to provide a nearly equivalent performance to that of conventional engine oils.

Over the past decade, nanoparticles have been emerged as versatile additives due to their ability to serve multiple purposes as antiwear and extreme pressure additives as well as friction modifiers. There are many studies which showed lubrication potential of nanoparticles as lubricant additives for engine piston ring–cylinder liner interaction. However, majority of the studies have used mineral oils and synthetic base oils. Despite potential tribological advantages, research contributions are lacking for various combinations of variety of nanoparticles and bio-based lubricants. Thus, research

contributions are required to investigate lubrication potential of nanoparticle as additives to chemically functionalized vegetable oils for engine piston ring–cylinder liner interaction.

This research investigates the tribological viability of palm oil trimethylolpropane (TMP) ester as bio-based base stock for piston ring–cylinder liner interaction. To improve the lubricity of palm TMP ester for piston ring–cylinder liner contact, a variety of nanoparticles were used as additives. The lubricant samples were tested in a laboratory under new and engine-aged conditions by experimentally simulating the lubrication conditions that are characteristic of piston ring–cylinder liner interaction.

1.3 Objectives of the Research

The objectives of the research are follows:

1. To investigate the tribological behavior of palm TMP ester as a bio-based lubricant for engine piston ring–cylinder interaction.
2. To improve the wear protection and friction reduction abilities of palm TMP ester by using nanoparticles as lubricant additives.
3. To determine lubricating oil degradation in actual engine conditions for bio-based nanolubricant in comparison to conventional engine lubricant.
4. To investigate the lubricant degradation effects on the friction and wear characteristics for piston ring–cylinder interaction.

1.4 Scope of Research

This study revolves around determining the tribological performance of nanoparticles as additives in palm oil-derived TMP ester for the purpose of realizing effective piston ring–cylinder liner lubrication. A variety of nanoparticles have been investigated which

include Copper (II) oxide (CuO), Molybdenum disulfide (MoS_2) and Titanium silicate (TiO_2/SiO_2). A range of concentration of selected nanoparticles (0.25 wt%, 0.5 wt%, 0.75 wt%, 1.0 wt%, 1.25 wt% and 1.50 wt%) in palm TMP ester was applied to identify the minimum friction and wear losses that occur during piston ring–cylinder liner sliding contact. A high-stroke reciprocating test rig was used to evaluate the tribological performance of bio-based lubricants and a conventional engine lube oil. The evaluation was based primarily on average friction coefficient (COF) and wear loss. New and engine-aged lube oils were assessed to analyze lubricant degradation and its effects on tribological performance. To this end, sump oil samples were collected during long duration engine tests using single-cylinder engine, and engine-aged oil samples were examined for friction behavior and wear losses. Given that the bio-based lubricant is detergent free, a strong base oil filter technology was adopted for prolonged use in a diesel engine. For the new and engine-aged oils, physicochemical properties were analyzed to look into lubricating oils degradation.

A comparison of the performance parameters related to the lubrication characteristics of the conventional engine oil and the bio-based lubricant provided insight into the feasibility of nanoparticle-enriched bio-based lubricants for engine piston ring–cylinder liner interaction.

1.5 Thesis Outline

This thesis is structured in five chapters, the content and function of which are:

Chapter 1 presents the background of this research, research objectives and scope of the research which are addressed through the state of the art work carried in this research. This chapter also outlines the structure of the thesis.

Chapter 2 provides the literature review of research topics related with this research thesis, including conventional lubricants, bio-based lubricants and additives. This chapter also include comprehensive literature review of nanoparticles as lubricating oil additives, piston ring-cylinder tribology, lubricant degradation and its effect on piston ring-cylinder tribology.

Chapter 3 outlines the different materials and experimental methods employed in this work with their detailed samples preparation techniques, procedures and testing conditions. It includes details about the development of nanolubricants, ultrasonic dispersion procedures and stability analysis methods using ultraviolet–visible (UV–vis) spectrophotometry. Tribo-testing procedures in controlled laboratory conditions are mentioned along with illustrations of testing rigs. For engine endurance testing, the specifications of single cylinder diesel engine test rig and sump oil sampling details are part of this chapter. For new and engine-aged lubricant samples, the details of adopted procedures and test equipment have been mentioned for viscosity, acidity, oxidation, soot and fuel residue. The test set-ups, working principles and illustrations of the surface analysis tools such as scanning electron microscopy (SEM), energy-dispersive X-ray spectroscopy (EDX), micro-Raman spectroscopy and 3-dimensional surface profilometry constitutes a major part of this chapter.

Chapter 4 is dedicated to results and discussions based upon findings of experimental work. This chapter starts with the tribological investigation of palm TMP ester for piston

ring–cylinder liner combination. In the next stage of experimentation, the compatibility of nanoparticles as additives to palm TMP ester, was investigated in terms of dispersion stability and tribological analysis. For all the developed nanolubricants, friction behavior, wear volume and extreme pressure characteristics were reported. For nanolubricant showing stable dispersion and suitable tribological behavior, engine endurance testing was carried out. The lubricating oil condition and its effect on piston ring–cylinder lubrication was investigated in comparison to conventional diesel engine lubricant. To understand the degradation rate of lubricating oil samples, collected over the drain interval, the lubricant physicochemical analysis (viscosity, acidity, fuel residue, soot content) is also covered in this part of thesis.

The friction and wear behavior was reported and discussed for new and engine-aged lubricant samples. Results obtained in the form of SEM micrographs, EDX spectra, Raman spectra and surface topography, were discussed to understand and report the potential lubrication mechanisms for considered lubricating oil samples.

Chapter 5 provides a summary of the key findings of this research and puts forward recommendations for potential areas of research for the future studies.

CHAPTER 2: LITERATURE REVIEW

There has been much research and development to improve engine lubricants and drain intervals for IC engines through minimizing frictional losses and wear. The formulation of suitable lubricant is a function of its ability to control friction, wear, and surface damage over the intended life of a system. For actual engine operation, the lubricant should provide effective lubrication performance over the complete drain interval. Therefore, after development of a potential engine lubricating oil, an understanding is required about lubricating oil degradation and its effect on friction and wear of engine components.

This chapter outlines the science and technology of bio-based lubricants. The potential of nanoparticles and related challenges has been discussed for their use as lubrication enhancement additives. To approach the realistic engine lubricating oil condition, the lubricant degradation and related tribological effect is also discussed in this chapter.

2.1 Lubricants

Lubricants are often classified into three categories: (1) mineral oils, that are predominantly petroleum-based lubricants and are the most common lubricants; (2) natural oils, that are derived from plant-based oils and animal-based fats or tallow; and (3) synthetic oils, that include polyalphaolefins (PAOs), synthetic esters, polyalkylene glycols (PAGs), alkylated aromatics, perfluoroalkylpolyethers (PFPEs), among others. In the last three decades, natural and synthetic oils (not mineral oils) derived from bio-based feedstock have seen a resurgence due to hazardous emissions, toxicity and slow degradability of conventional engine lubricants.

2.1.1 Conventional Engine Lubricants and Related Hazards

Commonly used lubricants are mixtures of hydrocarbons blended with additives for specific lubrication requirements. These mixtures consists of paraffins, isoparaffines, nephthalenes, aromates and compounds of Sulfur, Phosphours, Nitrogen and Oxygen (Basu, Sengupta, & Ahuja, 2005). The conventional engine oil composition consists of a hydrocarbon base oil (typically 75 – 83 wt%), viscosity modifier (5 – 8 wt%) and an additive package (12 –18 wt%).

Additives present in conventional engine oils contain Sulfur and Phosphorous based compounds, which are harmful to the environment (Z. Li, Li, Zhang, Ren, & Zhao, 2014; Zhang et al., 2015). The amount of unburned lubricant has been proved to be a predominant contributor to undesirable paraffins and hydrocarbons emissions (Brandenberger, Mohr, Grob, & Neukom, 2005). The use of conventional engine lubricants results in toxic exhaust emissions and harmful particulate matters. In addition to environmental hazards, the health risks include eye irritation, allergic contact dermatitis and mutagenicity (Isaksson, Frick, Gruvberger, Pontén, & Bruze, 2002; Jaiswal, Rastogi, Kumar, Singh, & Mandal, 2014). At present several regulations are implemented globally which limit the SAPS (Sulfated Ash, Phosphorous and Sulfur) contents of additives (Jaiswal et al., 2014).

Also, the disposal of lubricant wastes has been an alarming environmental concern due to their slow degradation and high toxicity. It is estimated that 30 to 40 million tons of lubricant are consumed annually, with 20 million tons of this lubricant entering the environment, totaling to a 55% loss of lubricant (Mang & Dresel, 2007). Over 95% of these lubricants entering the environment are petroleum-based and harmful to the environment (Schneider, 2006). As a result of their high toxicity and low

biodegradability, petroleum-based lubricants and functional fluids (hydraulic fluids) constitute a significant hazard to the environment.

2.1.2 Bio-based Lubricants

The lubrication industry is shifting to become more environmentally responsible due to estimates indicating that nearly 50% of all the lubricants sold globally contaminate the environment, through spillage, evaporation, and total loss applications (Reeves, Menezes, Jen, & Lovell, 2012). It is estimated that bio-based lubricants have the ability to replace over 90% of all petroleum-based lubricants (Reeves, 2013). The environmental advantages of bio-based lubricants and related marketing benefits have involved several companies for various relevant products (Table 2.1).

The term “bio-lubricant” has been ascribed to all lubricants, derived from bio-based raw materials (such as plant oils, animal fats, or other environmentally benign hydrocarbons), which are biodegradable and nontoxic to humans and other living beings where the impacts are more detrimental (Salimon, Salih, & Yousif, 2010). Bio-based lubricants are comprised of plant oils, animal fats, or chemical modifications of these oils and are widely regarded as environmentally benign because of their superior biodegradability and renewable feedstock.

The renewable and biodegradable nature of bio-based lubricants have made them suitable for various applications like, engine lubricants (Mannekote & Kailas, 2011), chain-saw bar lubricants (Battersby, Pack, & Watkinson, 1992; Randles, 1992), (Beitelman, 1998) and in fractional oil loss applications such as hydraulic fluids (Bartz, 2000; Kassfeldt & Dave, 1997) and greases (Dwivedi & Sapre, 2002).

For IC engine application, lubricants have to operate in extremely aggressive environments with high temperatures, acidic contaminants and in contact with compounds that cause oil degradation. These factors must be taken into account to develop bio-based lubricants while providing adequate engine protection and suitable oil drain interval.

Few studies have reported the use of bio-based lubricants in IC engines. Mannekote and Kailas (2011) studied the tribological and physical properties of fresh and engine-aged coconut and palm oils after endurance testing in a four-stroke engine. They observed that antiwear properties of fresh vegetable base oils and conventional engine oil were comparable but deviation was reported during engine endurance testing due to poor oxidation stability and the absence of additives in vegetable oil. Igartua et al. (2009) investigated the bio-based lubricant formulations in automotive applications and found them environmentally conformable due to the lower content of lubricant derived ash, Sulfur and Phosphorous. A. K. Singh (2011) reported that the chemically modified castor oil was as beneficial as the petroleum based two stroke engine oil in terms of physicochemical characteristics and lubricity requirement. In another experimental study reported by Arumugam S (2014), chemically modified rapeseed oil with copper oxide (CuO) nanoparticles as additives, found to have comparable lubrication characteristics to commercial diesel engine lubricant.

Table 2.1: Suppliers of bio-based lubricants, brand names and locations

Company	Bio-based lubricant Trade Name	Manufacturing Region	Applications
Fuchs	Locolub eco	USA/Europe	Greases, hydraulic fluids, gear oil and chain oils
Mobil	Mobil EAL	USA/Europe	Greases, hydraulic fluids and refrigeration oil
Shell	Ecolube	USA	Hydraulic fluids
Houghton Plc.	Cosmolubric	UK	Hydraulic oil
Aztec Oils	Biohyd & Biochain	UK	Hydraulic and chainsaw oil
Raisio Chemical	Raisio Biosafe	-	Hydraulic fluids, bar and chain oils
International Lubricants Inc	Lubegard	USA/Europe	Hydraulic fluids, gear oil and metalworking oils.
Karlshamns-Binol AB	Binol	USA/Europe	Hydraulic fluids, metalworking oils, bar and chain oils
Bioblend Lubricants International	Bioblend	USA/Europe	Greases, hydraulic fluids, gear oil, bar and chain oils
Karlshamns-Binol AB	Binol	USA/Europe	Hydraulic fluids, metalworking oils, bar and chain oils
Renewable Lubricants	Biogrease/oil	USA	Greases, hydraulic fluids, cutting oil, transmission oil, gear oil, metalworking oils, bar and chain oils, turbine drip oil, vacuum pump oil and crankcase oils.
Chevron Texaco	Biostar (Rando)	USA/Belgium	Hydraulic fluids
Environmental Lubricants Manufacturing Inc.	SoyTrak, SoyEasy	USA	Greases, hydraulic fluids, cutting oil, gear oil, metalworking oils, bar and chain oils
Moton Chemicals	Biolube	Europe	Greases, turbine drip oil, bar and chain oils.
Cargill Industrial Oils & Lubricants	Novus	USA/Europe/Japan	Hydraulic fluids, cutting oil, gear oil, metalworking oils, bar and chain oils

Source: Rudnick (2013)

2.1.3 Vegetable Oils

The use of vegetable oils as lubricants and fuels has been recognized for many years (Rudnick, 2013). There are a wide variety of plant-based oils such as avocado, canola (rapeseed), castor, coconut, corn, cottonseed, olive, palm, palm kernel, peanut, safflower, sesame, soybean, and sunflower, among many others that are native to particular regions of the world.

The efficacy of vegetable oils is determined by their chemical composition, where they predominantly consist of mixtures of fatty acid esters derived from glycerol. Vegetable oils which contains high concentration of monounsaturated fatty acid, oleic acid (18:1),

are considered as the best candidates for potential bio-based lubricants (Fan, 2010; Kodali, 2002). List and composition of common unsaturated fatty acids found in plant oils are provided in Table 2.2 (Erhan, Adhvaryu, & Sharma, 2006; Meier, Metzger, & Schubert, 2007; Ogunniyi, 2006). In addition to fatty acid compositions, triacylglycerols, TAG, is the key component in plant oils ideally used for biolubricant feedstocks production. TAG is the natural long-chain fatty acid tri-esters of glycerol that is structurally similar to petroleum base oils. Table 2.3 lists the average TAG content of common oil crops.

Table 2.2: Composition of unsaturated fatty acids in common oil crops

Plant Oil	Unsaturated Fatty Acid in Plant Oils (wt. %)			
	Mono		Poly	
	Oleic Acid C18:1	Ricinolenic Acid $C_{18}H_{34}O_3$	Linoleic Acid C18:2	Alpha Linolenic Acid C18:3
Sunflower	28	-	61	-
Palm Kernel	15	-	1	-
Castor Bean	7.4	87	3.1	-
Rapeseed	60	9	20	9
Soybean	53	0.5	8	0.5
Corn	28	1	58	1

Table 2.3: Average TAG content of common oil crops

Plant	(% dry weight)
Sunflower	55
Palm Kernel	50
Castor	45
Rapeseed	40
Soybean	20
Corn	07

2.1.4 Selection of Vegetable Oil

In addition to appropriate physicochemical characteristics, Rudnick (2013) listed the following major factors for the selection of suitable candidates for bio-based lubricant production

- Bio-based resources for oil production should be enough in quantity.
- Bio-based oils should have more mono-unsaturated fatty acid than polyunsaturated fatty acids.
- The bio-based resources should have a stable trading price.

With respect to above mentioned criteria palm oil has the potential to be used as lubricant while addressing the concern of Malaysia's domestic energy security and environmental legislations. Globally, palm oil contributes the maximum of the total world oil production i.e. about 36%. It is followed by soybean oil and rapeseed oil which have a share about 29 and 15%, respectively. Indonesia, Malaysia, Thailand, Nigeria and Colombia are among the major palm oil producing countries, which together produced about 93% of total world palm oil in 2012–2016 (Table 2.4)**.**

Table 2.4: Major contributing countries for palm oil production and supply

	Production (Thousand Metric Tons)				
Country	2012-13	2013-14	2014-15	2015-16	(Aug) 2016-17
Indonesia	28500	30500	33000	32000	35000
Malaysia	19321	20161	19879	18250	21000
Thailand	2135	2000	2068	2100	2300
Colombia	974	1041	1110	1273	1280
Nigeria	970	970	970	970	970
Others	4478	4670	4614	4809	4945
Total	56378	59342	61641	59402	65495

Source: USDA Economics (2016)

2.1.5 Properties of Vegetable Oils

The information of lubricant-related properties of vegetable oils is required to compare them with baseline lubricants. As different applications consist of different ambient as well as operating condition, therefore vegetable oils should be used in applications where their properties and lubrication performance are best matched. In this regard, lubricants properties like viscosity, low temperature fluidity, oxidation stability and tribological behavior are discussed.

2.1.5.1 Viscosity

For specific application, the viscosity of lubricant is considered as one of the most important parameter. In this regard, the chemical structure of the vegetable oil plays a vital role. Carbon chain length and degree of unsaturation are factors affecting the viscosity of oil. An increase in hydrocarbon length increases the viscosity. For example, if an oil that majorly contain of oleic, linoleic acids, or other unsaturated components is hydrogenated to produce a saturated version, the resulting product would have the properties of grease. Table 2.5 shows the viscosity of commonly used vegetable oils.

2.1.5.2 Low-temperature properties

Flow at low temperatures is one of the limitations of vegetable oils. In many studies, poor flow, and solidification has been observed at −10 °C (Kassfeldt & Dave, 1997; Quinchia, Delgado, Franco, Spikes, & Gallegos, 2012; Rhee, Velez, & Von Bernewitz, 1995). To characterize the low-temperature properties of lubricants, pour point is the commonly used property. Pour point is the lowest temperature at which a fluid becomes semi-solid and loses its flow behavior. Table 2.5 shows the pour point of various vegetable oils.

Table 2.5: Physical characteristics of vegetable oils

Vegetable Oil	Viscosity at 40 ^{o}C (cSt)	Density (g/cm^3)	Flash Point (^{o}C)	Pour Point (^{o}C)
Sunflower (Abolle, Kouakou, & Planche, 2009)	31.30	0.920	315	–12
Rapeseed (X. Wu, Zhang, Yang, Chen, & Wang, 2000)	34.75	0.917	323	–15
Soybean (Honary, 1996)	29	0.913	328	–10
Coconut (P. J. Singh, Khurma, & Singh, 2010)	28.05	0.926	228	–
Palm (Barnwal & Sharma, 2005)	39.60	0.918	267	–
Jatropha (Mofijur et al., 2012)	35.40	0.918	186	15
Castor (Scholz & da Silva, 2008)	260	0.950	229	–15

2.1.5.3 Oxidation stability

Oxidation stability of vegetable oils is generally lower than those of fully saturated synthetics such as PAOs, synthetic esters, etc. This is due to the necessary unsaturation in vegetable oils required for low-temperature properties. The extent of oxidation relates to the fatty acid composition of natural oils. The rate of oxidation is a function of unsaturation of fatty acyl chain as shown in Figure 2.1.

Due to this lower oxidation stability, vegetable oils degrade more rapidly than mineral oils. In general, oxidation stability is inversely proportional to the degree of unsaturation. Such degradation leads to breakdown products that are volatile and corrosive, and weakens lubricant structure and properties. This means that vegetable oil formulations generally require higher doses of antioxidants to provide comparable performance.

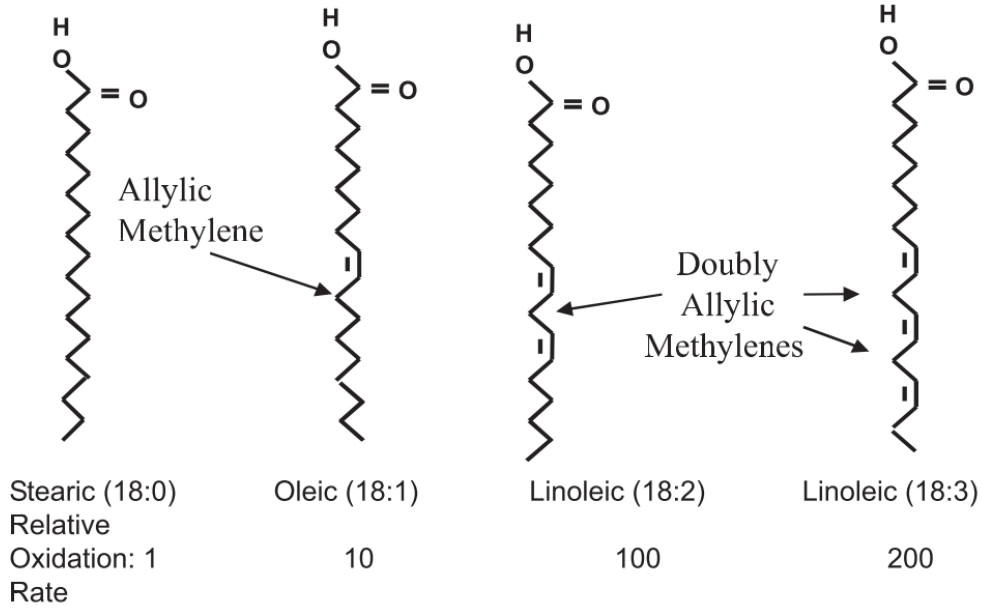

Figure 2.1: Approximate rates of oxidation of fatty acids
Source: Kodali (2002)

2.1.5.4 Tribological behavior

The fatty acids in natural oils are desirable in boundary lubrication for their ability to adhere to metallic surfaces. This behavior is due to the inherited polar carboxyl group that remain closely packed, and establish a monolayer film that is effective for reducing friction and wear by minimizing the metal-to-metal contact (Grushcow & Smith, 2005). The formation of protective complexes of the fatty acid molecules on the metal surfaces is shown in Figure 2.2 (Hsu, 1997). The polar heads of the fatty acid chains attach to metal surfaces by a chemical process that allows a monolayer film to form with the non-polar end of fatty acids sticking away from the metal surface resulting in reduction of COF (Jayadas & Prabhakaran Nair, 2007; Masjuki & Maleque, 1997; Masjuki, Maleque, Kubo, & Nonaka, 1999; Zulkifli et al., 2016).

But this tendency of protective film formation is adversely affected in an environment of high oxidation. In one of such study, the boundary lubrication properties have been analyzed for oxidized sunflower oil (Fox & Stachowiak, 2003). After aging for 28 days or more, the boundary lubrication characteristics of sunflower oil was degraded significantly. Due to the same reason, the direct use of vegetable oils is unsuitable for long durations in IC engines and other applications that require appropriate thermal and oxidative stability (Rudnick, 2013).

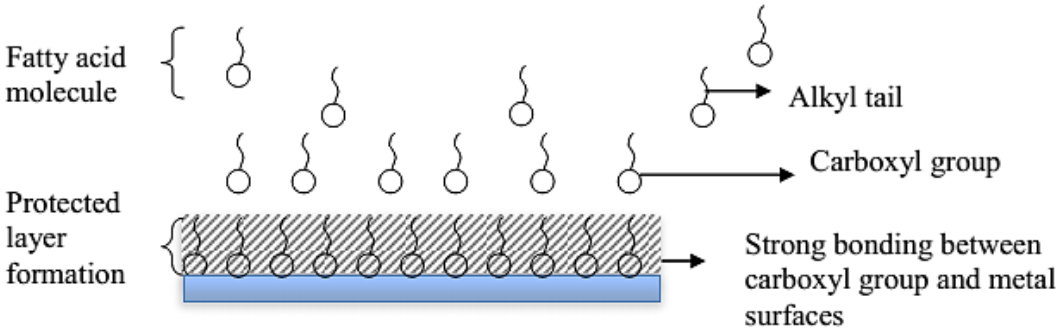

Figure 2.2: Protective film formation on metal surfaces by natural oil
Source: Zulkifli (2014)

2.1.6 Chemically Functionalized Vegetable Oils

Despite the lubrication properties of natural oils, direct use of vegetable oils are not suitable for prolonged use in IC engines because of their low thermal and oxidation stability (Rudnick, 2013). These deficiencies have been improved via the inducement of chemical changes, such as esterification, epoxidation, and hydroxylation. To improve thermo-oxidative stability, chemical modification of the vegetable oils is a subject under active investigation. Research has shown that chemically modified vegetable oils based biolubricants exhibit excellent oxidation stability and low-temperature flow properties (Arumugam & Sriram, 2012b; Kodali, 2002; Zulkifli, Kalam, Masjuki, Shahabuddin, & Yunus, 2013). Such chemically functionalized esters are produced from relatively pure raw materials to produce predetermined molecular structures formulated for high performance lubrication. Synthetic esters have improved thermo-oxidative stability, high viscosity indices, and advantage of absence of the undesirable impurities found in conventional petroleum based oils (Nagendramma & Kaul, 2012).

Similar to neat natural oils, synthetic esters maintain an affinity for metal surfaces due to their high degree of polarity which affords them the ability to establish monolayers that minimize the surface contact and enhance the tribological properties. Due to their sensitivity towards hydrolysis and thermal degradation, thermal properties of esters have been improved by replacing the glycerol with other polyols such as neopentylglycol (NPG), pentaerythritol (PE), trimethylolpropane (TMP), trimethylolhexane (TMH), and trimethyoloethane (TME) (Birova, Pavlovičová, & Cvenroš, 2002; Gryglewicz, Piechocki, & Gryglewicz, 2003; Nosonovsky & Bhushan, 2012) (Yunus, Fakhrul I-Razi, Ooi, Iyuke, & Idris, 2003) (Uosukainen, Linko, Lämsä, Tervakangas, & Linko, 1998; Yunus, Fakhru'I-Razi, Ooi, Biak, & Iyuke, 2004). Esters such as the NPG were originally developed for the lubrication of aircraft jet engines whereas PE esters have found use in gas turbines.

2.1.7 TMP Ester as a Lubricant

TMP esters, other polyol esters and complex esters have been found to be possible base oil candidates and have attained considerable importance in applications which include engine lubricants, gear oils, hydraulic oils, compressor oils, pump and turbine oils (Nagendramma & Kaul, 2012). For engine use in automotive and marine engine lubrication, esters such as TMP esters have found widespread use (Reeves, 2013). High viscosity index (VI) with moderate thermo-oxidative stability make TMP esters attractive lubricants for reciprocating engine applications.

2.1.7.1 Viscosity and low temperature fluidity of TMP esters

The physical properties like viscosity, VI and temperature fluidity define the viscometric behavior of lubricant. The viscosity and viscosity–temperature dependence of TMP ester is comparable to the conventional engine base oils like PAOs. Similarly, TMP ester show appreciable low temperature fluidity as compared to its counterparts which offer suitable viscosity behavior. Table 2.6 shows the details of physical properties of esters. Few studies have also been listed in Table 2.7 to show various research findings for synthesized TMP esters.

Table 2.6: Physical properties of esters

	Viscosity at 40 ◦C (cSt)	Viscosity at 100 ◦C (cSt)	VI	Pour Point
Crambe oil	51.5	10.5	199	− 9
TMP	56.9	11.0	190	−12
Neopentylglycol	32.2	7.3	203	− 6
PE	78.7	14.8	198	0
Methyl	5.8	2.1	199	− 6
Ethyl	6.1	2.2	207	3
Isopropyl	6.0	2.3	264	−27
2-ethylhexyl	10.5	3.2	190	−18

Source: Rudnick (2013)

2.1.7.2 Oxidation stability of TMP esters

TMP esters have improved oxidation stability as compared to raw vegetable oils. This stable behavior against oxidation and polymerization is attributed to the elimination of carbon β hydrogen as shown in Figure 2.3. Table 2.7 shows that chemical modification leading to formation of TMP ester resulted in enhanced oxidation stability in previous research findings.

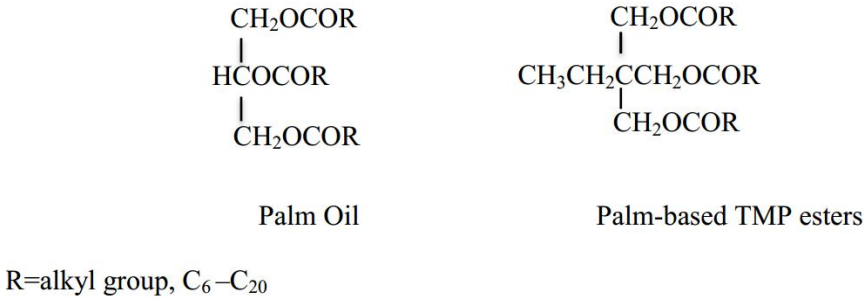

Figure 2.3: Structure of vegetable oil and TMP ester

Table 2.7: Oxidation stability and low temperature flow characteristics of TMP esters

Literature	Findings
(Gryglewicz et al., 2003)	TMP esters have better oxidation stability up to 30% with improved VI as compared to neat vegetable oil.
(Yunus et al., 2004)	Improved oxidation stability and high VI ranges (170 – 200) were recorded with relatively high pour point, between 4 to -1 °C.
(Arbain & Salimon, 2011)	Synthesized TMP esters showed good low temperature properties, improved hydrolytic stability, and high viscosity index.
(Salimon, Salih, & Yousif, 2012a) (Salimon, Salih, & Yousif, 2012b)	Favorable low temperature performance and higher oxidation stability is reported.

2.1.7.3 Lubricity, EP, and AW behavior

Antiwear and friction reduction characteristics of palm TMP ester found to comparable to mineral base oil using the four ball tribo-testing (Zulkifli, Kalam, Masjuki, Shahabuddin, et al., 2013). In another study, Okubo, Watanabe, Tadokoro, and Sasaki (2016), found that the TMP ester was helpful in causing ultra-low-friction during cylinder

on a disk sliding tests as compared to polypropylene glycol (PPG), and poly-alpha olefin (PAO).

More still, the use of appropriate AW and friction reduction additives to TMP esters are required to improve their tribological performance.

2.2 Lubricant Additives

During engine operations, lubricant is expected to maintain the effective lubrication for extended duration before it is drained. To meet these expectations, the base oil are combined with a number of additives, which must be carefully selected to develop the lubricant with the desired performance. The additive packages have evolved to play an increasingly important role in the oil formulation. The base oils comprise of typically 75 – 83 wt% of the commercial engine lubricant. For different engine applications, viscosity improvers (5 – 8 wt%) and small amounts of other additives (12 –18 wt%) are used to further enhance the lubricant properties (Watson, 2010). Conventional additives are synthetic chemical substances mixed with base oils to improve various characteristics of lubricants so the oils can placate the higher demand placed on them and satisfy specification requirements. Additives often improve existing properties, suppress undesirable properties, and introduce new properties to the base oils. One of the most important properties that additives enhance is a lubricant's ability to form protective films, which is especially important in boundary lubrication conditions. When blending additives with base oils, it is important to have a well-balanced and optimized composition to improve the performance of the lubricant. This usually requires the formulation of high performance base oils that are derived from highly refined oils and then mixed with additives to further enhance the lubricant's properties. Many of the most common additive bundles used in lubricant formulations are antiwear additives, extreme pressure additives, viscosity improvers, oxidation inhibitors, corrosion inhibitors,

detergents, dispersants and foam inhibitors. Similar to conventional engine lubricants, bio-based base material alone cannot achieve the effective lubrication performance therefore in addition to bio-based base stock, a variety of additives should also be a part of final formulation (Rudnick, 2013) .

2.2.1 Friction Modifiers and Antiwear Additives

In tribo-pairs, when two surfaces engage in metal-to-metal contact and begin to move relative to each other, AW additives and FMs are essential part of engine oil to prevent seizure, wear loss, and friction. Wear and friction improvers consist of chemical additives that can be divided into three groups: adsorption or boundary additives; AW additives; and extreme pressure (EP) additives.

'Boundary' additives are friction and wear modifiers such as fatty acids that are added to oil to minimize the asperity contact. All of these additives help in maintaining the lubricating performance of the oil which making their usage very important. In case of ineffective lubrication, high friction and extreme wear will occur, causing damage to the moving parts with usually an increase in energy consumption. Extensive research on the suitability and concentration of FMs and AW additives have been done for the conventional engine lubricants.

As the chemistry of bio-based base stock is different from conventional lubricants base oils, so the suitable additives selection is under investigation. Many researchers (Alves, Barros, Trajano, Ribeiro, & Moura, 2013; Arumugam S, 2014; Arumugam & Sriram, 2014; Thottackkad, Perikinalil, & Kumarapillai, 2012) found nanoparticles addition more effective for bio-based lubricants.

2.2.2 Nanoparticles as Additives

The quest for energy efficiency has led the research towards new materials, instead of traditional materials, for use as lubricant additives. Currently, various types of nanomaterials are under investigation as lubricant additives (Bakunin, Suslov, Kuzmina, & Parenago, 2005; Bakunin, Suslov, Kuzmina, Parenago, & Topchiev, 2004; Kheireddin, 2013; B. Li, Wang, Liu, & Xue, 2006; L Rapoport et al., 1997; Wang & Liu, 2013). In the development history of lubricant additives, nanoparticles are a relatively new class of lubricant additives as mentioned in Figure 2.4. Nanolubricants typically consist of base oils or fully formulated lubricants with colloidal solid particles suspended within them (Martin & Ohmae, 2008; Saidur, Kazi, Hossain, Rahman, & Mohammed, 2011). There are usually three components in a nanolubricant; the lubricant/base oil solvent, the nanoparticles that act as antiwear (AW)/extreme pressure (EP) additive or friction modifier (FM), and the surfactant that inhabits the interface area between the lubricating oil and the particles (Ohmae, Martin, & Mori, 2005).

Nanolubrication offers a solution to many problems associated with traditional lubricants that contain Sulfur and Phosphorus (Martin & Ohmae, 2008). However, few nanoparticles inhibit toxic nature, for related nanolubricants, the disposal of nanolubricants after drain interval is needed to be carried out according to local regulations with approved waste disposal facility, in consideration of the product characteristics at time of disposal. Nanoparticles are versatile, and many researchers have reported that a single type of nanoparticle served multiple purposes as AW, EP additive as well as FM (Chou et al., 2010; Z. S. Hu et al., 2002; Nallasamy, Saravanakumar, Nagendran, Suriya, & Yashwant, 2014; Thakur, Srinivas, & Jain, 2016; Verma, Jiang, Abu Safe, Brown, & Malshe, 2008). Due to the various types, sizes and morphology of nanoparticles, the combinations of nanoparticles and lubricants can result in several nanolubricants.

Table 2.8 shows the variation in types, sources, size and morphology for commonly used nanoparticles various studies. Although various studies have shown remarkable tribological improvement in lubricants dispersed with different types of nanoparticles, it is still difficult to select the suitable nanoparticle additive. The effectiveness of nanoparticles depends on various factors, including their compatibility with base oil/lubricant, their sizes and morphologies, as well as their concentrations (Peña-Parás et al., 2015).

In order to determine a suitable nanoparticle and lubricant combination, it is required to consider all these parameters while focusing on their tribological test conditions and related lubrication mechanisms.

This section provides an overview of the tribological essence of nanoparticles type, morphology and size as well as the role of lubricant/nanoparticle compatibility, range/optimum nanoparticles concentrations, and experimental tests conditions (geometry, load, contact, temperature, speed, time etc.).

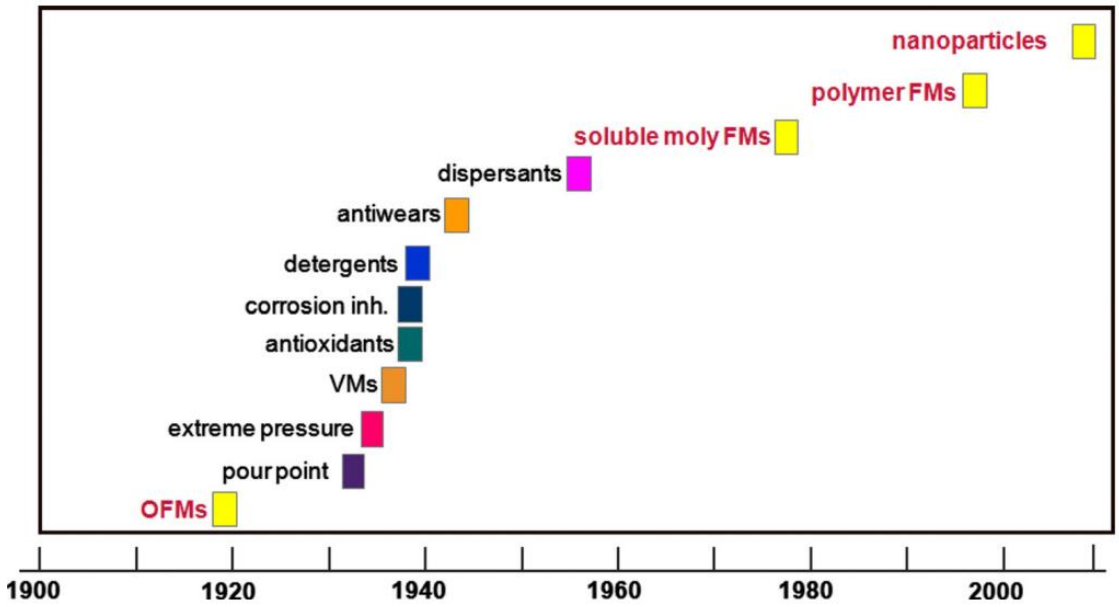

Figure 2.4: Timeline for development of lubricant additives
Source: Spikes (2015)

Table 2.8: Summary of sources and typical properties of nanoparticles used as lubricant additives

Type	Nano-particle	Source	APS (nm)	Shape	Reference
Metal	Cu	Commercial	25	Nearly spherical	(Viesca, Battez, González, Chou, & Cabello, 2011)
	Ni		20	Nearly spherical	(Chou et al., 2010)
	Al		65	Spherical	(Peng, Kang, Chen, Shu, & Chang, 2010)
	Pb	Fabricated	2.2	Spherical	(Kolodziejczyk, Martinez-Martinez, Rojas, Fernandez, & Sanchez-Lopez, 2007)
			40	Spherical	(Zhao, Zhang, & Dang, 2004)
Metal Oxides	CuO	Fabricated	5	Sphere-like	(Y. Y. Wu, Tsui, & Liu, 2007)
			4.35	Nearly spherical	(Alves et al., 2013)
	ZnO	Fabricated	11.71	Nearly spherical	(Alves et al., 2013)
		Commercial	20	Nearly spherical	(Battez et al., 2007)
	TiO_2	Fabricated	80	Sphere-like	(Y. Y. Wu et al., 2007)
Chalcogenides	MoS_2	Commercial	90	Layered lamellar flaky	(Koshy, Rajendrakumar, & Thottackkad, 2015)
		Fabricated	350, 150	Layered	(Rabaso et al., 2014)
			100	Rectangular, oblate	(Yadgarov et al., 2013)
	WS_2	Fabricated	100	Spherical	(L. Rapoport et al., 2003)
			120	Polyhedral, faceted	(Yadgarov et al., 2013)
Carbon based	Diamond	Commercial	10	Sphere-like	(Y. Y. Wu et al., 2007)
	Graphite		55	Spherical	(C.-G. Lee et al., 2009)
	Carbon nano horns		80	Dahlia like	(Zin, Agresti, Barison, Colla, & Fabrizio, 2015)
	Graphene	Fabricated	10	Spheroidal	(Joly-Pottuz, Vacher, Ohmae, Martin, & Epicier, 2008)
Nitrides	BN	Commercial	70	Spherical	(Abdullah et al., 2016)
			114	Non-spherical	(Çelik, Ay, & Göncü, 2013)
Ceramic	Al_2O_3	Fabricated	78	Spherical	(Luo, Wei, Huang, Huang, & Yang, 2014)
	SiO_2	Commercial	30	Spherical	(Xie, Jiang, He, Xia, & Pan, 2015)
		Fabricated	362, 215, 140, 58	Spherical	(Peng, Chen, Kang, Chang, & Chang, 2010)
Composites	Al_2O_3/SiO_2	Fabricated	70	Elliptical	(Jiao, Zheng, Wang, Guan, & Cao, 2011)

	ZrO_2/SiO_2		50-80	Nearly spherical	(W. Li, Zheng, Cao, & Ma, 2011)
Polymer	PTFE	Commercial	30-50	Spherical	(Mukesh, Jayashree, & SSV, 2013)

2.2.2.1 Role of dispersion stability

When added to a fluid medium, the size of the nanoparticles is small enough to remain dispersed in liquids by Brownian motion. This is due to the random motion of particles that was first observed by Robert Brown and proven by Albert Einstein in 1905 (Einstein, 1905). The particles in suspension may stick together and form larger agglomerates, which may settle down due to gravity. The agglomeration of nanoparticles results not only in sedimentation but also in the loss of wear protection and friction reduction ability. Therefore, dispersion stability is highly desirable for reliable lubrication performance. In the case of poor dispersion stability, sedimentation, and clogging may occur (K. Lee, Y. Hwang, S. Cheong, L. Kwon, et al., 2009). Stability means that the particles do not accumulate at a significant rate. Figure 2.5 shows two profiles for a dispersion of inorganic fullerene, IF-MoS_2 in a reciprocating test rig. Two cases of "stirred" and "not stirred" nanolubricant samples are considered showing loss of friction reduction ability of MoS_2 nanoparticles.

Stable suspension is considered as a prerequisite for an effective nanolubricant formulation. There are various studies in the related literature that lack information on the nanoparticles dispersion method (Chen & Liu, 2006; Ma, Zheng, Cao, & Guo, 2010; Ye et al., 2003) and stability of the nanolubricants (Joly-Pottuz et al., 2008; Ma et al., 2010; Viesca et al., 2011; Xie et al., 2015; Ye et al., 2003). As suspension stability is a vital issue that influences the nanolubricant lubrication performance, it is important to study and discuss the related influencing factors. This section will outline (a) the methods of nanoparticles dispersion in lubricating oils, (b) dispersion stability analysis methods for nanolubricants, and (c) methods to enhance the dispersion stability of nanolubricants.

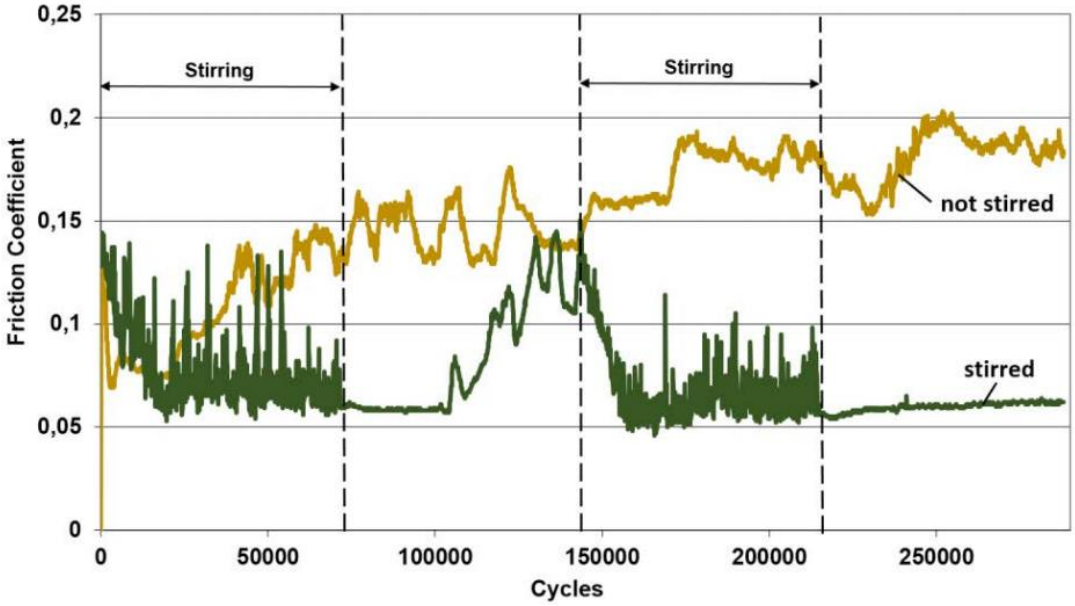

Figure 2.5: Friction behavior of "stirred" and "not stirred" lubricants showing effectiveness of stable dispersion for nanoMoS_2 enriched lubricant
Source: Rabaso (2014)

2.2.2.2 Methods of nanoparticles dispersion

For stable dispersion stability of nanolubricants, the selected method for dispersion is one of the governing parameter after the selection of base oil and nanoparticles. According to Rabaso (2014), agitating the IF-MoS_2 enriched oil before testing can help in reducing the size of agglomerates.

Various methods have been used including magnetic stirring (Rabaso, 2014), chemical agitation (Laad & Jatti, 2016), agitation using ultrasonic shaker (Thottackkad et al., 2012; Xie et al., 2015), agitation using mechanical ball milling agitation, ultrasonic probe (Alves et al., 2013; Battez et al., 2006; Battez et al., 2007; Mukesh et al., 2013; Viesca et al., 2011; H.-l. Yu et al., 2008; J. Zhou, Wu, Zhang, Liu, & Xue, 2000), and ultrasonic bath (Asrul, Zulkifli, Masjuki, & Kalam, 2013; K. H. Hu, Huang, Hu, Xu, & Zhou, 2011; Joly-Pottuz et al., 2008).

After the selection of dispersion method, the time duration of dispersion is also a key parameter in controlling the tendency of agglomerations. It has been observed that an increase in the mixing time leads to a decrease in the size of nanoparticles aggregates using ultrasonic bath (Joly-Pottuz et al., 2008). Rabaso (2014), has reported that the friction reduced significantly as the mixing time increased for IF-MoS_2 enriched oil.

Thus, agitation time duration plays an important role in dispersion stability and consequently affects the lubrication performance. Agitation duration as low as 2 minutes (Battez et al., 2006; Battez et al., 2007; Battez et al., 2008; Greco, Mistry, Sista, Eryilmaz, & Erdemir, 2011) and as high as 24 hours have been reported (Cho et al., 2012). Table 2.9 shows commonly used dispersion methods and the duration for different lubricants and nanoparticles combinations.

Table 2.9: Literature summary of commonly used dispersion methods, duration, techniques to improve dispersion stability and measuring methods

Particle	Oil	Dispersion Method and Duration	Surface Modification	Surface Modifying Agent/ Surfactant	Dispersion Stability Test	Reference
ZrO_2/SiO_2	$20^{\#}$ Machine oil	Ultrasonic dispersion, 30 min	Yes	Aluminum zirconium coupling agent	Zeta Potential, UV-Vis Absorbance	(W. Li, Zheng, Cao, & Ma, 2011)
Al_2O_3/SiO_2		Ultrasonic dispersion, 30 min	Yes	Silane coupling agent KH-560	Sedimentation	(Jiao et al., 2011)
Al_2O_3		Ultrasonic dispersion, 30 min	Yes	Silane coupling agent KH-560	Sedimentation, Zeta potential UV-Vis Absorbance	(Luo et al., 2014)
TiO_2	Servo 4T synth 10W-30	Chemical shaker for agitation, 30 min	No	-	UV-Vis Absorbance	(Laad & Jatti, 2016)
$ZnAl_2O_4$	Lubricating oil	-	Yes	OA	UV-Vis Absorbance	(Song et al., 2012)
CuO	Multi-grade engine oil	Ultrasonic agitation, 30 minutes	No	-	UV-Vis Absorbance	(Jatti & Singh, 2015)
	SAE-40, Coconut oil	Ultrasonic shaker, 40 minutes	No	-	UV-Vis Absorbance	(Thottackkad et al., 2012)
ZrO_2	20# machine oil	-	Yes	Silane coupling agent KH-560	No	(Ma et al., 2010)
ZnO	60SN base oil	Ultrasonic bath 30 minutes, stirrer 20 minutes	Yes	OA	Sedimentation	(Ran, Yu, & Zou, 2016)
CuO, MoS_2	Palm TMP ester	Ultrasonic bath, 60 min	Yes	OA	UV-Vis Absorbance	(M. Gulzar et al., 2015)
SiO_2	Liquid paraffin	Ultrasonic stirrer, 60 min	Yes	OA	Sedimentation	(Peng, Chen, et al., 2010)
PbS	Liquid paraffin	-	Yes	OA	No	(Chen & Liu, 2006)
hBN	SAE 15W-40	Ultrasonic homogenizer, 20 min	Yes	OA	No	(Abdullah et al., 2016)
hairy silica	PAO100	Stirrer	Yes	Amino Functional-ized	Sedimentation	(Sui et al., 2015)
Cu	PAO6	Ultrasonic probe, 30 min	No	-	Sedimentation	(J. Viesca et al., 2011)
Ni		Ultrasonic probe, 30 min	No	-	Sedimentation	(Chou et al., 2010)
Carbon onion, Graphite	PAO	Ultrasonic bath, 300 min	No	-	No	(Joly-Pottuz et al., 2008)
Carbon nano-onions		Ultrasonic bath, 300 min	No	-	Sedimentation	(Joly-Pottuz et al., 2008)
SiO_2, MoS_2	EOT5#	Ultrasonic shaker, 120 min	No	-	No	(Xie et al., 2015)

2.2.2.3 Dispersion stability analysis for nanolubricants

For investigation of dispersion stability, a number of different methods have been used. These methods include sedimentation, spectral absorbency, zeta potential, and metallographic micrographs stability test. Table 2.9 shows the commonly used methods in various research studies. The details of these stability investigation methods, procedures, and limitations are given below.

(a) ***Sedimentation method***

Sedimentation is the simplest method to evaluate the stability of nanolubricants. This method has also been termed as "observation stability test" (Azman, Zulkifli, Masjuki, Gulzar, & Zahid, 2016). For the stability evaluation, sedimentation photograph of samples in test tubes are usually taken (Amiruddin, Abdollah, Idris, Abdullah, & Tamaldin, 2015; Koshy et al., 2015; Mukesh et al., 2013; Peng, Chen, et al., 2010; Peng, Kang, et al., 2010; Sui, Song, Zhang, & Yang, 2015, 2016). The major disadvantage of this method is the long duration to acquire the results. In addition, precautions required the maintenance of same volume, temperatures, and surrounding conditions for all the considered samples. This stability analysis is usually carried out immediately after the dispersion of nanoparticles in the lubricant. Disturbance or movements should also be avoided to ensure reliability. Figure 2.6 shows the sedimentation of paraffin oil added with surface modified and unmodified aluminum nanoparticles that were recorder after 30 days from preparing.

The duration of this test varies from days to months. Peng et al. (2010) reported the sedimentation behavior after 30 days for silica and alumina nanoparticles dispersed in paraffin oil (Peng, Chen, et al., 2010; Peng, Kang, et al., 2010). In another study by Sui et al. (2016), the stability of the nano silica enriched polyalphaolefin (PAO) lubricants was studied by keeping the lubricants for 2 months. Amiruddin et al. (2015), evaluated

the dispersion stability of SAE15W40 enriched with nanohBN for 60 days. Koshy et al. (2015) have reported a test duration of 100 days for coconut oil and paraffin oil enriched with nanoMoS_2. Mukesh et al. (2013), carried out this test for 7 days for PTFE based nanolubricants. Thus, different test durations have been mentioned by researchers for different nanoparticles and lubricants combinations.

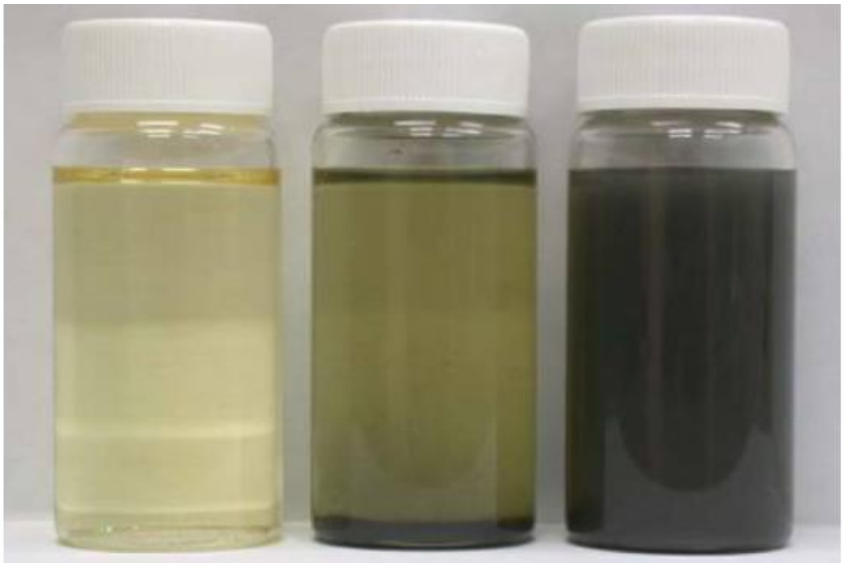

Figure 2.6: Sedimentation of aluminum nanoparticles dispersed in paraffin oil
Source: Peng, Kang, et al. (2010)

(b) ***Method of spectral absorbency***

Spectral absorbency is a commonly used method to evaluate the stability of nanolubricants (Table 2.9). In this method, ultraviolet–visible (UV–vis) spectrophotometry absorbance measurements are used to characterize the colloidal stability of the dispersions. It is an easy and reliable method to evaluate the dispersion stability given that the nanomaterials dispersed in fluids have characteristic absorption bands in the wavelength range of 190–1100 nm (Yu & Xie, 2012). In this method the lubricant samples are placed in quartz/glass cuvettes of typically 1 cm thickness and the absorption spectra are recorded on a spectrometer (Das, Bedar, Kannan, & Jasuja, 2015). The advantage of this method compared to other methods is that it can provide a

quantitative concentration of nanofluids (Yu & Xie, 2012). This quantitative analysis provides a linear relation between the supernatant nanoparticle concentration and the absorbance. This method is also considered to be helpful in determining the sedimentation kinetics (D. Zhu et al., 2009). Similar to the sedimentation method, different test durations have been reported by researchers for spectral absorbency analysis. Song et al. (2012), showed the absorbance profiles of lubricating oil enriched with nano$ZnAl_2O_4$ for an analysis duration of 140 hours. Koshy et al. (2015), has mentioned a test duration of 120 hours for coconut oil and paraffin oil enriched with nanoMoS_2. Jatti and Singh (2015), showed absorbance spectral behavior of nanoCuO enriched multi-grade engine oil over a time duration of 125 hours. Similarly, Luo et al. (2014), have shown optical absorbance for nanoAl_2O_3 enriched lubricating oil for 72 hours (Figure 2.7). From the analysis of various studies, it can be observed that the selection of test duration is based upon the observable variation in the absorbance behaviors of lubricant samples.

(c) *Zeta potential analysis*

This method shows dispersion stability in terms of the potential difference between the dispersion medium and the stationary layer of fluid attached to the dispersed particle (Yu & Xie, 2012). The absolute value of this parameter is used to illustrate the dispersion tendency of selected nanoparticles in the lubricating oil. The higher the value of zeta potential (negative or positive), the better is the electrical stability of the dispersion. The low values of zeta potential show higher tendency of agglomeration or flocculation. In general, a value of 25 mV (positive or negative) can be taken as reference value for deciding the stability of the suspension. For example, Figure 2.7 shows trend of zeta potential values for nanoAl_2O_3 showing poor and better dispersion behaviors in the same lubricating oil.

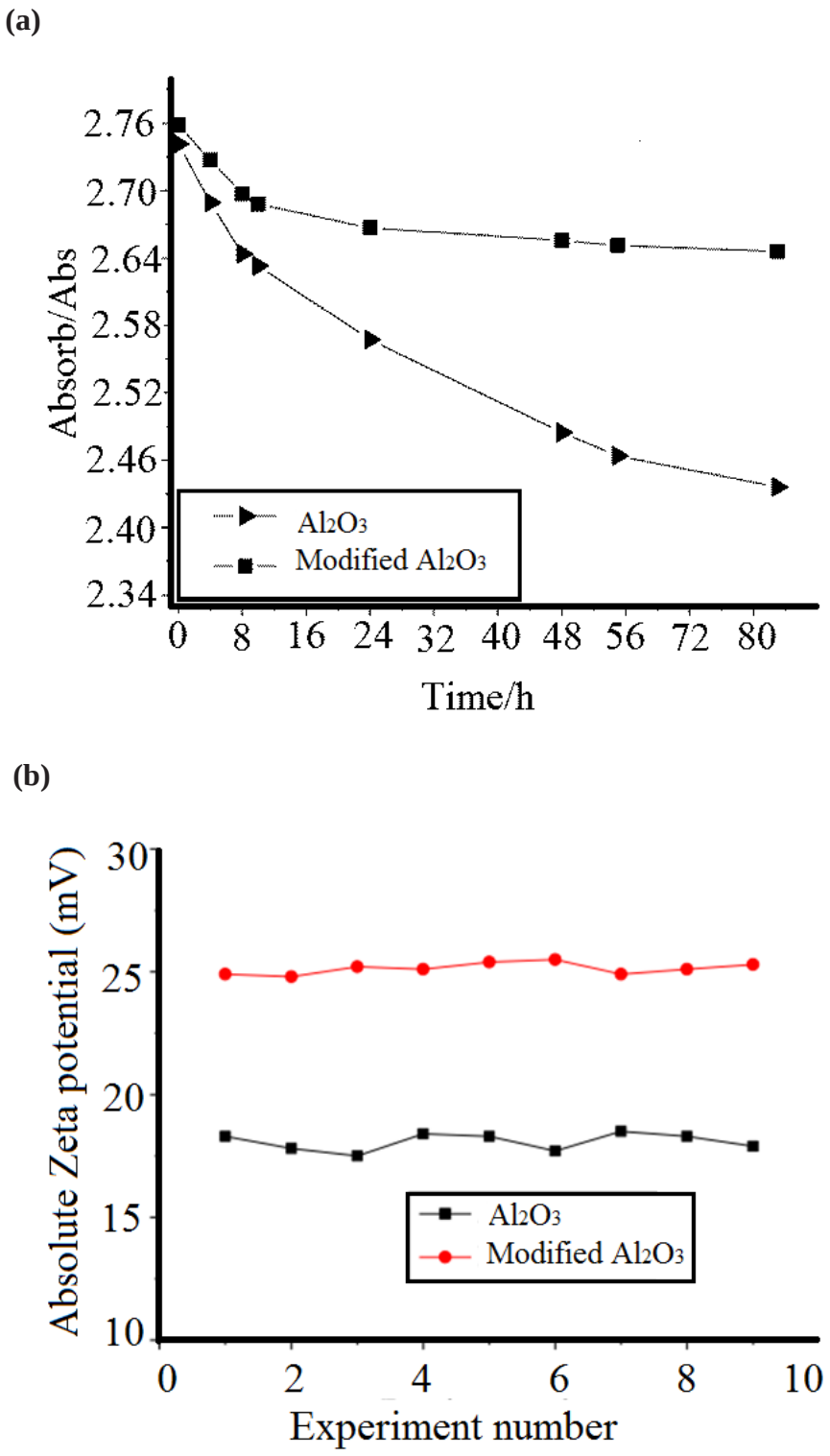

Figure 2.7: Dispersion stabilty analysis showing comparison of poorly disperesd (Al_2O_3) and better dispersed nano-oils (Modified Al_2O_3) using (a) spectral absorbency (b) zeta potential

Source: Luo et al. (2014)

2.2.2.4 Methods to enhance the dispersion stability of nanolubricants

To address the issue of dispersion stability of nanoparticles in lubricating oils, nanoparticles surface functionalization is considered an essential step (Akbulut, 2012). For stable dispersions through surface functionalization, the researchers have developed two methods: a) Electrostatic stabilization b) Steric stabilization. Electrostatic stabilization is usually incorporated via the adsorption of ionic surfactants on the nanoparticle surface. This interaction is based on the theory that like-charged repel each other in compliance with Coulomb's law. While, the steric repulsion is achieved by functionalizing the nanoparticle surface with a polymer or a surfactant monolayer (Min, Akbulut, Kristiansen, Golan, & Israelachvili, 2008). Commonly used surface functionalization techniques and relevant studies have been discussed below.

(a) ***Effect of surfactant***

Surfactants used in nanolubricants are also termed as dispersants. Adding surfactants in the nanolubricants is an easy and economic method to enhance the dispersion stability. Commonly used surfactant include OA (Abdullah et al., 2016; Demas et al., 2012) and sodium dodecyl sulfate (SDS) (Demas et al., 2012; Koshy et al., 2015). Demas et al. (2012) have studied five different surfactants to evaluate the dispersion of nanoMoS_2 and nanoBN in PAO (Table 2.10). They reported that the use of surfactant was not only beneficial in suspending the nanoparticles, but also reduced the friction and wear by itself.

(b) ***Nanoparticles surface modification***

In this method, the surface properties of the nanoparticles are tailored by the organic modification agents. Commonly used modification agents like oleic acid (OA) is adsorbed around the nanoparticle, reducing their surface energy effectively to prevent the agglomeration (Peng, Chen, et al., 2010). The presence of organic chains enhances their

dispersion stability in organic solvent. Studies have shown the effectiveness of surface modification as mentioned in Table 2.9. In addition to organic acids (Chen & Liu, 2006; Song et al., 2012; Ye et al., 2003), silane coupling agents (Jiao et al., 2011; Luo et al., 2014; Ma et al., 2010; Sui et al., 2015) are also found to be helpful in stable nanolubricant suspensions.

Table 2.10: Typical surfactants, their chemical structure and functionality

Surfactant	Functionality
#1 Sodium dodecyl sulfate 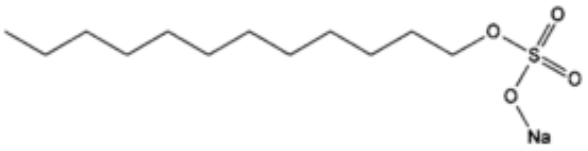	Anionic
#2 Benzethonium chloride 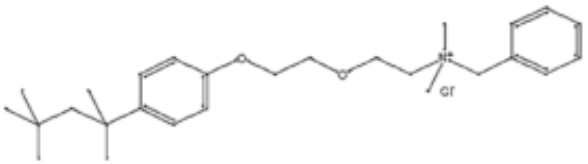	Cationic
#3 Benzalkonium chloride 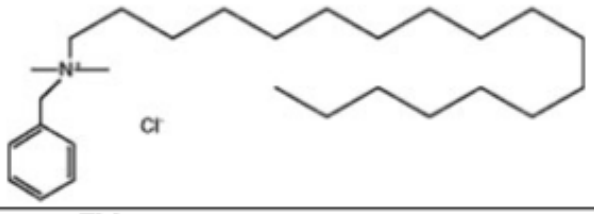	Cationic
#4 Triton™ X 102 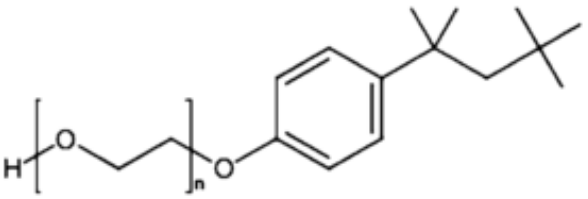	Non-ionic
#5 Oleic acid 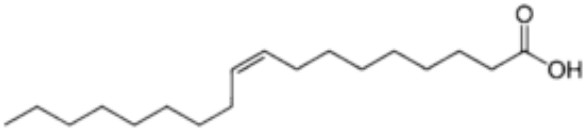	Anionic

Source: Demas et al. (2012)

2.2.2.5 Role of nanoparticles concentration

Suitable concentration is another important factor that affects the lubrication characteristics of nanolubricants (Koshy et al., 2015; Luo et al., 2014; Sui et al., 2015; Thottackkad et al., 2012). The addition of nanoparticles, either too little or too much, may cause harmful effects in some cases either by increasing friction or wear (Azman et al., 2016). The path to suitable nanoparticle concentration for a lubricating oil depends on three crucial factors which include dispersion method/time, role of nanoparticle (FM, AW or EP additive) and tribo-test conditions. Table 2.11 summarizes related literature, showing a range of concentrations and optimum concentrations along with the role of nano-additive for different lubricants and nanoparticles combinations.

It is interesting to observe that the same MoS_2 nanoparticles show different suitable concentrations for two different base lubricants i.e. 0.58 wt% for mineral oil and 0.53 wt% for coconut oil using pin on disk contact geometry (Koshy et al., 2015). Contradictorily, a fixed optimum concentration of 0.5 wt% nanoCuO and nanoZnO has been used for mineral, synthetic and vegetable oils for ball on disk contact geometry (Alves et al., 2013). It shows that the optimum concentration is strongly system specific which means it will vary for each test condition.

Table 2.11: Literature summary of role of nanoparticles and optimum concentrations for different lubricating oils

Nano-particle	Lubricant	Nanoparticle Role	Conc. (wt%)	Optimum Conc. (wt%)	Reference
ZnO	Mineral, PAO, Sunflower, Soybean	FM, AW	0.5	0.5	(Alves et al., 2013)
	60SN base oil	FM, AW	0.5	0.5	(Ran, Yu, & Zou, 2016)
CuO	Coconut oil	FM, AW	0.1-0.6	0.34	(Thottackkad et al., 2012)
	CMRO	FM, AW	0.1,0.5,1	0.5	(Arumugam & Sriram, 2014)
	Mineral based engine oil	FM, AW	0.5, 1, 1.5	1.5	(Jatti & Singh, 2015)
	SAE 75W-85	FM, AW, EP	0.5, 1.0, and 2.0	2	(Peña-Parás et al., 2015)
	PAO8	FM, AW, EP	0.5, 1.0, and 2.0	2	(Peña-Parás et al., 2015)
	Mineral, PAO, Sunflower, Soybean	FM, AW	0.5	0.5	(Alves et al., 2013)
MoS_2	Coconut oil	FM, AW	0.25,0.5,0.75,1	0.53%	(Koshy et al., 2015)
	Mineral oil	FM, AW	0.25,0.5,0.75,1	0.58%	(Koshy et al., 2015)
	EOT5#	FM, AW, EP	0.2, 0.5, 0.7 and 1.0	1	(Xie et al., 2015)
	SE 15W-40	FM, AW, EP	0.1, 0.5, 1.0, 2.0 and 5.0	~ 1	(Wan, Jin, Sun, & Ding, 2014)
SiO_2	Liquid paraffin	FM, AW	0.0125, 0.025, 0.05,0.1,0.2,0.5, 1, 2, 4	0.05-0.5wt%	(Peng, Chen, et al., 2010)
	EOT5#	FM, AW, EP	0.2, 0.5, 0.7 and 1.0	0.7	(Xie et al., 2015)
PbS	Liquid paraffin	FM, AW	0.05-0.2	0.2	(Chen & Liu, 2006)
Fe_3O_4	#40 engine oil	FM, AW	0.5, 1.0, 1.5, 2.0	1.5	(Gao, Wang, Hu, Pan, & Xiang, 2013)
hairy silica	PAO100	FM, AW	0.5,1,2,4	1	(Sui et al., 2015)
Cu	PAO6	AW, EP	0.5,2	0.5	(Viesca et al., 2011)
Carbon Coated Cu		AW, EP	0.5,2	0.5	(Viesca et al., 2011)
Ni		FM, AW, EP	0.5, 1 and 2	0.5	(Chou et al., 2010)
ZrO_2, ZnO, CuO		AW, EP	0.5%, 1.0% and 2.0%	0.5	
Carbon nano-onions	PAO	FM, AW	0.1	0.1	(Joly-Pottuz et al., 2008)
ZrO_2/SiO_2	20# machine oil	FM, AW	0.05, 0.1, 0.3, 0.5, 0.75,1	0.1	(W. Li et al., 2011)
Al_2O_3/SiO_2		FM, AW	.05, 0.1 0.5,1	0.5	(Jiao et al., 2011)
Al_2O_3		FM, AW	.05, 0.1 0.5,1	0.1	(Luo et al., 2014)
TiO_2	Servo 4T Synth 10W30	FM, AW	0.3,0.4,0.5	0.3	(Laad & Jatti, 2016)
$ZnAl_2O_4$	Lubricating Oil	FM, AW	0.05, 0.1, 0.5, 1	0.1	(Song et al., 2012)

2.2.2.6 Role of nanoparticle size

The tribological performance of nanolubricants has a direct linkage to the nanoparticle size in a number of ways. Firstly, the dispersion stability is a function of nanoparticle size which is a major requirement for proper nanolubricant formulation. In this regard, the sedimentation rate is an important parameter to determine the dispersion stability which can be calculated using Stokes' law

$$v_z = \frac{2(\rho_{NP} - \rho_F)\, g r^2}{9\mu} \qquad \text{Equation 2.1}$$

where, v_z is settling velocity, ρ_{NP} is density of nanoparticles, ρ_F is density of fluid, g is gravity, r is the radius of nanoparticle, and μ is the viscosity of the fluid. This simple equation shows that for 10-fold increase in nanoparticle size (e.g., 100 nm instead of 10nm), sedimentation time will decrease 100-fold. It shows the role of nanoparticle size in achieving stable nanolubricant.

Secondly, the small size of nanoparticles helps them to penetrate the rubbing surfaces and their reaction with the environment depending upon their surface-to-volume ratio. The intrinsic mechanical properties of nanoparticles such as hardness are determined by its size which in turn affects the tribological behavior. For materials in the size range of 100 nm or greater, the hardness increases with shrinking particle size (Schiøtz & Jacobsen, 2003; Weertman, 1993). If the hardness of nanoparticles is higher than the hardness of the material of tribo-pair, the result is indentation and scratching. The same phenomenon has been reported by Peña-Parás et al. (2015). According to their study, high hardness (8–9 Mohs) of nanoAl_2O_3 than the metal substrate resulted in abrasive wear and nanoparticle re-agglomeration. Therefore, the relationship between size and hardness of nanoparticles must be considered while formulating nanolubricant.

Lastly, while considering the suitable nanoparticle size selection, the ratio of root mean square roughness of lubricated surface to the radius of nanoparticle is an important parameter. If the nanoparticles size is too big as compared to the gap between asperities, they will not deposit on the contact zone which will lead to poor lubrication.

2.2.2.7 Role of nanoparticle shape and structure

For various types of tribological applications, the role of nanoparticle shape plays an important role. The shape of nanoparticle corresponds to pressure experienced by nanoparticles upon loading. Spherical shape nanoparticles show high load carrying capacity and EP characteristics due to their ball bearing effect (Luo et al., 2014). The reason for this behavior is based on the contact between the nanoparticle and the lubricated surface. The spherical shape of nanoparticles results in point contact with the counter surface. The line contact is associated with the nanosheets while the planar contact is the feature of nanoplatelets (Figure 2.8). In a majority of studies related to the use of nanolubricants, spherical shape nanoparticles have been used (Joly-Pottuz et al., 2008; Kolodziejczyk et al., 2007; C.-G. Lee et al., 2009; Luo et al., 2014; Peng, Chen, et al., 2010; Peng, Kang, et al., 2010; L. Rapoport et al., 2003).

While characterizing the morphology of nanoparticles, their internal nanostructure can influence their tribological properties. Commonly used nanoparticles, such as graphite, h-BN, and transition metal dichalcogenides, owe their lubrication performance to a layered structure (Demas et al., 2012). Figure 2.9 shows the molecular structure of MoS_2 as an example of layered crystal structure.

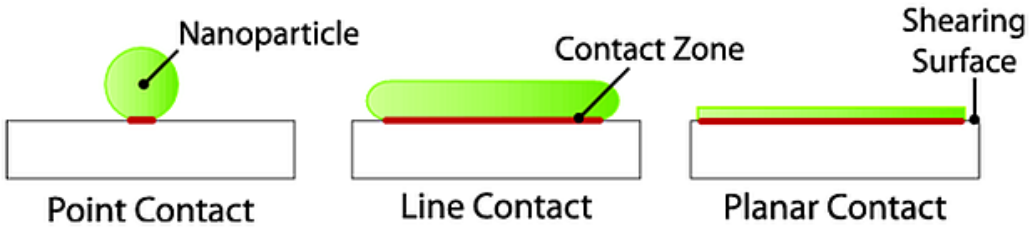

Figure 2.8: The effect of nanoparticle shape on the contact pressures upon loading
Source: Akbulut (2012)

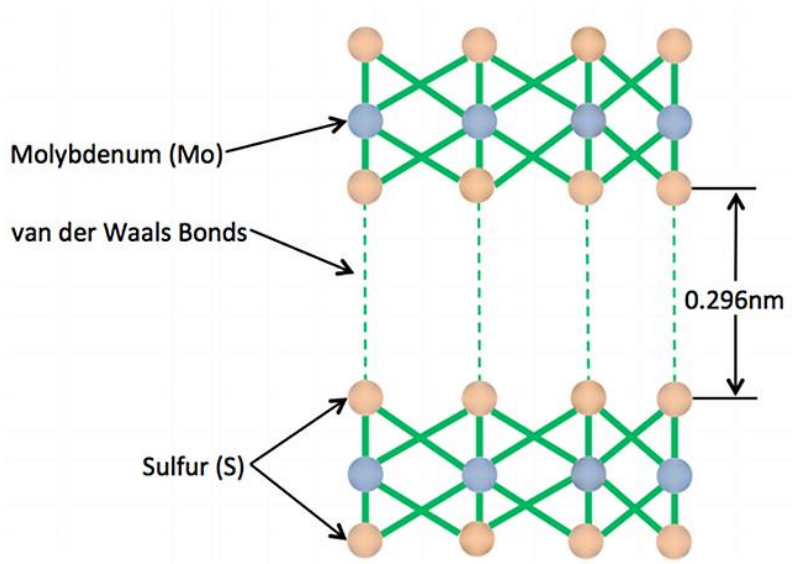

Figure 2.9: Illustration of the layered crystal molecular structure of MoS_2
Source: Reeves (2013)

2.2.2.8 Role of tribo-testing conditions

The tribological effectiveness of nanolubricants is likely to be very system-specific and as a result, a different performance is likely to be observed in different test conditions. M.R. Falvo and R. Superfine, have shown that the relative orientation of the interacting surfaces affects the frictional behavior for nanometer scale lubrication system (Falvo & Superfine, 2000).

To investigate the tribological performance of nanoparticles as additives in lubricating oils, various experimental studies were carried out using different geometric

configurations, which include four-ball, ball-on-flat, pin-on-disk, cylinder-on-flat, piston ring on cylinder liner and block on ring (Figure 2.10). Most of the studies were conducted at a normal operating temperature of an engine (i.e., 70–100 C) as mentioned in Table 2.12 and Table 2.13. Similarly, the values of other test parameters, such as normal load, sliding distance, sliding velocity, and test duration also varied. For EP characteristics and load carrying ability of nanolubricants, the majority of nanolubricants have been tested for four-ball test geometry using ASTM D2783 standard conditions (Abdullah et al., 2016; Chou et al., 2010; Viesca et al., 2011). Table 2.12 shows the summary of only four-ball test conditions by different researchers. For friction behavior and AW characteristics, most of the researchers have simulated the sliding contact between different counter bodies. Table 2.13 shows the test conditions for various type of geometric configurations other than the four-ball test geometry.

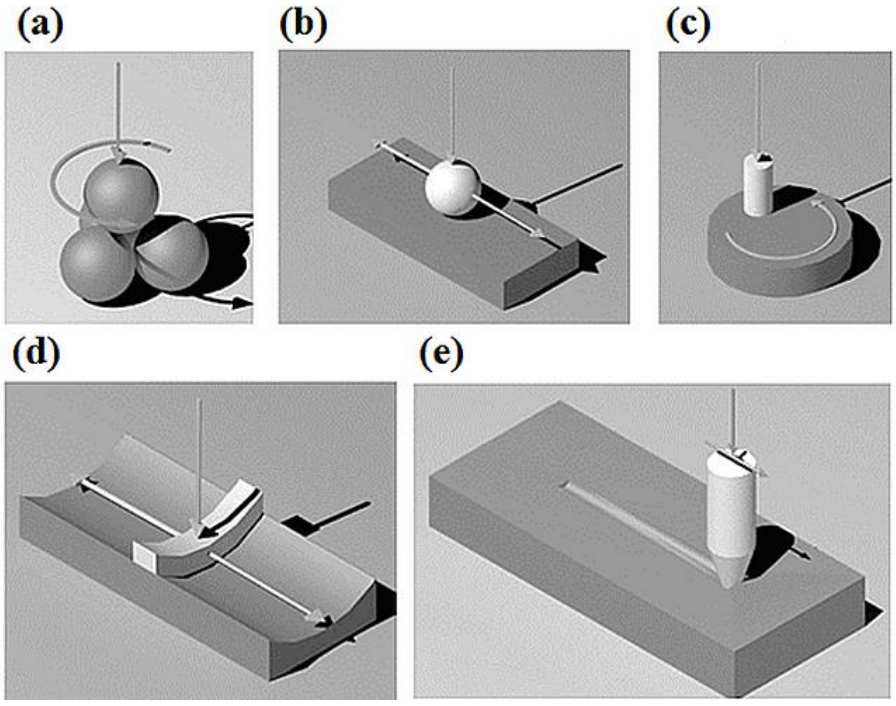

Figure 2.10: Commonly used tribo-testing geometric configurations (a) four-ball, (b) ball-on-flat, (c) pin-on-disk (d) piston ring-cylinder (e) pin -on-flat

Table 2.12: Literature summary of four-ball test conditions

Nano-particle	Oil	Test Duration (sec)	Temp (°C)	Normal Load (N)	Speed (rpm)	Output Parameters	Reference
ZnO	PAO6	3600	75	392	1200	WSD	(Battez et al., 2006)
		10/stage till weld	25	Varies/stage till weld	1470	ISL, LNSL, WL, LWI, WSD	(Battez et al., 2006)
	60SN base oil	1800	75	500	1000	WSD, Friction	(Ran et al., 2016)
CuO	Liquid paraffin	900	60-70	392	1200	WSD, Friction	(Asrul et al., 2013)
	PAO6	10 /stage till weld	25	Varies/stage till weld	1470	Friction, ISL, LNSL, WL, LWI, WSD	(Fernandez, Viesca, & Battez, 2008)
Cu	Liquid paraffin	1800	-	300	1450	WSD, Friction	(Zhang et al., 2015)
	PAO6	10 /stage till weld	25	Varies/stage till weld	1470	ISL, WL, LWI, WSD	(Viesca et al., 2011)
MoS_2	SAE 20W-40	3600	75	392	600, 1200	WL, WSD	(Thakur et al., 2016)
		10 /stage till weld	25	Varies/stage till weld	1470	ISL, WL, LWI, WSD	(Thakur et al., 2016)
Al_2O_3/SiO_2	20# machine oil	1800	75	147	1,450	Friction, WSD	(Jiao et al., 2011)
CuO, ZnO, ZrO_2	PAO6	10 /stage till weld	25	Varies/stage till weld	1470	ISL, LNSL, WL, LWI, WSD	(Battez et al., 2008)
PTFE	150N group II base oil	3600	75	392	1200	WL, WSD	(Mukesh et al., 2013)
ZrO_2/SiO_2	20# machine oil	1800	75	147	1,450	Friction, WSD	(W. Li et al., 2011)
Ni	PAO6	10 /stage till weld	25	Varies/stage till weld	1470	ISL, LNSL, WL, LWI, WSD	(Chou et al., 2010)
hBN	SAE 15W40	10 /stage till weld	25	Varies/stage till weld	1760	WSD	(Abdullah et al., 2016)
MoS_2/TiO_2	Liquid paraffin	1800	25	300	1450	WSD, Friction	(K. H. Hu et al., 2011)
Fe, Cu, Co	SAE10	3600	25	150	1420	WSD, Friction	(Padgurskas, Rukuiza, Prosyčevas, & Kreivaitis, 2013)
TiO2	palm TMP ester	300	25	392,784,1176, 1568	1200	WSD, Friction	(Zulkifli, Kalam, Masjuki, & Yunus, 2013)
$CaCO_3$	PAO+5 % palm TMP ester	3600	25	392	1200	WSD, Friction	(Zainal, Zulkifli, Yusoff, Masjuki, & Yunus, 2015)

Table 2.13: Literature summary of tribo-test conditions simulating sliding contact

Nano-particle	Oil	Contact Geometry	Test Time (sec)	Temp (°C)	Normal Load (N)	Contact Pressure (Gpa)	Speed	Reference
Cu	PAO6	Block-on-ring	3066	-	165	0.1	1 (m/s)	(Viesca et al., 2011)
MoS_2, BN	PAO10	Piston skirt- liner	10800	20,40,100	250	-	120 (rpm)	(Demas et al., 2012)
CuO	CMRO	Piston ring- liner	7200	60	80	0.005	600 (rpm)	(Arumugam & Sriram, 2014)
	Mineral oil	Pin-on-disk	400,600,1200	-	40,60	-	0.5, 1.0, 1.5 (m/s)	(Jatti & Singh, 2015)
	Coconut Oil	Pin-on-disc	178 to 714	-	49 to 98	0.001 to 0.002	1.4 to 5.6 (m/s)	(Thottackkad et al., 2012)
	Mineral, PAO, Sunflower, Soybean	Ball-on-disk	3600	50	10	-	1200 (rpm)	(Alves et al., 2013)
WS_2	SAE 30	Piston ring- liner	27000	70	160	0.01	2.29 (m/s)	(Gullac & Akalin, 2010)
	Paraffin oil	Pin-on-disk	24000	-	100–500	-	0.6 (m/s)	(L. Rapoport et al., 2003)
Pb	Paraffin oil	Pin-on-disk	5000	-	7	1.26	1 (m/s)	(Kolodziejczyk et al., 2007)
Cu, TiO_2, carbon horns	SAE40	Ball-on-flat	120 /step for 13 steps	25	-	0.6	0.001–1.8 (m/s)	(Zin et al., 2015)
CuO, ZnO, ZrO_2	PAO6	Block-on-ring	1533	-	165	0.1	2 (m/s)	(Battez et al., 2008)
Ni		Block-on-ring	1533	-	165	0.1	2 (m/s)	(Chou et al., 2010)
BN	SAE10W	Ball on disk	160	20	10	2.93	0.25 (m/s)	(Çelik et al., 2013)
Graphite	Vegetable based oil	Pin-on-disk	3600	24	2,10	-	100 (rpm)	(Su, Gong, & Chen, 2015)
Carbon Nano-onions, Graphite	PAO	Pin-on-flat	1000, 20000	25	2,5,10	0.83,1.12,1.42	0.25 (m/s)	(Joly-Pottuz et al., 2008)
MoS_2, SiO_2	EOT5# engine oil	Ball-on-flat	1800, 4500	25	1,3,5,8	0.223, 0.312,0.381, 0.446	0.08, 0.03 (m/s)	(Xie et al., 2015)
MoS_2	PAO4 + PAO 40	Ball-on-flat	144000 cycles	80	10	1.4	600 (rpm)	(Rabaso et al., 2014)
CuO, Al_2O_3	PAO8, SAE 75W-85)	Ball on disk	7200	50	200	-	3000 (rpm)	(Peña-Parás et al., 2015)

2.2.2.9 Lubrication mechanisms

The investigation of lubrication mechanisms is considered as a crucial parameter to completely understand the tribology of nanoparticles. However, defining the active mechanisms remain a subject of debate for many research studies related to nanoparticles based lubrication systems. A number of mechanisms have been proposed by researchers using the surface analysis techniques to explain the lubrication enhancement by the nanoparticle-suspended lubricating oil. These mechanisms include the ball bearing effect (Chiñas-Castillo & Spikes, 2003; L Rapoport et al., 2002; Y. Y. Wu et al., 2007), protective film formation (Ginzburg et al., 2002; Z. S. Hu et al., 2002; Xiaodong, Xun, Huaqiang, & Zhengshui, 2007), mending effect (G. Liu et al., 2004) and polishing effect (Tao, Jiazheng, & Kang, 1996). Sui et al. (2015), reported all these lubrication mechanisms for PAO enriched with amino functionalized hairy silica nanoparticles (Figure 2.11).

These mechanisms can be categorized into two main groups. The first is the direct effect of the nanoparticles that includes ball bearings effect and protective/tribofilm formation. The other is the secondary effect which contributes to surface enhancement by mending/repairing effect and polishing/smoothing effect. Table 2.14 shows the literature summary of majorly reported lubrication mechanisms for different nanoparticles/lubricating oils combinations.

For better understanding, the detail of potential lubrication mechanisms by the presence of nanoparticles, are further discussed below.

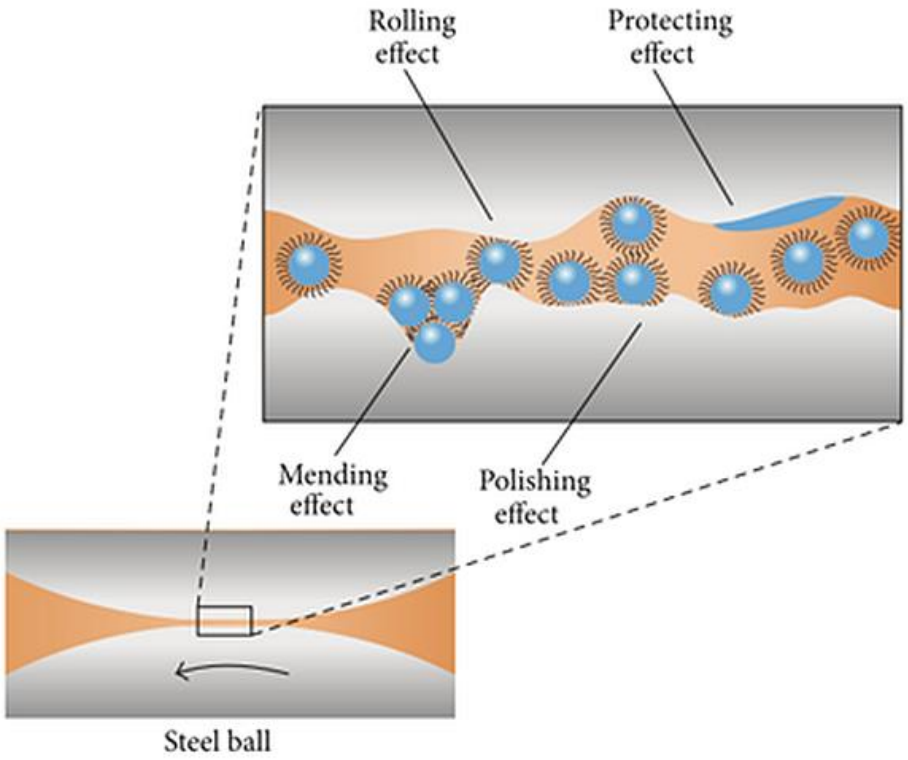

Figure 2.11: Schematic diagram of the lubrication mechanism of silica nanoparticle dispersed in PAO

Source: Sui et al. (2015)

(a) ***Ball bearing effect***

The spherical and quasi spherical nanoparticles are believed to function like tiny ball bearings which roll into the contact area. Nanoparticles with such shapes are believed to change the sliding friction to a mix of sliding and rolling friction. This lubrication mechanism is attributed to tribo-pair system having stable low-load conditions between the shearing surfaces to maintain the shape and rigidity of the nanoparticles. Figure 2.12 illustrates the ball bearing mechanism. This mechanism of surface protection has been reported by a number of researchers (Table 2.14).

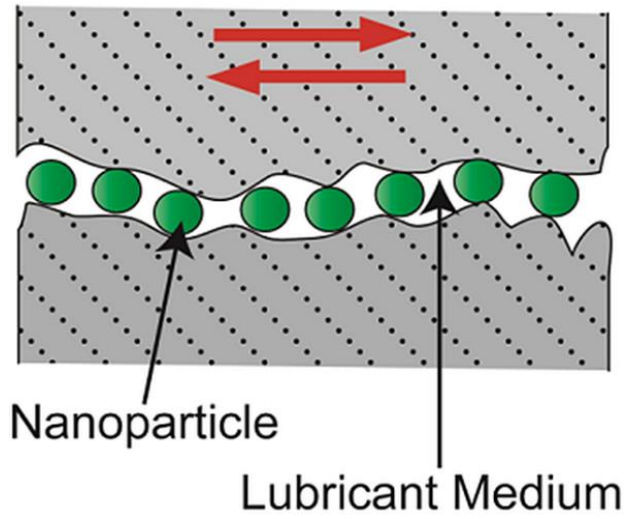

Figure 2.12: Illustration of ball bearing mechanism by nanoparticles based lubrication

Source: Kheireddin (2013)

(b) ***Protective film formation***

Protective film on the tested surfaces is also referred as tribofilm. Tribofilms and near-surface materials govern the tribological behaviors of interacting surfaces. This film formation is triggered by the reaction between the treated material and the additives under the provided environment or tribo-sintered (Chou et al., 2010; Viesca et al., 2011). There are many experimental studies that have reported tribofilm formation mechanism for superior lubrication (Table 2.14). Verma et al. (2008), reported the formation a durable tribofilm with Mo, S, and P elements, reducing the chances of severe wear, friction, and seizure for nanoMoS_2 based lubricant. Some other studies have shown friction as well as wear reduction by this mechanism of protective film formation (Demas et al., 2012; L. Rapoport et al., 2003). However, in an experimental study using CeF_3 based nanolubricant, poor anti-wear behavior has been observed due to corrosion from F-surface atoms (Sunqing, Junxiu, & Guoxu, 1999). Figure 2.13 shows the schematics of tribofilm formation, which not only provides surface protection but also helps to protect the material from crack propagation by reducing friction between asperities. The formation of this tribofilm can be verified by using analysis techniques like scanning

electron microscopy/energy dispersive spectrometer (SEM/EDS), Raman spectroscopy, and X-ray photoelectron spectroscopy (XPS), as given in Table 2.14.

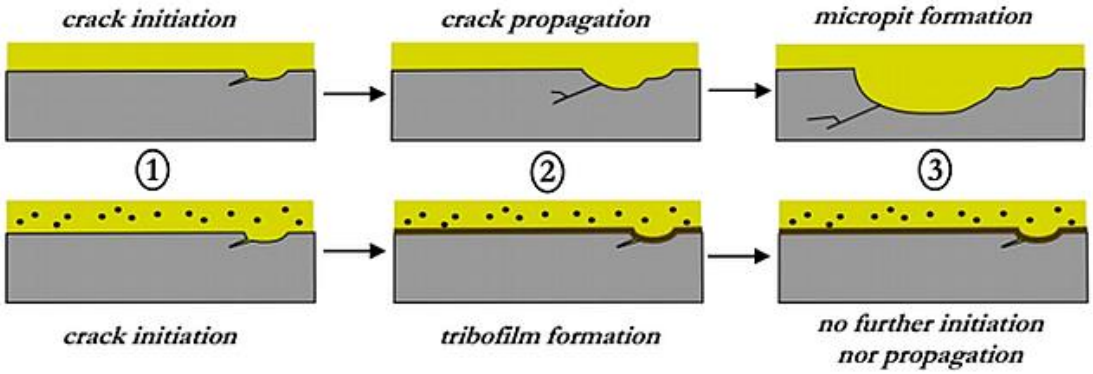

Figure 2.13: Illustration of lubrication by base oil alone (top) and tribofilm formation and surface protection by nanoparticles (bottom)
Source: Rabaso (2014)

(c) ***Mending effect***

The mending effect or self-repairing effect is characterized by nanoparticles deposition on the interacting surfaces and compensation for the loss of mass. During this phenomenon, the nanoparticles deposit on wear surface to reduce abrasion (Song et al., 2012). Nanoparticles in the lubricating oil have the ability to fill scars and grooves of the friction surface. Figure 2.14 shows the schematics of the friction surface where scars and grooves have been filled up with nanoparticles. A majority of studies reporting the mending effect, have used EDX analysis to confirm the deposition of nanoparticles on the rubbing surface.

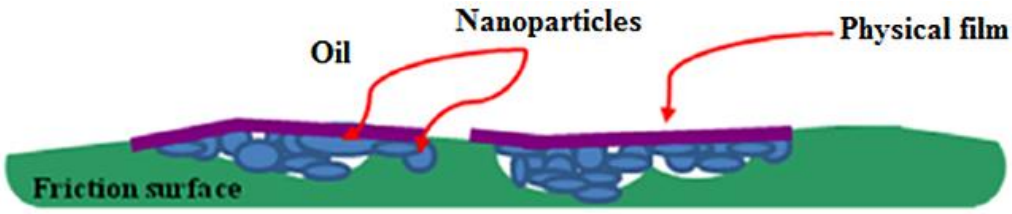

Figure 2.14: Schematics of nanoparticles filled up in scars and grooves on friction surface

Source: Choi et al. (2009)

(d) ***Polishing effect***

The polishing effect, also termed as smoothing effect, is believed to be reported when the roughness of the lubricating surface is reduced by nanoparticle-assisted abrasion. In the tribological contacts, the nanoparticles may fill-up the gaps of the rough asperities, which may act as reservoirs of solid lubricants (nanoparticles) within the contact, as shown schematically in Figure 2.15 (Kalin, Kogovšek, & Remškar, 2012). This process of filling up rough valleys is referred as the smoothing out process. This "artificial smoothing" or polishing mechanism lead to improved tribological performance mainly due to the reduced surface roughness (Kheireddin, 2013). To characterize this effect, the surface roughness analysis tools are found to be helpful as they can provide the effect of nanoparticles on surface roughness.

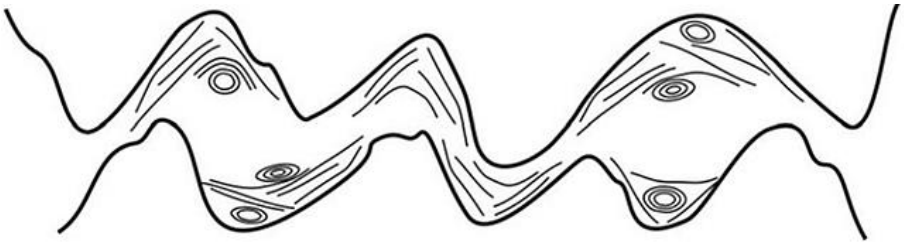

Figure 2.15: Illustration of smoothing/polishing effect by filling up of rough valleys of rubbing surfaces

Source: Kalin et al. (2012)

2.2.2.10 Investigation of lubrication mechanism

To investigate the lubrication mechanisms for lubricating oils enriched with nanoparticles, a number of surfaces characterization techniques have been used by researchers. The analysis techniques include SEM/EDS, AFM, X-ray diffraction (XRD), XPS, and Raman Spectroscopy (Alves et al., 2013; Chou et al., 2010; Demas et al., 2012; Ettefaghi, Ahmadi, Rashidi, & Mohtasebi, 2013; Ginzburg et al., 2002; Greenberg, Halperin, Etsion, & Tenne, 2004; K. H. Hu et al., 2011; Z. S. Hu et al., 2002; Kolodziejczyk et al., 2007; C.-G. Lee et al., 2009; J. Lee et al., 2009; Gang Liu, Li, Lu, & Fan, 2005; G. Liu et al., 2004; Padgurskas et al., 2013; Peng, Kang, et al., 2010; Song et al., 2012; Thakur et al., 2016; Viesca et al., 2011; Y. Y. Wu et al., 2007; Xiaodong et al., 2007).

Table 2.14 shows the summary of various studies which have used surfaces analysis technique and reported lubrication mechanism. However, it has been observed that due to the existence of various lubrication mechanisms by nanolubricants, these surface analysis tools are not enough to distinguish the role of nanoparticles amongst these mechanisms. There are various studies that have reported multiple mechanisms for nanolubricants; an example has been given in Figure 2.11.

This situation becomes more complex when it has to draw a line between direct effect (e.g., ball bearing/tribofilm) of nanoparticles and the surface enhancement effects (e.g., mending/polishing) (K. Lee, Y. Hwang, S. Cheong, Y. Choi, et al., 2009).

Table 2.14: Summary of reported effects of nanoparticles on tribological properties, lubrication mechanisms and rubbing surfaces characterization

Nano-Particle	Lubricant	Additives Role	Mechanism	Surface Analysis Technique	Reference
Cu	PAO6	AW, EP	Tribosinterization	SEM, EDS	(Viesca et al., 2011)
Ni		FM, AW, EP	Tribosinterization	SEM, EDS	(Chou et al., 2010)
ZnO, ZrO_2, CuO		AW, EP	Deposition	SEM, EDS	(Battez et al., 2008)
Graphite	Supergear EP220	FM, AW	Polishing	SEM, AFM	(C.-G. Lee et al., 2009)
Fullerene, Carbon nanoballs	SAE-20W50	AW	Mending	SEM	(Ettefaghi et al., 2013)
Al/Sn	SE15W/40	AW, EP	Mending	SEM, EDS	(Gang Liu et al., 2005)
Pb	Liquid paraffin	FM, AW	Ball bearing Tribofilm	SEM, EDS	(Kolodziejczyk et al., 2007)
Fe, Cu, Co	SAE10	FM, AW	Tribofilm	SEM, EDS	(Padgurskas et al., 2013)
Al	Liquid paraffin	FM, AW	Tribofilm	SEM, EDS	(Peng, Kang, et al., 2010)
CuO	SAE30	FM, AW	Ball Bearing, Mending	SEM, EDS	(Y. Y. Wu et al., 2007)
	Mineral oil	FM, AW	Deposition, Polishing	SEM, EDS	(Jatti & Singh, 2015)
	Liquid paraffin	FM, AW	Ball bearing	-	(Asrul et al., 2013)
BN, MoS_2	PAO10	FM, AW	Tribofilm	Raman spectroscopy	(Demas et al., 2012)
MoS_2	SAE 20W-40	FM, AW, EP	Mending	SEM, EDS	(Thakur et al., 2016)
	PAO	FM, AW, EP	Tribofilm	SEM, EDS	(Nallasamy et al., 2014)
	Liquid paraffin	FM, AW, EP	Tribofilm	SEM, EDS	(Verma et al., 2008)
MoS_2, TiO_2, MoS_2/TiO_2	Liquid paraffin	FM, AW	Mending, Tribofilm	XPS	(K. H. Hu et al., 2011)
ZnO	60SN base oil	FM, AW	Mending	SEM	(Ran et al., 2016)
hBN	SAE 15W40	FM, AW	Ball bearing, Polishing	SEM	(Abdullah, Abdollah, Amiruddin, Tamaldin, & Nuri, 2014)
Al_2O_3	SAE 15W40	FM, AW	Ploughing effect	SEM	(Abdullah et al., 2014)
ZnO, CuO	Mineral oil	FM, AW	Deposition, Tribofilm	SEM, EDS	(Alves et al., 2013)
	PAO	FM, AW	Deposition, Tribofilm	SEM, EDS	(Alves et al., 2013)
	Sunflower oil	FM, AW	Tribofilm	SEM, EDS	(Alves et al., 2013)
	Soybean oil	FM, AW	Tribofilm	SEM, EDS	(Alves et al., 2013)
TiO_2	10W-30	FM, AW	Ball bearing, Deposition	-	(Laad & Jatti, 2016)
$ZnAl_2O_4$	-	FM, AW	Mending	SEM, EDS	(Song et al., 2012)

2.3 IC Engine Lubrication

The reciprocating IC engine as shown in Figure 2.16 is considered the primary means of propulsion, whether that be for ground or sea transport. Due to its reliability, performance, and versatility, a huge number of reciprocating IC engines is use in industry and transport. However, thermal and mechanical efficiencies of IC engines are relatively low, with much of the energy wasted as heat loss and friction. While considering the frictional losses, worldwide, one passenger car uses on average of 340 liters of fuel per year, which would corresponds to an average driving distance of 13,000 km/year (Holmberg, Andersson, & Erdemir, 2012). To minimize friction and wear losses, with a minimum hazardous effect on the environment, the modern engine tribology demands effective lubrication of all moving engine components with less hazardous lubricant formulations. As worldwide a huge numbers of reciprocating IC engines are in operation, even the small improvement in engine efficiency, emissions and reliability can have a significant effect on the global fuel economy and the environment in a long-term. Concerning energy consumption within the IC engine, 48% of the energy consumption developed in an engine is due to frictional losses (Tung & McMillan, 2004). The decrease in the amount of energy wasted from the fuel as a result of frictional losses can make substantial reductions in fuel consumption. For example, for the case of a medium sized passenger car during an urban cycle, a reduction of 10% in mechanical losses would lessen the fuel consumption by 1.5% (Priest & Taylor, 2000). Mechanical losses comprise approximately 15% of the energy lost from the fuel, 40-60% of which is thought to be due to the action of the piston assembly (Taylor & Coy, 2000) (Nakada, 1994) (Smith, Priest, Taylor, Price, & Cantley, 2005). Figure 2.17 shows the fuel energy losses distribution in a typical IC engine.

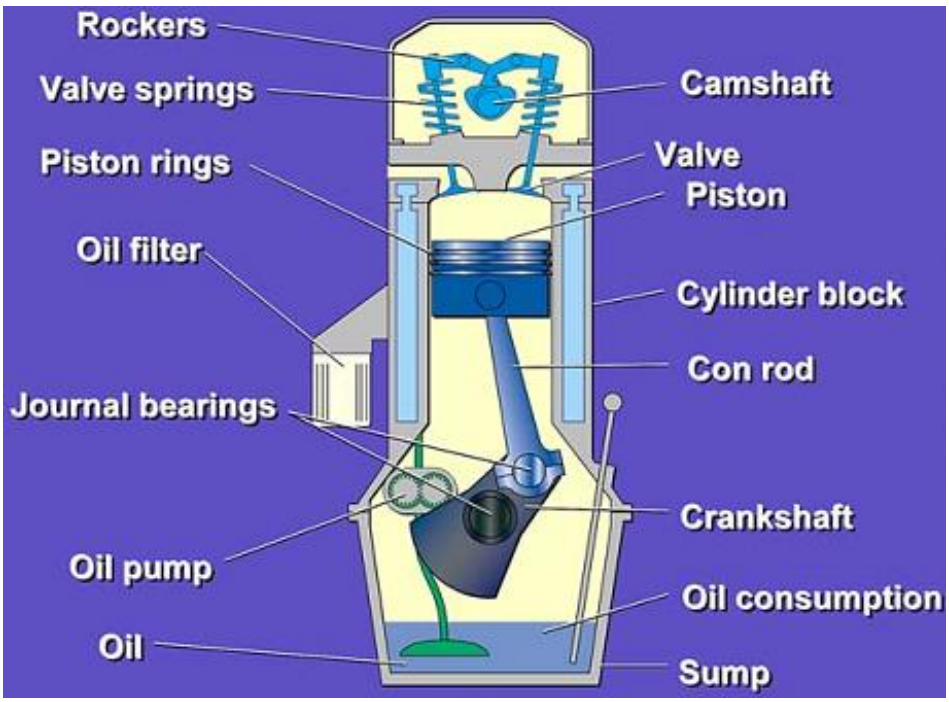

Figure 2.16: Main components in a typical IC engine
Source: Tung and McMillan (2004)

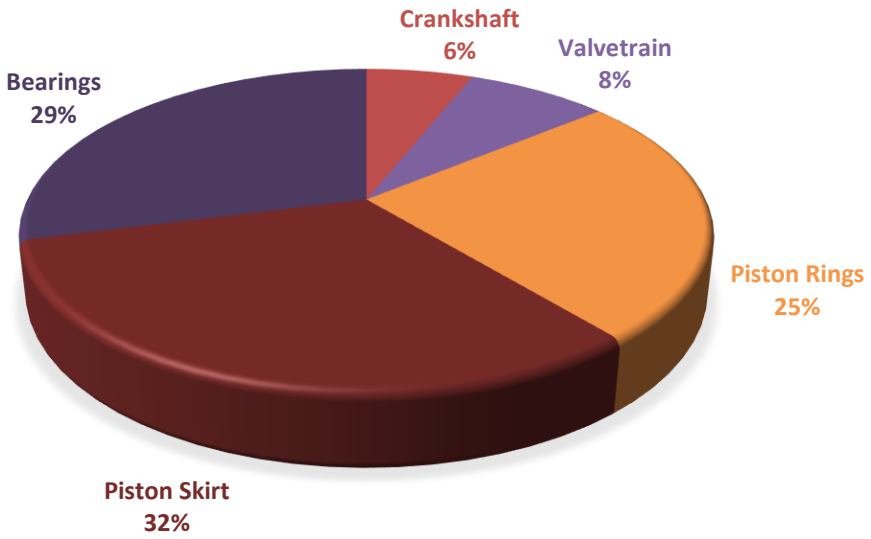

Figure 2.17: Fuel energy losses distribution in a typical IC engine
Source: Notay (2013)

2.3.1 Engine Piston Assembly

Engine piston assembly is considered as the heart of IC engines, establishing a link to transform the fuel combustion energy into useful kinetic energy. It is exposed to high combustion temperatures and repeated loading, presenting a need for it to resist thermal shock and cyclic fatigue. As a result, the piston assembly operates in one of the most arduous environments found in any machine. The combustion process results in extremely high pressure gas which forces the piston's motion. This high-pressure gas acts behind the piston rings forcing them to thrust against the cylinder liner which restricts their radial expansion. Here a thin film of lubricant exists to reduce the friction and wear between the piston ring–cylinder liner conjunctions, thereby ensuring smooth running and satisfactory service life of these engine parts.

Previously many experimental and theoretical studies have reported tribological performance of lubricants on the piston ring–cylinder liner conjunction (Arumugam & Sriram, 2012a; Avan, Spencer, Dwyer-Joyce, Almqvist, & Larsson, 2013; Çakir & Akçay, 2014; Cesur, Ayhan, Parlak, Savaş, & Aydin; De Silva, Priest, Lee, Coy, & Taylor, 2011; Johansson, Nilsson, Ohlsson, & Rosén, 2011; Lee et al., 2006; Shayler, Leong, Pegg, & Murphy, 2009; Truhan, Qu, & Blau, 2005b; Usman, Cheema, & Park, 2015; Y. F. Xu et al., 2013).

2.3.1.1 Piston ring–cylinder lubrication

Piston rings for current IC engines have to ensure the sealing function for linear motion that operates under demanding thermal and chemical conditions. Piston rings, which serve as labyrinth seal, attain this function by closely conforming to their grooves in the piston against the cylinder wall (Figure 2.18). Of the oil in the piston ring pack, only a small oil flows to the top ring zone, which is in close proximity to the combustion chamber. Thus, low oil supply and tough engine conditions require effective piston ring-

cylinder lubrication during complete oil drain interval. Figure 2.19 shows the transition of lubrications regimes for piston rings as well as other engine components.

2.3.1.2 Experimental investigation of piston ring–cylinder lubrication

Piston ring–cylinder lubrication has been studied by using different experimental setups include laboratory simulations and motored as well as firing engines (Daniels & Braun, 2006; Kohashi, Kimura, Murakami, & Drouvin, 2013; Richardson, 2000; Shayler et al., 2009). Previously, researchers have found that it is difficult to obtain any meaningful and statistically significant correlations between the testing parameters and tribological performance during actual engine testing (Morina, Lee, Priest, & Neville, 2011). In this regard, better accuracy was achieved by laboratory controlled tribo-testing at very low costs as compared to complexity and high costs involved in modifications and instrumentation in actual engines. Due to the availability of controlled testing conditions and possibility of simulating a variety of contact geometries, majority of reported experimental research studies have carried out tribo-testing for piston ring–cylinder contact. Table 2.15 shows summary of experimental studies which simulated the piston ring–cylinder interaction in controlled tribo-testing environment.

In various such tribo-testing, the condition of oil samples as well as test conditions were different from actual engine running conditions (Arumugam & Sriram, 2012a, 2014; Avan et al., 2013; Blau, 2002; Çakir & Akçay, 2014; Johansson et al., 2011). To study the piston ring tribology using realistic lubricant samples, the engine-aged oil samples had been collected and investigated in laboratory testing for piston ring-cylinder contacts by Truhan, Qu, and Blau (2005a) and Truhan et al. (2005b). Thus, the engine oil

performance in new as well as engine-aged conditions can be evaluated using the reciprocating bench tribometer tests.

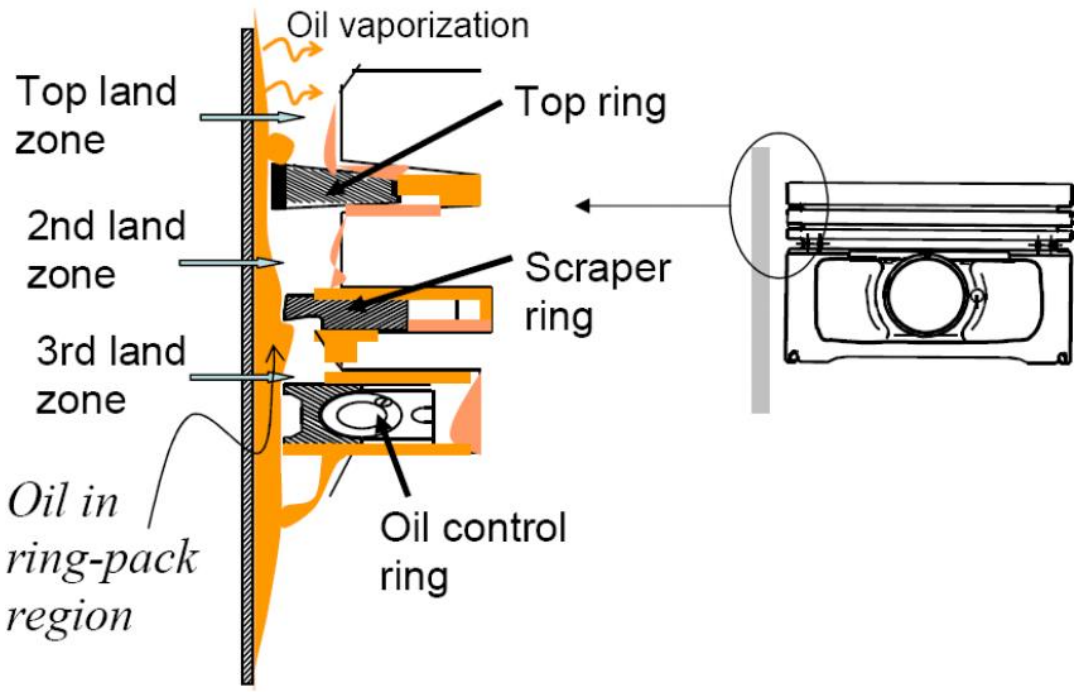

Figure 2.18: A schematic of the piston ring pack geometry in a typical diesel engine
Source: Wong, Thomas, and Watson (2007)

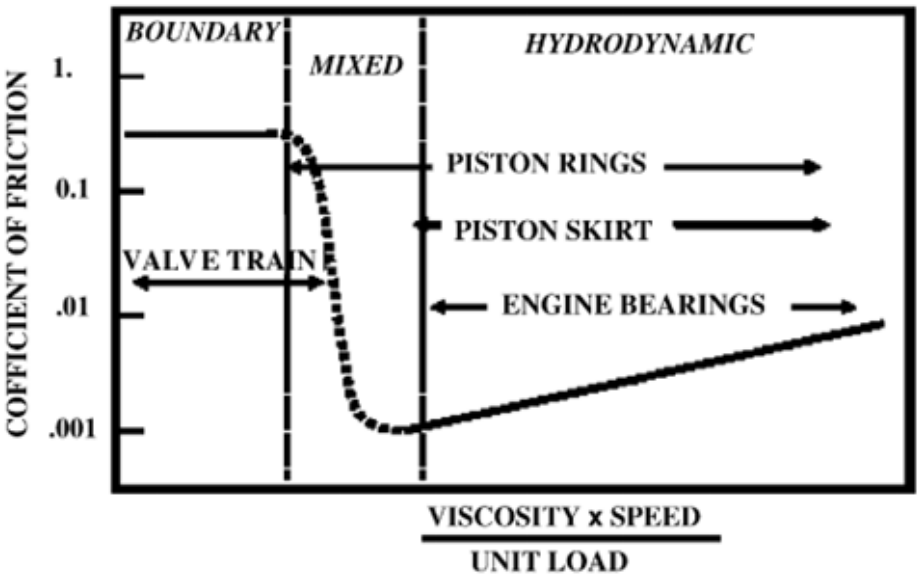

Figure 2.19: Lubrication regimes for engine components
Source: Tung and McMillan (2004)

Table 2.15: Summary of studies using tribo-testing for piston ring–cylinder liner contact

Equipment	Relevant Output Parameters	Lubricants	Temperature ^{o}C	Lubricant Condition	Reference
Sliding Tribometer	Friction	SAE 30, SAE 30 + Nanoadditives	70	New	(Gullac & Akalin, 2010)
Sliding Tribometer	Friction, Wear Rate, Viscosity	SAE 15W40	100	New and Used	(Truhan et al., 2005a)
Sliding Tribometer	Friction, Wear Rate, Viscosity	SAE 15W40, Aviation fuel, Mineral Oil	100	New and Used	(Truhan et al., 2005b)
Sliding Tribometer	Friction, Viscosity, Film Thickness	SAE 5W-30 with ethanol and water	25, 40, 70 and 110	New	(De Silva et al., 2011)
Pin on disk Tribometer	Wear, Friction	SAE 20W40 Biodiesel+ SAE 20W40 Bio-lubricant	120	New and Used	(Arumugam & Sriram, 2012a)
Sliding Tribometer	Wear	Fully formulated oil	100	New	(Morina et al., 2011)
Sliding Tribometer	Wear, Friction	SAE 20W40 Biodiesel+ SAE 20W40 Bio-lubricant	60	New	(Arumugam & Sriram, 2012b)
Sliding Tribometer	Friction, Wear	Bio-oil, Diesel and Emulsified bio oil	Room Temperature	New	(Y. F. Xu et al., 2013)
Sliding Tribometer	Wear, Friction	Nano Bio-lubricant	60	New	(Arumugam & Sriram, 2014)
Sliding Tribometer	Friction	SAE 30 and SAE 30 + 5% soluble MoS_2	-	New	(Çakir & Akçay, 2014)
Pin on Disk	Wear, Friction	SAE 20W50 with nanoparticles	20-25	New	(Ettefaghi et al., 2013)

2.3.2 Lubricant Degradation in Diesel Engine

For compression ignition engine, the quality and effectiveness of lubricants is degraded by contamination and thermal (oxidative) degradation. As it degrades, the lubricant loses its performance, until it must finally be replaced to maintain engine performance and prevent damage to components (Watson, 2010). The problem of short useful lubricant life is serious in such engines due to oil degradation by contaminations such as soot, unburnt fuel, metal particles, and acid by-products of fuels. Irreversible changes in viscosity are also linked to the additives degradation, soot content, oxidation products, fuel residue, and base oil evaporation. These undesirable changes in lubricant viscosity and formulation results in ineffective engine lubrication, consequently increase the engine parts wear and friction. The quality of lubricant affects the wear and friction of engine components as well as the engine performance and engine exhaust emissions (Masjuki et al., 1999). Various factors affected by oil viscosity during engine use are summarized in Table 2.16. Typically, formulation changes and oil aging over a few hours of engine operation gave rise to friction.

The quality of engine oil lubricant not only affects the interacting engine parts but also reduce the drain intervals. Unused diesel engine oils contain active additives to protect the engine moving parts but due to severe engine operating condition, additives in the lubricant depletes over the time and it gets contaminated by combustion particles, soot content and wear particles.

Due to acidic contaminations, solid particles cause abrasive wear and corrosion and tribochemical wear (P. Andersson, J. Tamminen, & Sandstrom, 2002). The contaminations of solid particles of sufficient size in engine oil results in abrasive wear of piston rings as well as cylinder liner (Truhan et al., 2005a). Researchers have also reported scratches on cylinder liner as well as undesirable polishing on it due to small

abrasive particles in used oils (Godfrey, 1987) (Jiang & Wang, 1998). It is evident by previous research that not only the physicochemical properties but also the friction and wear characteristics of engine-aged oils are different from new engine oil (Truhan et al., 2005a, 2005b). Despite the fact that the use of engine-aged oil is more realistic in laboratory simulation of the piston ring–cylinder liner interactions, little research has been done in this lubricating environment (Truhan et al., 2005a, 2005b).

Table 2.16: Parameters affecting the lubricant viscosity

Viscosity change	Reversible	Irreversible (oil aging)
Increase	Pressure	Oxidation products Soot formation Base oil evaporation
Decrease	Temperature Shear	VI Improver degradation Fuel dilution

Source: Bukovnik, Dörr, Čaika, Bartz, and Loibnegger (2006)

2.3.2.1 Effect of fuel blends

Amidst concerns over energy security, environmental legislation, and increasing costs of fossil fuels, many countries are taking action to promote the use of biodiesel (Zdrodowski et al., 2010). Around the world, 419.2 thousand barrels of biodiesel are being consumed each day. The two largest biodiesel consumers are the European Union and the United States, accounting for 218.4 and 60 thousand barrels per day, respectively (EIA).

With the implementation of biodiesel mandate, the effect of fuel, on lubricating oil condition, become significant for higher blends of biodiesels. Biodiesel is composed of fatty acid methyl esters (FAME), synthesized by the transesterification of crude vegetable oils and animal oil/fats. Common biodiesel feedstocks include corn and soy oil (US), rapeseed oil (Europe), and palm and jatropha oil (Southeast Asia). It is worth mentioning

here that palm biodiesel blending has been implemented in Malaysia several years ago, and the blending ratio is continuously increasing with a target of B20 blend in 2018.

During normal engine operations, the engine oil is exposed to combustion gases and carbon based acids. In such situations, the oxidation of base oil results in accumulation of the weak organic acids in the engine oil. The problem becomes more intense for biodiesel operated engines where the researchers have reported increased dilution and polymerization of engine oil which in turn requires more frequent oil changes (Devlin, Passut, Campbell, & Jao, 2008; Fang, Whitacre, Yamaguchi, & Boons, 2007). The esters available in biodiesels are hydrolyzed to increase the concentrations of weak acids in the lubricants (Devlin et al., 2008; Fang et al., 2007; Sugiyama, Maeda, & Nagai, 2007). The related problems include high carbon deposits, piston oil ring sticking, and increased engine oil viscosity (Petraru & Novotny-Farkas, 2012; Rakopoulos, Antonopoulos, Rakopoulos, Hountalas, & Giakoumis, 2006).

2.3.2.2 Role of additive technology

Other than thermo-oxidative stability and tribological enhancement, an excessive alkaline reserve is required for use of bio-based lubricant in diesel engines. Like synthetic base oils, bio-based base stocks have low alkaline reserve therefore acidity control is required for their use in long hour diesel engine operations. In conventional engine lubricant, over based detergents are used to neutralize the acidic contamination. Such over based detergents reported to work well in bio-based lubricants but their use result in toxic compounds (R. K. Singh, Kukrety, Thakre, Atray, & Ray, 2015). These over based detergents are major source of Sulfur and ash in a typical conventional diesel engine lubricant as shown in Table 2.17.

Other than conventional engine oil additives, by pass filtration and slow additive release filters are two filter technologies currently being used to control acidity and improve oil drain intervals (Watson, Wong, Brownawell, & Lockledge, 2009). In by pass filtration technique the contamination particles are removed mechanically, leaving the acidic contaminants untrapped. On the other hand, control over release rate is the main shortcoming in the filter technology which is based upon slow release of additives like detergents, dispersants and antioxidants etc. The accumulation of these additives increases ash content in lubricant.

Table 2.17: Sources of Sulfur and ash in conventional diesel engine oil

Component	Sulfur (wt%)	Ash Contribution (wt% of oil)
Detergent	0.05-0.25	0.6-1.3
Zinc dithiophosphate (Antiwear)	0.20-0.25	0.15
Other (Antioxidants, viscosity improvers, friction modifiers)	0.0-0.10	0.0-1.5
Total	0.25-0.60	0.75-1.6
Typical Group II base oil	0.0001-0.003	0.0

Source: Watson (2010)

(a) ***Strong base filter technology***

For additive requirements of a zero-detergent lubricant, the effectiveness of novel approach of chemical modification of oil filter element has been highlighted by the various earlier researchers (Lockledge & Brownawell, 2013b; Rohrbach, Jones, Unger, & Bause, 2007; Watson, 2010; Watson, Wong, Brownawell, & Lockledge, 2009; Watson, Wong, Brownawell, Lockledge, & Harold, 2009). This approach is unique compared to conventional additive technology because it has the ability to induce a chemical change in the lubricant without releasing compounds into the oil. The technique was found to be simple to adopt. The major benefits include control of oil acidity, low variation in oil viscosity, total base number (TBN) retention and reduced engine wear and corrosion.

A strong base filter can be used in combination with a lubricant containing no detergent additives to minimize the detrimental effects of ash. The technique found to be simple to adopt as well as economically suitable for various engines, fuels and lubricants. The related studies pointed out several benefits of strong base filter technique for diesel engines fueled with Ultra Low Sulfur Diesel (ULSD) (Watson, Wong, Brownawell, & Lockledge, 2009; Watson, Wong, Brownawell, Lockledge, et al., 2009). The major benefits include improvement in oil degradation rate, control of oil acidity, oil viscosity, total base number (TBN) retention and reduced engine wear and corrosion.

(b) *Oil conditioning mechanism*

Strong base filter works by cyclic regeneration of the weak base. It displaces the weak base from combustion acids-weak base complex. The combustion acid-weak base complex forms at piston ring zone by interaction between combustion acids and lubricant detergent additives and travels within the lubricant. While passing through the strong base filter, the weak base is displaced from combustion acid-weak base complex resulting in formation of combustion acid-strong base complex. This displacement happens via ion exchange as NaOH disposed on strong base filter exchanges with weak base in the combustion acid-weak base complex.

It results in regeneration and recycling of weak base in lubricant to travel back and neutralize additional acid in piston ring zone. This cyclic process helps in extending the alkaline reserve provided by over-based detergents which are most often used in fully formulated diesel lubricants. The proposed mechanism for action of strong base oil filter has been discussed previously by different researchers (Brownawell, Thaler, Bannister, & Ladwig, 1990; Lockledge & Brownawell, 2013a) and is illustrated in Figure 2.20.

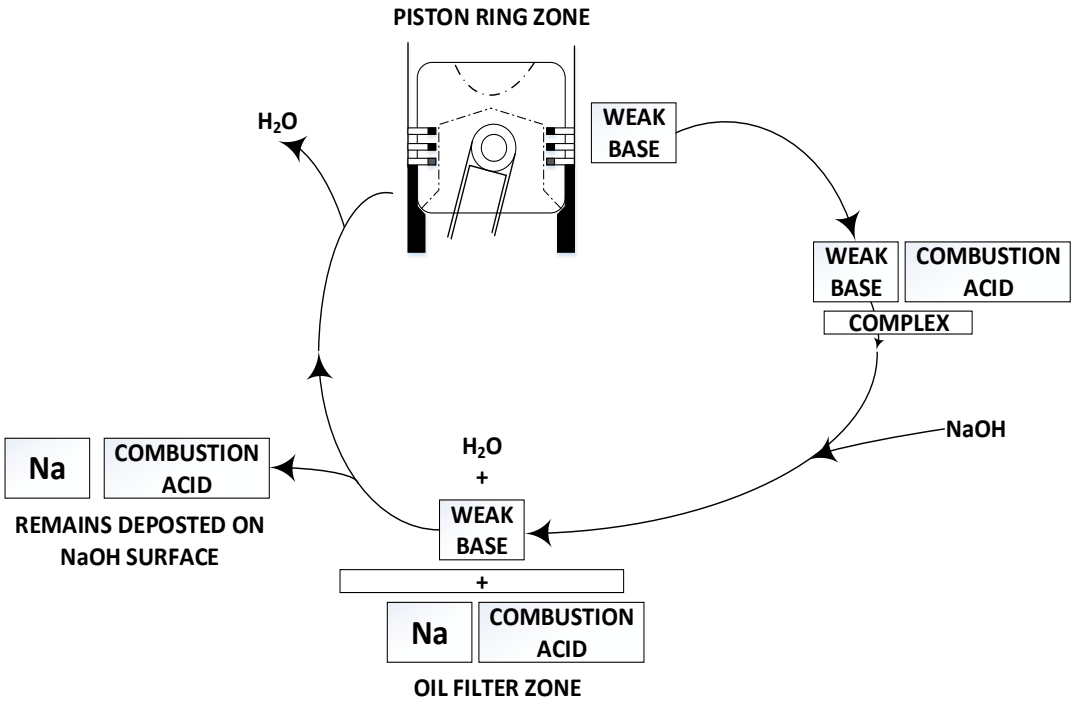

Figure 2.20: Mechanism for lubricant conditioining by strong base filter

2.4 Summary

The literature review highlights the studies showing the potential of chemically modified vegetable oils for various applications in general and specifically the use of TMP esters for IC engine lubrication. However, it has been found that, like conventional base oils, bio-based base stocks alone cannot give the high lubrication performance for IC engine tough lubrication environment. In this regard, the interesting friction and wear protection behavior of nanoparticles make them suitable candidates as additives to improve the tribological performance.

For piston ring–cylinder liner interaction, a number of research studies showed improved tribological behavior of conventional base oils and fully formulated traditional lubricants, when added with a variety of nanoparticles. Though nanolubrication developed by the conventional base oils with nanoparticles, offered a solution to many problems associated with traditional lubricants that contain Sulfur and Phosphorus,

significant improvement in terms of environmental conformity can be achieved by replacing the conventional base oils by bio-based base stocks. As it has been discussed previously that palm TMP ester has such characteristics to be used as base stock for engine lubricant formulation, the environmental hazards can be reduced by replacing the traditional base oils which comprises of typically 80% of lubricant formulation.

In this regard, the dispersion stability and tribological compatibility of variety of nanoparticles as additives to bio-based base stocks, is required to be investigated for IC engines application. Figure 2.21 shows the research gap for development of suitable lubricant to achieve the high environmental suitability as well as adequate lubrication performance.

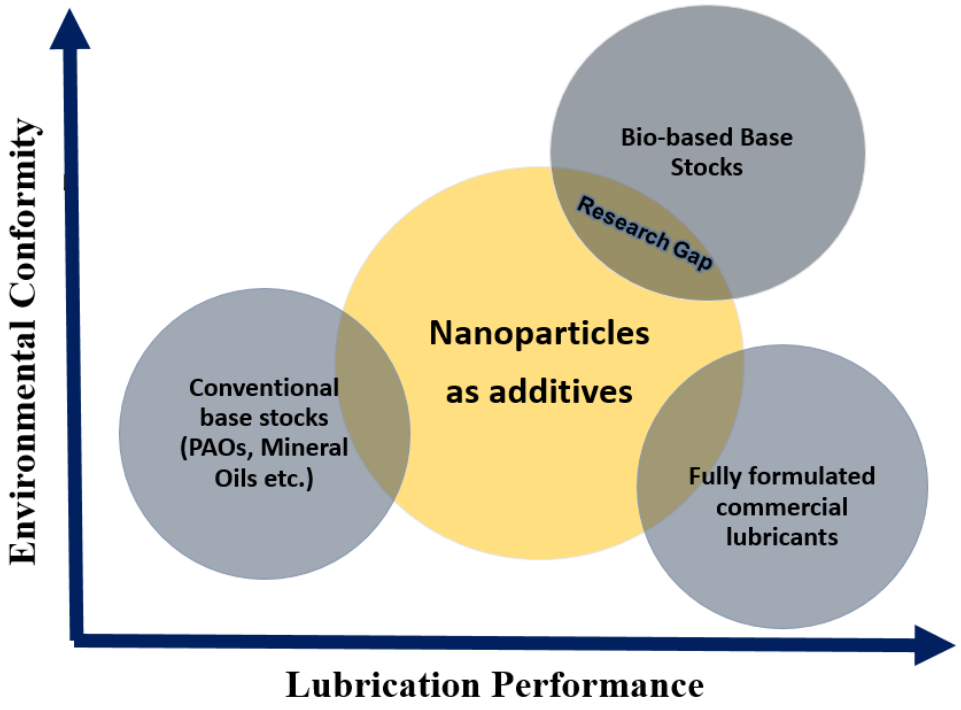

Figure 2.21: Potential research gap of IC engine bio-based nanolubrication

CHAPTER 3: RESEARCH METHODOLOGY

A step by step and extensive research methodology has been adopted for effective bio-based lubrication of piston ring–cylinder liner interaction. This endeavor began by investigating palm TMP ester as bio-based lubricant to gain an understanding of the tribological performance for piston ring–cylinder liner interaction in the absence of any additive. It was followed by the investigation of suitable type and concentration of nanoparticles for stable and tribologically improved suspensions. Oleic acid (OA) was used as anionic surfactant to improve the dispersion stability. Ultrasonic dispersion technique was adopted for homogenous and stable suspensions. UV-vis spectroscopy was carried out to analyze the dispersion stability of suspensions. Friction and wear characteristics of lubricant samples were investigated by simulating the engine piston ring–cylinder contact in laboratory controlled conditions.

In the next phase of experimentation, engine-aged sump oil samples were collected during long hours testing of single cylinder diesel engine. During this phase of research study, chemically active oil filter technology was adopted to control the bio-based lubricant acidity and additive requirements for bio-based nanolubricant. In the last, new as well as engine-aged oil samples were analyzed via standard in-situ lubricant diagnostics and tribological analysis and compared with conventional engine lubricant samples.

To provide an overview of this research study, the sequential details of major research activities are listed in the flow chart as shown in Figure 3.1.

.

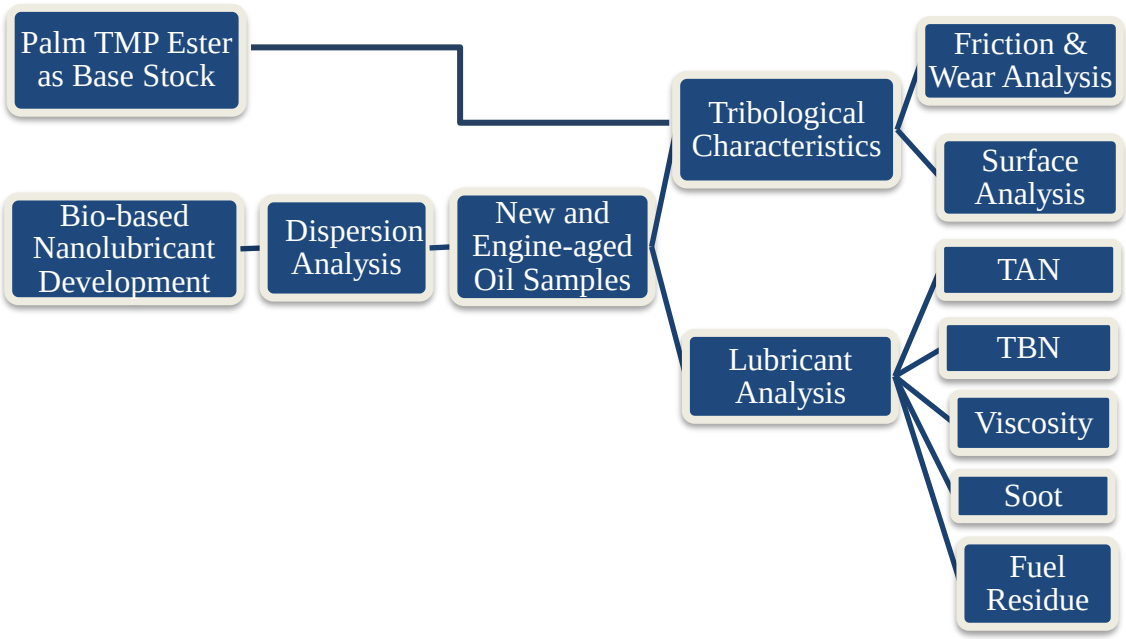

Figure 3.1: Flowchart of research activities

3.1 Palm TMP Ester as Bio-based Base Stock

Palm TMP ester mentioned as, Oil A, in this thesis, was used as bio-based base stock to develop bio-based lubricant. The friction behavior and antiwear characteristics of palm TMP ester were investigated using tribo-testing for piston ring on cylinder contact as well as four ball EP tests. The details for tribo-test setups and testing conditions have been mentioned in Section 3.4 of this chapter. The worn surfaces were then analyzed by surface characterization tools. The details about surface analysis tools and related procedures are discussed in Section 3.5 of this chapter.

3.1.1 Palm TMP Ester

The development of palm TMP ester was carried out at Institute of Advanced Technology, University Putra Malaysia. For the desired physicochemical characteristics, Palm TMP ester was synthesized as per the materials and procedure adopted by Zulkifli (2014). The details of chemical modifications and related procedures are discussed below.

3.1.1.1 Procedure for Development of Palm TMP Ester

In the synthesis, palm-based methyl esters (POME) were used as starting materials, and TMP was used as a polyol. Palm TMP ester is produced when the transesterification reaction replaces an ester group from POME (i.e., RCOO–) with an –OH group from TMP. Given that three –OH groups exist in TMP, the process results in an intermediate formation of monoesters, diesters, and triesters. Methanol, a by-product, was removed to ensure that the reaction was completed.

Transesterification reaction was induced in a 500-mL three-necked flask equipped with a reflux condenser, a thermometer, and a sampling port. The condenser was coupled to a vacuum line with a relief valve, an accumulator, and a vacuum trap. The reactor was then immersed in a temperature-controlled silicon oil bath, and the solution was agitated with a magnetic stirrer. A 200-g volume of methyl ester and a known amount of TMP were placed in the reactor, and the mixture was heated to the operating temperature before a catalyst was added. Vacuum was gradually applied after catalyst addition to avoid the spillover of reaction materials. TMP triesters were obtained at a POME-to-TMP molar ratio of 10:1. This ratio helped maintain the reaction temperature by providing a heat reservoir and driving forward reaction. Sodium methoxide was used as the catalyst because it minimizes the saponification of esters. The amount of catalyst used was 0.4% w/w, determined on the basis of the total mass at a 10:1 molar ratio. Samples were taken at pre-determined time intervals for the gas chromatographic analysis of product yield.

After the reaction was completed, the catalyst was separated from the product mixture by vacuum filtration. Vacuum distillation was conducted to remove un-reacted methyl esters from the final product. Overall reaction for synthesis of palm TMP ester is illustrated in Figure 3.2.

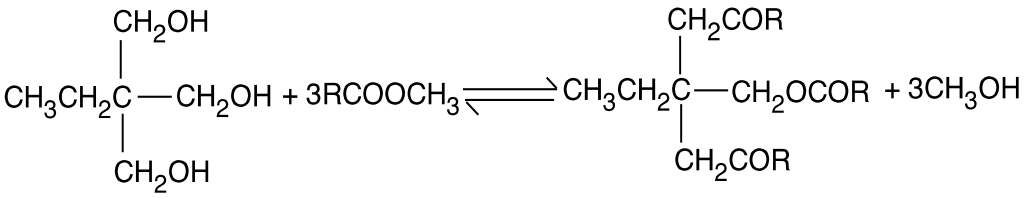

TMP POME TMP ester Methanol

R=alkyl group C_6-C_{20}

Figure 3.2: Overall reaction for synthesis of palm TMP ester

3.1.1.2 Composition and Physicochemical Characteristics

The final composition of palm TMP ester contained 93% w/w of triesters, 4.2% w/w of monoesters and 2.8% w/w of diesters. The physicochemical properties of starting material (POME) and the final product (Palm TMP ester ester) are given in Table 3.1.

The high VI value shows the ability of palm TMP ester to maintain its viscosity over wide temperature range. The ideal oil for most purposes is one that maintains a constant viscosity throughout different temperature changes. High VI is a desirable property for IC engine lubricants as it results in considerable thickening when the engine is cold and, consequently, promotes rapid starting and prompt circulation. It also promotes excessive thinning when the engine is hot and thus provides full lubrication and prevents starvation. The viscosity of palm TMP ester conforms to viscosity class of SAE30 lubricant (Zulkifli, 2014).

Table 3.1: Physicochemical properties of POME and Palm TMP ester

Sample	Properties					
	Viscosity		VI	Pour Point	Flash Point	Density 15 °C (g/cm^3)
	40 °C (cSt)	100 °C (cSt)				
POME	4.32	-	-	12	157	0.8783
Palm TMP ester (Oil A)	40.03	9.15	221	-10	270	0.9011

3.2 Development of Bio-based Nanolubricants

The design of experiments was inspired by full factorial design approach in which the different nanoparticles with varying weight concentrations were used. The effect of these parameters was observed on friction and wear characteristics. To investigate the role of nanoparticles as AW/EP additives and FMs, a variety of nanoparticles in different concentrations (0.25 wt%, 0.50 wt%, 0.75 wt%, 1.0 wt%, 1.25 wt%, 1.50 wt%), have been investigated as additives. For the considered nano-additives, the suitable type and weight concentrations were investigated by the tribo-testing for piston ring and cylinder interaction. For this purpose, high stroke reciprocating test rig was used while EP characteristics were analyzed by four ball tribo-testing. The details of tribo-testing and worn surfaces characterization are provided in Section 3.4 and Section 3.5 of this chapter. The details of nanomaterials used in this thesis and procedure for development of nanolubricants are given below.

3.2.1 Nanoparticles

Three different type of nanoparticles were used in this research which include Molybdenum disulfide (MoS_2), Copper(II) oxide (CuO) and Titanium silicate (TiO_2/SiO_2). Commercially available nanoparticles were obtained from M/S Sigma-Aldrich (M) (Sdn. Bhd., Malaysia), and the true size and density of the nanoparticles were

provided by the supplier. Figure 3.3, Figure 3.4 and Figure 3.5, illustrate the morphology of the nanostructures. The morphologies of the nanoCuO and nanoTiO_2/SiO_2 were fairly spherical. Table 3.2 presents the detailed materials properties of the nanoparticles used in this research. For particles size range, the data were statistically analyzed by measuring the size of isolated nanoparticles on the basis of several different SEM micrographs (500 particles). The nominal particle size for nanoTiO_2/SiO_2 was less than 50 nm while CuO and MoS_2 powder had comparatively larger sizes. Figure 3.6 (a-c), shows the size distribution of the nanoCuO, nanoMoS_2 and nanoTiO_2/SiO_2 respectively

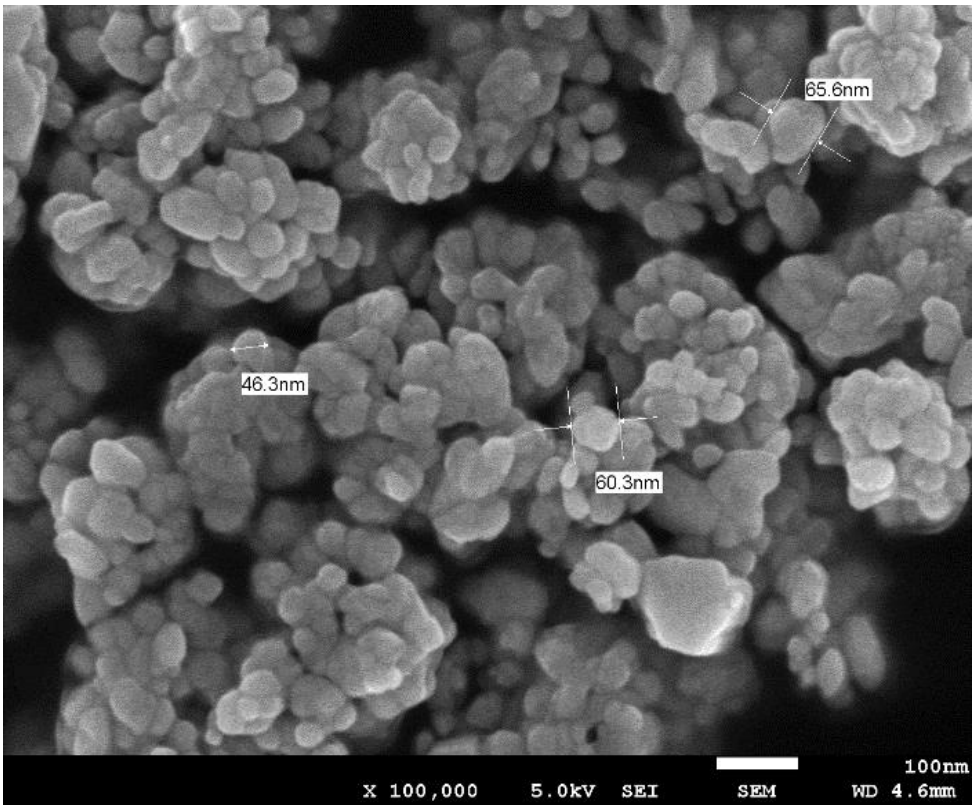

Figure 3.3: SEM micrograph of CuO nanoparticles

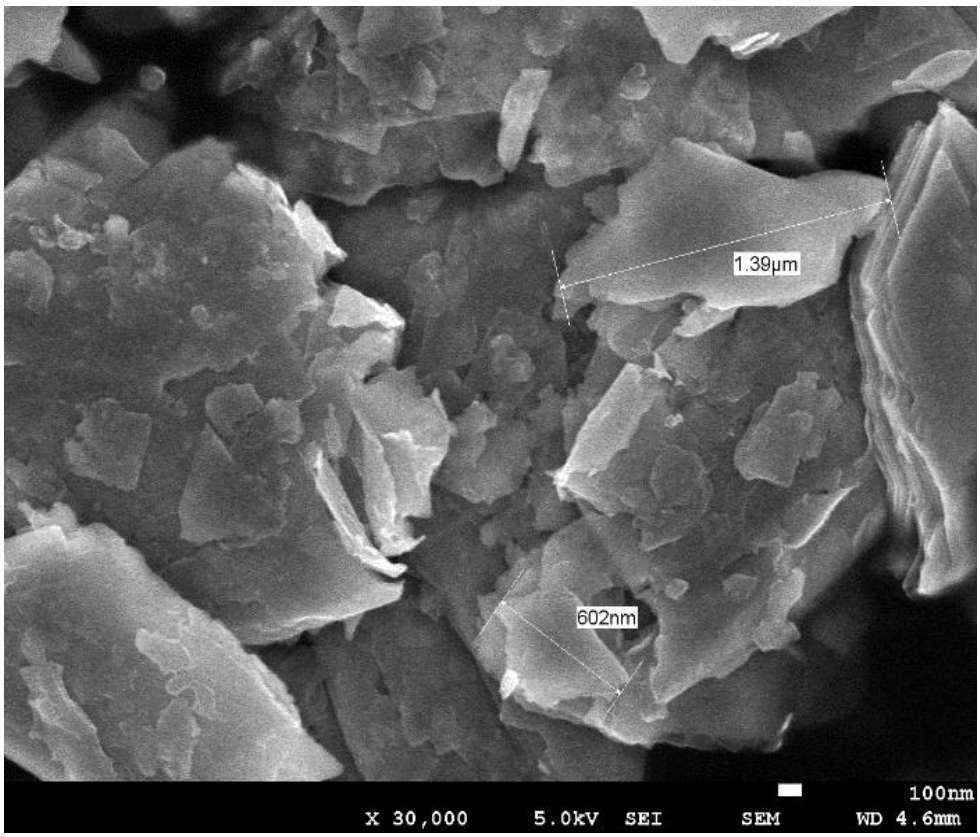

Figure 3.4: SEM micrograph of MoS_2 nanoparticles

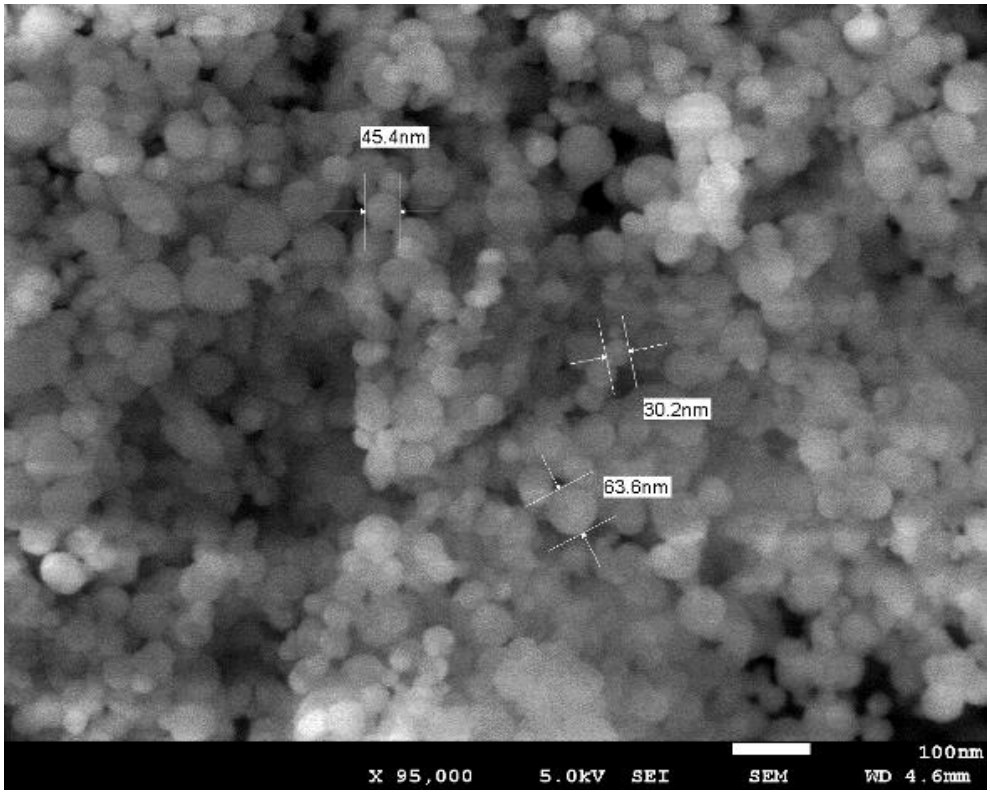

Figure 3.5: SEM micrograph of TiO_2/SiO_2 nanoparticles

Table 3.2: Nanoparticles material properties

Materials	Properties					
Nano-particles	Appearance (Form)	Appearance (Color)	Purity (%)	Morphology	Relative Density (g/cm^3)	Melting Point (^0C)
CuO	Powder	Black	99.99	Nearly spherical	6.32	1336
MoS_2	Powder	Black	99	Non-spherical	5.06	2375
TiO_2/SiO_2	Powder	White	99.8	Nearly spherical	3.39	-

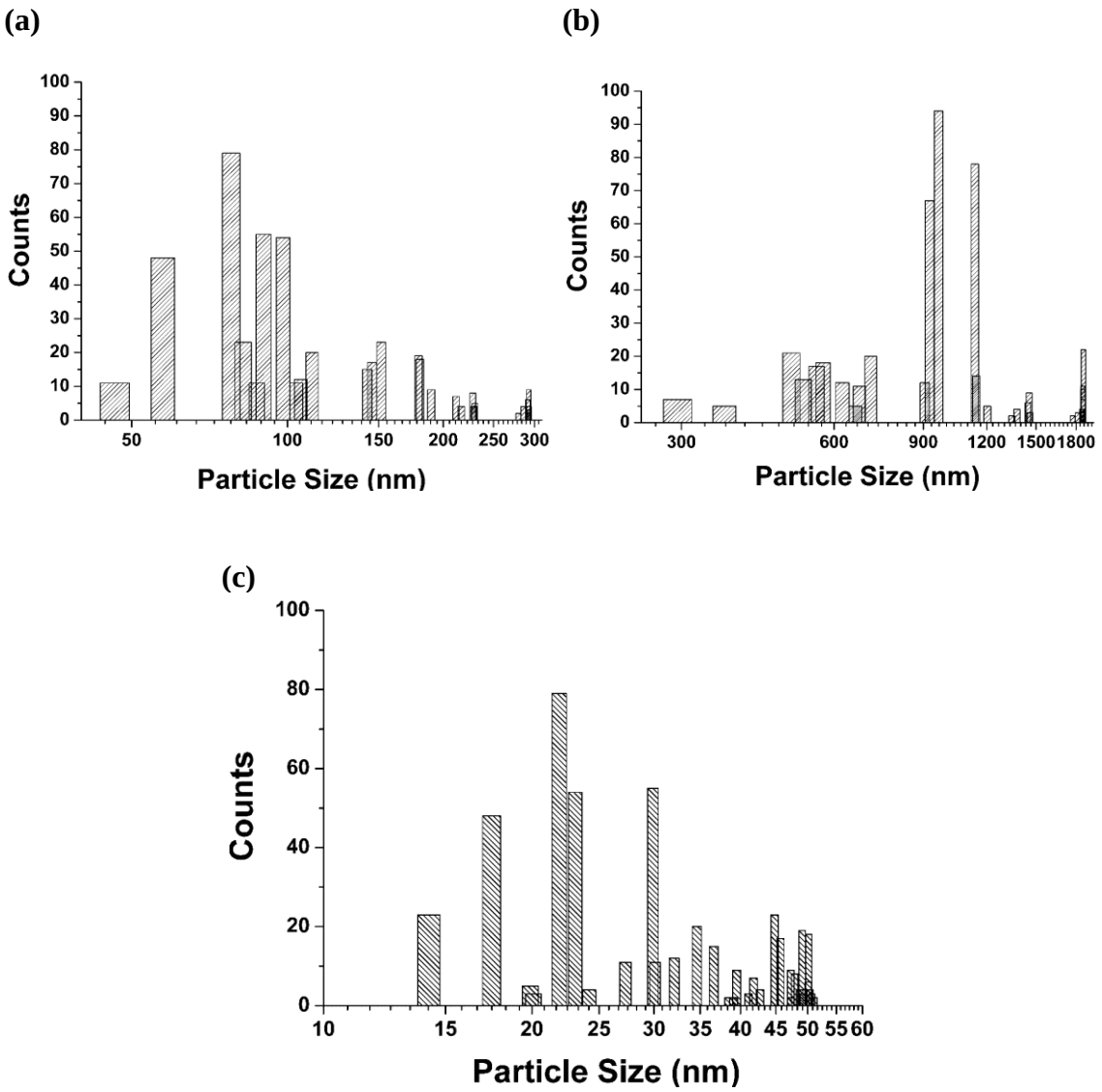

Figure 3.6: Size distributions of nanoparticles used in this study (a) CuO (b) MoS_2 and (c) TiO_2/SiO_2

3.2.2 Ultrasonic Dispersion

For long stationary applications like IC engines, stable nanolubricants are required to maintain effective lubrication. In the absence of any surfactant, MoS_2 and CuO nanoparticles started separating out of suspensions within 24 hours while homogeneity of nanoTiO_2/SiO_2 enriched suspensions lasted for 72 hours. To improve the dispersion stability, anionic surfactant, OA was used for all the suspensions. All types of nanoparticles were used in six different wt % concentrations: 0.25%, 0.5%, 0.75%, 1%, 1.25% and 1.5%. Nanoparticles as well as 1 wt% OA were sonicated in Palm TMP ester at room temperature for 2 hours. The process of dispersion was carried out using an ultrasonic probe as shown in Figure 3.7. Sonic Dismembrator Model 505 by Fisher Scientific™ was used at continuous mode.

Figure 3.7: Sonic dismembrator for homogeneous dispersion of nanoparticles in palm TMP ester

3.2.3 Dispersion Stability Analysis

The dispersion ability of the nanolubricant samples was evaluated by measuring the corresponding optical absorbance spectrum. A SPEKOL® 1500 UV-vis

spectrophotometer with a wavelength range of 190 to 1100 nm was used. The SPEKOL® 1500 is a single beam spectrophotometer with wavelength accuracy of ± 2 nm and a repeatability of 1 nm. The nanolubricant samples were placed in glass cuvettes, and blank palm TMP ester was used as a reference solution. Figure 3.8 shows the glass cuvettes filled with nanolubricant samples containing 1wt% of each type of considered nanoparticles. The glass cuvettes were placed in the spectrophotometer as shown in Figure 3.9. The dispersion stability test lasted for two weeks (336 hours). The rate at which changes in the absorbance of visible light occurred was observed to evaluate the dispersive ability of the nanolubricants.

3.2.4 Nano-lubricants

Eighteen nanolubricants were developed and used in this study; identified in this thesis as oils B to S (Table 3.3). The relevant physicochemical characteristics of bio-based nanolubricants are given in Table 3.3.

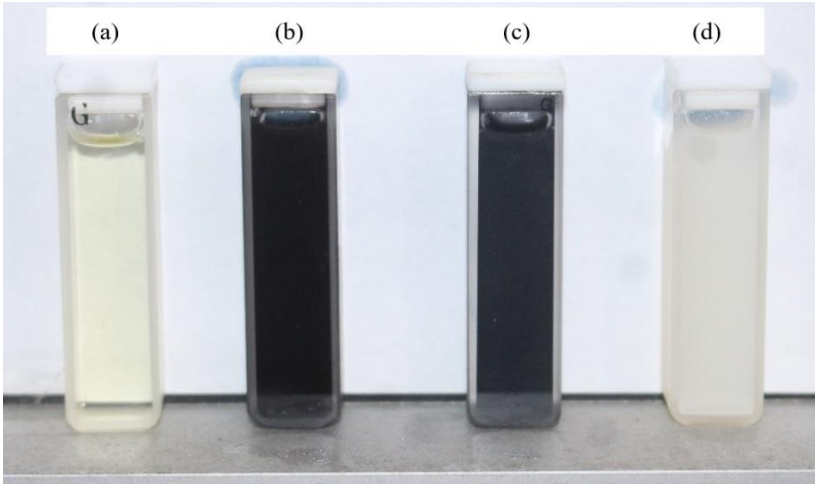

Figure 3.8: Glass cuvettes with lubricant samples (a) Palm TMP ester (b) Palm TMP ester + 1 wt% CuO + OA (c) Palm TMP ester + 1 wt% MoS_2 + OA (d) Palm TMP ester + 1 wt% TiO_2/SiO_2 + OA

Figure 3.9: UV-vis spectrophotometer with nanolubricants filled glass cuvettes

Table 3.3: Lubricant samples properties

Sample	Oil	Properties		
		Viscosity (cSt) 100 °C	VI	Density (g/cm^3) 15 °C
Palm TMP + 0.25 % CuO + OA	B	9.166	220	0.9024
Palm TMP + 0.50 % CuO + OA	C	9.174	220	0.9031
Palm TMP + 0.75 % CuO + OA	D	9.179	222	0.9045
Palm TMP + 1.00 % CuO + OA	E	9.184	221	0.9067
Palm TMP + 1.25 % CuO + OA	F	9.191	221	0.9075
Palm TMP + 1.50 % CuO + OA	G	9.198	221	0.9081
Palm TMP + 0.25 % MoS_2 + OA	H	9.156	222	0.9010
Palm TMP + 0.50 % MoS_2 + OA	I	9.159	220	0.9015
Palm TMP + 0.75 % MoS_2 + OA	J	9.161	221	0.9018
Palm TMP + 1.00 % MoS_2 + OA	K	9.163	221	0.9022
Palm TMP + 1.25 % MoS_2 + OA	L	9.167	219	0.9028
Palm TMP + 1.50 % MoS_2 + OA	M	9.171	219	0.9034
Palm TMP + 0.25 % TiO_2/SiO_2 + OA	N	9.197	220	0.9047
Palm TMP + 0.50 % TiO_2/SiO_2 + OA	O	9.221	221	0.9064
Palm TMP + 0.75 % TiO_2/SiO_2 + OA	P	9.277	220	0.9088
Palm TMP + 1.00 % TiO_2/SiO_2 + OA	Q	9.311	220	0.9103
Palm TMP + 1.25 % TiO_2/SiO_2 + OA	R	9.331	219	0.9118
Palm TMP + 1.50 % TiO_2/SiO_2 + OA	S	9.350	219	0.9125

3.3 Engine Testing and Lubricating Oil Degradation

To investigate the friction and wear behavior of piston ring and liner materials by using more realistic lubricants, engine-aged lubricant samples were collected and tested in laboratory.

3.3.1 Engine Test Setup

Naturally aspirated, single cylinder diesel engine (YANMAR TF120) was used for long duration tests. The engine test setup is shown in Figure 3.10. The engine specifications for relevant parameters of this study are given in Table 3.4. Tests of 200-hrs were conducted by using conventional diesel engine lubricant as well as bio-based nanolubricant. Engine schematics is shown in Figure 3.11.

Table 3.4: Engine specifications

Parameter	Specification
Model	YANMAR TF 120-M
Configuration	Single cylinder
Air aspiration	Naturally aspirated
Maximum Power	7.7 kW at 2400 rpm
Fuel injection	Mechanical direct injection
Displacement	0.638 cc
Oil capacity	2.8 L
Drain Interval	200 Hours

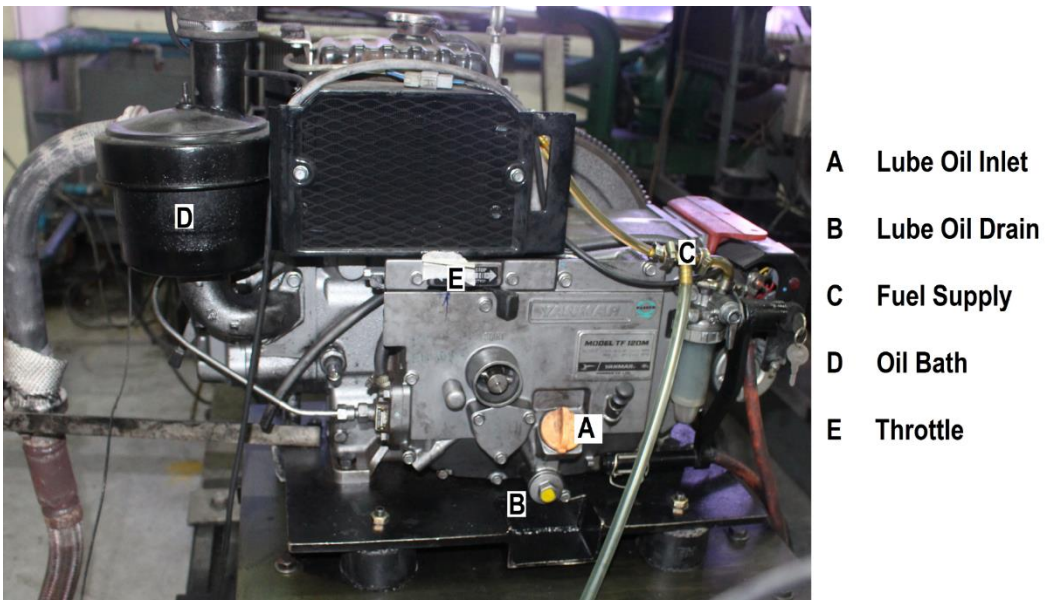

Figure 3.10: Engine test bench showing YANMAR single cylinder diesel engine

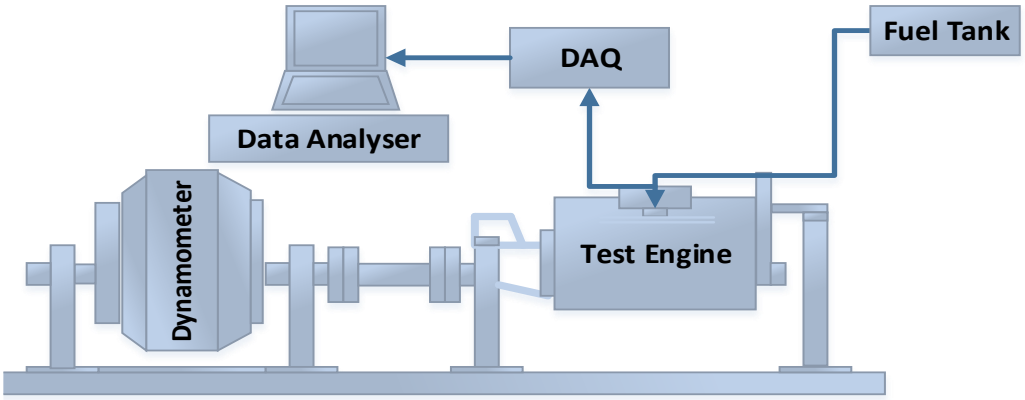

Figure 3.11: Schematics of the engine test bench

3.3.2 Fuels for Engine Testing

Due to implementation of the biofuel mandate in different countries, this study has considered the conventional diesel fuel (DF) as well as palm biodiesel blend (PB20) which consists of 20% palm methyl ester and 80% DF. The role of fuel on lubricant degradation and its effect on piston ring–cylinder lubrication was investigated. The commercially available fuels were used in this study for which the significant characteristics are provided in Table 3.5.

Table 3.5: Properties of diesel fuel and bio-diesel

Properties	ASTM standard	Test Equipment	DF	PB20
Kinematic viscosity at 40°C (cSt)	D7042	SVM 3000	3.32	3.62
Flash point (°C)	D93	Pensky-martens NPM 440	69	89
Density at 15°C (kg/m^3)	D7042	SVM 3000	822	833
Calorific value (MJ/kg)	D240	C2000 basic calorimeter	45.55	43.83
Cetane number	D6890	Advanced engine technology IQT™	51	53.10

3.3.3 Engine Oil Filter Conditioning

Other than AW, EP and FM additive requirements, the conventional engine lubricants are typically additivated by over based detergents, dispersants, antioxidants, viscosity modifiers and corrosion inhibitors. Therefore, similar additive technology was required to use the bio-based nanolubricant in actual engine conditions. In this regard, chemically modified engine oil filter technology has been found as replacement to additive requirements by controlling acidity, providing corrosion protection and extending the drain interval for zero detergent diesel engine lubricant (Watson, Wong, Brownawell, Lockledge, et al., 2009).

This approach was adopted in this work as the formulated bio-based nanolubricant contained low alkaline reserve to neutralize the acidic contaminations in diesel engine for long hour tests. For conventional engine lubricants, this technique has been found useful to reduce the requirements of dispersants and over-based detergent additives and extended drain intervals has been achieved (Watson, 2010). This technology has an additional benefit of environmental conformity unlike the conventional detergent and anti-corrosion additives which are source of environmental hazards and high ash content.

3.3.3.1 Development of Strong Base Filter

A variety of strong bases have been mentioned by researchers that can be effectively used as neutralizing agents for acid contaminations in the engine-aged oil (Lockledge & Brownawell, 2014; Rohrbach et al., 2007). In this research, sodium hydroxide (NaOH) was selected as strong base for flocculation of strong base particles on standard filter element surface. Reagent grade sodium hydroxide pellets with a molecular weight of 40 g/mol, pH=14 and purity of 99% were used. High molecular weight Polyacrylamide (PAM) was used as flocculent. For the chemical process, 31.25 grams of PAM was added in 250 ml of filtered tap water. For uniform dispersion, the solution was constantly agitated by a magnetic stirrer for 30 minutes. NaOH slurry was prepared by diluting 5 grams of NaOH in 200 grams of filtered water. To this solution, 0.5 wt % of PAM dispersion was added by weighing into a container. For micro particle retention aid, 0.1 wt% of cationic starch (CATO302) was added. After filtration, the strong base flocs were transferred to the standard filter element and allowed to set overnight in oven at 105 ^{0}C. Scanning electron microscopy (SEM) and energy dispersive X-ray spectroscopy (EDX) analysis provides strong base filter paper characteristics and elemental details in strong base filter showing the contents of NaOH. Figure 3.12 provides the morphology and elemental details for strong base filter paper.

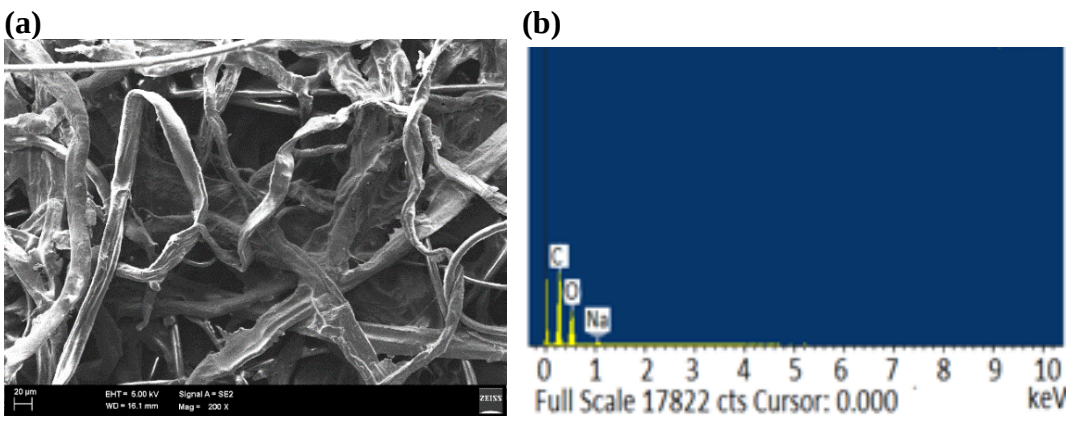

Figure 3.12: (a) SEM micrograph of strong base filter paper (b) EDX analysis showing elemental details

3.3.4 Engine-aged Lubricants

In addition to the use of optimized bio-based nanolubricant, conventional diesel engine lubricant (SAE15W40), with API category of CI-4 was also used for comparison in this part of study. As two type of lubricants and two different fuels were used, therefore, a total number of four long duration engine experiments were carried out. Lubricant samples were collected during long duration engine testing to investigate lubricant degradation and related effect on tribological behavior. For each test, the tests duration was 200 hours, which was based on the drain interval. The sump oil samples were collected at regular intervals of 40 hrs and standardized oil analysis procedures were used to measure the lubricant quality.

3.3.5 Lubricant Analysis

3.3.5.1 Viscosity

The kinematic viscosity was measured using ASTM D2270. This method provides the lubricant's kinematic viscosities at 40 ^{0}C and 100 ^{0}C. The experiments were carried out using an Anton Paar´s Stabinger Viscometer™ SVM™ 3000. For the viscosity measurements, the test apparatus has a reproducibility of 0.35% and a repeatability of 0.1%.

3.3.5.2 Total Acid Number (TAN)

For the TAN analysis, the ASTM D664 test method was used to measure the samples acidity by using TAN/TBN analyzer (Metrohm 716 DMS Titrino). In this analysis, potassium hydroxide = 0.1 mol/l (concentration) isopropanol was the titrant, whereas toluene, isopropanol, and distilled water were the solvent. The sample size was varied on the basis of conventional and bio-based lubricants. The measurements were accurate to ± 0.003.

3.3.5.3 Total Base Number (TBN)

For the TBN measurement, the ASTM D2896 test method was used to evaluate the alkaline reserves of lubricant samples. This test was also carried out using the Metrohm 716 DMS Titrino, but the titrant and solvent were different than TAN analysis as per standard procedure. In this analysis, perchloric acid = 0.1mol/l (concentration) in acetic acid was the titrant whereas 1:2 i.e. glacial acetic acids:chlorobenzene, was the solvent. The measurements were accurate to ± 0.003.

3.3.5.4 Infrared Spectroscopy

To analyse lubricant degradation, Fourier transform infrared (FTIR) spectroscopy was carried out for fresh as well as engine-aged oil samples. In a typical FTIR analysis the lubricant sample is placed between the infrared source and detector (Watson, 2010). These infrared radiations are required to pass through the lubricant sample to be absorbed and provide corresponding spectra. The absorbance spectra for lubricant samples were analysed for functional groups and related absorbance peaks were determined. This series of experimentation was carried out using a PerkinElmer Spectrum 400 FTIR spectroscopy instrument with a data acquisition system. A background spectrum was obtained as reference before FTIR measurements were conducted. It was ensured that the crystal surface was clean and properly installed before the background spectrum was obtained. The spectra were acquired over a spectral range of 4000–500 cm^{-1} at 2 cm^{-1} spectral resolution; 16 scans per test were selected. The absorbance spectra mode was chosen for data analysis.

This research investigated and reported the IR absorption data corresponding to fuel residue, oxidation, and soot loading. The monitoring parameters for lubricant oil condition and reporting methods are listed in Table 3.6. Functional groups in a typical FTIR absorbance spectrum of used oil is illustrated in Figure 3.13.

Table 3.6: Lubricant condition monitoring parameters and reporting using FTIR

Parameter	Measurement Region (cm^{-1})	Baseline Point(s) (cm^{-1})	Reporting*	Interferences	Type of Measurement	Relative Sensitivity
Fuel Residue	815 to 805	Minima 835 to 825 and 805 to 795	(Value + 2) × 100	Fuel evaporation, variation in fuel aromaticity	Contaminant screening	extremely sensitive
Oxidation	1800 to 1670	Minima 2200 to 1900 and 650 to 550	Report Value as Measured	Dispersants, moisture contents, VI improvers	Trending lubricants degradation	fairly insensitive
Soot Loading	2000	None	Value × 100	Particle size, particle density, engine make/model	Trending carbon load for diesel engine	insensitive

* Reporting values in absorbance/0.1mm

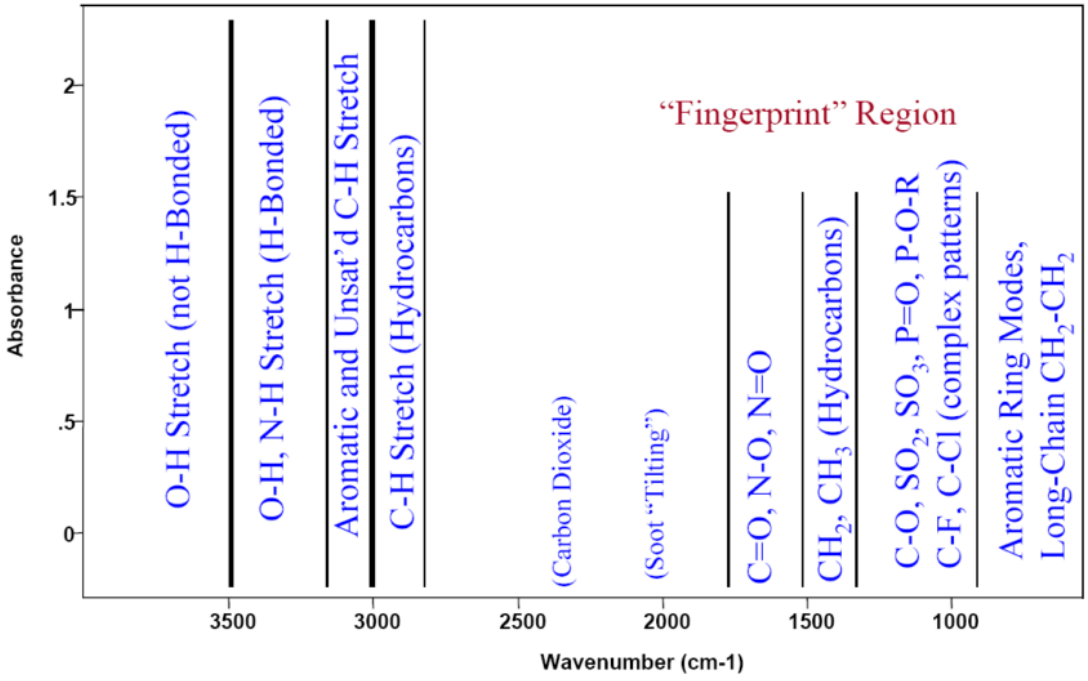

Figure 3.13: Functional groups corresponding to absorbance peaks in FTIR spectra of used oil

Source: Watson (2010)

3.4 Tribometer Investigation

3.4.1 Test Specimen Preparation

The piston rings and cylinder liner specimen were extracted from actual new engine parts of a commercial single cylinder diesel engine. Piston ring specimens were machined from new top compression piston rings (uncompressed outer diameter of 92.00 mm) into

several small segments of 25.4 mm. The machining process was carried out using Sodick Fine Mark 21 CNC Wire Electrical Discharge Machine to prevent damage to surface finish and treatments. The extracted piston ring and cylinder liner specimen are shown in Figure 3.14. Material properties of piston ring and cylinder liner are given in Table 3.7.

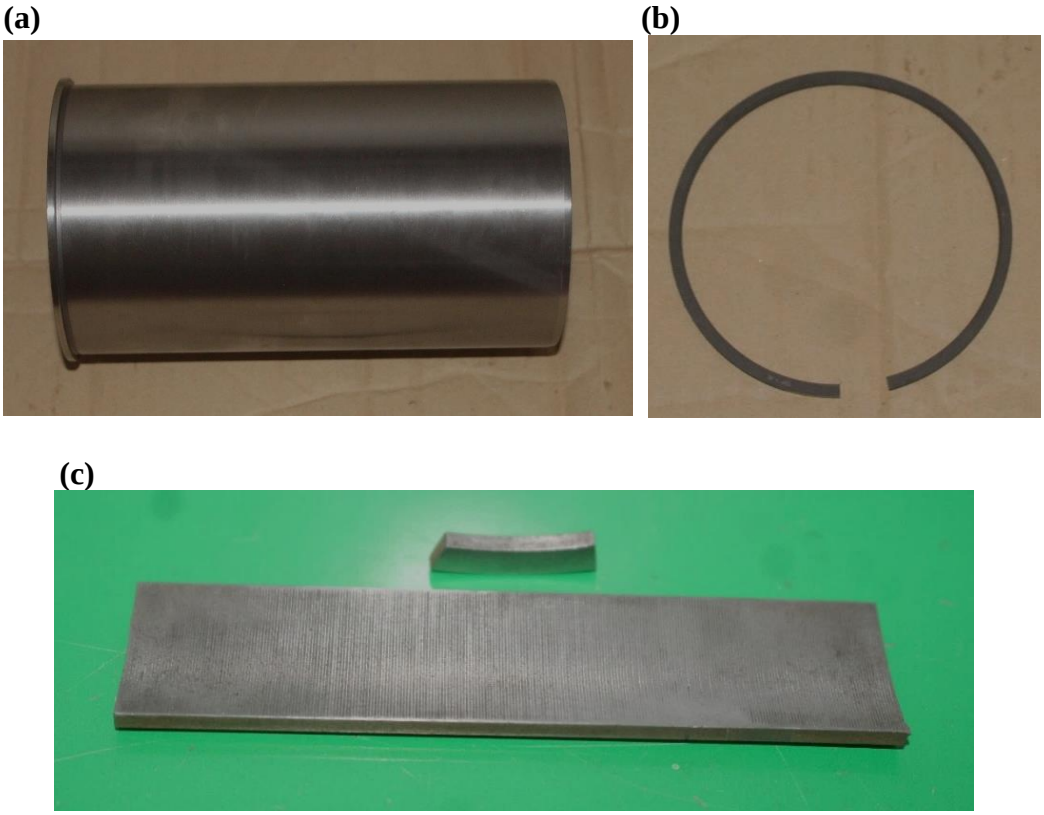

Figure 3.14: Extraction of piston ring and cylinder liner specimen (a) actual cylinder liner (b) actual piston ring (c) extracted piston ring segment and extracted cylinder liner specimen

Table 3.7: Piston ring and cylinder specifications

Specimen	Material	Surface Treatment	Roughness (Rq, micron)	Elastic Modulus (GPa)
Cylinder	Cast Iron	Honing	1.215	200
Ring	Cast Iron	Chrome Coated	0.138	210

3.4.2 High Stroke Reciprocating Tribo-testing

A high-stroke reciprocating test rig (Figure 3.15) was used to ensure that the piston ring was stationary in the holder at the top and that the specimen of the cylinder liner exhibited a reciprocating motion. The relevant testing conditions are given in Table 3.8. After load application, the piston ring specimen established conformal contact with the surface of the cylinder liner (Figure 3.16). Normal load was distributed in a uniform manner across the contact area. To simulate engine oil temperature, the oil bath was equipped with a temperature controller, a thermocouple, and a heater system. The 3-D schematics of piston ring-cylinder tribo-test setup and related contact geometry of test specimen is demonstrated in Figure 3.17. Running in duration lasted for 2 hours such that the sharp asperities on the new surfaces were shaved off before each test. Average COF was measured for test duration of two hours. For wear test, the contact between piston ring and cylinder liner lasted for six hours and the wear was measured by weight loss method as direct wear volume measurements were not possible due to curvature specimen profiles. Samples were cleaned ultrasonically and weighed to an accuracy of 0.1 mg, before and after each test. The wear loss was then reported in terms of wear volume for cylinder liner as well as piston ring specimen. Each test was repeated three times using a new piston ring and cylinder liner specimen each time.

Table 3.8: Test specifications of high stroke reciprocating test rig

Normal load	160 N
Temperature	70 ^{0}C
Stroke	84 mm
Contact width	25.4 mm
Speed	240 rpm
Lubricant feed rate	5 mL/hr

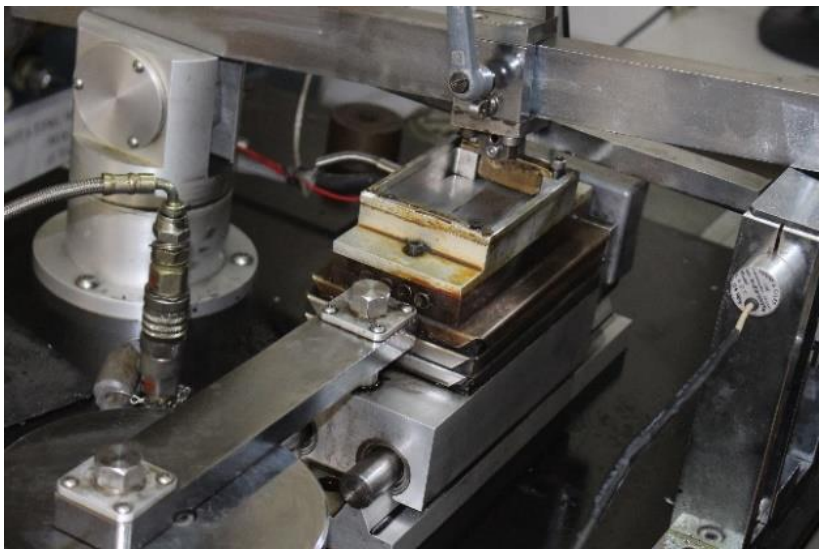

Figure 3.15: High stroke reciprocating test rig

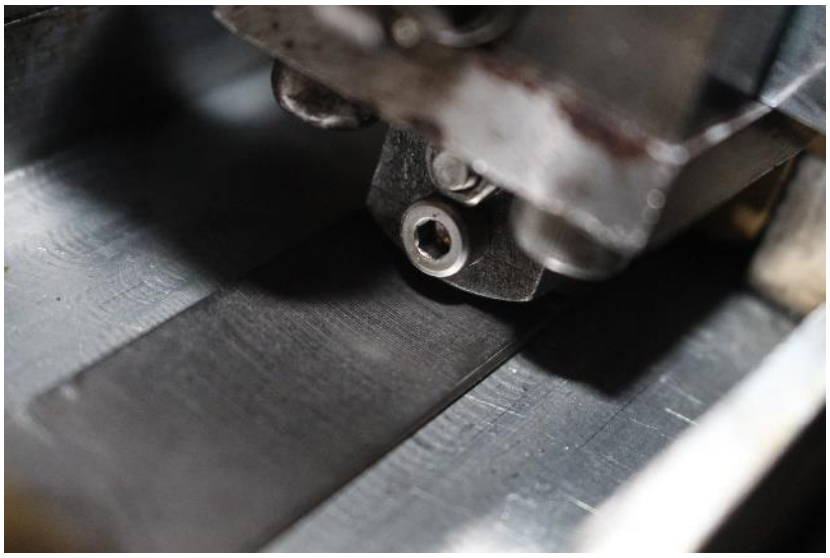

Figure 3.16: Contact between piston ring and cylinder liner

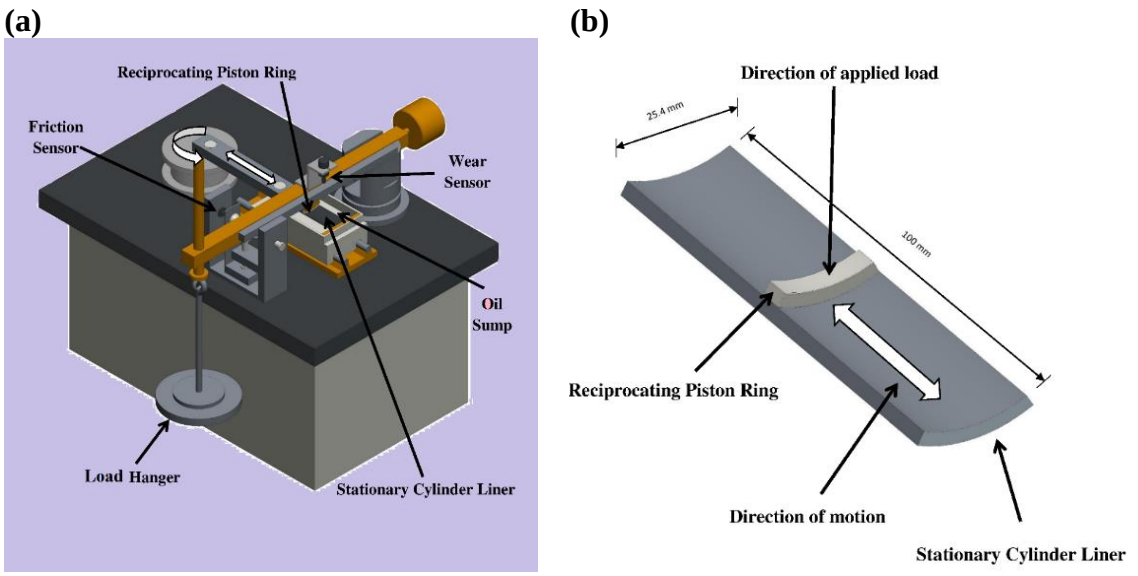

Figure 3.17: (a) 3-D schematics of piston ring-cylinder tribo-testing. (b) Schematics of contact between piston ring segment and cylinder specimen

3.4.3 Four-Ball Extreme Pressure (EP) Tribo-Testing

A four-ball test configuration was used to investigate EP characteristics of fresh nanolubricants. For this purpose, DUCOM's four ball tester model TR-30H was used as shown in Figure 3.18. In this series of experiments, lubricant samples were tested by using ASTM D2783 standard. The balls and the pot were thoroughly cleaned with toluene before each experiment. The significant experimental conditions are summarized in Table 3.9. Commonly used EP parameters, namely, last non-seizure load (LNSL), initial seizure load (ISL), weld load (WL) and mean wear scar diameter (WSD) were evaluated. Each test was repeated three times so as to minimize data scatter.

Table 3.9: Test conditions for four-ball tests

Condition	Value
Test Temperature (^{o}C)	25±5
Test Duration (sec)	10
Spindle Speed (rpm)	1770 ± 30
Load (Kg)	Varies, 10-sec/stage
Ball Material	AISI 52100
Ball Diameter (mm)	12.7
Ball Hardness (HRC)	64-66

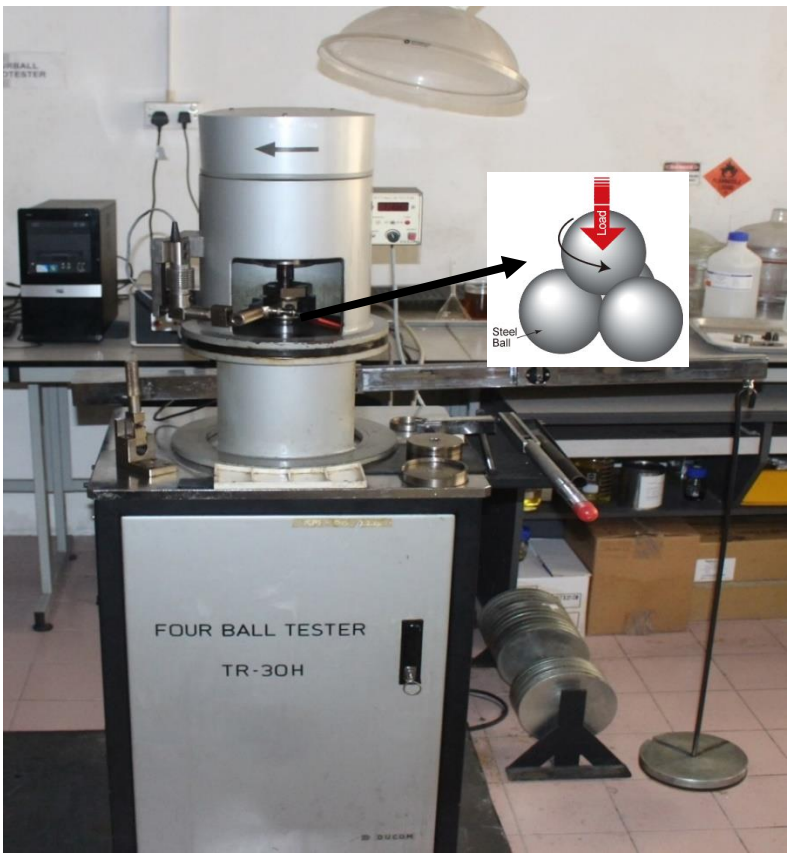

Figure 3.18: Four-ball tribo-testing using DUCOM TR-30H four ball tester

3.5 Surface Analysis

To understand the lubrication mechanism for piston ring−cylinder conjunction, the tested specimens of cylinder liner were analyzed by using surface characterization techniques. For this purpose, surface analysis tools were used which include scanning electron microscopy (SEX), EDX spectroscopy, 3-D surface profilometry and Raman spectroscopy.

3.5.1 Scanning Electron Microscopy (SEM)

Using this surface analysis tool, a focused electron beam is scanned across the sample surface and related imaged is taken. It is a versatile tool for the investigation of surfaces at an extensive range of magnifications and high resolution. SEM provides qualitative information about topography, morphology and general appearance of tested surfaces.

SEM was used to study the morphology of worn surfaces in this thesis which helped in understanding the lubrication mechanisms contributed by lubricant samples. The equipment used for the SEM analysis was Carl Zeiss UltraPlus scanning electron microscope, model AG ULTRA55, as shown in Figure 3.19 (a). Due to the compact design of specimen holder and test chamber of SEM equipment, all cylinder liner specimens inspected were needed to cut to the size of 10mm x 10mm. The cutting of cylinder liner specimens was carried out in a bench top cut-off machine. Figure 3.19 (b) shows the installation of cylinder liner specimens on the sample mount for SEM analysis.

3.5.2 Energy Dispersive X-ray Spectroscopy (EDX)

The chemical composition of elements deposited on worn surfaces was investigated using Oxford Instruments energy dispersive x-ray (EDX) analysis system integrated with SEM setup.

The working principle of this tool is based on the excitation of characteristic x-rays by the incidence of primary electrons. By studying the energy spectra of X-rays emitted from the sample, it is possible to determine its elemental composition. The elemental information by EDX originates from approximately the first 1 μm below the surface of tested sample. In this study, EDX helped in analyzing the lubrication mechanisms by comparing the chemical composition of the elements on the worn surfaces with the known composition of specimen before tribo-testing. It provides the evidence of mending/repairing by deposition of nanoparticles on tribologically tested surfaces.

(a) **(b)**

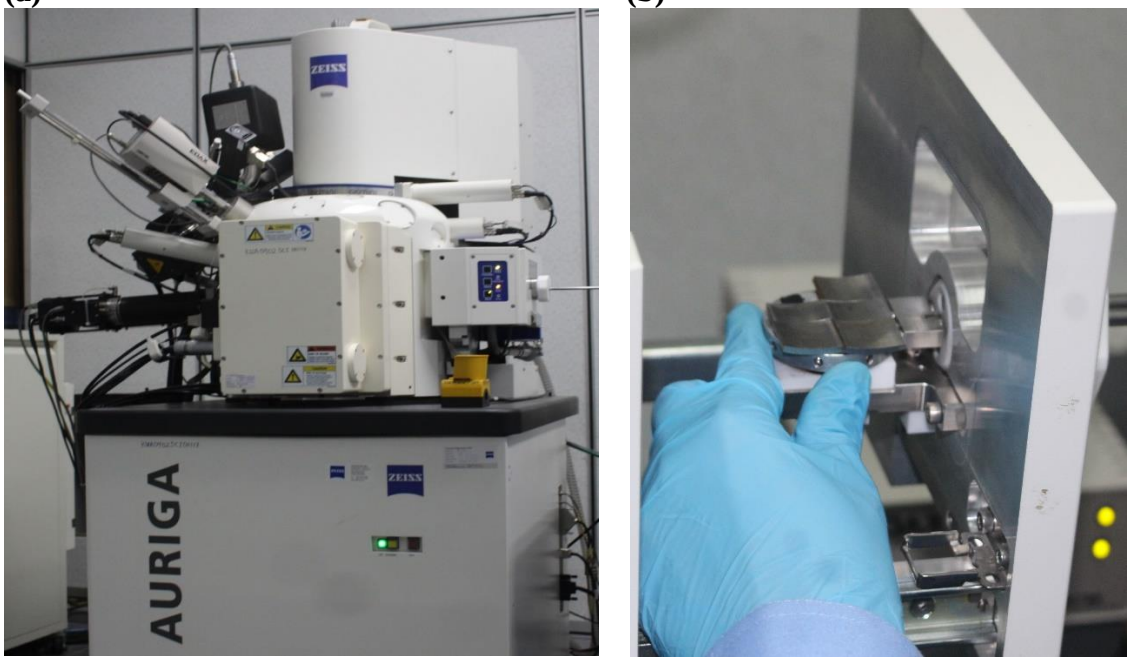

Figure 3.19: (a) SEM setup for analysis of worn surfaces (b) Samples installation on the sample mount

3.5.3 Raman Spectroscopy

Raman spectroscopy is an optical spectroscopic method in which the test sample is illuminated with monochromatic laser light, and the light dispersed from the test surface is studied. A majority of these scattered light rays have the same wavelength as that of incident light, but there is little scattering with different wavelength. This change or shift of wavelength is a result of excitation of vibrational modes in the sample material. Such vibrations are a result of either molecules or combined motion of atoms. The energy difference between the vibrational states provides the wavelength shift.

Raman spectroscopy was adopted in this study due to its advantage of providing information about compounds on the sample surface rather relying only on elemental composition by EDX. But it has limitation to detect a limited selection of compounds, meaning that some compounds tend to be “invisible” in the analysis. RENISHAW inVia confocal Raman microscope (Figure 3.20) was used to carry out inVia Raman

spectroscopy using argon-ion laser having excitation wavelength of 514 nm and 10 mW laser power.

Figure 3.20: Raman microscope used to analyze worn cylinder liner specimen

3.5.4 Surface Profilometry

The surfaces topography after tribo-testing was investigated using optical 3D surface measurement. For this purpose, Alicona Infinite Focus 3D surface analyzer was used as shown in Figure 3.21 (a).

The measurement principle is based on focus-variation with non-contact, optical, three-dimensional characteristics. This tool combines the small depth of focus of an optical system with vertical scanning to provide topographical and color information. Novel and unique algorithms reconstruct this into a single 3D data set with accurate topographical information. Surface depth resolution can be as low as 10nm making the instrument ideal for surface study of both homogeneous and compound materials.

For surface roughness profile, objective magnification of 20x with a vertical resolution of 50 nm was used. Related height step accuracy was 0.05 % with maximum measurable area of 10000 mm². Figure 3.21 (b) shows the placement of cylinder liner specimen.

(a) **(b)**

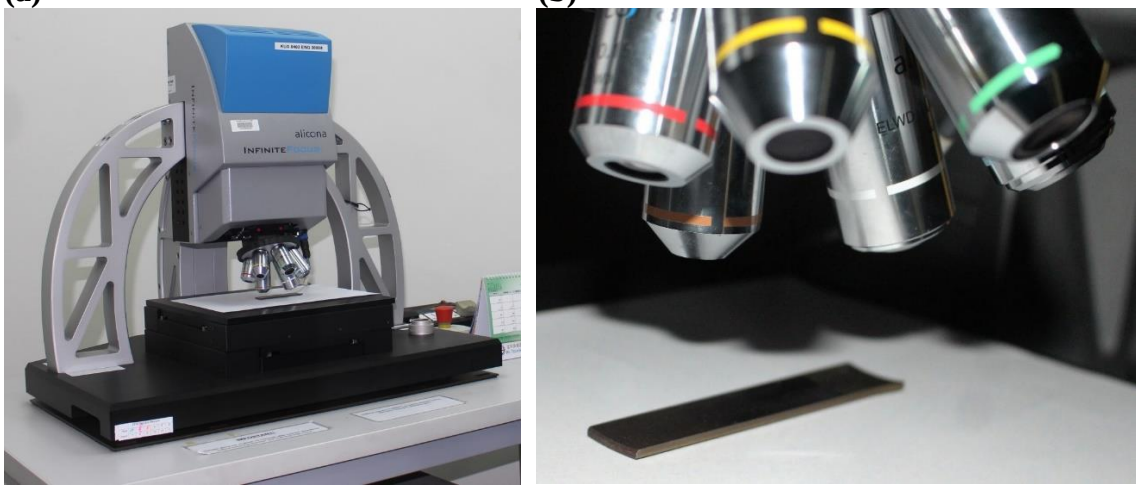

Figure 3.21: (a) Alicona Infinite Focus 3D surface analyzer (b) Non-contact surface roughness measurement of cylinder liner specimen

CHAPTER 4: RESULTS AND DISCUSSION

In this chapter, the results of the considered performance parameters for fresh as well as engine-aged oil samples have been provided and discussed. In the first stage, average COF profiles and wear volume of piston ring as well as cylinder liner specimen, have been reported and discussed for blank palm TMP ester. It is followed by the investigation of dispersion stability and discussion of tribological parameters for all the nanolubricant samples. After this, the EP behavior of all the lubricant samples has been discussed.

In the next phase, the results of considered degradation parameters (viscosity, TAN, TBN, fuel residue, oxidation and soot loading), are reported and discussed for engine sump oil samples collected at regular interval during long duration engine tests. Then, the effect of lubricating oil degradation on friction and wear behavior for piston ring–cylinder liner interaction is reported and discussed. Also, the detailed surface analysis and related discussions are also part of this chapter.

4.1 Tribological Behavior of Palm TMP Ester

4.1.1 Friction Results

The friction behavior of blank Palm TMP ester (Oil A) is shown in Figure 4.1 (a-b). The friction profiles indicate that the Oil A exhibits an initial friction reduction because of the high polarity of the TMP ester, which creates a strong affinity to the metal and provides a barrier between surfaces (Zulkifli, Kalam, Masjuki, Al Mahmud, & Yunus, 2014). According to Rudnick (2013), such chemically modified vegetable oils have a high degree of polarity which is ascribed to ester linkages in the molecules. It results in their physical bonds with metal surface using electron lone pairs on the oxygen atom of ester linkage.

However, in the absence of any additive and at high contact temperatures, friction starts increasing after 25 minutes of sliding (Figure 4.1). Such a trend of increasing friction may be attributed to the breakdown of fluid film at high contact temperatures which results in deterioration of initial protective film formed by metal affinity to palm TMP ester. Similar trends have been reported for blank palm TMP ester in an earlier study (Zulkifli, Kalam, Masjuki, Shahabuddin, et al., 2013). The average COF of 0.15 has been reported for Oil A. The lubrication behavior of palm TMP ester was further explored by characterizing the worn cylinder liner surfaces (Section: 4.1.3.1).

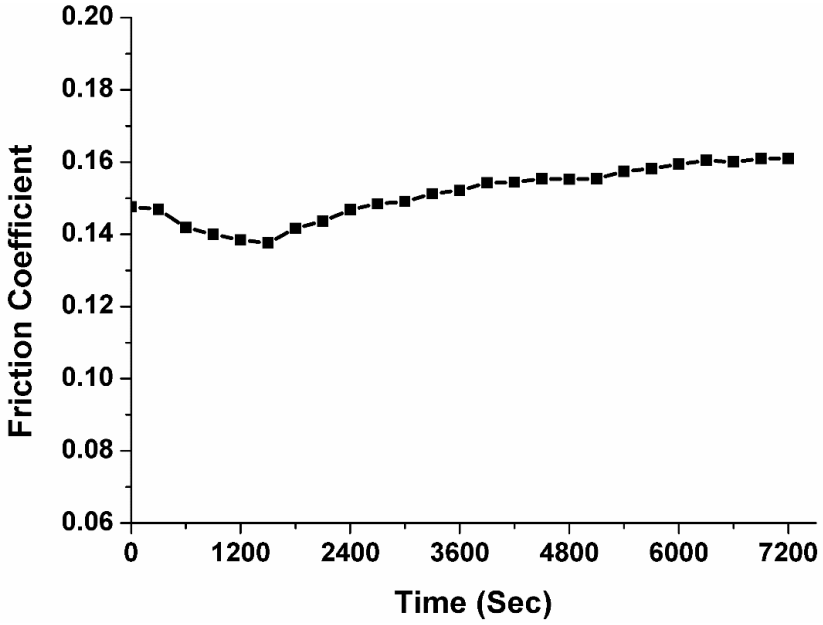

Figure 4.1: COF as a function of sliding time for Oil A

4.1.2 Wear Results

The wear volumes of piston ring as well as cylinder liner specimen were considered to investigate the AW characteristics of palm TMP ester (Oil A). Figure 4.2 shows the antiwear characteristics of Oil A in the absence of any additives. The wear volumes of cylinder liner specimen as well as piston ring segment are illustrated in Figure 4.2. In the absence of any AW additive, a wear volume of 0.315 mm^3 has been observed for cylinder liner specimen as illustrated in Figure 4.2. Similarly, for piston ring segment,

a wear volume of 0.026 mm^3 has been obtained. Such wear losses by palm TMP ester were due to accelerated adhesive and abrasive wear over the sliding test duration. Such trend is in accordance to previously reported study by Waara, Norrby, and Prakash (2004). They have reported severe adhesive and abrasive wear for two pure TMP esters, i.e. TMP–oleate and a TMP-C_8–C_{10}. The wear behavior of palm TMP ester was further investigated by surface analysis in Section: 4.1.3.1.

Though polar nature of TMP ester help reducing the severe wear, the base oil has limited wear protection ability. Therefore, like conventional base oils, the AW behavior of palm TMP ester can be further improved by addition of appropriate AW additives. Such additives are beneficial in wear protection as they usually have much stronger attraction to the surfaces than base fluids.

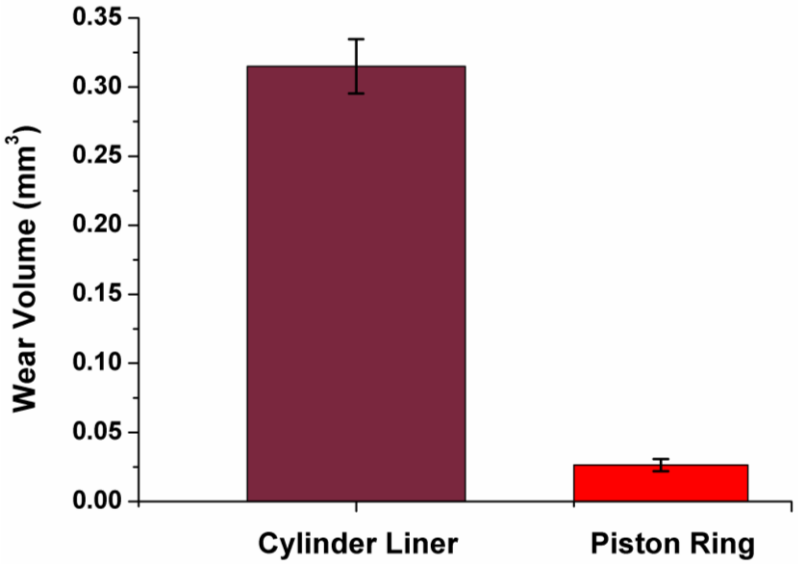

Figure 4.2: Wear volume by Oil A for cylinder liner specimen and ring segment

4.1.3 Surface Analysis

4.1.3.1 SEM Analysis

SEM analysis provides the micrographs of cylinder liner worn surfaces. The micrographs at low magnification (20x) as well as high magnifications (200x) are demonstrated for tested surface by each type of lubricant sample. In each figure the

micrographs given in the left side represent the low magnification i.e. 20x while corresponding high magnification micrographs (200x) are mentioned at the right side.

Figure 4.3 (a) illustrates the SEM micrographs of new cylinder liner specimen which clearly shows the honing on the surface. Figure 4.3 (b) show worn cylinder liner specimen which was tested using Oil A. In the absence of AW additives and FMs, the surface tested with Oil A shows material removal from the worn surface as shown in Figure 4.3 (b-b_1). The SEM micrograph at high magnification show highly rough surface with grooves, pits by adhesive wear and scratching line marks by abrasive wear (Figure 4.3 (b_1)). SEM analysis support the high wear volume trends by Oil A was used as reported and discussed previously in Section 4.1.2.

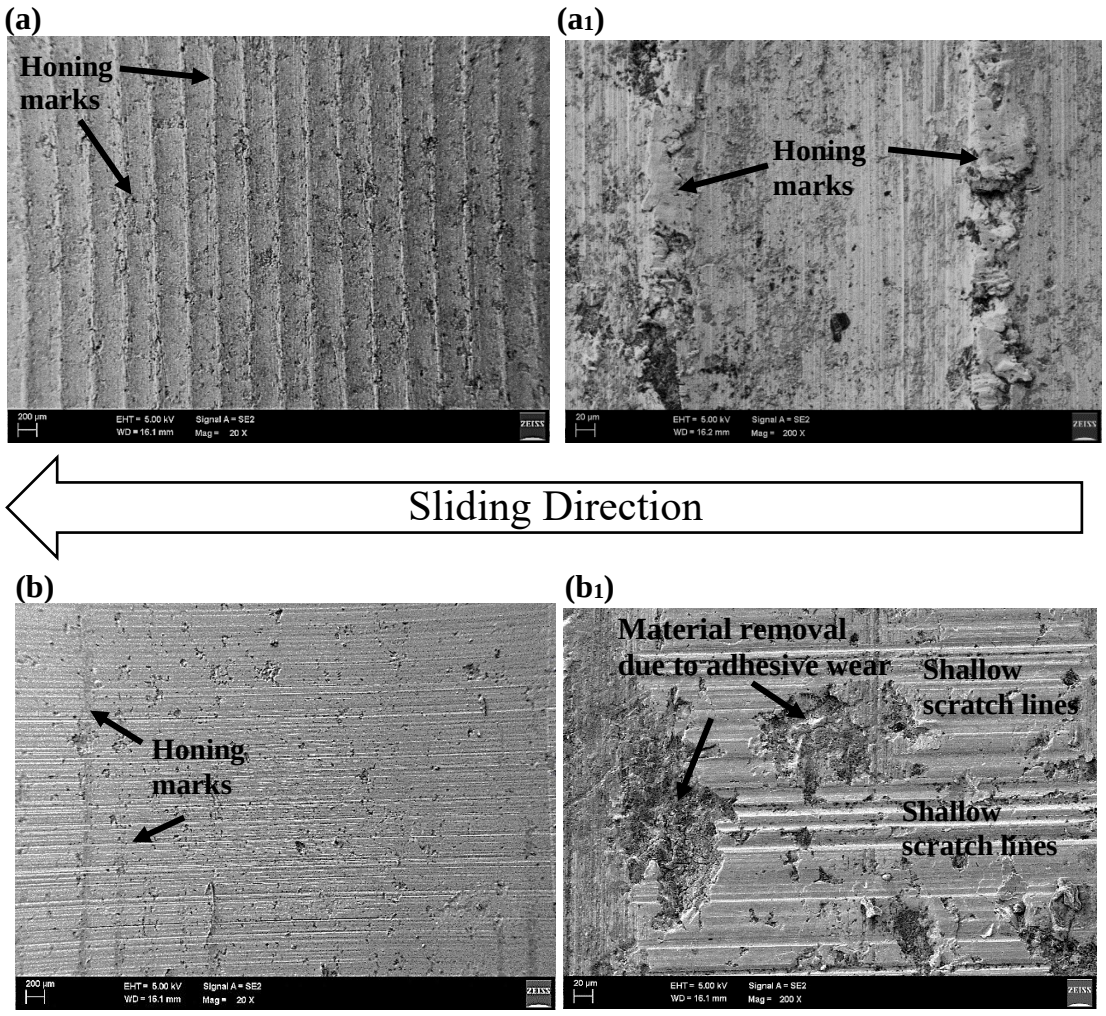

Figure 4.3: SEM micrographs cylinder liner specimen (a) new 20x, (a_1) new 200x, (b) tested with Oil A 20x, (b_1) tested with Oil A 200x

4.1.3.2 Surface Profilometry

The effect of palm TMP ester on surface roughness of worn cylinder liner specimen, is provided in terms of 3-D surface profiles. The adopted technique of surface profilometry showed surfaces roughness distribution in terms of height, quantifying the range of height by color bars. Apart from apparent surface texture and height distribution, the roughness is quantified in terms of commonly used roughness parameters like "Roughness Average (Ra), Root Mean Square roughness (Rq) and Mean Roughness Depth (Rz)". Figure 4.4 shows the 3-D texture of cylinder liner specimen before tribo-testing while corresponding 2-D roughness profile is illustrated in Figure 4.5.

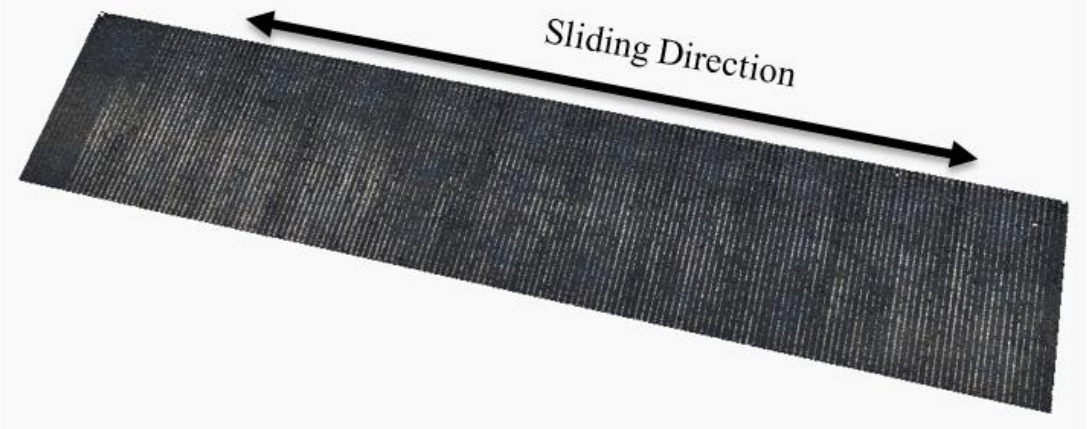

Figure 4.4: Surface texture of new cylinder liner specimen

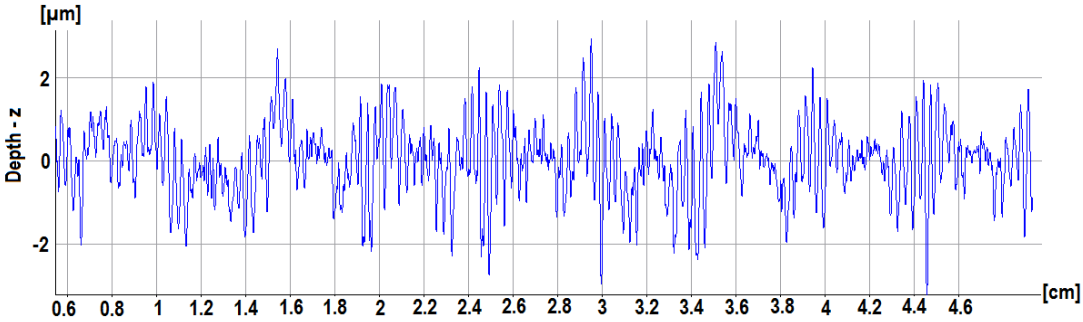

Figure 4.5: Roughness profile of new cylinder liner specimen

For new cylinder liner specimen and specimen tested with Oil A, Figure 4.6 (a-b) shows 3-D surface textures. Comparing the values of roughness parameters, it can be observed that in comparison to new cylinder liner specimen, surface roughness was decreased when cylinder liner specimens was tested with Oil A. However, shallow grooves are visible as shown in Figure 4.6 (b).

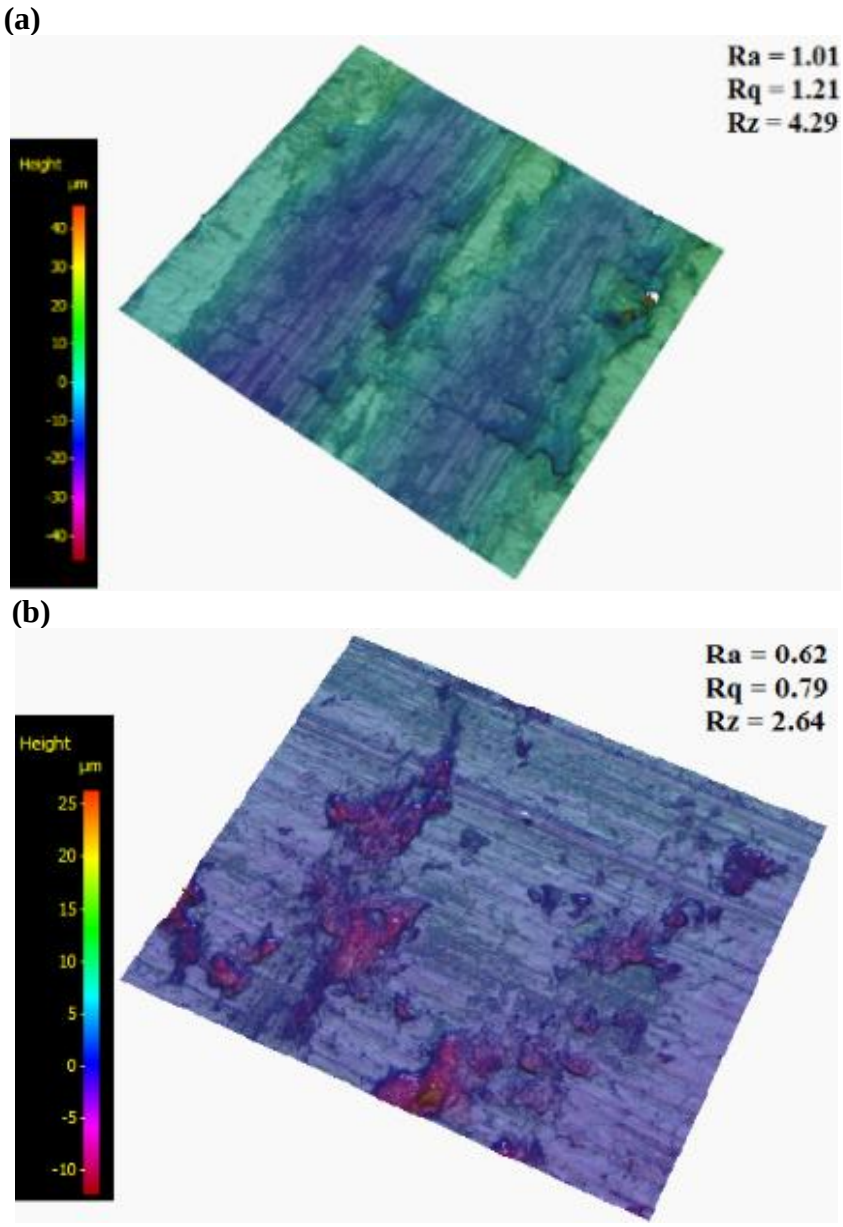

Figure 4.6: 3-D surface profile of liner specimen (a) new (b) tested with Oil A

4.2 Tribological Analysis of Nanoparticles Enriched Palm TMP Ester

After investigation of friction behavior and AW characteristics of palm TMP ester, the tribological behavior of the nanolubricants was investigated by tribo-testing. The most suitable type and concentration of nanoparticles was evaluated in terms of low COF and wear volumes, which was then tested for lubrication performance during long duration engine testing.

4.2.1 Dispersion Stability of Nanolubricants

For long stationary applications as well as consistent tribological performance, stable nanolubricant suspensions were required. To present the quantitative dispersion stability analysis of nanolubricant samples, UV-vis spectral absorbency tests were carried out. Generally, there is a linear relationship between the absorbance and the concentration of nanoparticles in the nanolubricant. Higher the value of optical absorbance, the stable will be the dispersion. The degree of absorbance is proportional to the amount of particles per unit volume, and thus, this measure can be used to denote variations in supernatant particle concentration in the solution with time (Amiruddin et al., 2015; Yu & Xie, 2012). UV–vis spectrophotometer absorbance test was performed immediately after the ultrasonic dispersion of nanoparticles in the lubricant. Time rate changes in the absorbance level of visible light were recorded to measure the dispersion capability of the samples.

4.2.1.1 Dispersion Analysis of nanoCuO Enriched Lubricants

Figure 4.7 indicates the profiles of optical absorbance for lubricant samples dispersed with the nanoCuO. The spectral absorbency profiles show a continuous improvement in dispersion stability when nanoCuO concentration is increased from 0.25 wt% (Oil B) to 1 wt % (Oil E). Oil E shows the most stable trends in terms of optical absorbency as shown in Figure 4.7. But a further increase in nanoCuO concentrations i.e. 1.25 wt % (Oil

F) and 1.5 wt% (Oil G), results in poorly stable dispersions. The poor dispersion stability for Oil F and Oil G was resulted due to tendency of agglomeration and sedimentation which has been observed after first 24 hours. For all the CuO enriched nanolubricants, a continuously low dispersion stability has been witnessed at the end of two weeks. The separation interfaces between the sediment and the supernatant were sharp after being initially stable. At the end of dispersion tests, all CuO-enriched suspensions tended to isolate into sediments. This behavior of nanoCuO enriched suspensions shows that these nanolubricant samples tend to lose their lubrication performance over the period of their use. Further investigation of the effect of dispersion stability on lubrication performance has been investigated by tribo-testing.

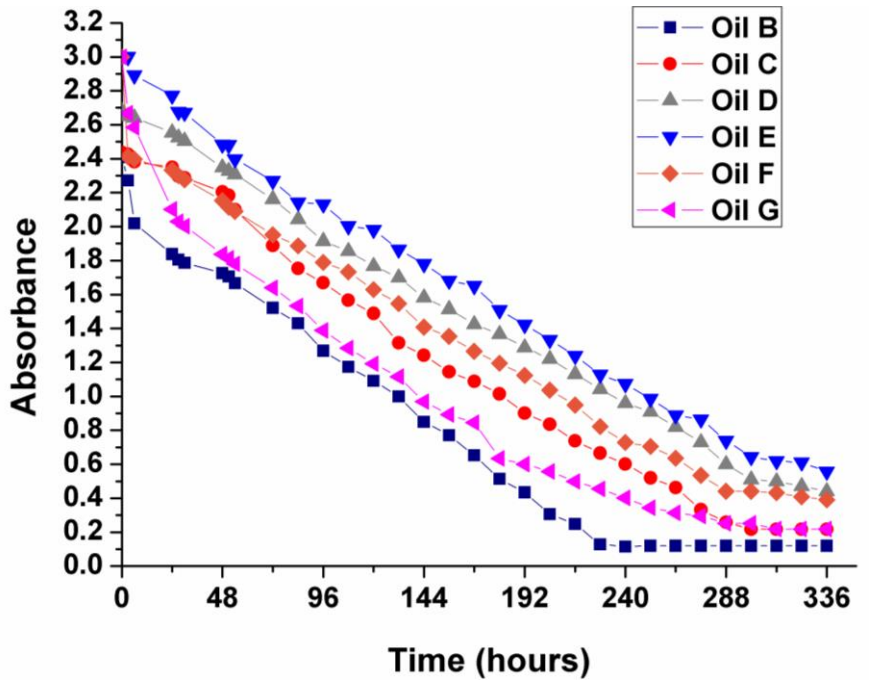

Figure 4.7: The optical absorbance profiles of nanolubricants added with different concentrations of CuO nanoparticles

4.2.1.2 Dispersion Analysis of nanoMoS$_2$ Enriched Lubricants

For nanoMoS$_2$ enriched lubricants, Figure 4.8 shows the spectral absorbency trends over a period of two weeks. Lowest spectral absorbency has been shown by nanolubricant enriched with 0.25 wt% nanoMoS$_2$ (Oil H) while most stable dispersion has been obtained

when 1 wt% nanoMoS_2 was added in palm TMP ester (Oil K). For dispersions containing nanoMoS_2 in higher concentrations i.e. 1.25 wt% (Oil L) and 1.5 wt% (Oil M), relatively low dispersions stability has been observed.

In comparison to nanolubricants enriched with nanoCuO, higher dispersion stability has been observed for dispersions containing nanoMoS_2. However, after a duration of two weeks, sedimentations and low spectral absorbency showed that dispersions are not suitable for long stationary application.

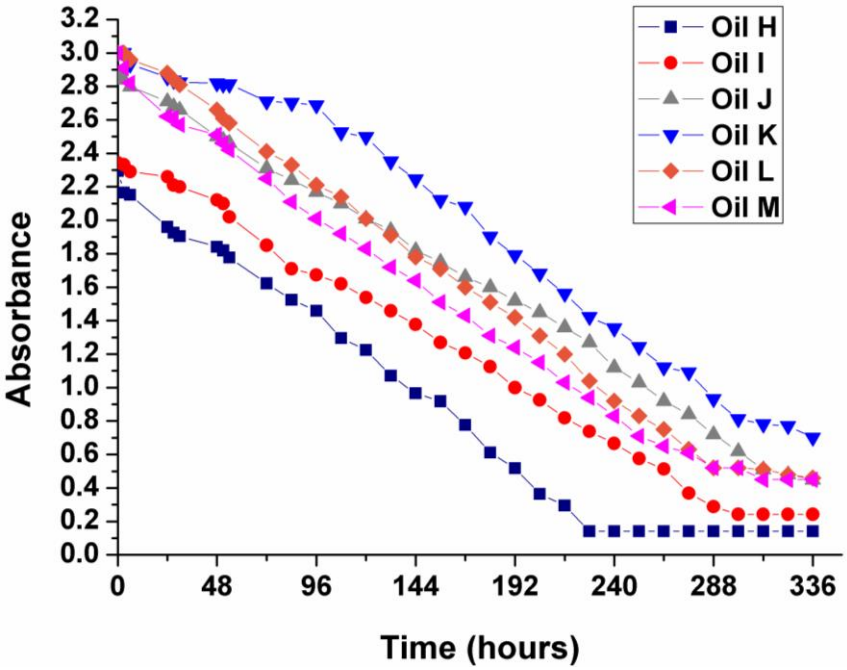

Figure 4.8: The optical absorbance profiles of nanolubricants added with different concentrations of MoS_2 nanoparticles

4.2.1.3 Dispersion Analysis of nanoTiO_2/SiO_2 Enriched Lubricants

Figure 4.9 shows the dispersion stability of the nano-TiO_2/SiO_2-enriched lubricants in terms of optical absorbance. The optical absorbance profiles show that the increasing concentration of nanoTiO_2/SiO_2 from 0.25 wt% to 0.75 wt% raises the optical absorbance. Figure 4.9 shows the stable trend of the nano-TiO_2/SiO_2-enriched lubricant samples as compared to the spectral absorbency profiles by nanoCuO enriched and nanoMoS_2

enriched lubricants. At the end of dispersion analysis, low sediments were observed that can be attributed to tiny size of nano-TiO_2/SiO_2 than those of nanoCuO and nanoMoS_2 nanoparticles as per Stokes' law. Thus, the sedimentation time was increased for all nano-TiO_2/SiO_2 enriched samples and low sedimentation was observed for all samples even after two weeks of static tests. In addition to effect of size, trends of stable dispersions can be attributed to the part of nano-SiO_2 in the TiO_2/SiO_2 nanocomposite given that nano-SiO_2 exhibits a homogenous and stable dispersion in oil for long periods (Jiao et al., 2011; Xie et al., 2015). Figure 4.9 shows that 0.75 wt% nano-TiO_2/SiO_2 (Oil P) provided the most suitable dispersion stability among all the considered lubricants in this work. The dispersion stability was seen to be a function of weight concentration of the nano-additives as a rapid decline in absorbance can be seen for nanolubricants containing 1 wt% - 1.5 wt%, of nano-TiO_2/SiO_2. Such trend can be attributed to increase in agglomeration tendency and sedimentation at higher concentrations of nano-TiO_2/SiO_2.

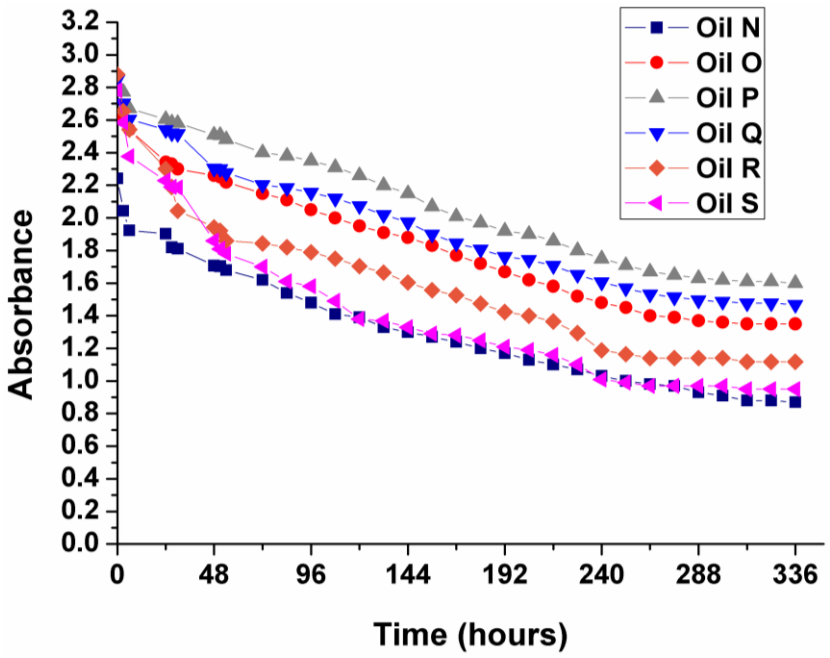

Figure 4.9: The optical absorbance profiles of nanolubricants added with different concentrations of TiO_2/SiO_2 nanoparticles

4.2.2 Friction Results for Nanolubricants

4.2.2.1 Friction Behavior of nanoCuO Enriched Lubricants

Figure 4.10 shows the COF trends over the tribo-test duration for nanoCuO enriched lubricants. For piston ring–cylinder line r sliding tests, highest friction resistance has been observed for suspensions containing 1 wt% concentrations of CuO nanoparticles ((Figure 4.10) and (Figure 4.11)). Initially the friction resistance was improved by addition of nanoparticles from 0.25 wt% to 1 wt% but further increase resulted in increased friction. An average COF as low as 0.14 has been shown by Oil E as illustrated in Figure 4.11. An improvement of 11.7% has been observed for Oil E as compared to Oil A. The higher concentrations of nanoCuO (Oil F and Oil G) resulted in higher COF than that of Oil E and even higher as compared to Oil A. Similar trends of increased COF at increased concentrations than optimum concentration, have been reported by a number of previous research works (Chou et al., 2010; Thottackkad et al., 2012). Such variation in friction behavior by changing nanoparticles concentration, can be attributed to the dispersion stability. Oil E showed better dispersion stability than other oil samples containing CuO nanoparticles. For nanolubricants such friction reduction may also be attributed to the tribofilm formation on the sliding surfaces and secondary effect of surface enhancement resulting by the surface polishing effect by nanoparticles. To understand the lubrication mechanism by these nanolubricants, surface analysis was required to investigate the potential lubrication mechanism. Therefore, surface analysis tools including SEM, EDX, Raman spectroscopy and 3-D surface profilometry were used to explore the possible lubrication mechanism in subsequent sections of this chapter.

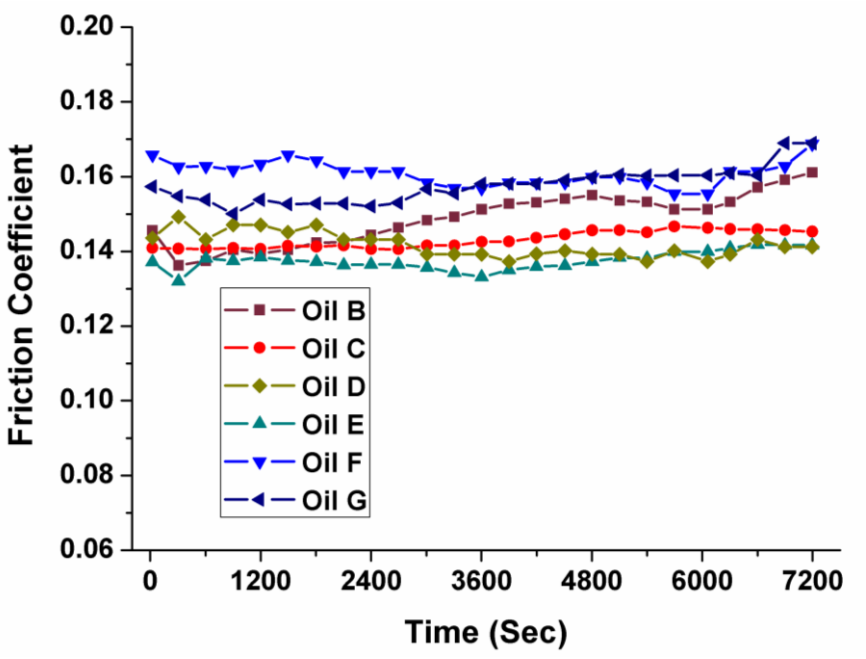

Figure 4.10: COF as a function of sliding time for nanoCuO enriched lubricants

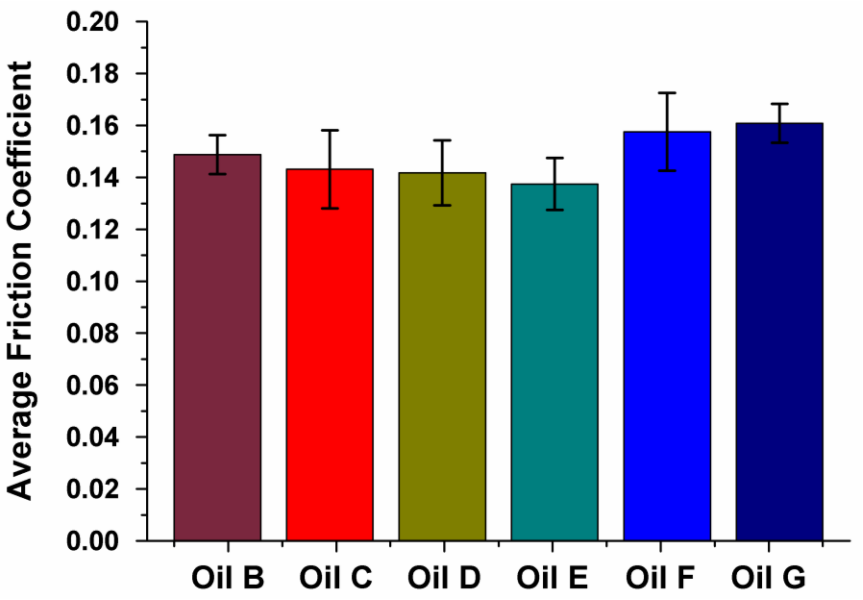

Figure 4.11: Average COF for nanoCuO enriched lubricants

4.2.2.2 Friction Behavior of nanoMoS$_2$ Enriched Lubricants

For nanoMoS$_2$ enriched lubricants, low resistance to shear was expected due to a layered structure having weak van der Waals forces between its molecular layers (Sahoo & Biswas, 2014; Xie et al., 2015). Figure 4.12 shows the profiles of COF for considered nanoMoS$_2$ enriched lubricants over the complete test duration. It can be observed that increasing nanoMoS$_2$ concentration from 0.25 wt% to 1 wt% has reduced the average COF. Further increase i.e. 1.25 wt% (Oil L) and 1.5 wt% (Oil M), resulted in higher friction. An average COF as low as 0.11 has been shown by Oil K. Thus, a significant improvement (42.2%) has been observed in friction behavior for Oil K as compared to Oil A (Figure 4.13). Such improved behavior of nanoMoS$_2$ enriched lubricants can be related to layered structure of MoS$_2$ which can significantly reduce boundary friction. There is a possibility of chemical interaction of MoS$_2$ with the sliding surfaces and formation of a tribofilm. The possibility of protective film formation and polishing effects were investigated by surface analysis of tested cylinder liner specimen.

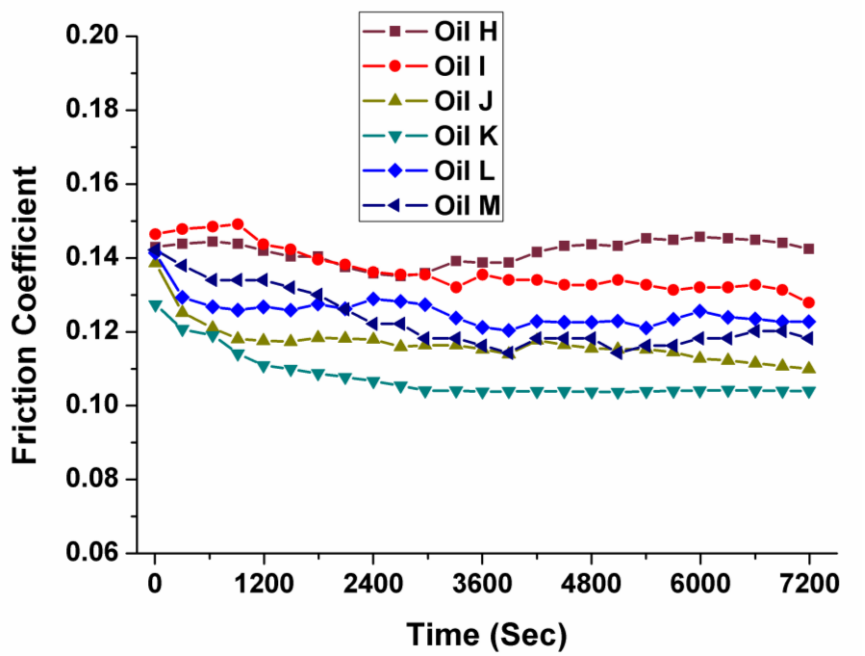

Figure 4.12: COF as a function of sliding time for nanoMoS$_2$ enriched lubricants

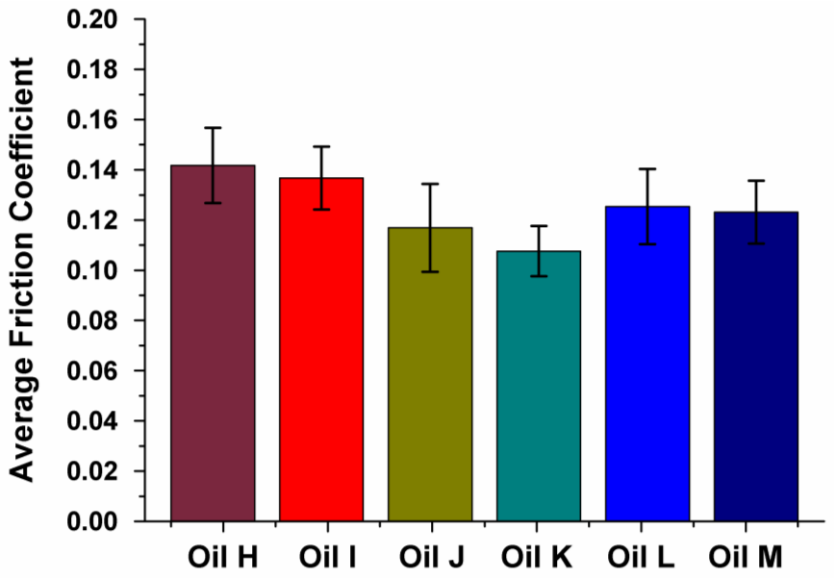

Figure 4.13: Average COF for nanoMoS2 enriched lubricants

4.2.2.3 Friction Behavior of nanoTiO_2/SiO_2 Enriched Lubricants

Figure 4.14 shows friction behavior of nanoTiO_2/SiO_2 enriched lubricants over the sliding test duration. It can be observed that COF for these lubricant samples were significantly lowered than those of nanoCuO (Figure 4.11) as well as nanoMoS_2 enriched lubricants (Figure 4.13). Lowest average COF value of 0.09 has been observed for nanolubricant containing 0.75 wt% nanoTiO_2/SiO_2 (Oil P) as compared to all other nanolubricants (Figure 4.15). A significant improvement as high as 70% has been shown by Oil P as compared to base oil i.e. Oil A. While investigating the factors for this improved friction behavior, uniform and stable dispersions of nanoTiO_2/SiO_2 enriched lubricants believed to be the major contributor. Stable dispersion helped in providing the continuous resistance against friction over the test duration. Due to uniform distribution and continuous availability of nanoTiO_2/SiO_2 in the lubricating oil samples, there were more chances of enhancement of rubbing surfaces and penetrations of tiny size particles in the pits and grooves of worn surfaces. This tendency was further investigated by analyzing the worn surfaces for tribofilm formation and potential surface enhancement mechanisms.

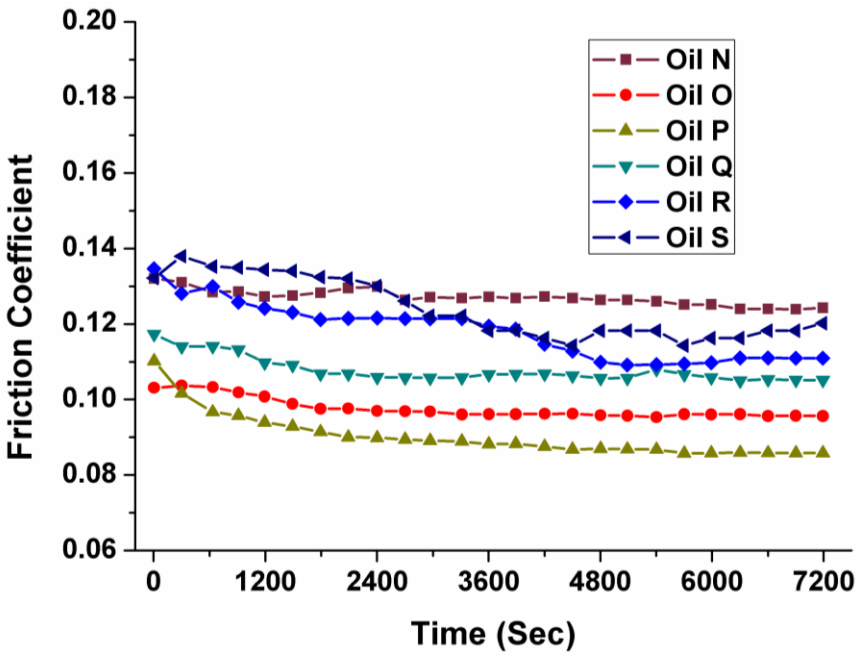

Figure 4.14: COF against sliding time for nanoTiO$_2$/SiO$_2$ enriched lubricants

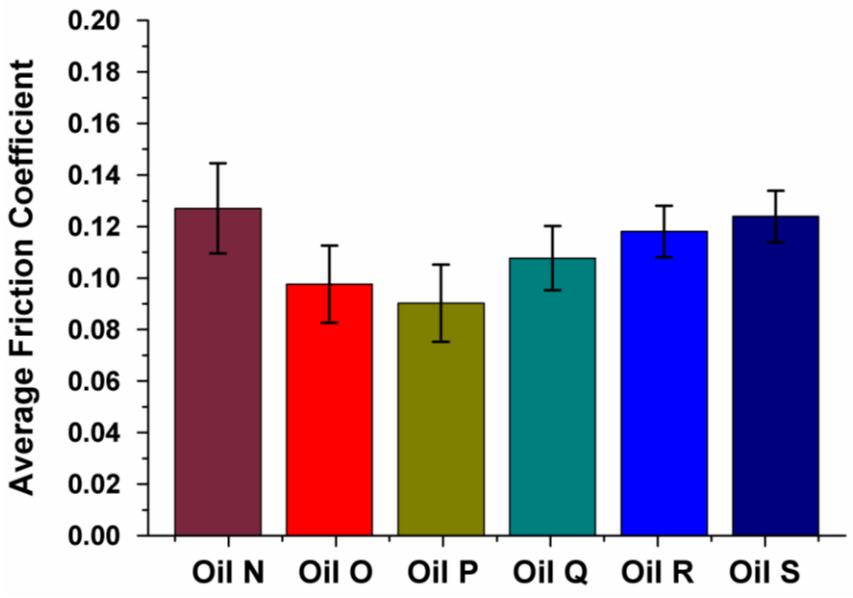

Figure 4.15: Average COF for nanoTiO$_2$/SiO$_2$ enriched lubricants

While analyzing all the friction results, it can be observed that the nanoparticles concentrations play a significant role in the development of stable dispersions which in turn results in improved friction behavior. Figure 4.16 shows the average COF as a function of nanoparticles concentration. As discussed earlier, lowest COF has been observed for nanolubricant containing 0.75 wt% nanoTiO$_2$/SiO$_2$ (Oil P). To get suitable

nanoparticle concentration and type, AW and EP characteristics were also taken into consideration.

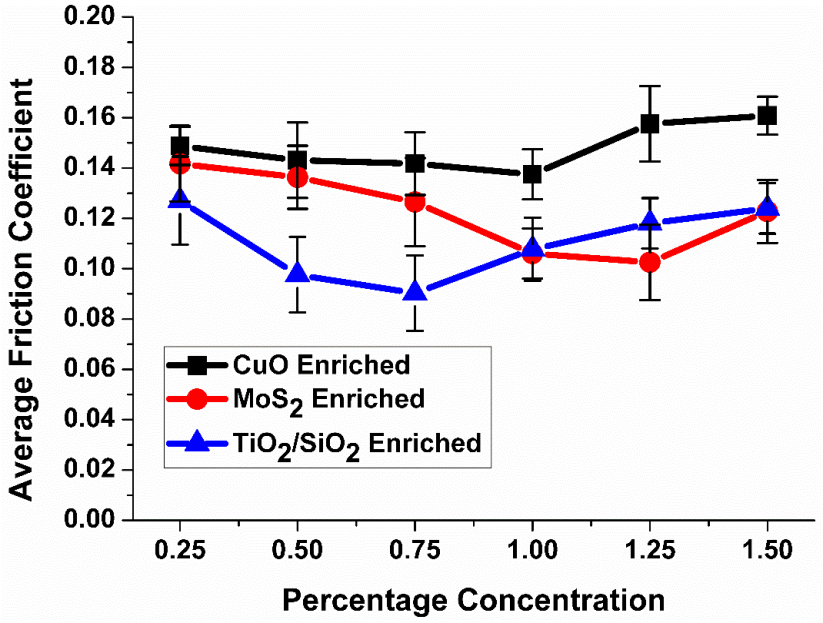

Figure 4.16: Effect of nanoparticles concentration on COF

4.2.3 Wear Results for Nanolubricants

4.2.3.1 Wear Loss for nanoCuO Enriched Lubricants

Figure 4.17 (a-b) illustrates the wear volume of cylinder liner as well as piston ring specimen for tribo-tests carried out using nanoCuO enriched lubricants. Significant reduction in wear volume has been achieved as the nanoCuO concentration was increased from 0.25 wt% to 1.5 wt%. Unlike the friction behavior, wear volume was reduced even at higher concentrations for nanoCuO enriched lubricants. For cylinder liner specimen, an improved wear protection as high as 44.3% has been shown by Oil G as compared to wear volume resulted by using Oil A. While piston ring wear was reduced to one-third by Oil F and Oil G as compared to Oil A. This trend of wear behavior can be related to the mending effect which seemed to be improved by increasing the nanoparticles concentrations. This effect of mending was further investigated by SEM and EDX analysis in Section 4.2.5 and Section 4.2.6 of this chapter.

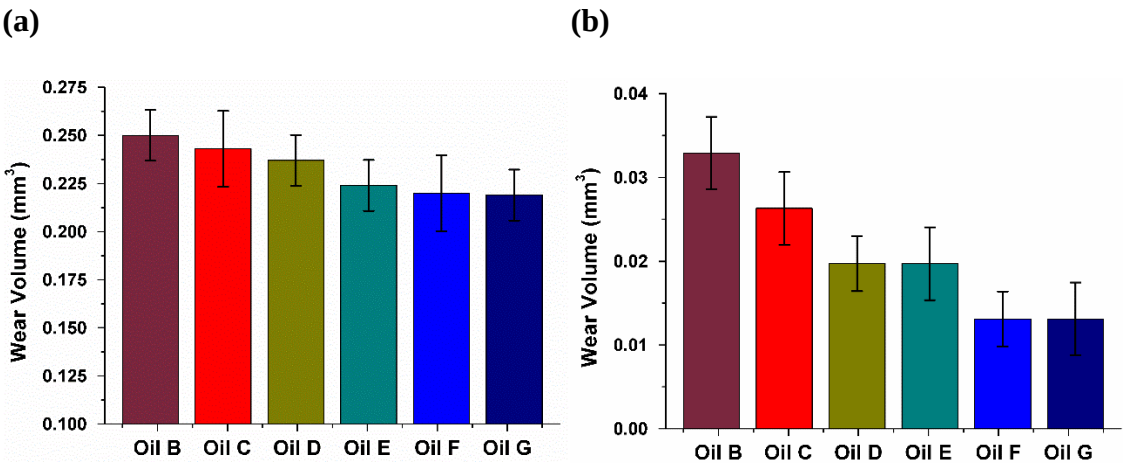

Figure 4.17: Wear volume by nanoCuO enriched lubricants for (a) Cylinder liner specimen (b) Piston ring specimen

4.2.3.2 Wear Loss for nanoMoS$_2$ Enriched Lubricants

For nanoMoS$_2$ enriched lubricants, wear volumes are illustrated in Figure 4.18. Likewise, nanoCuO enriched lubricants, it can be observed that increase in the nanoparticles concentrations from 0.25 wt% to 1.5 wt% improved the AW properties of palm TMP ester for cylinder liner specimen. For nanoMoS$_2$ enriched lubricants a constant piston ring wear volume has been observed for 1 wt% (Oil K), 1.25 wt% (Oil L) and 1.5 wt% (Oil M). While CuO enriched suspensions showed significant improvement in piston ring wear volume at 1.25 wt% (Figure 4.18(b)). A maximum reduction of 77.5% has been achieved in wear volume of cylinder liner by Oil M as compared to Oil A. This shows that nanoMoS$_2$ enriched lubricants showed better wear protection as compared to nanoCuO enriched lubricants. Such wear protection ability of nanoMoS$_2$ based lubricants may be attributed to the comparatively uniform dispersions as compared to nanoCuO based lubricants. Thus, a uniform mending effect of worn surfaces was believed to help in reduction of material loss. This phenomenon of improved AW behavior was further investigated by using surface analysis tools in Section 4.2.4 of this chapter.

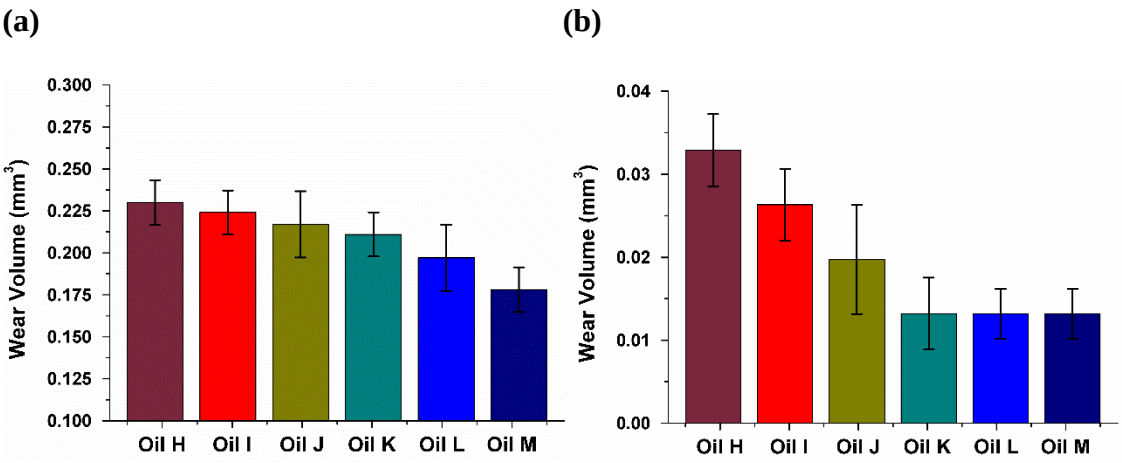

Figure 4.18: Wear volume by nanoMoS$_2$ enriched lubricants for (a) Cylinder liner specimen (b) Piston ring specimen

4.2.3.3 Wear Loss for nanoTiO$_2$/SiO$_2$ Enriched Lubricants

For nanoTiO$_2$/SiO$_2$ enriched lubricants, lowest wear volumes have been observed as illustrated in Figure 4.19. Like other nanolubricant samples, the AW characteristics were improved initially by increasing nanaoTiO$_2$/SiO$_2$ but unlike suspension containing nanoCuO and nano MoS$_2$, no improvement has been observed after 0.75 wt% (Oil P). It can be observed that lowest wear loss has been shown by Oil P, Oil Q and Oil R. This is the significant reduction of wear loss as compared to all nanoCuO based lubricants as well as nanoMoS$_2$ based lubricants for piston ring as well as cylinder liner specimen. In this case the wear loss has been reduced to at least half than that of Oil A. Thus, Oil P is reported to be the most suitable nanolubricant which showed highest wear protection with minimum nanaoTiO$_2$/SiO$_2$ concentrations. For cylinder liner wear, Oil P proved to be nearly 1.5 times effective than its counterparts of nanoCuO enriched and nanoMoS$_2$ enriched samples.

As compared to other nanolubricants, such behavior can be owed to uniform and stable dispersions and relatively smaller size of nanaoTiO$_2$/SiO$_2$ which made them able to penetrate the contact zones more easily than larger ones, and provide uniform surface mending effect. This surface enhancement effect of mending was believed to be

facilitated by higher supply and availability of nanoparticles between interacting surfaces. On the other side, larger particles tend to accumulate in front of the leading edge of the base body and counter-body which leads to the lubricant starvation of the contact zone. Thus, high material loss has been observed for nanoCuO and nanoMoS_2 enriched lubricants in comparison to nanoTiO_2/SiO_2 based nanolubricants. The potential wear protection mechanism was analyzed and discussed by using surface analysis tools like SEM, EDX, Raman spectroscopy and 3-D surface profilometry (Section 4.2.4).

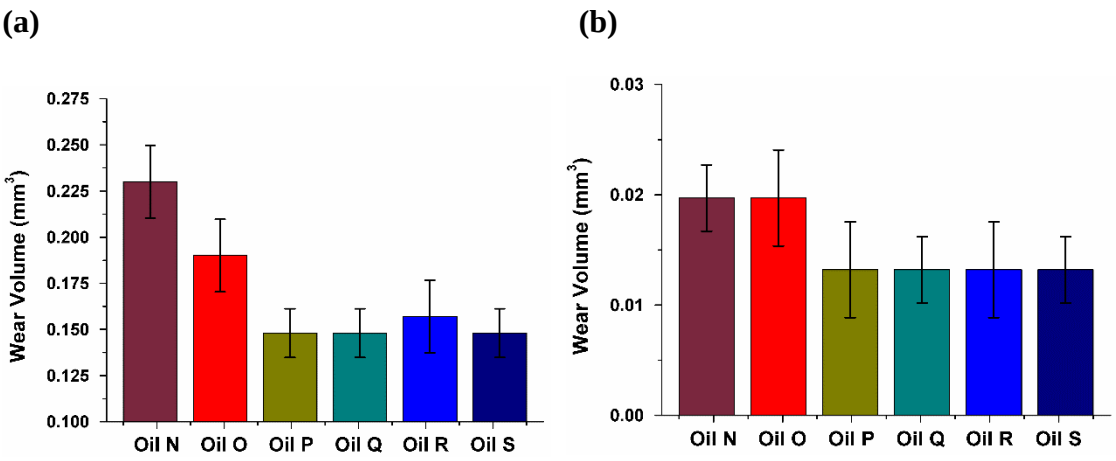

Figure 4.19: Wear volume by nanoTiO_2/SiO_2 enriched lubricants for (a) Cylinder liner specimen (b) Piston ring specimen

While analyzing all the friction results, it can be observed that the wear protection ability has been improved or remained constant, by increasing the nanoparticles concentrations for all three types of nanoparticles (Figure 4.20 and Figure 4.21). The most suitable antiwear characteristics are shown by 0.75 wt% nanoTiO_2/SiO_2 and relatively constant behavior has been shown at higher concentrations i.e. 1 wt % (Oil Q), 1.25 wt% (Oil R) and 1.5 wt% (Oil S).

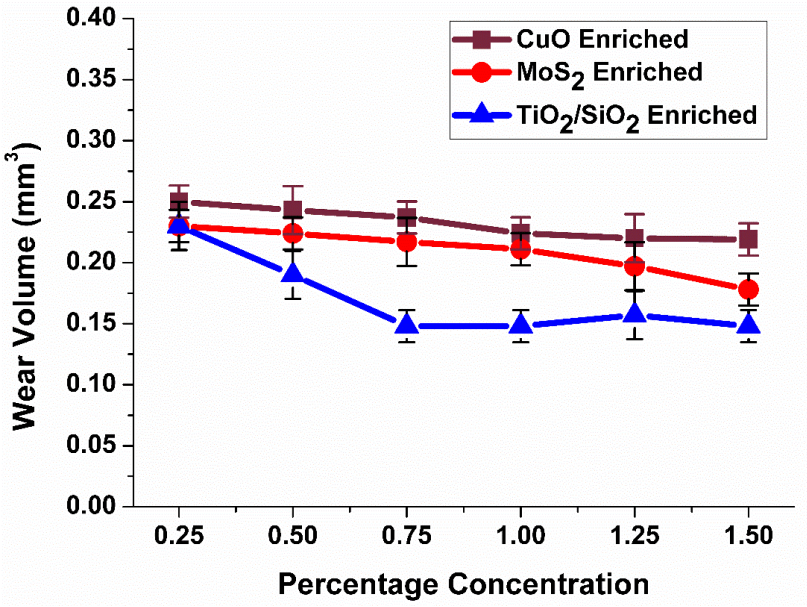

Figure 4.20: Effect of nanoparticles concentration on wear of cylinder liner specimen

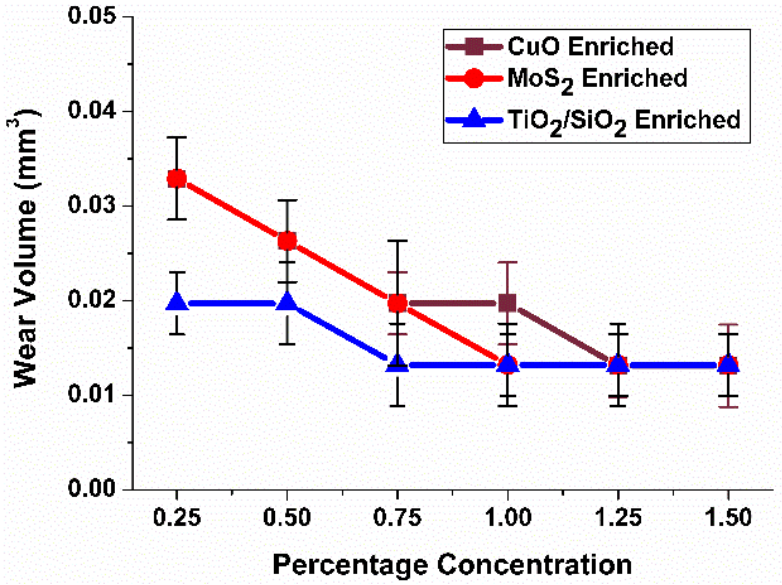

Figure 4.21: Effect of nanoparticles concentration on wear of piston ring specimen

4.2.4 Surface Analysis

To understand the lubrication mechanisms of nanoparticles enriched suspensions, worn surfaces of cylinder liner test specimen were analyzed by using surface

characterization tools. Surface analysis was performed for cylinder liner specimen tested with all nanoparticles enriched suspensions to compare with that of Oil A.

4.2.5 SEM Analysis

SEM analysis was carried out for all the cylinder liner specimen tested with nanolubricant samples. In majority of the cases, surface enhancement effect has been observed for considered nanolubricant samples. The worn surfaces micrographs and related surface morphology are discussed in this section.

4.2.5.1 SEM Analysis for nanoCuO Enriched Lubricants

Figure 4.22 shows SEM micrographs of cylinder liner specimen tested with nanoCuO enriched lubricants. Low magnification micrographs at 20x magnification are shown in Figure 4.22 (a-f) while corresponding micrographs at higher magnification of 200x are illustrated in Figure 4.22 (a_1-f_1). It can be observed that increasing nanoparticles concentrations helped in the surface mending by the nanoparticles deposition on the cylinder liner surface. At low concentrations of nanoCuO i.e. 0.25 wt% - 0.75 wt% (Oil B, Oil C, Oil D) higher tendency of shallow grooves and pits have been observed. Increasing the nanoCuO concentrations i.e. 1 wt% - 1.5 wt% (Oil E, Oil F, Oil G) resulted in improved surface mending effect by filling the shallow grooves as illustrated in Figure 4.22 (d-f) and Figure 4.22 (d_1-f_1). The demonstrated surface filling and mending by nanoparticles deposition support the wear volume results of tested cylinder liner surfaces as mentioned in Section 4.2.3.1.

The mending mechanism by the material filling using the nanoparticles has been reported by various researchers (Choi et al., 2009; Padgurskas et al., 2013; H. L. Yu et al., 2008). Such an effect of surface enhancement improves the wear protection ability (Chang, Zhang, Breidt, & Friedrich, 2005; Peng, Kang, et al., 2010).

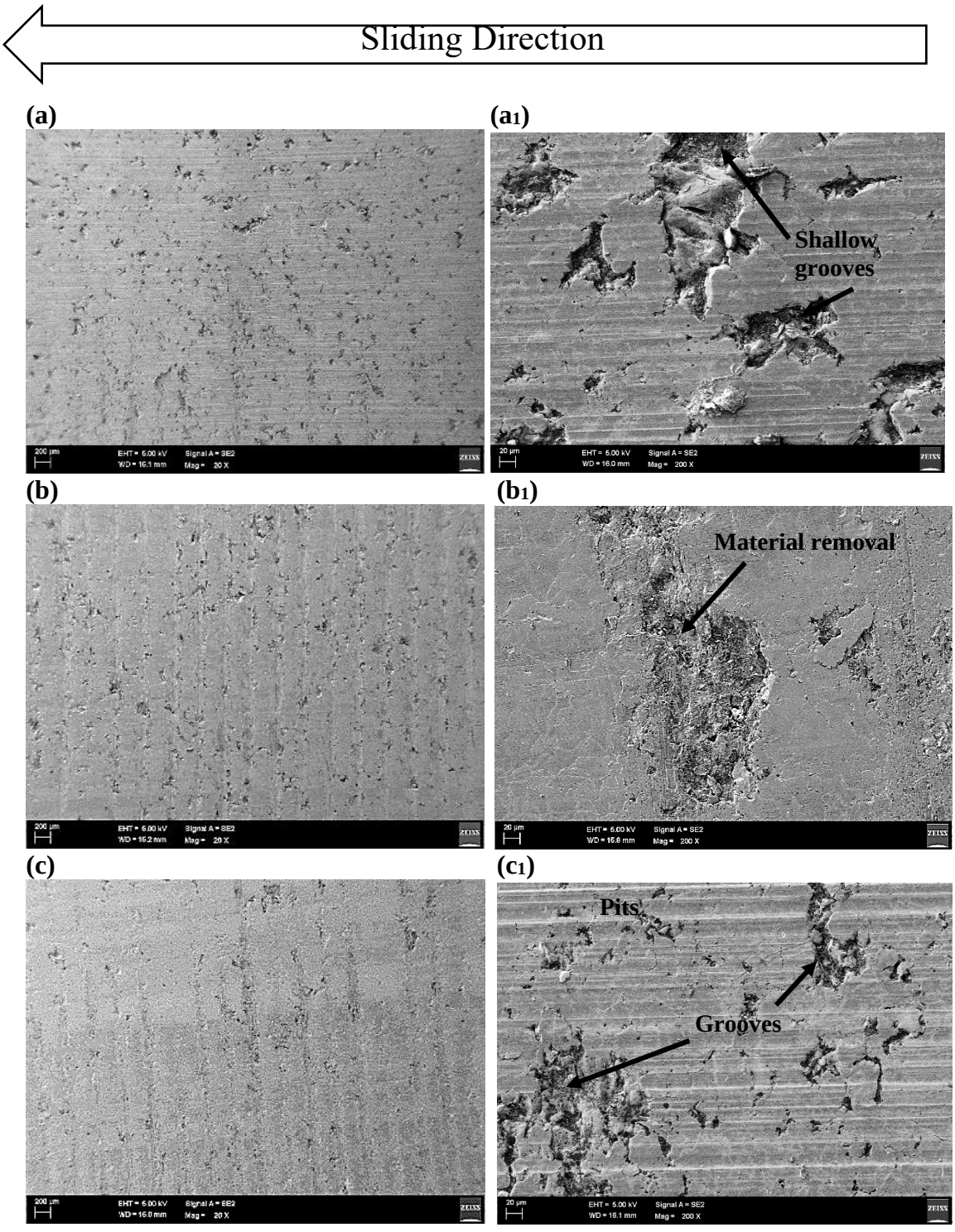

(Continued on next page)

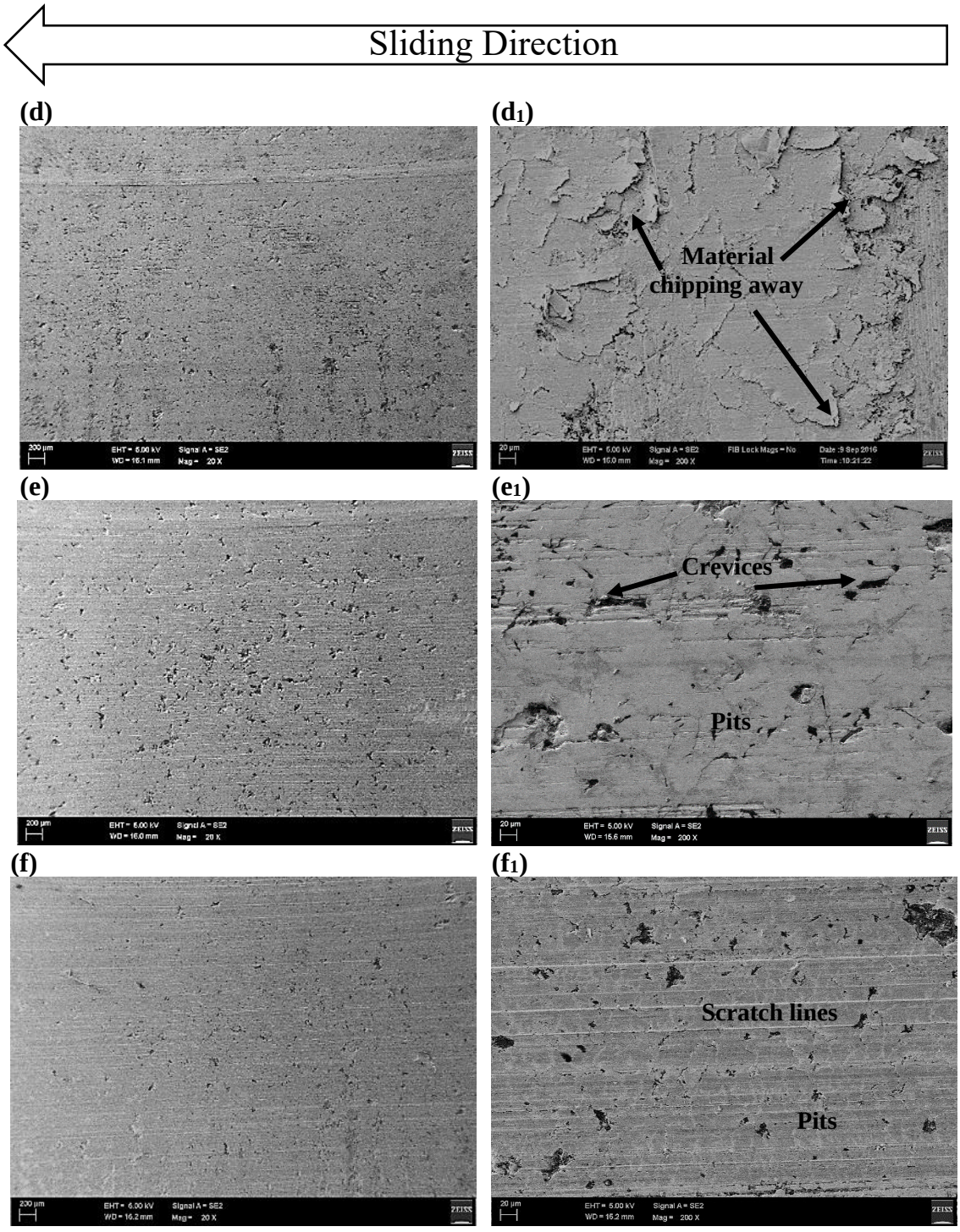

Figure 4.22: SEM micrographs of worn cylinder liner specimen tested with (a) Oil B 20x, (a_1) Oil B 200x, (b) Oil C 20x, (b_1) Oil C 200x, (c) Oil D 20x, (c_1) Oil D 200x, (d) Oil E 20x, (d_1) Oil E 200x, (e) Oil F 20x, (e_1) Oil F 200x, (f) Oil G 20x, (f_1) Oil G 200x

4.2.5.2 SEM Analysis for nanoMoS_2 Enriched Lubricants

Figure 4.23 shows SEM micrographs of cylinder liner specimen tested with nanoMoS_2 enriched lubricants. As compared to nanoCuO enriched lubricants, improved surface enhancement can be observed for all the nanoMoS_2 enriched dispersions. Due to this higher tendency of surface mending, low wear volumes were exhibited by nanoMoS_2 based lubricants than those of lubricant samples developed by adding nanoCuO. Significant material removal was observed for 0.25 wt% nanoMoS_2 (Oil H) as shown in Figure 4.23 (a) and Figure 4.23 (a_1). The surface mending can be observed for cylinder liner specimen tested with 0.5 wt% - 1.5 wt% nanoMoS_2 enriched lubricants as shown in Figure 4.23 (b-f)) and Figure 4.23 (b_1-f_1).

It can be observed that increasing nanoparticles concentrations helped in the surface mending by the nanoparticles deposition on the cylinder liner surface. The improved behavior of nanoMoS_2 based nanolubricants can be related to the uniform and stable dispersions as compared to lubricants added with nanoCuO. Due to stable dispersions, there is more availability of nanoparticles to penetrate the rubbing surfaces and fill up the wear scars and grooves.

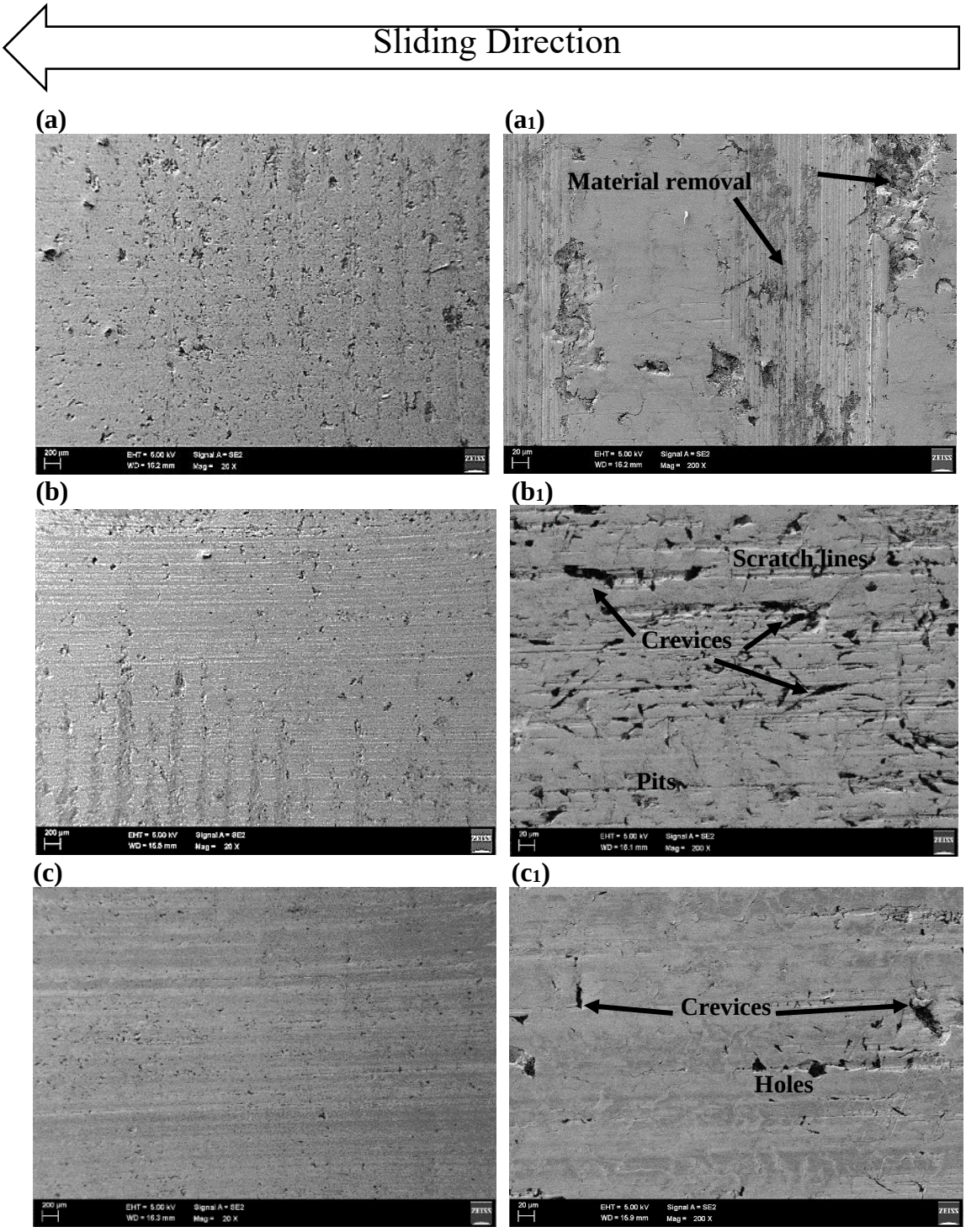

(Continued on next page)

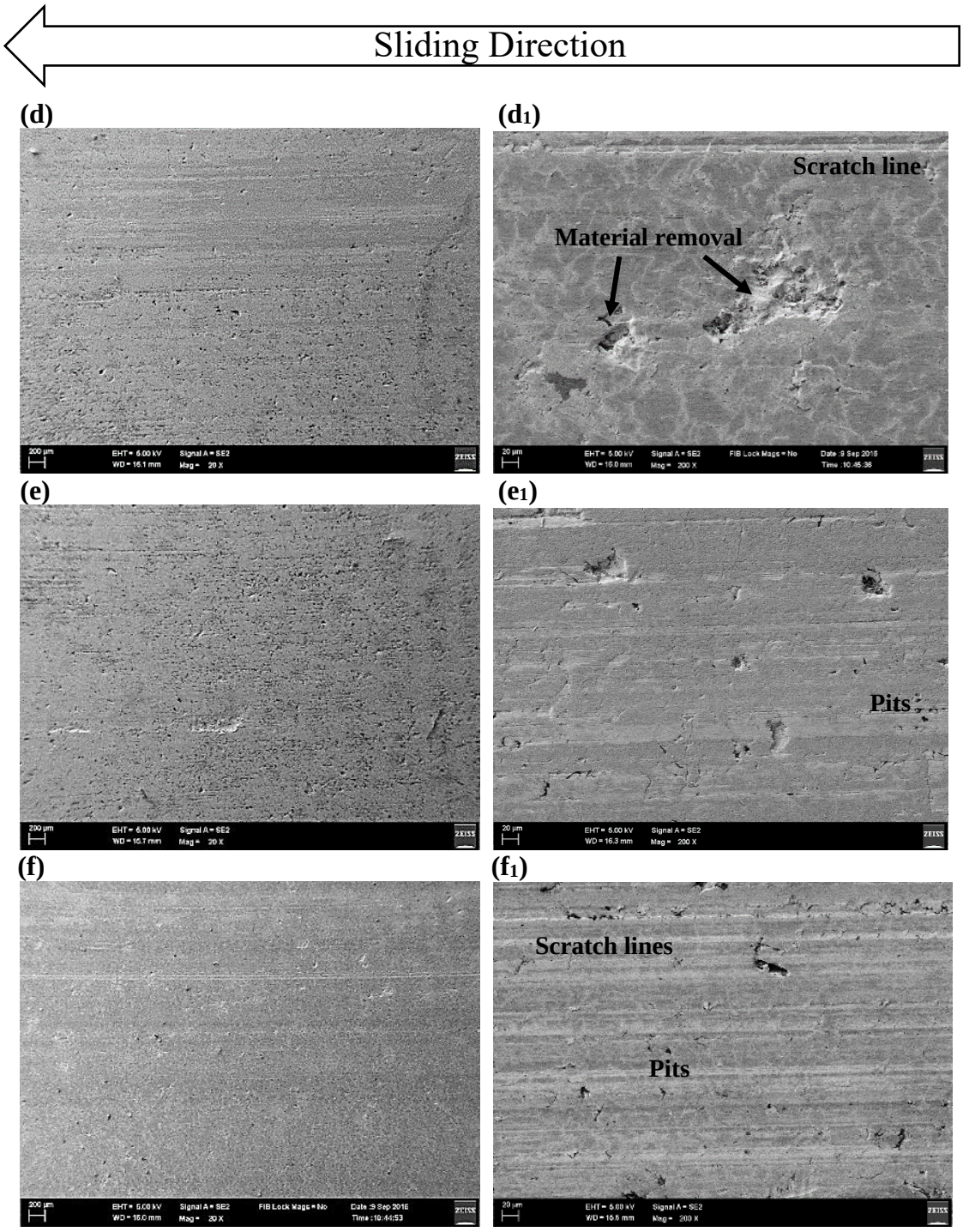

Figure 4.23: SEM micrographs of worn cylinder liner specimen tested with (a) Oil H 20x, (a_1) Oil H 200x (b) Oil I 20x, (b_1) Oil I 200x, (c) Oil J 20x, (c_1) Oil J 200x, (d) Oil K 20x, (d_1) Oil K 200x, (e) Oil L 20x, (e_1) Oil L 200x, (f) Oil M 20x and (f_1) Oil M 200x

4.2.5.3 SEM Analysis for nanoTiO_2/SiO_2 Enriched Lubricants

SEM micrographs of cylinder liner specimen tested with nanoTiO_2/SiO_2 enriched lubricants are given at low magnification (20x) (Figure 4.24 (a-f)) and high magnification (200x) (Figure 4.24 (a_1-f_1)). The significant surface enhancement effect in terms of surface mending has been observed for all nanolubricants containing nanoTiO_2/SiO_2. Oil P showed highest surface mending and polishing as demonstrated at low magnification in Figure 4.24 (c) and at high magnification in Figure 4.24 (c_1). The tendency of surface enhancement was observed to be prominent for nanoTiO_2/SiO_2 enriched lubricants as compared to its counterparts i.e. nanoCuO and nanoMoS_2 based lubricant samples. The mending effect of material filling using nanoparticles has been reported by various researchers (Choi et al., 2009; Padgurskas et al., 2013; H. L. Yu et al., 2008). Such surface enhancement effect of polishing and mending resulted in reduced friction and improved wear protection capability (Chang et al., 2005; Peng, Kang, et al., 2010). This significant improvement in the wear protection ability of nanoTiO_2/SiO_2 lubricants may be related to the most stable dispersions which help in providing continuous nanoparticles supply to precipitate on the rubbing surfaces. In addition to stable dispersions, the tiny size of nanoTiO_2/SiO_2 was also believed to provide this mending and surface smoothening.

It is worth mentioning here that stable and uniform distribution of nanoparticles plays the vital role and its effect was prominent as compared to the role of other influencing factors like size, shape and structure of nanoparticles. Due to this reason MoS_2 enriched lubricants showed better lubrication performance than lubricating oils added with CuO nanoparticles. Similarly, the lubricating oil samples containing nanoTiO_2/SiO_2, outperformed the other counterparts due to most stable dispersion stability behavior.

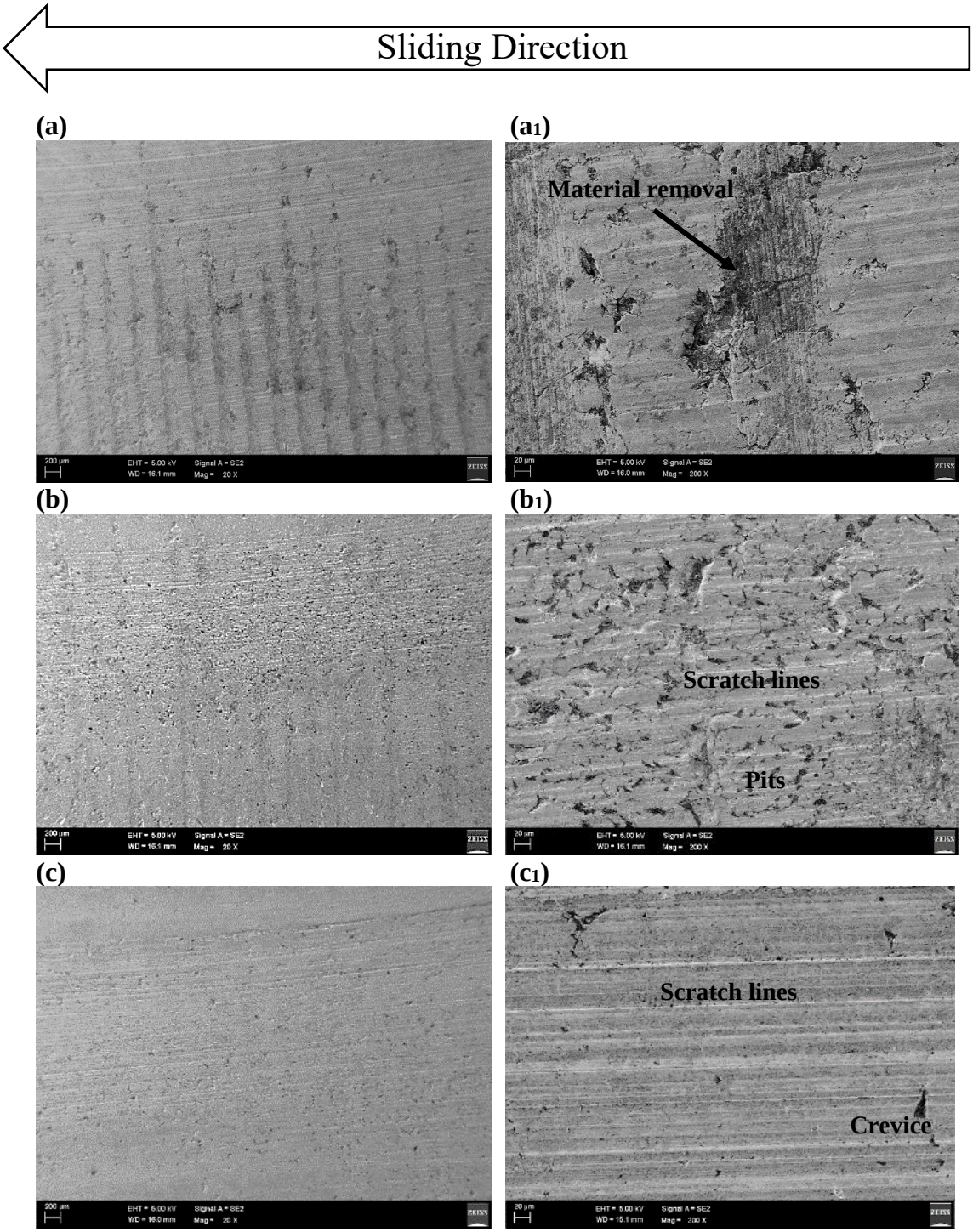

(Continued on next page)

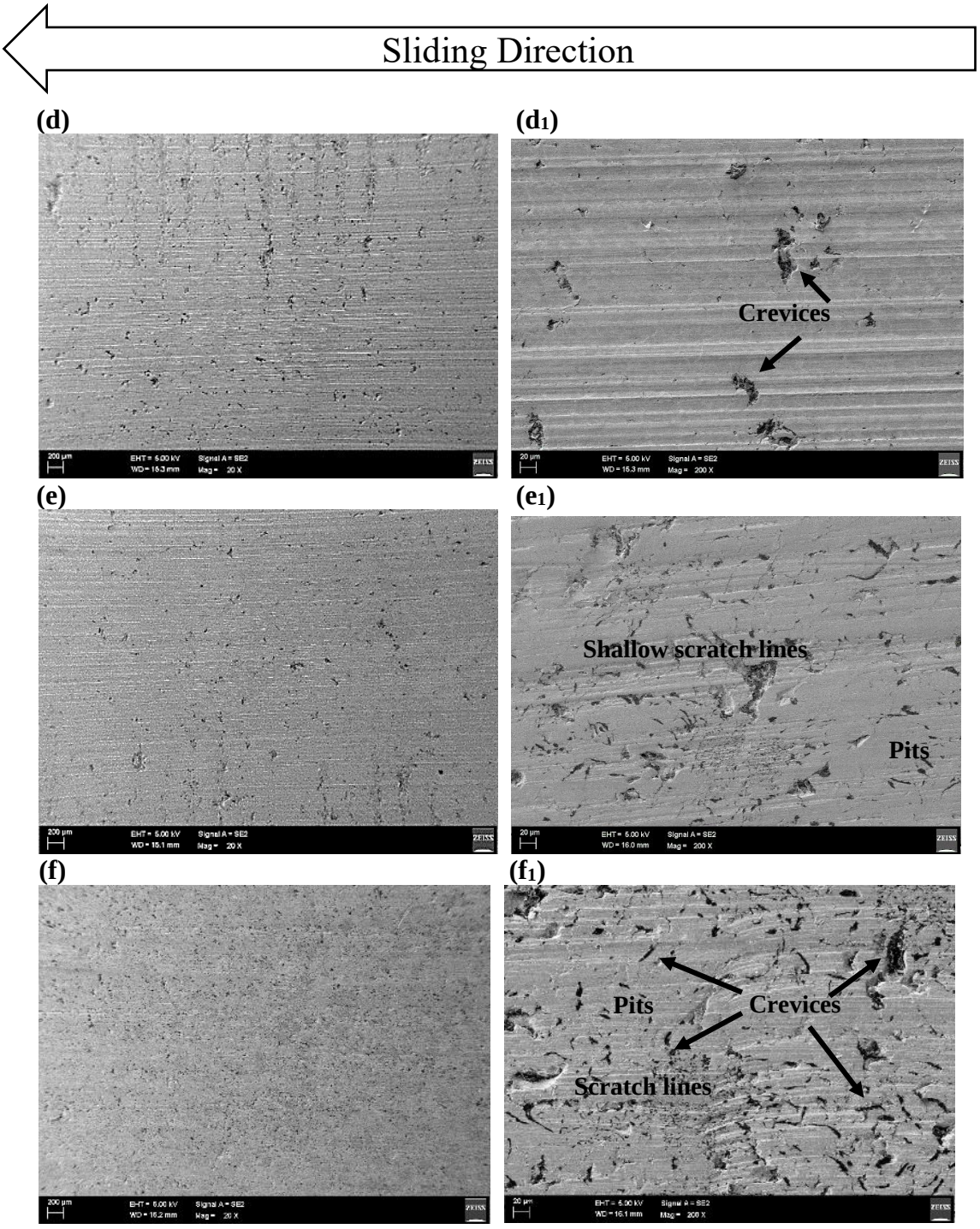

Figure 4.24: SEM micrographs of worn cylinder liner specimen tested with (a) Oil N 20x, (a_1) Oil N 200x (b) Oil O 20x, (b_1) Oil O 200x, (c) Oil P 20x, (c_1) Oil P 200x, (d) Oil Q 20x, (d_1) Oil Q 200x, (e) Oil R 20x, (e_1) Oil R 200x, (f) Oil S 20x and (f_1) Oil S 200x

4.2.6 EDX Analysis

SEM surface characterization was further aided by EDX analysis to understand the lubrication mechanism. EDX analysis provide the elemental details on the worn

surfaces. This tool helps in evaluating the ability of nanoparticles deposition on the contacting surfaces. EDX analysis shows the elemental spectra for the region in SEM micrographs.

Figure 4.25, Figure 4.26 and Figure 4.27 illustrate the elemental spectra for liner surface tested which showed highest element concentrations among nanoCuO, nanoMoS_2 and nanoTiO_2/SiO_2 enriched lubricants respectively. For all the nanolubricant samples, Table 4.1 shows the details of elemental weight percentages obtained by EDX elemental spectra of the cylinder liner tested surfaces. The values of elemental concentrations confirm the existence of elements due to deposition of nanoparticles on the worn surfaces. This confirms the mending effect by all type of nanolubricants. It is also worth mentioning here that the nanolubricants for which higher elemental concentration were observed, the same nanolubricants helped in providing wear protection in terms of minimum loss of wear volume. For nanoTiO_2/SiO_2 enriched lubricants, silicon concentration on the worn surface was negligible while significant concentration of titanium has been observed as depicted by Oil N, Oil O, Oil P, Oil Q, Oil R, Oil S in Table 4.1.

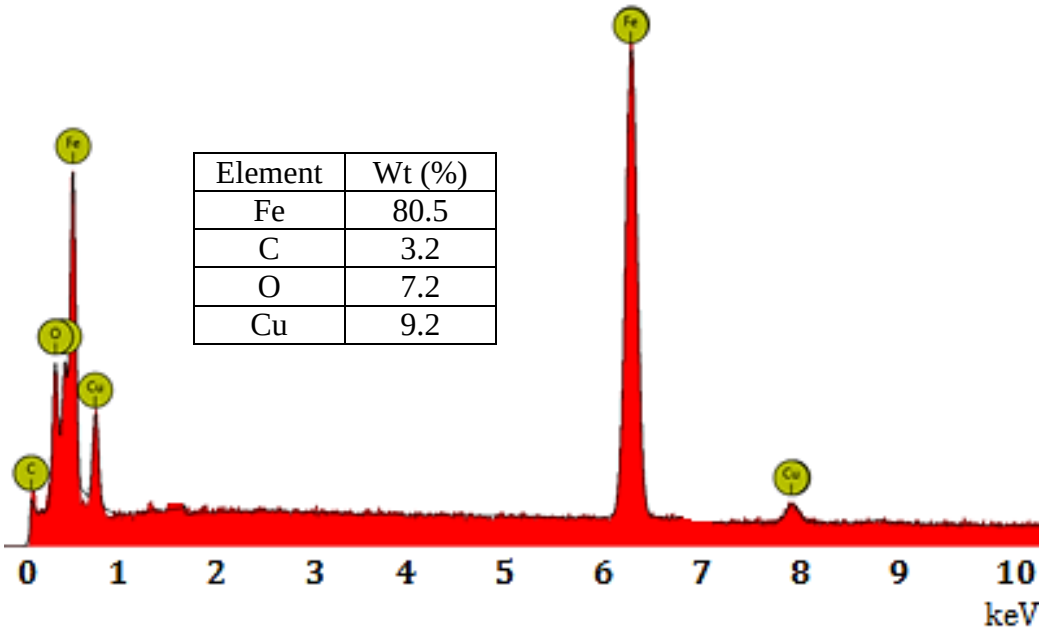

Element	Wt (%)
Fe	80.5
C	3.2
O	7.2
Cu	9.2

Figure 4.25: EDX elemental spectra of cylinder liner specimen tested with Oil F

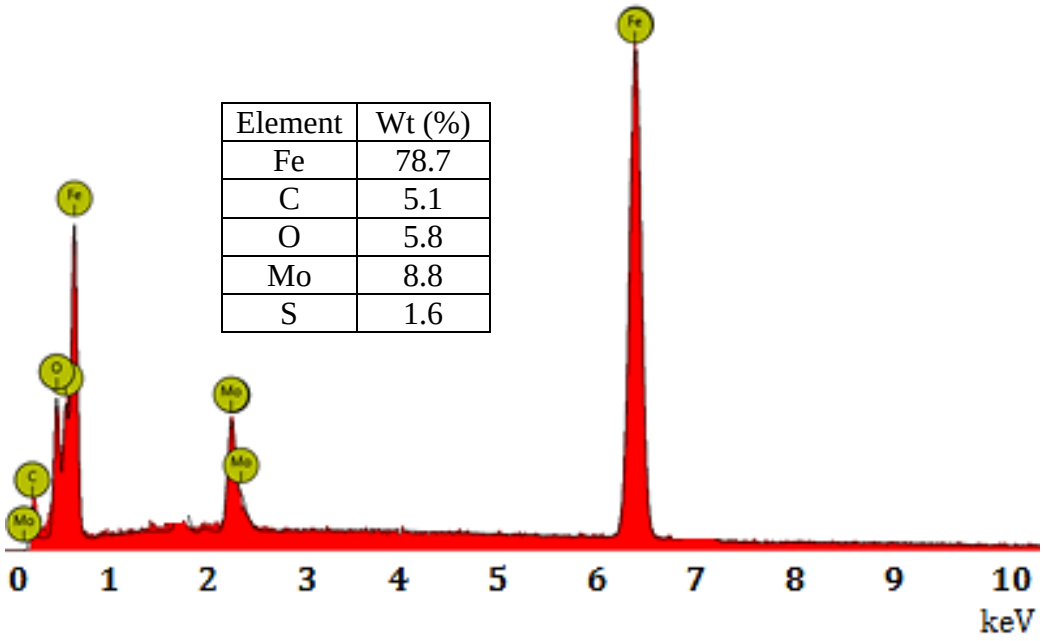

Figure 4.26: EDX elemental spectra of cylinder liner specimen tested with Oil M

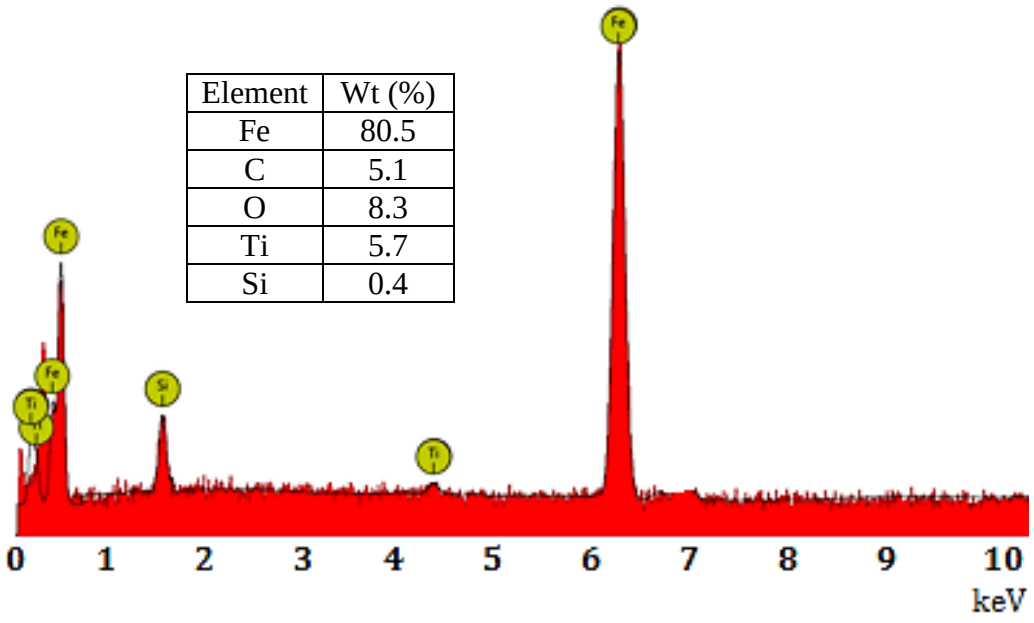

Figure 4.27: EDX elemental spectra of cylinder liner specimen tested with Oil P

Table 4.1: Elemental details by EDX analysis of tested cylinder liner surfaces

Oil Sample	Element wt (%)							
	C	O	Fe	Cu	Mo	S	Ti	Si
B	7.2	7.8	83.7	1.3	0.0	0.0	0.0	0.0
C	4.3	5.6	86.9	3.1	0.0	0.0	0.0	0.0
D	5.1	6.6	82.4	5.9	0.0	0.0	0.0	0.0
E	3.2	7.0	81.6	8.2	0.0	0.0	0.0	0.0
F	3.2	7.2	80.5	9.2	0.0	0.0	0.0	0.0
G	3.8	6.9	80.6	8.7	0.0	0.0	0.0	0.0
H	9.7	7.0	82.9	0.0	0.2	0.2	0.0	0.0
I	3.8	5.5	89.0	0.0	1.4	0.3	0.0	0.0
J	3.5	5.2	85.3	0.0	5.2	0.8	0.0	0.0
K	6.6	8.1	76.1	0.0	8.1	1.1	0.0	0.0
L	5.9	7.5	76.4	0.0	8.5	1.7	0.0	0.0
M	5.1	5.8	78.7	0.0	8.8	1.6	0.0	0.0
N	5.3	8.4	85.3	0.0	0.0	0.0	0.9	0.1
O	4.7	8.8	82.9	0.0	0.0	0.0	2.9	0.7
P	5.1	8.3	80.5	0.0	0.0	0.0	5.7	0.4
Q	4.4	9.3	81.8	0.0	0.0	0.0	4.1	0.4
R	4.8	8.4	81.6	0.0	0.0	0.0	4.5	0.7
S	5.3	8.7	80.2	0.0	0.0	0.0	4.7	1.1

4.2.7 Raman Spectroscopy

Tribofilms and near-surface materials govern the tribological behaviors of interacting surfaces. There is a tendency of nanolubricants to form surface protecting tribofilms, thereby facilitating the effective lubrication. As EDX analysis provide the information of elements present on the worn surfaces, suitable surface analysis technique is required to investigate the relevant compounds which results from tribo-chemical reaction. Thus, micro-Raman spectroscopy was performed to further investigate protective film formation.

4.2.7.1 Raman Spectra for nanoCuO Enriched Lubricants

The CuO enriched nanolubricants formed tribofilms, thereby facilitating the reduction of sliding friction and wear than that of blank palm TMP ester. The Raman peaks corresponding to CuO resonance modes for the treated cast-iron cylinder liner specimen are shown in Figure 4.28. The wavelength range of 200 – 700 cm^{-1} is selected to show the bands of a CuO resonant Raman mode.

For the tested specimen, the three expected CuO Raman peaks are clearly visible. CuO belongs to the C^{6}_{2h} with nine zone-center optical phonon modes, out of which only three (A_g+$2B_g$) modes are Raman active (J. Xu et al., 1999). The three Raman peaks can therefore be assigned to the Raman modes A_g and B_g as given in Table 4.2. The Raman peaks produced by the cylinder liner specimen treated with the CuO nanolubricant are closely related to those produced by the CuO nanocrystals discussed in previous research (H. Xu, Wang, & Zhu, 2006; J. Xu et al., 1999; J. Zhu et al., 2008). This similarity confirms the tribofilm formation on the cylinder liner surface; the formation was triggered by the reaction between the treated material and the nanoadditives under the provided environment. Thus, all the nanolubricants containing CuO nanoparticles showed tendency to form protective layer of CuO on the cylinder liner surface which helped in surface enhancement.

Table 4.2: Raman shifts showing active Raman peaks for specimen tested with CuO nanolubricant.

Raman Shift (cm^{-1})	Mode
283-296	A_g
334-343	B_g
621-627	B_g

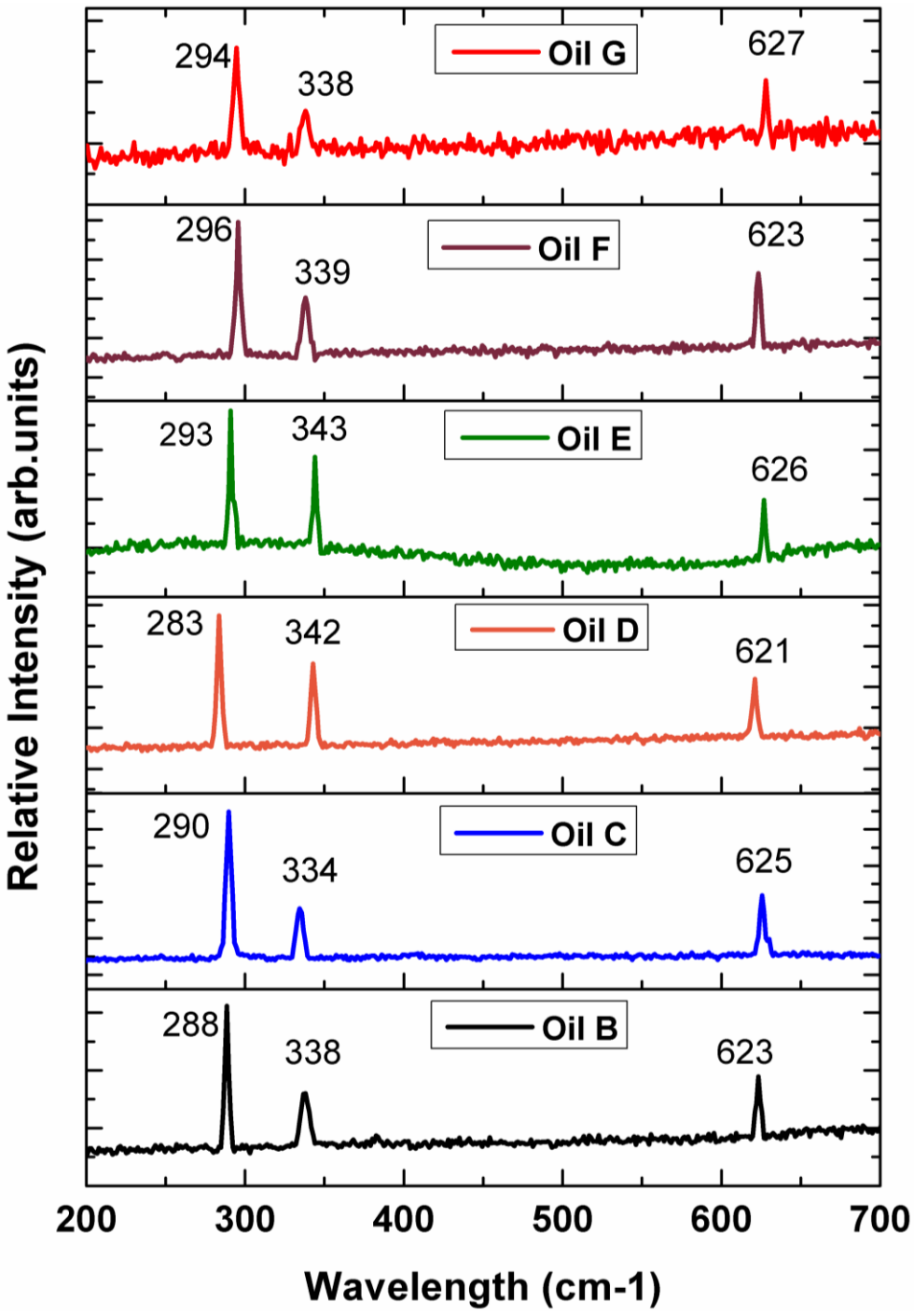

Figure 4.28: Raman spectra of cast iron cylinder liner specimen tested with CuO enriched nanolubricants

4.2.7.2 Raman Spectra for nanoMoS$_2$ Enriched Lubricants

The Raman spectra of the MoS_2 enriched nanolubricants are shown in Figure 4.29. The wavelength range of 100–900 cm^{-1} is selected to show the bands of a MoS_2 resonant Raman mode. In most of the Raman spectroscopic studies related to identification of MoS_2, four Raman resonant modes have been reported at wavelengths of 286 cm^{-1}, 383 cm^{-1}, 408 cm^{-1} and 32 cm^{-1} (Demas et al., 2012; Windom, Sawyer, & Hahn, 2011). In this thesis, three first order Raman active modes are reported i.e. 286 cm^{-1}, 383 cm^{-1} and 408 cm^{-1}, as the Rayleigh filter has a cut off wavelength of 100 cm^{-1}. Raman peaks for obtained MoS_2 samples are summarized in Table 4.3. Relative intensity is shown in the graphs but it has been observed that low concentrations of MoS_2 (i.e. < 1wt%) nanoparticles show low intensity. Such less intense MoS_2 resonance Raman peaks may be due to poor dispersion of nanoparticles or stronger scattering of laser radiation (Demas et al., 2012). The analysis of Raman spectra presented in Figure 4.29, showed that the nanoMoS$_2$ enriched lubricating oils tend to form the tribofilm of S–Mo–S which helped in friction reduction as well as wear protection as compared to the blank palm TMP ester.

Table 4.3: Raman shifts showing vibration of atoms within S–Mo–S layer

Raman Shift (cm^{-1})	Mode
284-286 (first order)	E_{1g}
378-383 (first order)	E^1_{2g}
405-408 (first order)	A_{1g}

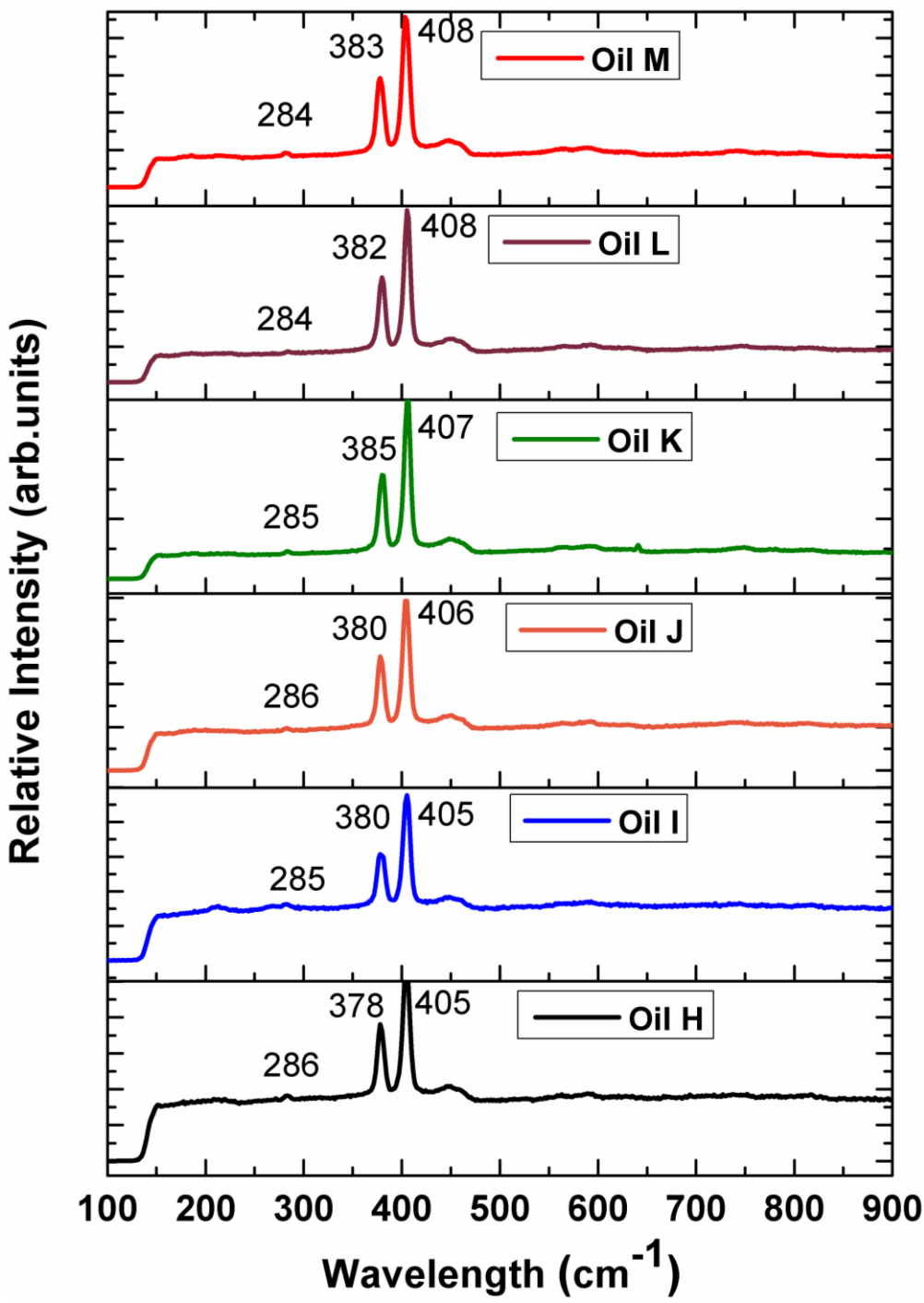

Figure 4.29: Raman spectra of cast iron cylinder liner specimen tested with MoS_2 enriched nanolubricants

4.2.7.3 Raman Spectra for nanoTiO_2/SiO_2 Enriched Lubricants

For specimen tested with nanoTiO_2/SiO_2 enriched lubricants, Raman spectra is shown in Figure 4.30. To investigate the TiO_2 as well as SiO_2 vibrations the Raman spectra was carried out for wavelength range of 100 cm^{-1} to 1500 cm^{-1}. The spectra are shown for wavelength range of 100 cm^{-1} to 700 cm^{-1} as no peaks have been observed at higher wavelength. The spectra show TiO_2 vibrational bands at 147, 197-198, 397-400, 518-519, and 639-641 cm^{-1} corresponding to Raman modes of E_g, E_g, B_{1g}, A_{1g} or B_{1g} and E_g, respectively (Ingole et al., 2013). The obtained Raman shifts and corresponding modes are listed in Table 4.4. The region below 200 cm^{-1}, can be used to distinguish between rutile and anatase of TiO_2 (Socrates, 2004). The sharp and intense peak at 147 cm^{-1} is characteristic of anatase phase (E_g mode) of TiO_2. The remaining peaks (weak) at 197-198, 397-400, 518-519, and 639-641 cm^{-1} are also correspond to anatase TiO_2 nanoparticle (Ingole et al., 2013).

Thus, in case of nanoTiO_2/SiO_2 enriched lubricants, the tribofilm of anatase TiO_2 nanoparticles was formed. On the other hand, no vibrational bands have been observed for Si-O bonds. Therefore, in case of lubrication performance of nanoTiO_2/SiO_2 enriched lubricants, the protective film formation on the tested surface is contributed by TiO_2 part of nanoTiO_2/SiO_2.

Table 4.4: Raman shifts of the TiO_2 anatase bands and corresponding Raman modes.

Raman Shift (cm^{-1})	Mode
147	$E_g(1)$
196, 197, 198	$E_g(2)$
397,398,399,400	$B_{1g}(1)$
516, 518, 519	$B_{1g}(2)$ / A_{1g}
639,641	$E_g(3)$

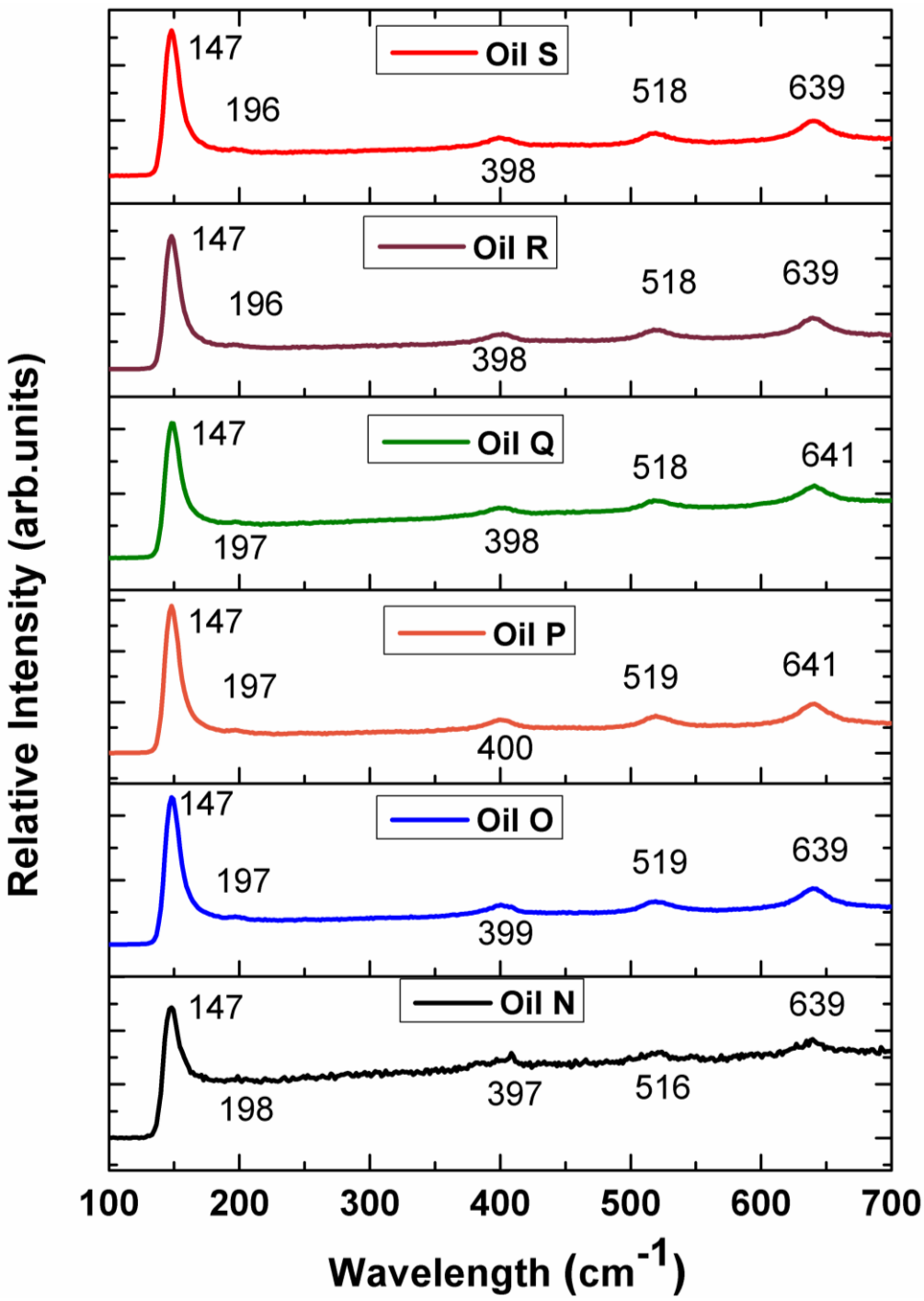

Figure 4.30: Raman spectra of cast iron cylinder liner specimen tested with nanoTiO_2/SiO_2 enriched nanolubricants

4.2.8 Surface Profilometry

Nanoparticle-assisted abrasion results in surface smoothening and polishing effects. Such smoothening and polishing of worn surfaces is characterized by reduction of surface roughness. As a result, friction and the related shear stress are reduced. Thus, polishing effect can be related to frictional behavior of nanolubricants to understand the friction mechanism. To investigate the surface polishing effect, the surface textures of worn surfaces are analyzed quantitatively in terms of surface roughness.

4.2.8.1 Surface Profiles for nanoCuO Enriched Lubricants

For lubricating oils added with CuO nanoparticles, an initial increase in nanoparticles concentrations (0.25 wt% - 1 wt%), helped in reducing surface roughness as shown in Figure 4.31 (a-f). Maximum surface smoothness in terms of low values of roughness parameters has been observed for Oil E (Figure 4.31 (d)). The corresponding values of surface roughness are Ra = 0.16 µm, Rq = 0.24 µm and Rz = 0.92 µm. While high surface roughness has been demonstrated by nanolubricants added with 1.25 wt% (Oil F) and 1.5 wt% (Oil G). The higher roughness for Oil F and Oil G may be attributed to the low dispersion stability and high tendency of agglomeration. Thus, uniform polishing effect was not observed by less stable dispersions and even Oil G shows the highest roughness (Ra = 1.17 µm, Rq = 1.36 µm and Rz = 3.21 µm) as compared to all other nanoCuO based lubricants. These trends showed the possible linkage between surface polishing and frictional behavior of nanolubricants. As highest surface polishing effect was observed for Oil E, the related COF was the lowest among nanoCuO enriched lubricants (Figure 4.10). Similarly, Oil G shows highest COF (Figure 4.10) and related surface roughness was highest as compared to other nanoCuO based lubricants (Figure 4.31 (f)).

Polishing effect in terms of surface smoothness by CuO enriched lubricants and related improvement in friction has also been reported by Choi et al. (2009). For nanoCuO

enriched bio-based lubricants, researchers have shown significant reduction of surface roughness as compared to blank bio-based base stocks (Arumugam & Sriram, 2014; Thottackkad et al., 2012).

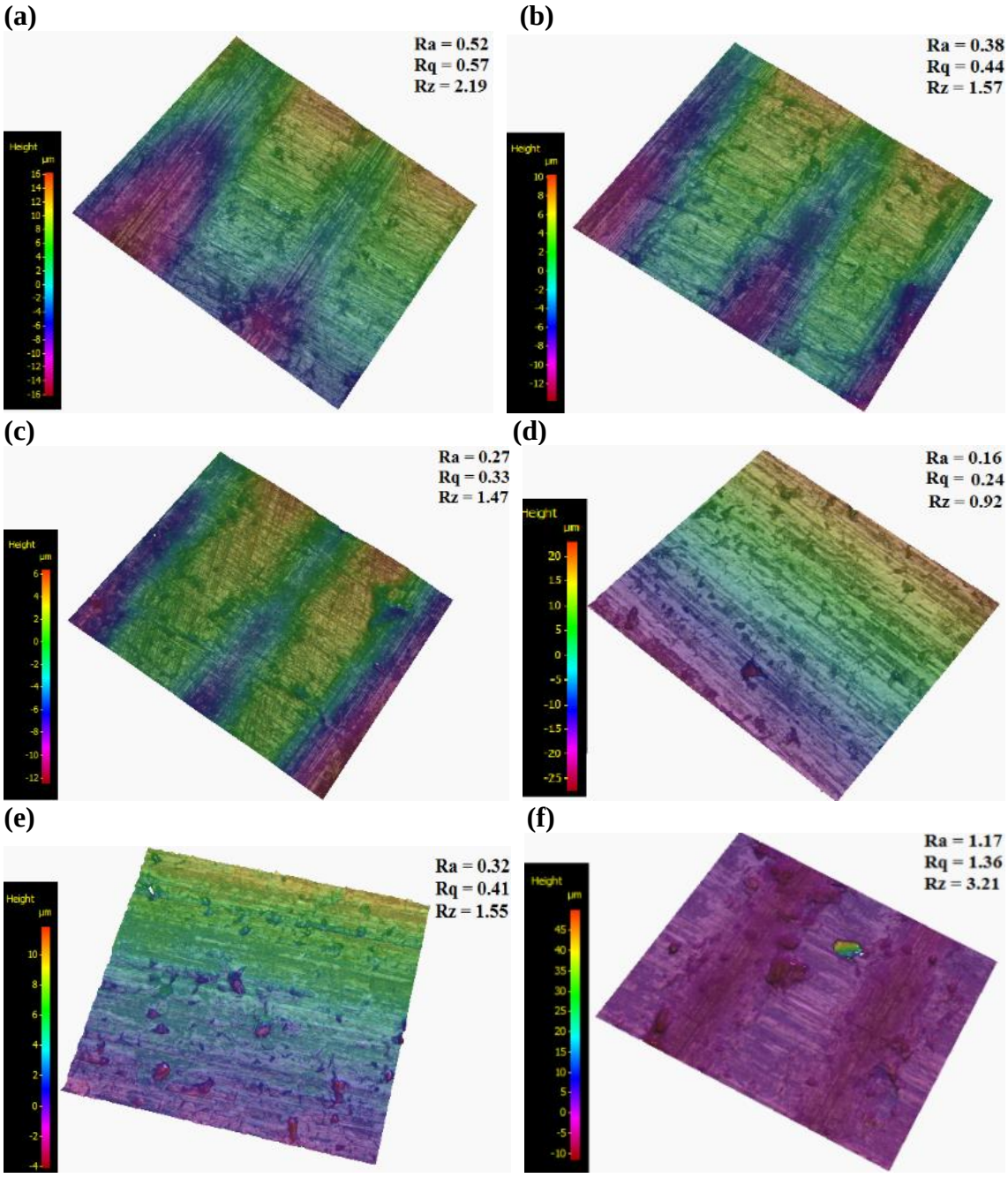

Figure 4.31: 3-D surface profile of cylinder liner specimen tested with CuO nanoparticles enriched lubricants (a) Oil B (b) Oil C (c) Oil D (d) Oil E (e) Oil F (f) Oil G

4.2.8.2 Surface Profiles for nanoMoS$_2$ Enriched Lubricants

For nanoMoS$_2$ enriched lubricants, Figure 4.32 (a-f) shows the 3-D surface textures and related roughness parameters. By analyzing the surface profiles, improved surface polishing effect can be reported with an increase in wt% concentration of nanoMoS$_2$ form 0.25 wt% to 1 wt%. Highest polishing and surface smoothness effect in terms of low values of roughness parameters has been depicted by Oil K (Figure 4.32 (d)). The corresponding values of surface roughness parameters are Ra = 0.11 µm, Rq = 0.16 µm and Rz = 0.57 µm. Similar to nanoCuO enriched lubricants, high roughness has been shown by nanoMoS$_2$ based lubricants at higher concentrations i.e. 1.25 wt% (Oil L) and 1.5 wt% (Oil M). In common with nanoCuO based lubricants with high concentrations, Oil L and Oil M have shown poor behavior in terms of uniform and stable dispersions. Thus, Oil M shows the highest roughness (Ra = 0.58 µm, Rq = 0.71 µm and Rz = 1.82 µm) as compared to all other nanoMoS$_2$ based lubricants. While looking into the link between effect of surface polishing with friction, it can be observed that Oil K showed the least surface roughness thus showing lowest average COF (Figure 4.12). Similarly, Oil H and Oil M showed higher average COF (Figure 4.12) which can be linked to high surface roughness of surfaces tested with these nanolubricants as compared to other nanoMoS$_2$ doped lubricants (Figure 4.32 (a) and (Figure 4.32 (f)). For nanoMoS$_2$ enriched lubricants, relatively low values of surface roughness parameters have been observed as compared to their CuO enriched counterparts. Thus, in comparison to CuO based lubricants low friction by nanoMoS$_2$ based lubricants can be linked with their higher tendency of surface polishing, consequently reducing shear stress between rubbing surfaces. In a previous research for nanoMoS$_2$ based lubricants, the surface roughness was reduced 10 times and obtained smooth surface provided an effective larger contact area, i.e., a lower average load, which resulted into a reduced friction and wear (Yadgarov et al., 2013). For coconut oil enriched with nanoMoS$_2$, Koshy et al. (2015), reported that

optimum concentration and suitable surfactants are required for polishing effect and it help in smoother surfaces and reduced friction. Similarly, smooth surfaces have been reported as a result of testing with lubricating oils added with nanoMoS_2 (Wan et al., 2014; Xie et al., 2015).

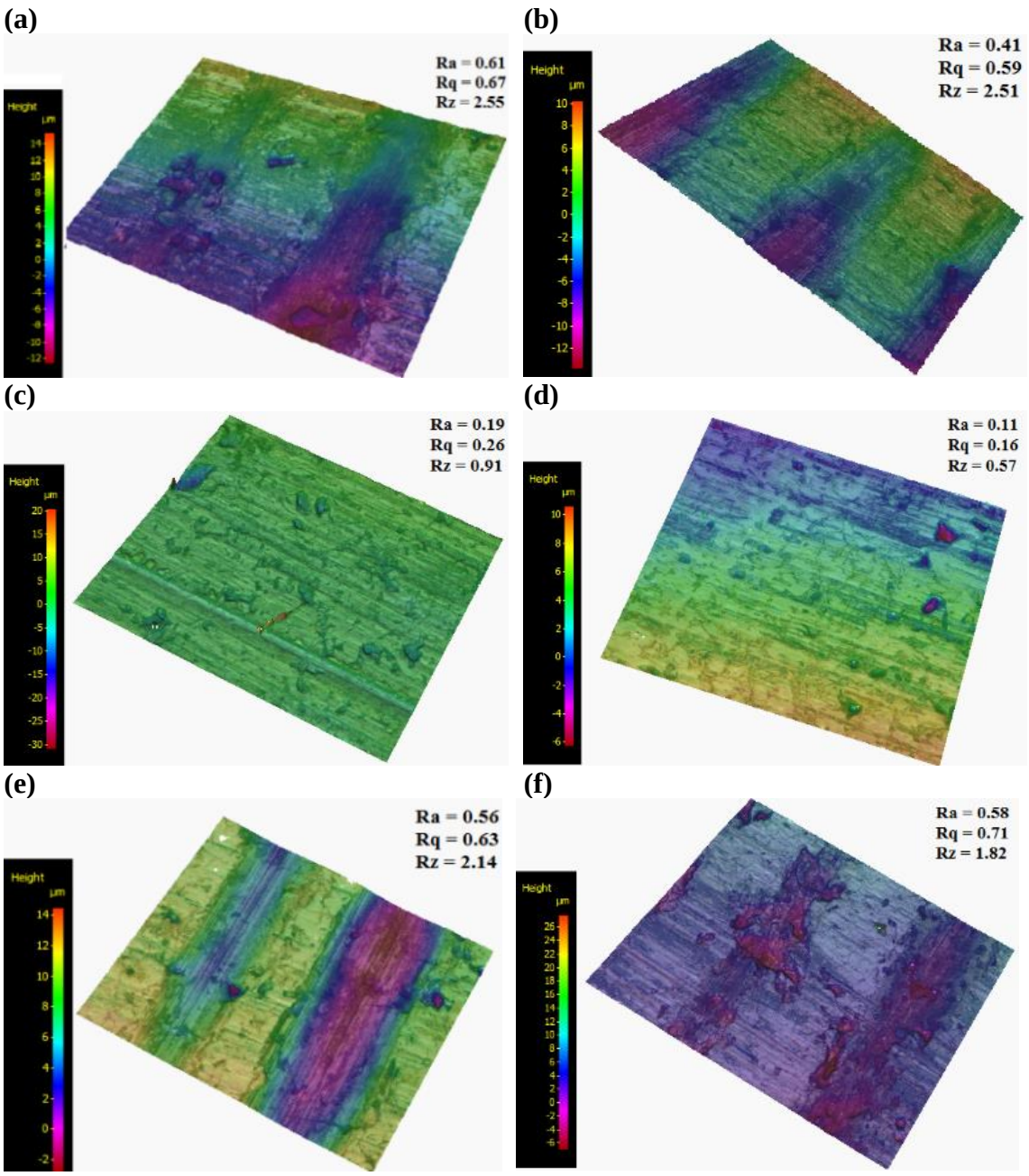

Figure 4.32: 3-D surface profile of cylinder liner specimen tested with MoS_2 nanoparticles enriched lubricants (a) Oil H (b) Oil I (c) Oil J (d) Oil K (e) Oil L (f) Oil M

4.2.8.3 Surface Profiles for nanoTiO_2/SiO_2 Enriched Lubricants

Figure 4.33 (a-f) shows the three dimensional (3D) topographic features of worn cylinder liner specimen tested with nanoTiO_2/SiO_2 enriched lubricants. It can be observed that an initial increase in nanoTiO_2/SiO_2 concentration from 0.25 wt% to 0.75 wt% resulted in smoother flat surfaces. The related surface topographic features have been illustrated in Figure 4.33 (a-c). It is worth mentioning here that Oil P shows the smoothest surface as compared to the worn surfaces tested by all other nanolubricants. The average surface roughness, Ra, as low as 0.08 µm has been observed while values of other roughness parameters were also comparatively low i.e. Rq = 0.11 µm and Rz = 0.42 µm. For nanoTiO_2/SiO_2 concentration > 0.75 wt%, roughness parameters show relatively higher values for worn surfaces as shown in Figure 4.33 (d-f). In this regard, highest values of roughness parameters (Ra = 0.44 µm, Rq = 0.49 µm and Rz = 2.11 µm) have been resulted for the surface tested with Oil N as shown in Figure 4.33 (f). The uniform surface polishing effect by Oil P can be related to its highest stable dispersion as compared to all other nanolubricants. Therefore, continuous and sufficient supply of nano-additives resulted in uniformly smooth flat surface. As mentioned previously, the degree of surface smoothness is linked with friction behavior, the lowest average COF was resulted when Oil P was used for tribo-testing (Figure 4.14). Such surface enhancement mechanism by reducing the surface roughness is believed to reduce shear stress between rubbing surfaces which ultimately reduce friction.

For the sliding friction tests, the polishing effect has also been reported by Chang et al. (2005), for nanoTiO_2 enriched lubricating oil. Such polishing effect was also verified when SiO_2 nanoparticles (Peng, Chen, et al., 2010) and aluminum nanoparticles (Peng, Kang, et al., 2010) were added to lubricating oils.

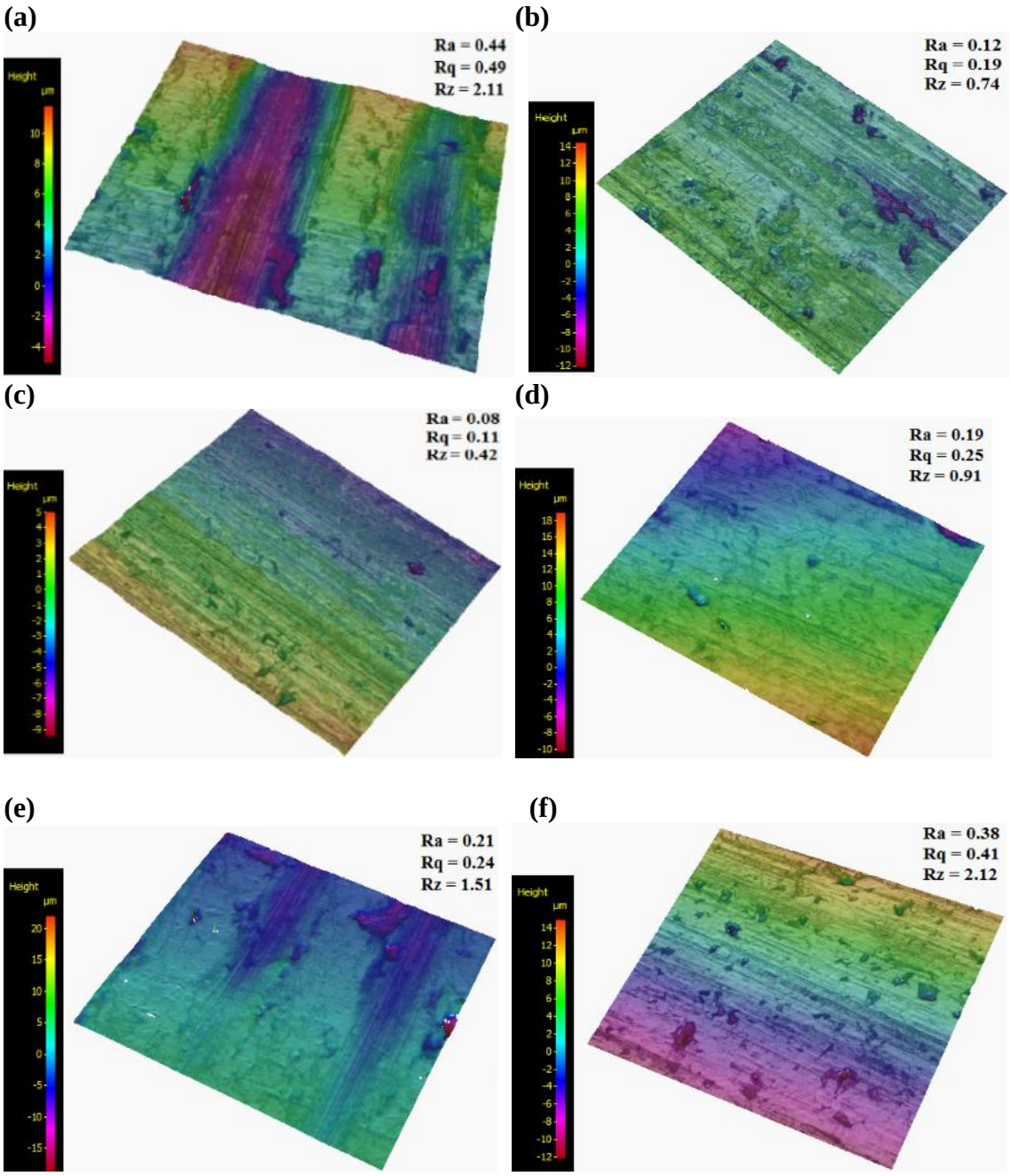

Figure 4.33: 3-D surface profile of cylinder liner specimen tested with TiO_2/SiO_2 nanoparticles enriched lubricants (a) Oil N (b) Oil O (c) Oil P (d) Oil Q (e) Oil R (f) Oil S

4.2.9 Surface Enhancement Mechanism

As per the understanding built from the tribological behavior and surface analysis in this research, the AW and friction reduction mechanisms of nanoparticles as additives in palm TMP ester are shown in Figure 4.34. For the nanoparticles, entering into the contact area between tribo-pair, they would tend to fill in the shallow grooves and holes on the metal surface (mending effect). In addition to surface mending, the nanoparticle-assisted abrasion results in reduced surface roughness (polishing effect). Such surface enhancement ability of nanoparticles resulted in reduced friction and wear.

Apart from surface enhancement by mending and polishing, the primary effect was observed when nanoparticles interact with the metal surface and form transfer films on it, which could protect the surface (protective tribofilm).

For spherical nanoparticles, i.e. CuO and TiO_2/SiO_2, there may also be contribution in terms of the rolling to support the metal surfaces and prevent them from contacting each other (ball bearing effect).

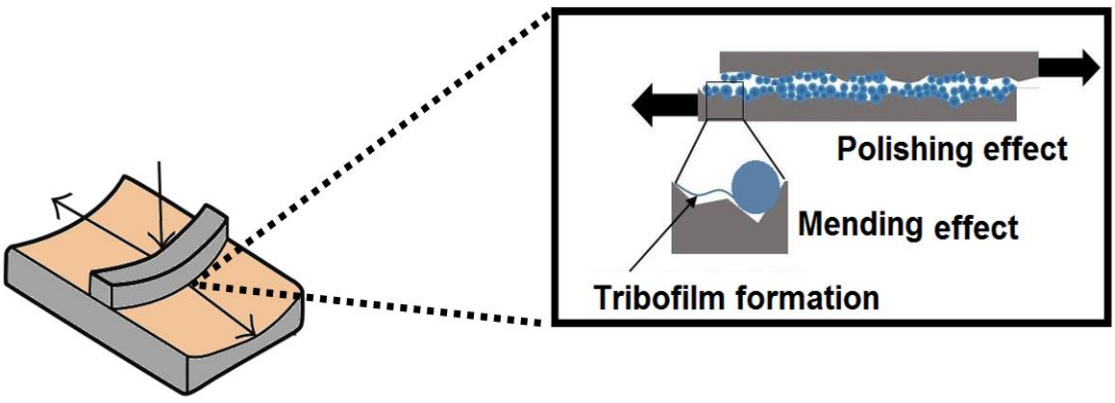

Figure 4.34: The schematic diagram of the lubrication mechanism of nanoparticles

4.2.10 EP Characteristics

For the considered EP parameters, i.e. LNSL, ISL, WL, and mean WSD, Table 4.5 shows the performance of all considered nanolubricants. Figure 4.35 shows the profiles of WSD under increasing loads for the pure bio-based base oil (palm TMP ester). For all the nanolubricants, it can be observed that increasing the nanoparticles concentrations resulted in improved EP characteristics.

As compared to nanoCuO based nanolubricants (Figure 4.36), nanoMoS_2 enriched (Figure 4.37) and nanoTiO_2/SiO_2 (Figure 4.38) based lubricants showed comparatively improved EP behavior. Figure 4.35 illustrates that without addition of nanoparticles, low load carrying capacity has been shown by Oil A i.e. ISL as low as 80 Kg and WL as low as 160 Kg have been observed (Table 4.5). For nanoCuO enriched lubricants (Figure 4.36), the addition of nanoparticles increased the LNSL for the suspensions > 1 wt% of nano-particles concentration while ISL increased for suspensions having nanoCuO concentration greater than 0.25 wt% (Figure 4.36). While improved EP behavior for LNSL and ISL values have been observed for all the suspensions added with nanoMoS_2 (Figure 4.37) as well as nanoTiO_2/SiO_2 (Figure 4.38). Though the suspensions added with nanoMoS_2 as well as nanoTiO_2/SiO_2 showed nearly similar LNSL, the corresponding mean WSD were lower for the nanoTiO_2/SiO_2 enriched lubricants. This contracted WSD behavior of the cited suspensions was witnessed at all the loadings (Figure 4.38). Overall an improved behavior with low values of mean WSD has been observed for nanoTiO_2/SiO_2 enriched lubricants (Figure 4.38). It was witnessed that high concentrations i.e. >1 wt% of all nanolubricants showed improved EP behavior. By comparing the values of EP parameters (Table 4.5), it can be observed that nanoTiO_2/SiO_2 based lubricants showed reduced mean WSD in addition to improvement in other parameters. For the EP test conditions investigated, high temperatures were achieved at non-conformal ball contact under ISL which could have resulted in tribo-sintering.

According to Y.-H. Zhou, Harmelin, and Bigot (1989), tribo-sintering initializes as soon as temperature increases to above-room levels for the very fine metal powders in a lubrication system. By the analysis of considered EP parameters it is evident that a single EP parameter is not enough to declare the superiority of lubricating oil sample in terms of EP behavior. For all the considered EP parameters, nanoTiO_2/SiO_2 enriched lubricants provide better performance than that of other nanolubricants.

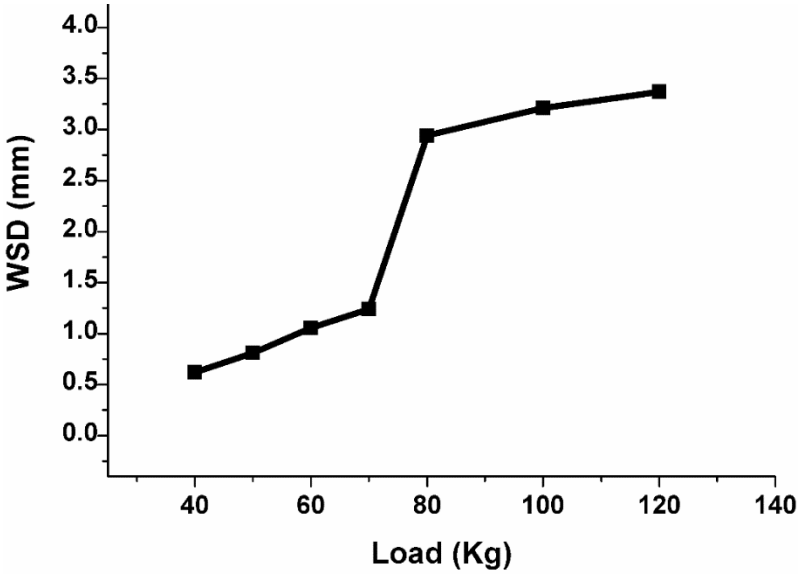

Figure 4.35: Load vs. mean WSD for Oil A

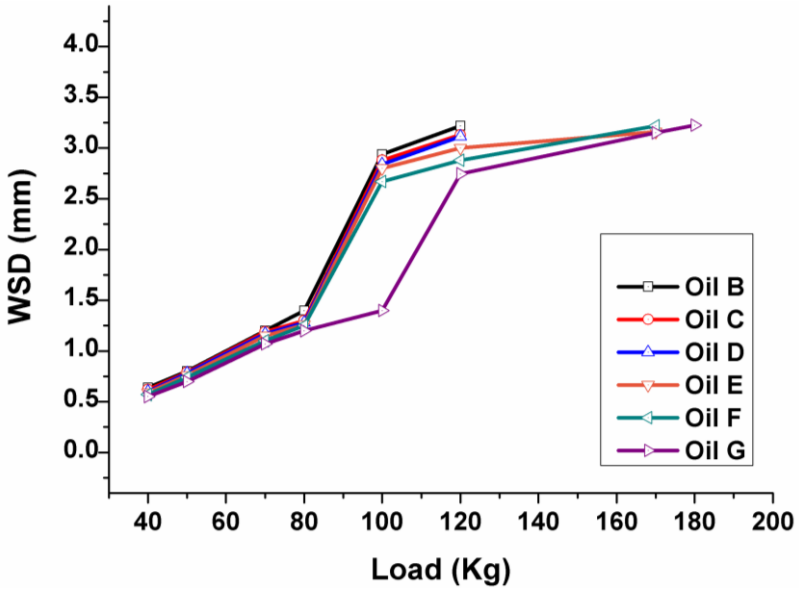

Figure 4.36: Load vs. mean WSD for nanoCuO enriched oils

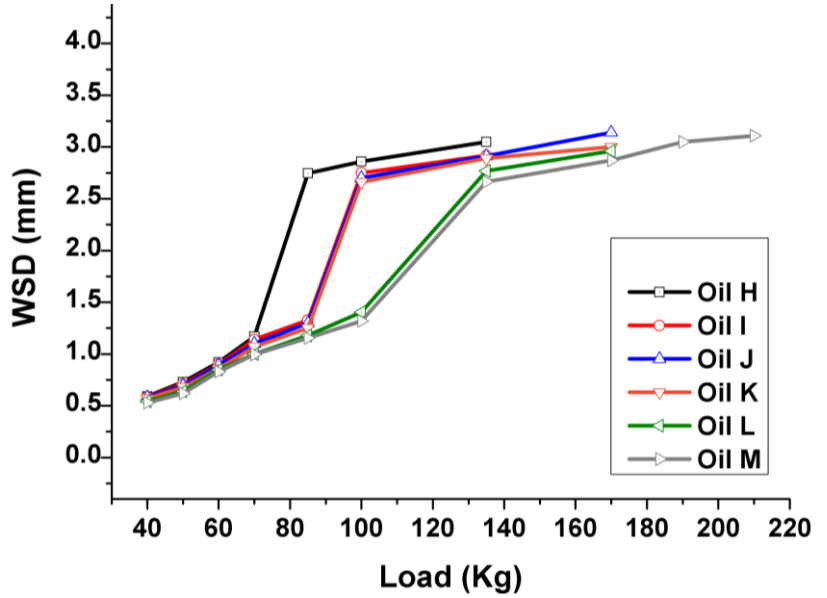

Figure 4.37: Load vs. mean WSD for nanoMoS_2 enriched oils

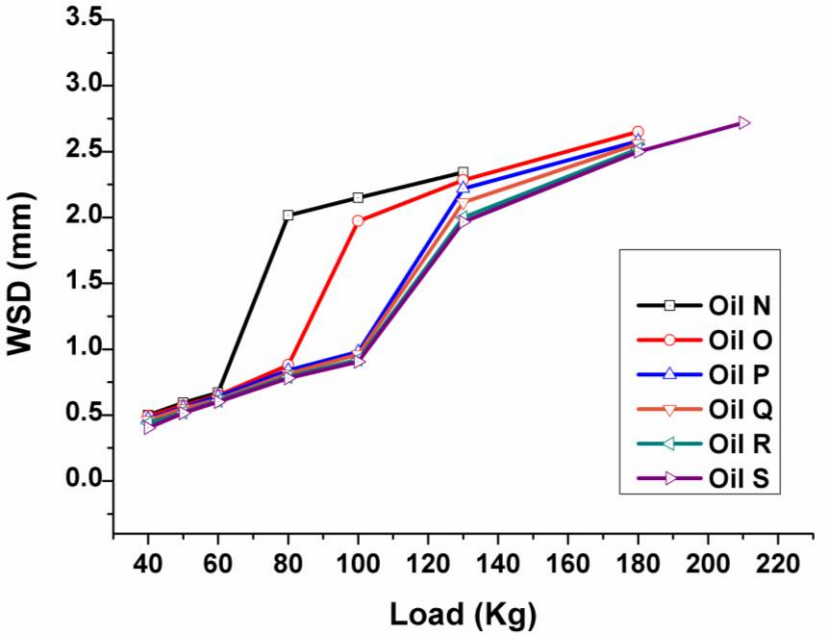

Figure 4.38: Load vs. mean WSD for nanoTiO_2/SiO_2 enriched oils

Table 4.5: LNSL, ISL, WL and WSD values for nanoparticles enriched suspensions

	Oil Sample	LNSL (kg)	ISL (kg)	WL (kg)	Mean WSD at ISL (mm)
	A	70	80	160	2.94
CuO enriched	B	70	80	165	2.74
	C	70	83.4	170	2.79
	D	70	86.7	170	2.81
	E	70	90	180	2.78
	F	80	100	195	2.91
	G	80	120	200	2.97
MoS_2 enriched	H	70	83.4	165	2.73
	I	70	93.4	170	2.78
	J	70	96.7	185	2.71
	K	80	100	190	2.66
	L	80	113.3	205	2.64
	M	90	125	220	2.51
TiO_2/SiO_2 enriched	N	70	80	175	2.41
	O	80	100	195	2.22
	P	80	110	205	2.17
	Q	80	120	205	2.12
	R	90	125	210	2.26
	S	90	130	220	2.29

4.3 Lubricating Oils Degradation

By analyzing the dispersion stability, tribological performance and surfaces analysis for all the considered nanolubricants, it can be clearly observed that 0.75 wt% nanoTiO_2/SiO_2 (Oil P) provided the high wear protection, friction reduction as well as surfaces enhancement. Therefore, bio-based nanolubricant (Oil P) was used for long duration engine testing to analyze its compatibility to actual engine condition in terms of degradation and tribological performance. Fully formulated lubricant (FFL), SAE15W40, was taken as reference to evaluate the lubrication performance of Oil P, by comparing the results of lubricant analysis and tribological behavior. As mentioned in previous chapter, two type of fuels are used i.e. petrodiesel (DF) and biodiesel (PB20). As previously highlighted, in Malaysia, petrodiesel has been completely replaced by palm biodiesel blends, therefore, lubricant-fuel combinations and related effects on lubricant degradation and lubrication performance, were also considered.

4.3.1 Lubricant Analysis

4.3.1.1 Viscosity

Engine oil viscosity is one of the key physical parameters for assessing oil condition during engine testing. Figure 4.39 and Figure 4.40 illustrates the trend with which the kinematic viscosity changed during the duration of the engine tests for Oil P and FFL respectively. In the absence of any viscosity improver, the viscosity of Oil P was relatively lower to FFL.

To compare the viscosity trends with previous studies related to long duration engine testing, viscosity results at 100 ^{o}C are reported (Stepien, Urzedowska, Oleksiak, & Czerwinski, 2011; Watson, 2010; Watson, Wong, Brownawell, & Lockledge, 2009; Zdrodowski et al., 2010). The researchers have mentioned that 100 ^{o}C is close to the average engine operating temperature (Truhan et al., 2005a, 2005b). Therefore, viscosity trends at 100 ^{o}C were compared for engine sump oil samples collected at regular intervals for Oil P and FFL.

Figure 4.39 shows the viscosity values and trends for Oil P over the engine testing. The viscosity of Oil P tends to decrease over the total duration of engine testing. For DF and PB20 fueled engine testing, similar trends have been observed with a little variation in resulting values. A viscosity value as low as 4.69 cSt has been observed at the end of DF fueled long duration engine testing. This trend of oil thinning was observed to be more significant for PB20 fueled engine testing. For PB20 fueled engine test, lowest viscosity of 4.56 cSt has been observed. Such trend of continuous oil thinning during long hours' engine operations have been reported in previous studies (Petraru & Novotny-Farkas, 2012; Stepien et al., 2011; Zdrodowski et al., 2010). The majorly reported causes include unburnt fuel which mix with lubricant as well as the degradation of polymers if part of

oil additive package. Therefore, investigation of fuel residue was also a part of lubricant samples analysis.

In comparison to Oil P, FFL shows an initial oil thinning at 40 hours, while insignificant variation in engine oil viscosity has been observed at 80 hours (Figure 4.40). Later on, the high degradation rate of polymers used as viscosity modifiers was likely to cause oil thinning over long hours operations (Stepien et al., 2011). For the case of FFL, kinematic viscosities dropped to as low as 10.7 and 11.1 cSt in the engine tests featuring the PB20 and DF, respectively (Figure 4.40). On the other hand, a continues decrease of viscosity has been observed for samples of Oil P as shown in Figure 4.39. This trends of oil thinning is dominant for PB20 fueled engine tests for both considered lubricating oils. Zdrodowski et al. (2010), also reported a reduction in the engine viscosity for B20-fuelled vehicles compared with ULSD-fueled vehicles when engine oil samples were collected over long mileage. They reported kinematic viscosity as low as 6.6 cSt for engine running on B20 fuels when 15W-40 engine oil was used. Similarly, Stepien et al. (2011), reported that, for heavy duty engine testing, the engine oil viscosity decreased significantly with rapeseed biodiesel. Therefore, the use of PB20 fuel resulted in oil thinning over the long hour test duration which in turn reduce the lubricant film thickness between engine interacting parts. This high tendency of fuel residue by PB20 was further investigated by FTIR spectroscopy.

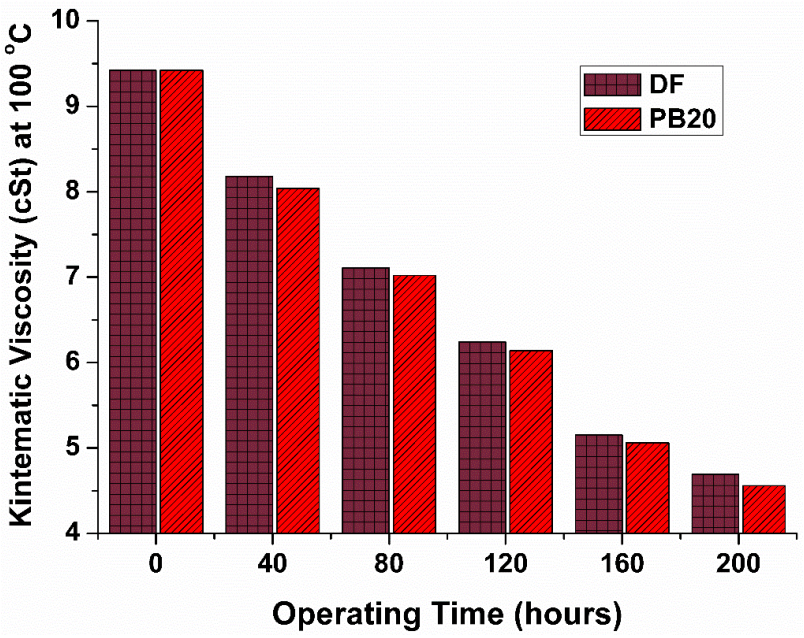

Figure 4.39: Kinematic viscosity of Oil P during long duration engine tests

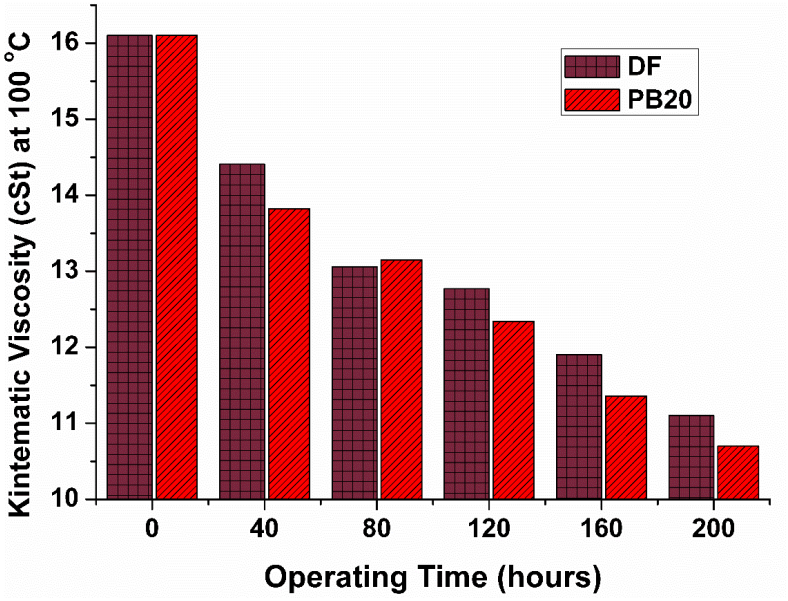

Figure 4.40: Kinematic viscosity of FFL during long duration engine tests

4.3.1.2 Total Acid Number (TAN)

Low acidity of lubricant is desirable to avoid corrosion, viscosity change and lubricant oxidation (Lockledge & Brownawell, 2013a). It is considered as one of the main indicator of the oil change timing in the diesel engines. The total acidity, mentioned as

the Total Acid Number (TAN), is a representation of the mutual concentration of organic and inorganic acids. TAN typically has an increasing trend over the lubricant life.

As Oil P is free of detergent and other acidity controlling additives, the lubricant acidity tends to rise over diesel engine operation (Figure 4.41). For Oil P than that of FFL, the use of strong base filter provided a continuous supply of alkaline reseve to neutralize the acidic contamination such that the Oil P sustain during the long duration engine testing. This was the main reason for using strong base filter so that adequate acidity control, oxidation resistance and protection to corrosion attacks could be provided. The acidic contamination in engine operation resulted in sharp rise of acidity as illustrated in Figure 4.41. An exponential rise has been observed for initial sample at 40 hours but later on this trend was controlled which may be related to the neuatraliztion performance of strong base filter. The acid control tendency at later duration of engine testing was improved for detergent free bio-based nanolubricant. The tendency for lowering the value of TAN can be related to the chemically active filter employing a strong base material that is capable of neutralizing weak acids in the fluids which come into contact with the strong base particles. Similar trends have been observed by Watson (2010), for zero detregent conventional diesel engine lubricant.

In comparison to acid control by Oil P, TAN charcteristics of engine-aged samples of conventional engine lubricant (FFL) are provided in Figure 4.42. In this case, the initial value of TAN was much higher than that of Oil P. But the rate of TAN increase was consistant due to alkaline reserve provided by detergent and dispersant in FFL. It is to be noted that for both type of lubricating oils, PB20 fueled engine testing showed high values of TAN. This behavior is due to the esters available in biodiesels which get hydrolyzed to increase the concentrations of weak acids in the lubricants (Devlin et al., 2008; Fang et al., 2007; Sugiyama et al., 2007). As acidity control is essential for lubricant to use in

engine operation, the continuous supply of alkaline reserve is required. This may be provided by conventional additive technology like detregents but their compatability with lubricant and related hazards must be studied. In this study the use of strong base filter technology proved to be effective in the given engine test conditions without any additional additive requirements.

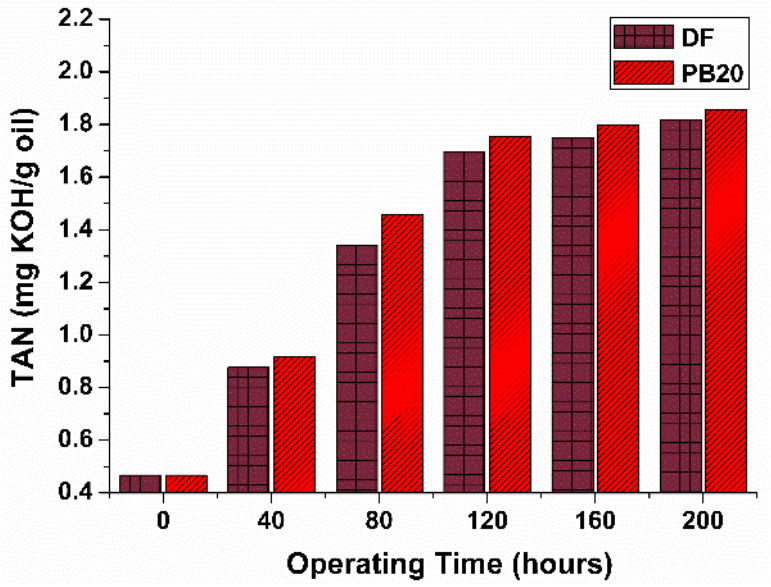

Figure 4.41: Total acid number of Oil P during long duration engine tests

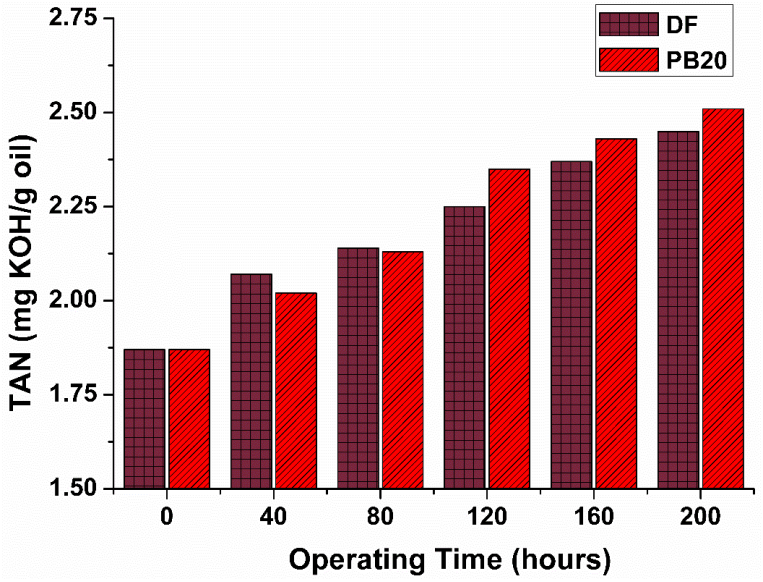

Figure 4.42: Total acid number of FFL during long duration engine tests

4.3.1.3 Total Base Number (TBN)

Total base number (TBN) indicates the quantity of alkaline reserve in the lubricant for controlling the acid contaminations. Lubricants with lower TBN are less effective in suspending the wear causing contaminants and results in engine damage due to corrosion by acid attack. Oils for most diesel engine applications typically have a TBN between 8 and 12 mgKOH/g. This high TBN is contributed by detergent in the cnventional additive package.

The values and trend of TBN for fresh and engine-aged Oil P samples are illustrated in Figure 4.43. As there is no alkaline supplying additive in Oil P, it shows very low value of TBN in fresh condition i.e. 0.42 mgKOH/g. But the use of strong base filter helped in maiantaing the TBN value as shown in Figure 4.43. The TBN retention was improved over the test duration for DF as well as PB20 fueled engine testing. This effectiveness is related to neutralization rate of strong base filter as discussed in previous section for TAN. Watson (2010) reported that the rate of TBN retention was improved by 50% when strong base filter was used for conventional engine lubricant.

In comaprison to Oil P, the TBN of engine-aged oil samples of FFL is illustrated in Figure 4.44. High values of TBN have been observed for all the engine-aged samples of FFL due to the presence of detergent. Compративley slow and consistant drop in TBN values was observed while low TBN retention has been observed for PB20 fueled engine test as shown in Figure 4.44. By comparing the TBN values in Figure 4.43 and Figure 4.44, it can be concluded that Oil P remained short of excessive alakline reserve throughout the engine testing. Though strong base filter helped in maintaining the minimum TBN values but the inherent value of TBN was very low. This shows the need of relevant additive which must be compatible to lubricant while meeting the environmental legislation.

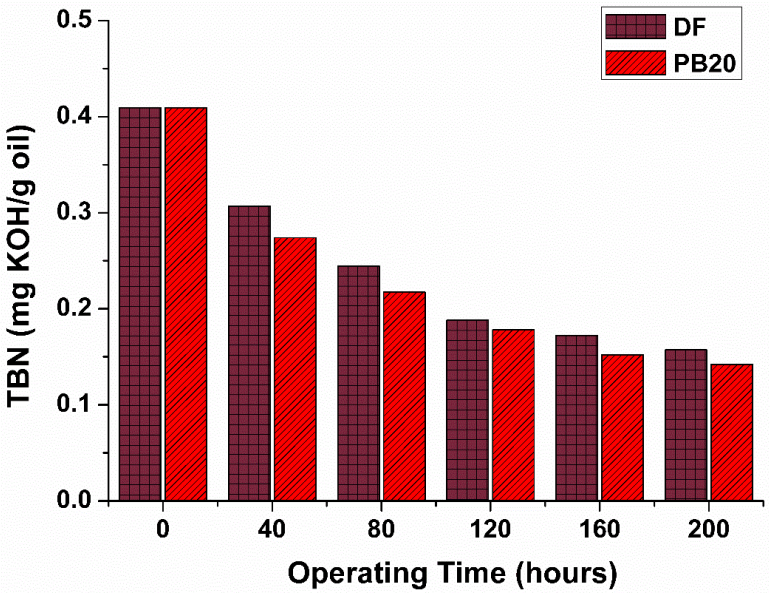

Figure 4.43: Total base number of Oil P during long duration engine tests

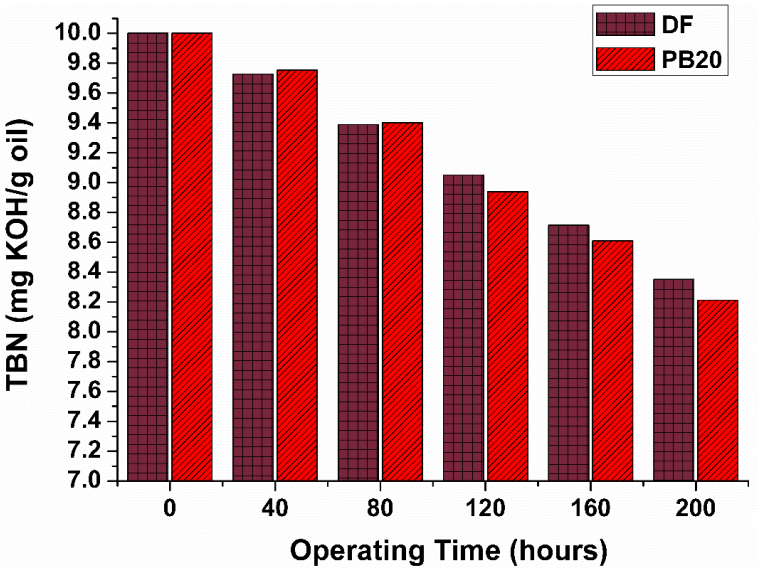

Figure 4.44: Total base number of FFL during long duration engine tests

4.3.1.4 Fuel Residue

As previously discussed, fuel residue decreases oil viscosity which in turn results in reduced film thickness and dilution of additives concentration. Therefore, it is taken as significant parameter to understand the lubricant degradation and its link to lubrication performance. Detecting fuel residue in engine oil by any method is difficult because fuel and base oil differ in terms of molecular weight, boiling temperature range, and aromatic compound content. The IR absorption method enables the examination of the aromatic compounds in engine oil, and thereby, the determination of fuel residue. The difference in aromatic compound content between engine oil and fuel reflects fuel residue. In this work, therefore, the FTIR absorbance spectra of the fresh engine oil around 800 cm^{-1} was taken as the baseline for detecting possible fuel residue. The absorption intensity of the fresh engine oil was measured, and the change in its absorption spectrum was determined as it was being diluted. The bio-diesel fraction of engine-aged oil samples was taken as the IR absorption of ester peak near 1746 cm^{-1}. The IR absorption value of each absorbance spectrum was derived for all the collected samples and plotted for comparative analysis. Figure 4.45 and Figure 4.46 show the IR absorption values corresponding to fuel residue in the used engine oil samples for Oil P and FFL respectively. Though there is a little difference in the values but overall similar trends have been observed for both type of lubricating oils. For Oil P, initially the fuel residue was low corresponding to PB20 fueled engine test as compared to DF fueled engine test. This can be related to continuous accumulation of esters in the lubricating oil and low evaporation tendency of these esters available in PB20. Thus, the accumulation rate was seemed to be higher than the evaporation rate which resulted in continuous rise in fuel residue as shown in Figure 4.45 and Figure 4.46. The high fuel residue of the engine oils in the biodiesel-fueled engines is expected because biodiesels have a volatility lower than that of DF (Watson & Wong, 2008). The fuel residue of the B20 fuels therefore remained

in the oil sump and gradually evaporated at the related oil sump temperatures. Other factors that influence the production of fuel residue in engine oils include the fuel mass post-injected into cylinders and the frequency of DPF regeneration (Zdrodowski et al., 2010). For DF fueled engine testing, consistent increase in fuel residue was observed which show a linear relationship between DF accumulation and evaporation. Though relative to Oil P, low fuel residue was observed by FFL, the trends are similar over the tests duration (Figure 4.46). This shows fuel residue was one of the major factor for continuous oil thinning over the engine testing as discussed in section 4.3.1.1.

This tendency of high fuel residue during B20 fueled engine testing shows higher acidic contamination due to hydrolysis of esters in biodiesels. This acidic contamination results in higher degradation rate of engine lubricant. At the end of 200 hours' test, the percentage values of fuel residue have been given in Table 4.6. The percentage change in the fuel residue show that high fuel residue has been observed for engine tests when Oil P was used as compared to FFL samples.

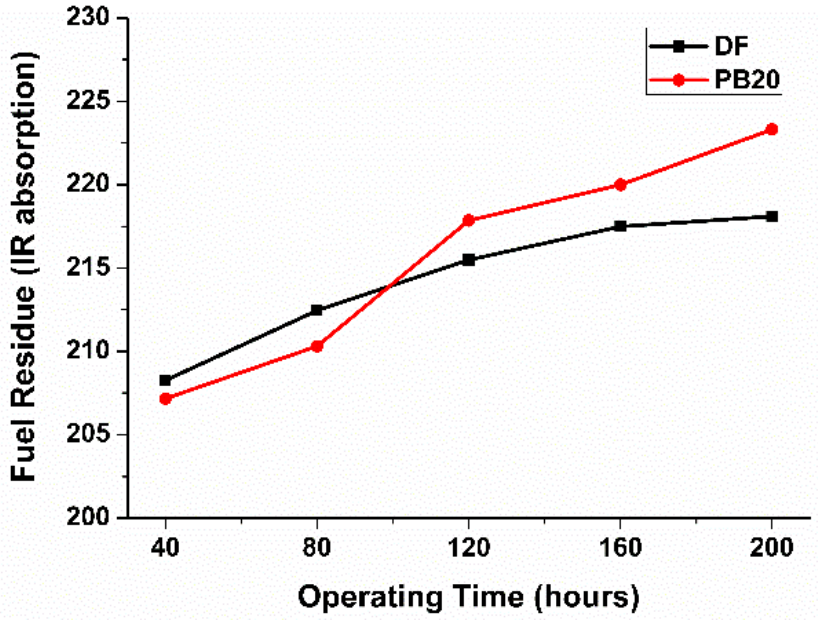

Figure 4.45: Fuel residue during long duration engine testing for Oil P

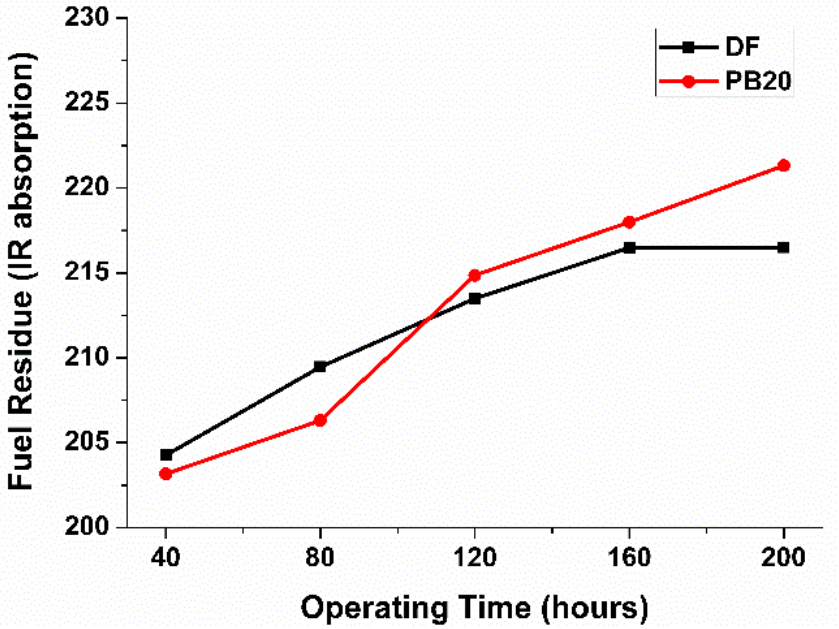

Figure 4.46: Fuel residue during long duration engine testing for FFL

Table 4.6: Fuel residue at the end of engine endurance tests

Fuel	Fuel Residue		Percentage change
	Oil P	FFL	
DF	218.101	216.509	0.74%
PB20	223.319	221.436	0.85%

4.3.1.5 Oxidation

The quality of the base oil is badly affected by oxidation as it is exposed to the high temperatures in an engine. The highly-oxidized lubricants show discoloration and a burnt odor. With aging during engine operations, the undesirable effects include rise in viscosity and acidic oxidation products. The related problems include corrosive attacks on engine parts, engine parts wear, high lubricant viscosity, sludge, varnish and piston deposits (Watson, 2010). The IR-derived oxidation values were obtained from the spectrum peaks between 1800 to 1670 cm^{-1}**.** The oxidation values at absorption mode were due to the absorption of IR energy by the carbon oxygen bonds in the degraded oil.

Only a limited number of fresh petroleum oil compounds exhibited significant absorptions in the 1800–1670 cm^{-1} region. For the used oil, therefore, the spectral peaks in this region serve as a direct measurement of the oxidation level in the engine oil. For each oil sample, the highest IR absorption peak was determined on the basis of the above-mentioned wavenumber range.

Figure 4.47 and Figure 4.48 illustrate the oxidation levels of the analyzed lubricant samples for Oil P and FFL respectively. Comparing the oxidation number profiles for Oil P (Figure 4.47) and FFL (Figure 4.48), high variation has been observed during initial 80 hours of engine testing. Such variation may be related to relatively low oxidation stability of Oil P which resulted in high oxidation number from the start of engine testing (Figure 4.47). On the other hand, the presence of antioxidant additives in FFL helped in controlling the oxidation number at the start of long duration engine testing (Figure 4.48). Later on, for FFL, the trend of increasing oxidation number for PB20 fueled engine can be related to the depletion of antioxidants in the corresponding engine oil samples; the depletion is caused by high fuel residue and increased acidic contamination. Since the tendency of fuel residue was higher for PB20 fueled engine, the related oxidation number was higher at the end of engine testing. Previous researchers have also reported this linkage between percentage dilution of FAME and the oxidation of used engine oils (Stepien et al., 2011; Zdrodowski et al., 2010). Relatively higher oxidation number has been shown by engine-aged samples of Oil P as compared to FFL. This control of oxidation over the tests duration can be related to the oxidation controlling ability of strong base filter. Such behaviour of strong base filter has been reported in earlier research for conventional engine lubricants (Watson, Wong, Brownawell, Lockledge, et al., 2009). Therefore, for engine-aged samples of Oil P, it is reasonable to assume that the controlled base oil oxidation rates were due to improved oxidation stability of base oil and absorption of oxidation by-products by the strong base filter. This shows that for actual

engine long duration operations, either antioxidant additives or other oxidation controlling mechanism is required.

Comparing the oxidation numbers and related trends in Figure 4.48 and Figure 4.48, the bio-based base oil show the tendency to sustain during high temperature engine conditions. Table 4.7 shows the percentage change in the oxidation number for the engine-aged samples of Oil P in comparison with FFL at the end of long duration engine testing.

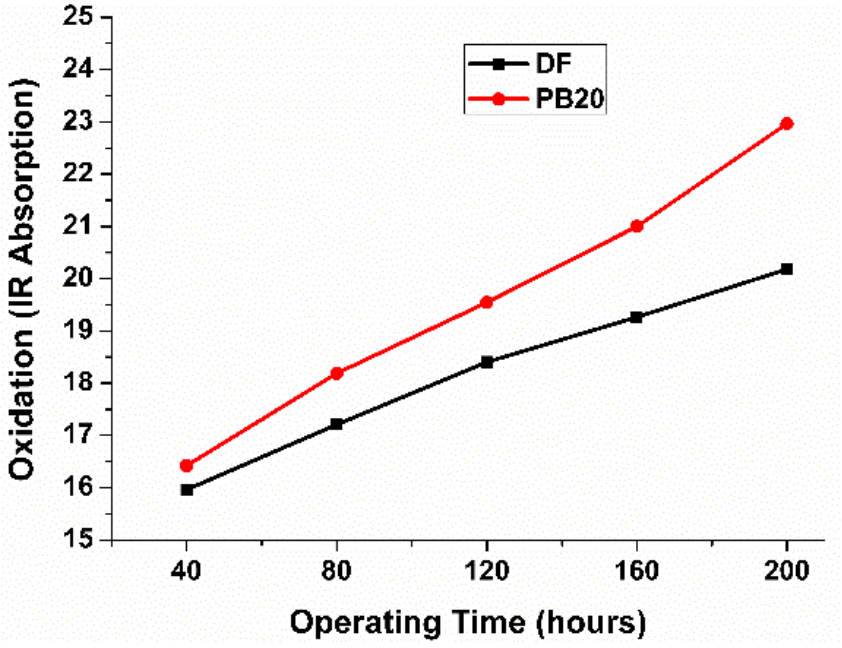

Figure 4.47: Oxidation number during long duration engine testing for Oil P

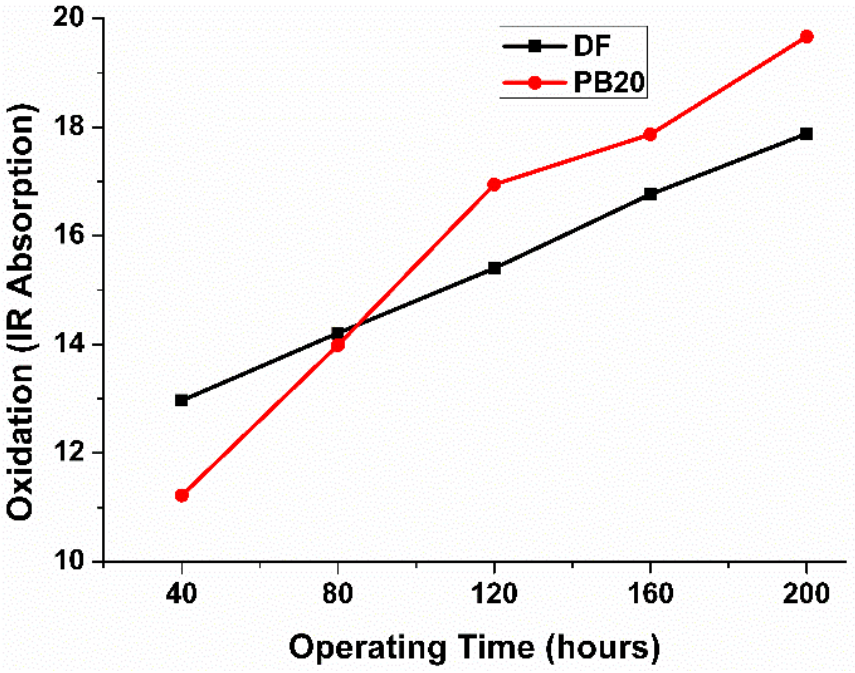

Figure 4.48: Oxidation number during long duration engine testing for FFL

Table 4.7: Oxidation number variation at the end of long duration engine testing

Fuel	Oxidation Number		Percentage change
	Oil P	FFL	
DF	20.180	17.880	12.8%
PB20	22.968	19.667	16.8%

4.3.1.6 Soot Loading

The combustion of highly rich fuel/air mixtures produces soot and soot particles as a result of incomplete fuel combustion. Petroleum diesel exhibits a high tendency toward soot formation because of its low H/C ratio, but diesel blends with high H/C contents can reduce the occurrence of this problem (Asfar & Hamed, 1998). Soot formation in engine oils increases oil viscosity and prematurely blocks the oil filter and oil circuit. Although soot has no particular IR absorption bands in an FTIR spectrum, it causes a scattering of IR radiation, which tends to be severe at high wavenumbers. In this work, therefore, soot loading was considered the absorbance intensity value at 2000 cm^{-1}.

Figure 4.49 and Figure 4.50 indicates that soot loading trends over the duration of engine testing for Oil P and FFL respectively. For all the collected engine-aged samples of Oil P (Figure 4.49), low soot loading has been observed than those of FFL (Figure 4.50). The lowest soot content has been reported for bio-based nanolubricant and biodiesel combination as illustrated by profile of Oil P related to PB20 in Figure 4.49. It is quite reasonable to believe that relatively high H/C contents during Oil P and PB20 combination helped in suppressing the tendency of soot formation. Similarly as low as half soot content for bio-based lubricant and biodiesel combination has been reported earlier as compared to conventional engine lubricant used with rapeseed biodiesel (Arumugam S, 2014).

The soot content steadily increased throughout the engine tests for both type of oil samples. Given that biofuels help reducing particulate matter emissions and smoke opacity (Agency., 2002; Labeckas & Slavinskas, 2006; Mohsin, Majid, Shihnan, Nasri, & Sharer, 2014), the value of soot loading was low for both Oil P and FFL for oil samples collected after PB20-fuelled engine testing. The results show that the bio-based nanolubricant and biodiesel combination resulted in reduction of soot content, showing the related environmental advantage over traditional lubricant and fuels. Table 4.8 shows the percentage change in the soot loading for Oil P and FFL at the end of long duration engine testing.

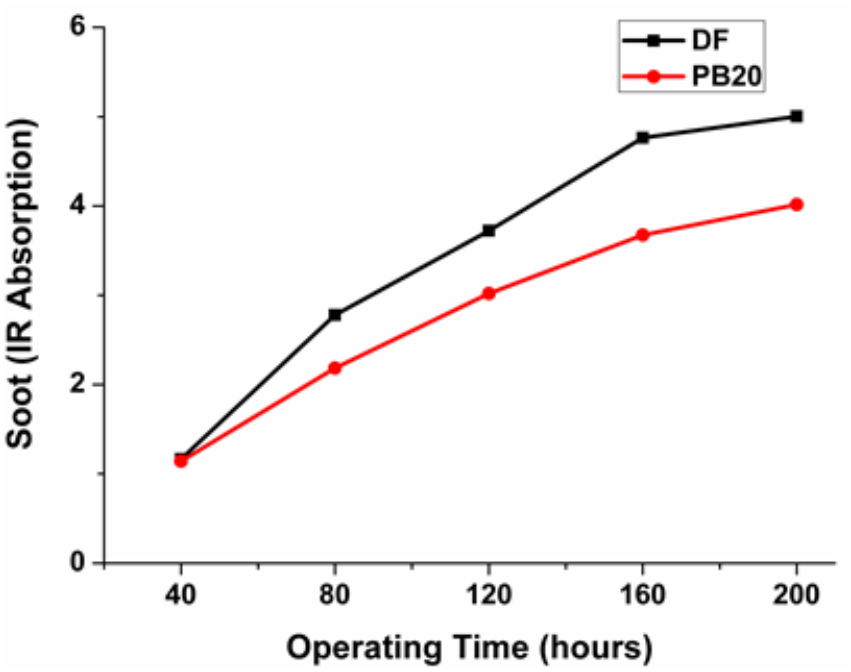

Figure 4.49: Soot loading during long duration engine testing for Oil P

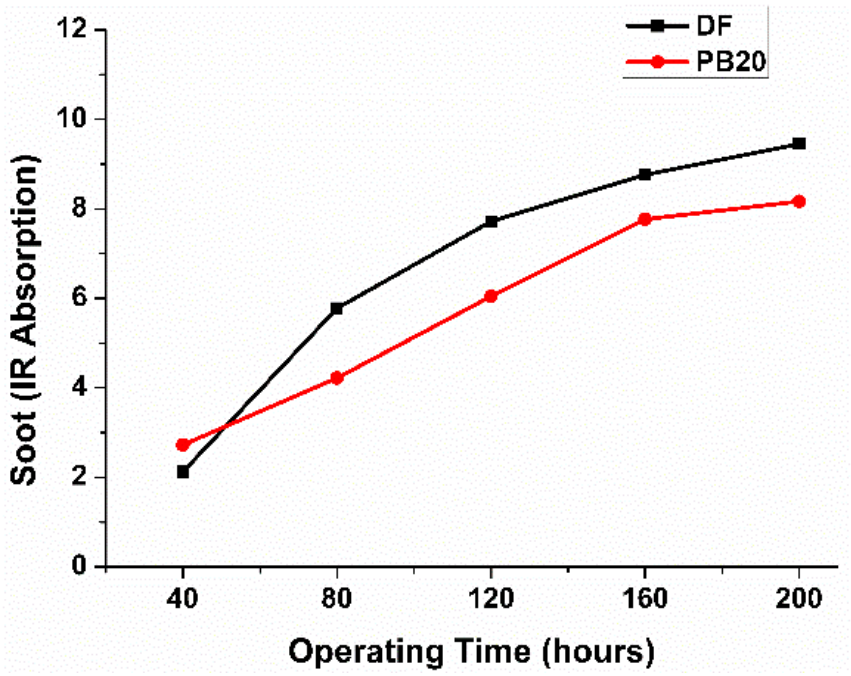

Figure 4.50: Soot loading during long duration engine testing for FFL

Table 4.8: Soot content at the end of long duration engine testing

Fuel	Soot Loading		Percentage Reduction
	Oil P	FFL	
DF	5.003	9.451	88.9%
PB20	4.016	8.167	103.4%

4.4 Effect of Lubricant Degradation on Tribological Performance

In this part of thesis, the lubricating oil condition based approach was adopted and the effects of lubricants degradation on tribological characteristics were investigated. It is to be worth mentioning here that the scaling to the in-situ engine real tests will result in variation of friction and wear results due to the effects of a number of parameters including piston secondary motions and gas pressures. However, the engine-aged samples helped in simulating the realistic lubrication conditions.

4.4.1 Friction Results

Figure 4.51 shows the COF trends over the tribo-test duration for Oil P. High friction profile has been shown for PB20 fueled engine as compared to DF fueled engine testing (Figure 4.51). Such higher frictional behavior for PB20 fueled engine testing may be attributed to high fuel residue. While comparing the friction behavior of Oil P (Figure 4.52) and FFL (Figure 4.54) the difference of average COF was not as high as the significant difference in lubricants viscosity. This shows the effectiveness of nanoTiO_2/SiO_2 as friction reducing additive, after degradation under engine tough conditions. This behavior of Oil P may be attributed to the tendency of surface polishing effect by which surface roughness is reduced by nanoparticle-assisted abrasion. As mentioned earlier, such smooth surfaces tend to reduce the shearing force between rubbing surfaces. This mechanism of surface polishing was further investigated by 3-D

surface topographic analysis in next section of surface analysis. For engine-aged Oil P samples, percentage increase of 67% (DF fueled) and 84.5% (PB20 fueled) has been observed in average COF than that of fresh Oil P.

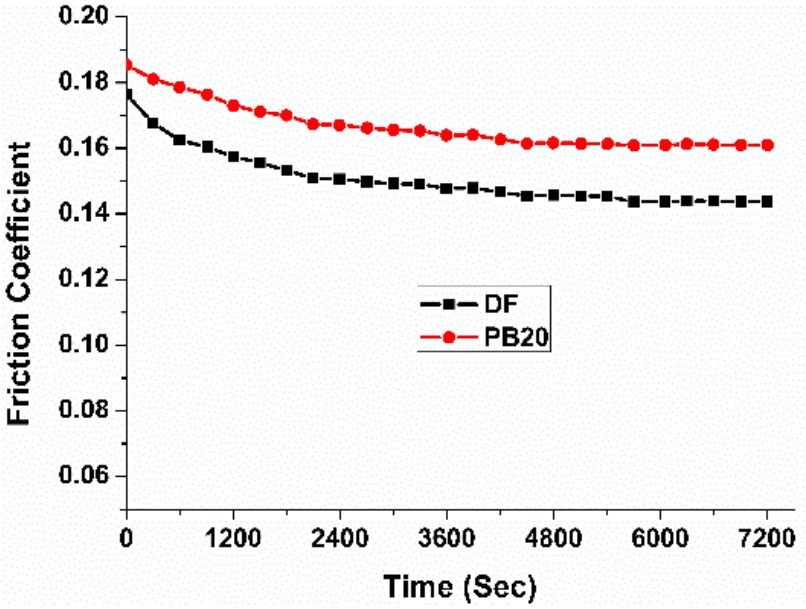

Figure 4.51: COF as a function of sliding time by engine-aged samples of Oil P

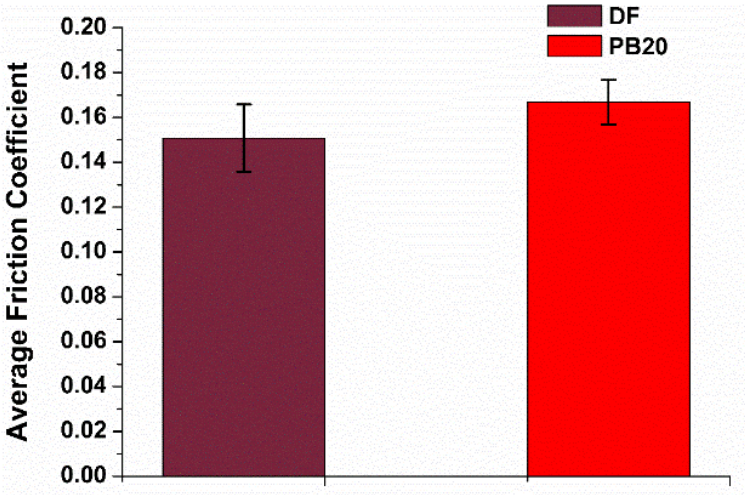

Figure 4.52: Average COF by engine-aged samples of Oil P

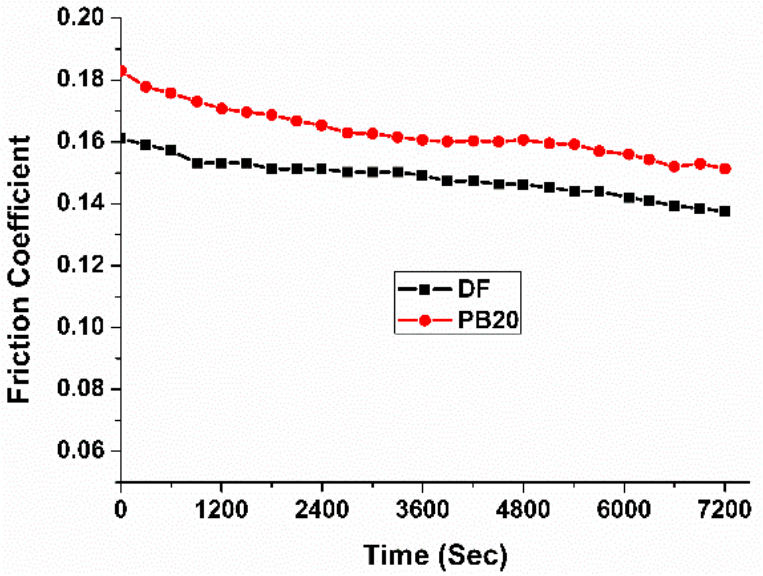

Figure 4.53: COF as a function of sliding time by engine-aged samples of FFL

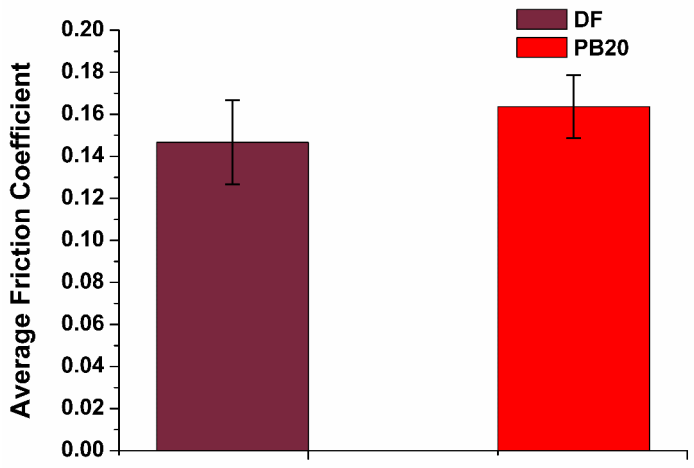

Figure 4.54: Average COF by engine-aged samples of FFL

4.4.2 Wear Results

For used engine sump oil samples, Figure 4.55 (a-b) and Figure 4.56 (a-b) shows the wear volume for engine-aged samples of Oil P and FFL respectively. High wear volumes have been observed for Oil P as compared to FFL. Such higher wear volumes by Oil P may be attributed to factors including increased fuel residue, higher oxidation and reduced oil viscosity. On the other hand, relatively low wear volumes have been shown by engine-aged samples of FFL. This improved behavior can be related to relatively high lubricant

viscosity, low oxidation and less acidic contamination. Such trends for conventional engine lubricant (SAE 15W40) have been reported previously by Zdrodowski et al. (2010). Though low wear loss was observed by FFL as compared to Oil P, the wear volumes were high for oil P than that of obtained in fresh condition (Figure 4.19). High fuel residue, soot particles and acidic contamination enhances wear rate. The acidic contaminations can cause corrosive wear. Furthermore, the active chemical characteristics of soot content badly affect the wear resistance of tribofilm-forming additives, such as ZnDDP (Ratoi, Castle, Bovington, & Spikes, 2004). Such high wear rate by conventional engine-aged lubricant as compared to fresh lubricant has been reported in earlier research due to ZnDDP reduction at the end of endurance engine tests (Petraru & Novotny-Farkas, 2012).

The wear mechanism for degraded bio-based nanolubricant was then investigated by using SEM, EDX analysis, Raman spectroscopy and surface profilometry.

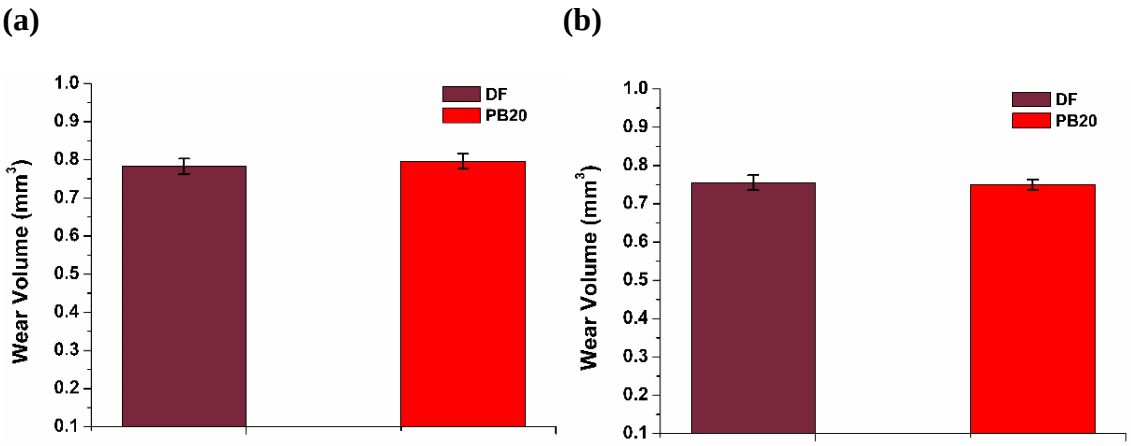

Figure 4.55: Cylinder liner wear volume by engine-aged samples of (a) Oil P (b) FFL

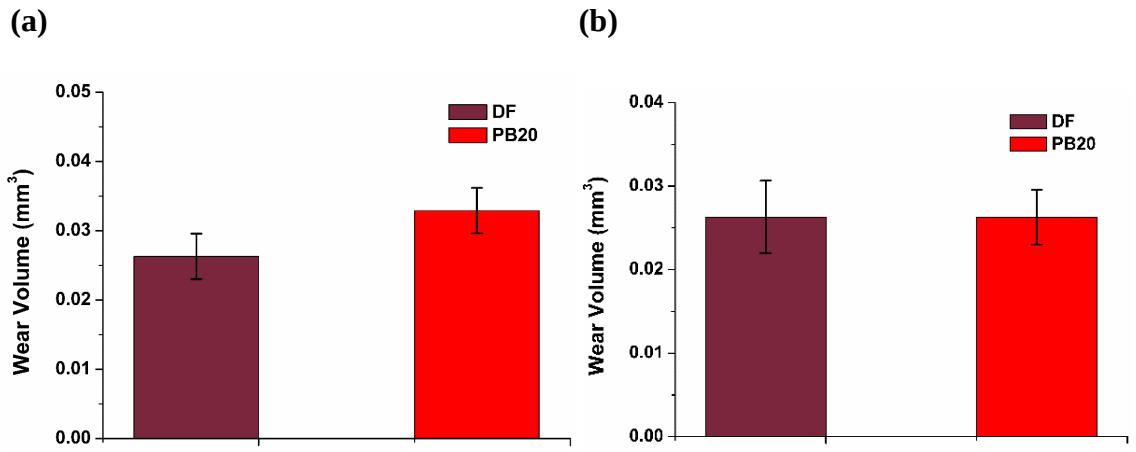

Figure 4.56: Piston ring wear volume for engine-aged samples of (a) Oil P (b) FFL

4.4.3 Surfaces Analysis of Worn Surfaces

To analyze the tribological effectiveness and related lubrication mechanism of nanoparticles enriched palm TMP ester in actual engine environment, the corresponding worn surfaces of cylinder liner test specimen were analyzed using surface characterization tools as already used for fresh nanolubricants including SEM, EDX analysis, Raman spectroscopy and 3-D surface profilometry.

4.4.3.1 SEM Analysis

For Oil P, SEM micrographs of cylinder liner specimen tested with engine-aged oil samples are illustrated in Figure 4.57 (a-a_1). For DF fueled engine testing, Figure 4.57 (a) shows the micrographs at low magnification (20x) and high magnification (200x) micrograph (Figure 4.57 (b)). Small pits can be observed at higher magnification while some material transfer was also visible in micrograph as shown in Figure 4.57 (a_1). This shows that the lubricant degradation negatively affect the mending/repairing tendency of Oil P such that adhesive wear was increased and high wear volume was observed as reported earlier in Figure 4.55 and Figure 4.56. As lubricant degradation was high in terms of fuel residue, acidic contamination and oxidation, the related wear surfaces shows pits and shallow holes even at lower magnification as mentioned by micrograph in Figure

4.57 (b). The corresponding higher magnification micrograph (Figure 4.57 (b_1)) also show shallow grooves resulting in high wear loss. This trend supports the high wear volume of cylinder liner by engine-aged lubricant (Oil P) as provided earlier in Figure 4.55. It is worth mentioning here that Oil P partially loose its wear protection after long duration engine testing which shows its ability to sustain engine conditions.

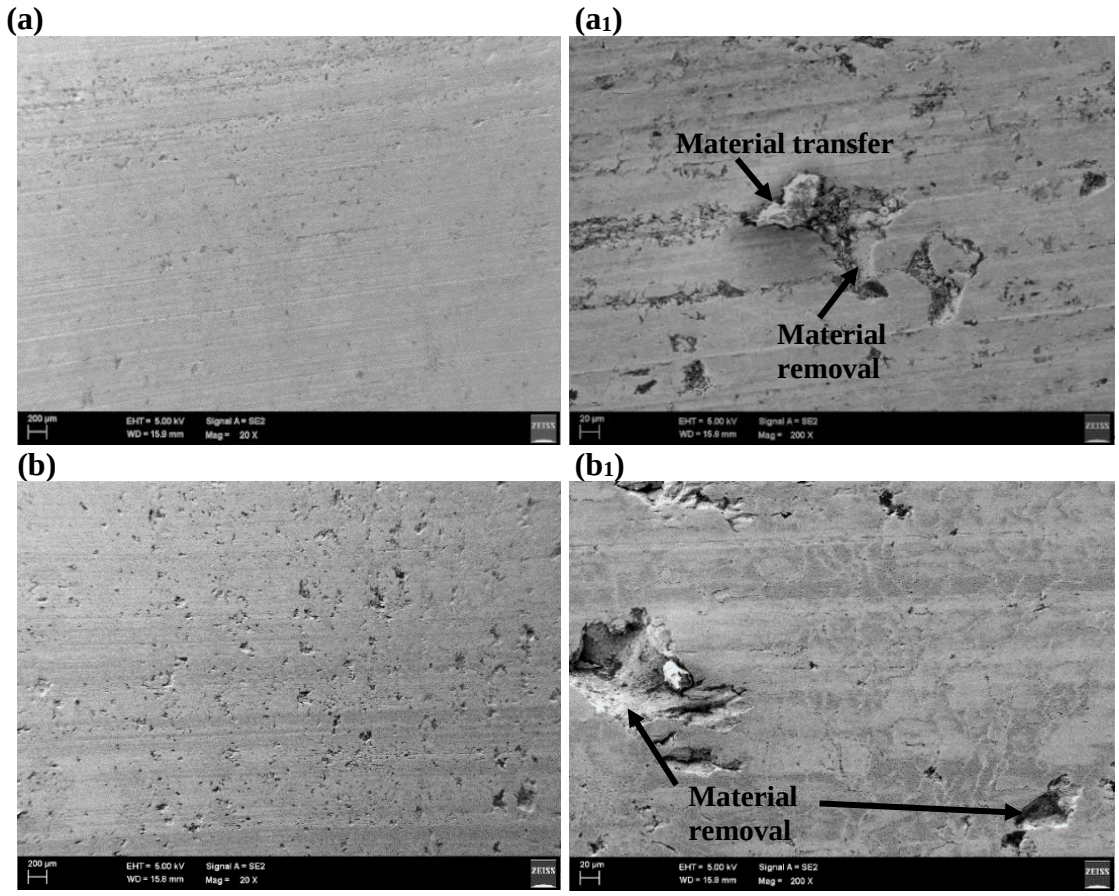

Figure 4.57: SEM micrographs of cylinder liner specimen tested with engine-aged samples of Oil P for engine fueled by (a) DF 20x (a_1) DF 200x (b) PB20 20x (b_1) (PB20) 200x

4.4.3.2 EDX Analysis

EDX analysis was performed for the region of SEM micrographs to find the chemical elements present on the worn cylinder liner specimen. Table 4.9 shows detailed percentage of elements found on the selected region. It can be observed that, engine-aged samples of Oil P show the presence of 'Ti' for samples collected from both DF fueled

and PB20 fueled engine testing. Though the deposition weight percentage was less than that of fresh Oil P (Table 4.1), the presence of 'Ti' shows the ability of Oil P to provide partial mending effect even after degradation by long hours' engine testing. It can be observed that carbon 'C' weight percentage has been increased than those of fresh oil samples. This increased 'C' element may be related with high soot content on the surface which appeared due to oil degradation. Further investigation of compounds existing on the worn surfaces, was carried out by Raman spectroscopy and discussed in subsequent section.

Table 4.9: Elemental details by EDX analysis for tribo-tests using engine-aged oils

Element wt (%)	Bio-based Nanolubricant (Oil P)	
	DF	PB20
Carbon	9.1	8.9
Oxygen	9.3	12.1
Iron	77.8	75.6
Titanium	3.1	2.6
Silicon	0.7	0.8

4.4.3.3 Raman Spectroscopy

To investigate the sources of elements on the worn surfaces in terms of corresponding compounds, the Raman spectra of engine-aged samples of Oil P are illustrated in Figure 4.58. For Raman peaks related to engine-aged samples of Oil P, it has been observed that Oil P maintained to provide sufficient lubrication performance in terms of forming the protective tribofilm on the worn cylinder liner surface. However, the relative intensities of obtained peaks were as low as five time than those of tested with fresh sample of Oil P (Figure 4.30).

Major factors influencing the peaks intensity for nanofluids include laser power, material purity and dispersion stability. In the considered case, the laser power and material purity were not varied which shows that the foreign contaminations like soot,

fuel residue, dust and acidic content may affect the dispersion by deteriorating the base oil-nanoparticles compatibility. Therefore, anatase TiO_2 peaks intensities were relatively low for PB20 fueled Oil samples as compared to oil samples collected from DF fueled engine tests. Thus, Raman spectra shows the ability of bio-based nanolubricant (Oil P) to form tribofilm on the worn surface even after long duration engine testing.

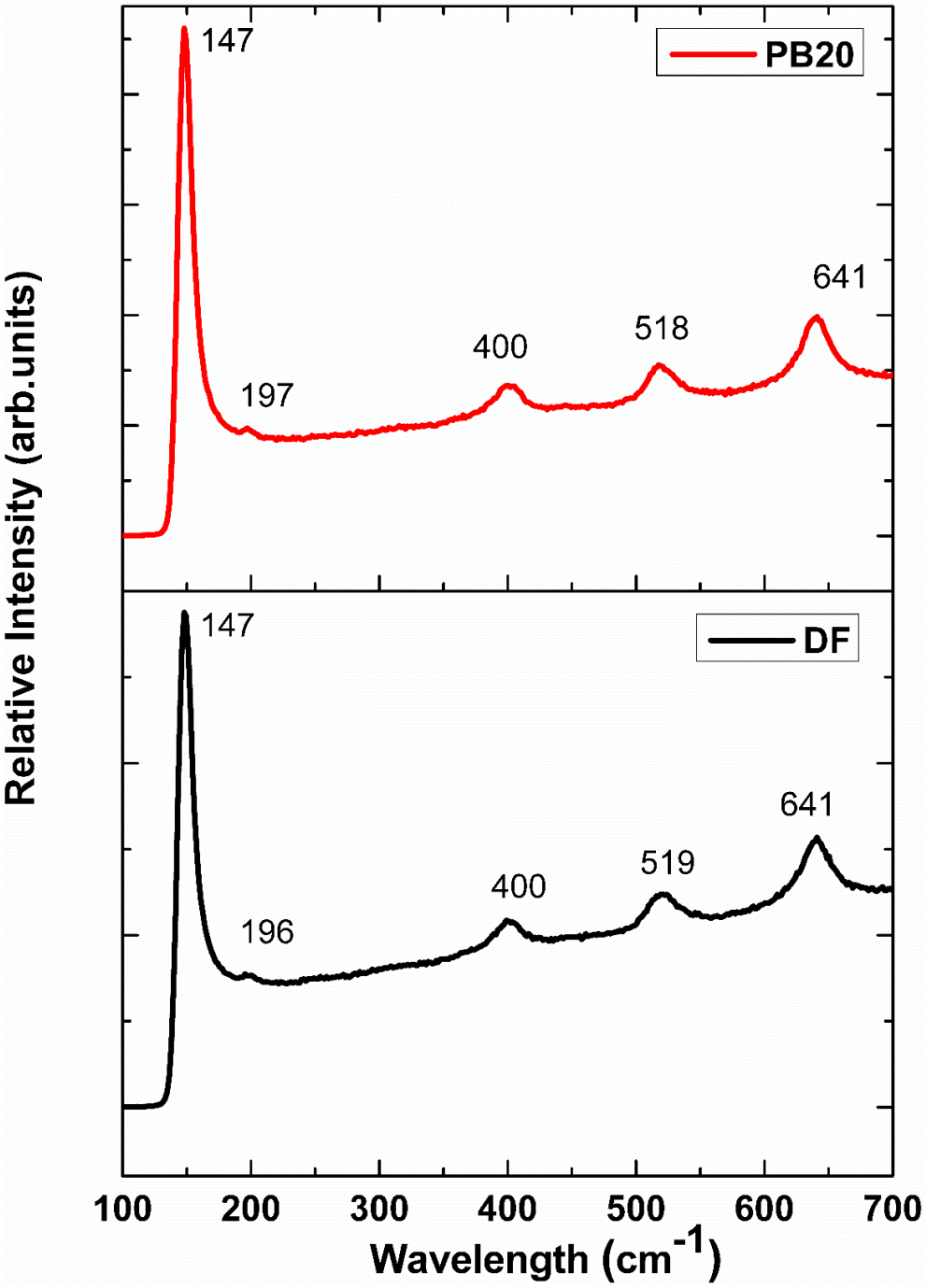

Figure 4.58: Raman spectra of cast iron cylinder liners specimen tested with engine-aged samples of Oil P

4.4.3.4 Surface Profilometry

Figure 4.59 (a-b) shows 3-D surface topography of the cylinder liner specimen tested with engine-aged samples of Oil P for DF fueled and PB20 fueled engine testing respectively. Comparatively higher surface roughness in terms of peak heights has been observed for oil samples collected for PB20 fueled engine testing. Though higher surface roughness has been observed than that of fresh Oil P (Figure 4.33), the engine-aged oil samples provide sufficient surface polishing effect. The surface roughness parameters show low surface roughness for engine-aged samples of Oil P (Figure 4.59) as compared to blank palm TMP ester (Figure 4.6). It shows that polishing effect by nanoTiO_2/SiO_2 in engine-aged oil samples of Oil P. Though surface enhancement tendency has been observed for engine sump oil samples but it was not as effective as that of fresh Oil P. This trend may be attributed to the higher tendency of adhesive and corrosive wear due to oil degradation by fuel residue and oxidation induced corrosion.

While looking into the 3-D surface topographic images for engine-aged oil samples collected from PB20 fueled engine tests, it can be observed that relatively higher surface roughness has been achieved as compared to those of DF fueled engine testing. For PB20 fueled engine testing, a higher roughness value i.e. Ra = 0.23 µm, Rq = 0.34 µm and Rz = 1.37 µm (Figure 4.59 (b)) has been observed for Oil P sample as compared to DF fueled engine testing for which Ra = 0.17 µm, Rq = 0.27 µm and Rz = 0.89 µm (Figure 4.59 (a)).

Analyzing the surface texture images and values of considered roughness parameters (Figure 4.59 (a-b)), it can be declared that nanoTiO_2/SiO_2 showed appropriate lubrication performance in terms of polishing effect even after degradation during long duration engine testing.

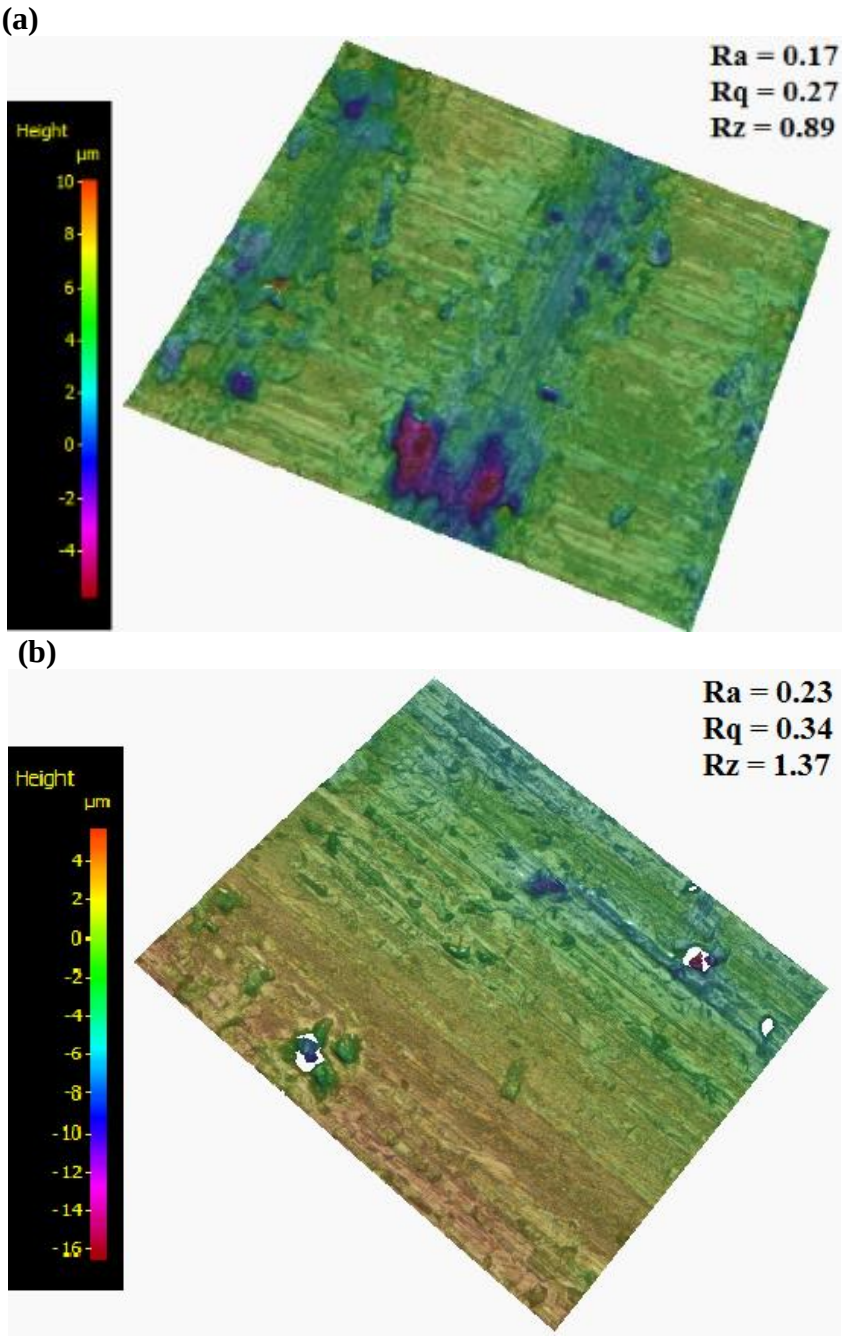

Figure 4.59: 3-D surface profile of cylinder liner specimen tested with engine-aged Oil P for engine fueled with (a) DF (b) PB20

CHAPTER 5: CONCLUSIONS AND RECOMMENDATIONS

This dissertation was dedicated to study the lubrication performance of a variety of nanoparticles as additives to bio-based base stock (palm TMP ester) for engine piston ring–cylinder interaction. The goal of the research was on the lubrication performance enhancement of palm TMP ester to minimize the sliding friction and wear losses for piston ring–cylinder combination. The significant contribution of this dissertation was developing a tribologically enhanced bio-based lubricant while enlightening the lubrication enhancing mechanisms of a variety of nanoparticle additives.

This research has illuminated the potential of bio-based nanolubricants in hopes that in future the macroscale development, industrial and economical competence, will move the lubrication industry one step further towards clean and safe lubrication solutions.

5.1 Conclusions

The major conclusions on the basis of experimental results are as follows:

1. Blank palm TMP ester exhibited comparable viscosity, improved VI but high average COF (approximately 25% higher) than that of petroleum mineral oil.

2. (a) The appropriate concentrations of considered nanoparticles showed significantly improved friction behavior and wear protection when added to palm TMP ester in the presence of surfactant. A reduction of 68% in average COF has been observed while wear volume was reduced to half for cylinder liner and piston ring segments using 0.75 wt% TiO_2/SiO_2 nanoparticles.

(b) An increase in nanoparticle concentrations helped in improving its EP behavior for all type of nanolubricants which showed high load carrying capacity of solid nano-additives by providing a cushion between rubbing surfaces.

(c) The poorly dispersed nanoparticles resulted in partial or complete loss of lubrication performance. In this regard, it is worth mentioning here that lowest average COF of 0.09 has been shown by most stable dispersion while highest value of average COF of 0.16 has been reported for poorly dispersed nanoparticles. Similarly, lowest wear volume loss of 0.013 mm^3 (piston ring) and 0.148 mm^3 (cylinder liner) has been observed for the most stable dispersion.

(d) The tribo-interface of piston ring and cylinder liner surfaces benefited from the lubricity of smaller nano-sized particles for their lubrication mechanisms of surfaces enhancement by forming protective tribofilm on the rubbing surfaces and secondary effects which included surface mending and surface polishing.

3. For engine-aged lubricant samples, high rate of degradation has been witnessed for bio-based nanolubricant as compared to conventional engine lubricant. At the end of drain interval, 17% higher oil thinning, 30% increased TAN and 16.8% high oxidation was observed for corresponding oil samples. However, an advantage of lowest soot content has been observed for bio-based engine-aged oil samples (reduced to half). This result showed environmental benefits over traditional lubricants and fuels combinations.

4. (a) The tribological analysis of engine-aged bio-based nanolubricant showed 84.5% higher average COF and four times higher wear volumes than that of corresponding fresh oil sample. The significant difference in the values of average COF and wear volumes of piston ring and cylinder liner for fresh and engine-aged

lubricants showed that the effect of lubricating oil condition must be taken into account while looking into the tribological performance of a lubricant for piston–cylinder interaction.

(b) The comparative analysis of friction and wear behavior for bio-based nanolubricant and conventional engine lubricant showed the potential of nanolubricant (0.75 wt% TiO_2/SiO_2+palm TMP ester+1 wt% OA) to provide adequate lubrication performance in fresh as well as engine-aged conditions.

5.2 Recommendations for Future Work

On the basis of obtained results, the following actions are recommended to carry out related future studies.

1. *Focus on understanding and establishing the stable dispersions by using suitable type and concentrations of nanoparticle along with surfactant or surface modification* – the dispersion stability results show that for same base stock and surfactant, the suspensions stability changes by varying the nanoparticles concentrations. The dispersion stability is directly linked to the tribological performance of nanoparticles added to a lubricant. In this regard future studies, can explore a number of combinations between variety of bio-based base stocks, surfactants, nanoparticles (types, size, structure, morphology, concentrations), surface modification techniques and dispersion techniques.

2. *Controlling the degradation rate of bio-based nanolubricant by investigating the role of additives like viscosity modifiers, detergents, antioxidants, corrosion inhibitors etc.* – though oil filter modification helped in maintaining the low alkaline reserve and oxidation for zero detergent bio-based nanolubricant, the additives are required to provide comparable viscosity, alkaline reserve and

protection of engine parts from corrosive attacks. Thus, future studies can investigate the suitability of such additives while focusing on the environmental conformity. In addition, such additives can be investigated in combination with strong base filter.

3. *For specific application, investigate the lubricants performance by establishing realistic lubricating oil condition* – a significant difference in the values and behaviors of COF and wear volumes showed that fresh as well as engine-aged lubricants must be investigated to understand the compatibility of lubricant for specific application. In this regard extraction of engine oil directly from top piston ring may provide more realistic tribological behavior for piston ring–cylinder lubrication. A comparative analysis between sump oil samples and oil samples collected directly from engine top piston ring would be more helpful to achieve realistic lubricant degradation and related tribological behavior.

4. *Exploring the nanolubricants tribological performance in combination with ionic liquids (ILs)* - Recent advances in the use of ionic liquids as potential candidates for lubricants and lubricant additives would be helpful to address the environmental concerns. In this regard, various combinations of nanoparticles, ILs and bio-based lubricants can be explored.

REFERENCES

Abdullah, M. I. H. C., Abdollah, M. F., Amiruddin, H., Tamaldin, N., & Nuri, N. R. M. (2014). Effect of hBN/Al_2O_3 nanoparticle additives on the tribological performance of engine oil. *Jurnal Teknologi, 66*(3).

Abdullah, M. I. H. C., Abdollah, M. F. B., Tamaldin, N., Amiruddin, H., Mat Nuri, N. R., Gachot, C., & Kaleli, H. (2016). Effect of hexagonal boron nitride nanoparticles as an additive on the extreme pressure properties of engine oil. *Industrial Lubrication and Tribology, 68*(4).

Abolle, A., Kouakou, L., & Planche, H. (2009). The viscosity of diesel oil and mixtures with straight vegetable oils: Palm, cabbage palm, cotton, groundnut, copra and sunflower. *Biomass and Bioenergy, 33*(9), 1116-1121.

Agency., E. P. (2002). A Comprehensive Analysis of Biodiesel Impacts on Exhaust Emissions: US Environmental Protection Agency Washington DC.

Akbulut, M. (2012). Nanoparticle-based lubrication systems. *Journal of Powder Metallurgy & Mining, 2012*.

Alves, S. M., Barros, B. S., Trajano, M. F., Ribeiro, K. S. B., & Moura, E. (2013). Tribological behavior of vegetable oil-based lubricants with nanoparticles of oxides in boundary lubrication conditions. *Tribology International, 65*(0), 28-36.

Amiruddin, H., Abdollah, M., Idris, A., Abdullah, M., & Tamaldin, N. (2015). Stability of nano-oil by pH control in stationary conditions. *Proceedings of Mechanical Engineering Research Day 2015: MERD'15, 2015*, 55-56.

Arbain, N. H., & Salimon, J. (2011). Synthesis and characterization of ester trimethylolpropane based jatropha curcas oil as biolubricant base stocks. *Journal of Science and Technology, 2*(2).

Arumugam S, e. a. (2014). Bio-lubricant-biodiesel combination of rapeseed oil: An experimental investigation on engine oil tribology, performance, and emissions of variable compression engine. *Energy, 72*, 618-627.

Arumugam, S., & Sriram, G. (2012a). Effect of bio-lubricant and biodiesel-contaminated lubricant on tribological behavior of cylinder liner–piston ring combination. *Tribology Transactions, 55*(4), 438-445.

Arumugam, S., & Sriram, G. (2012b). Synthesis and characterisation of rapeseed oil bio-lubricant–its effect on wear and frictional behaviour of piston ring–cylinder liner combination. *Proceedings of the Institution of Mechanical Engineers, Part J: Journal of Engineering Tribology, 227*(1), 3-15.

Arumugam, S., & Sriram, G. (2014). Synthesis and characterization of rapeseed oil bio-lubricant dispersed with nano copper oxide: Its effect on wear and frictional behavior of piston ring–cylinder liner combination. *Proceedings of the Institution of Mechanical Engineers, Part J: Journal of Engineering Tribology, 228*(11), 1308-1318.

Asfar, K. R., & Hamed, H. (1998). Combustion of fuel blends. *Energy Conversion and Management, 39*(10), 1081-1093.

Asrul, M., Zulkifli, N. W. M., Masjuki, H. H., & Kalam, M. A. (2013). Tribological properties and lubricant mechanism of nanoparticle in engine oil. *Procedia Engineering, 68*, 320-325.

Avan, E. Y., Spencer, A., Dwyer-Joyce, R. S., Almqvist, A., & Larsson, R. (2013). Experimental and numerical investigations of oil film formation and friction in a piston ring–liner contact. *Proceedings of the Institution of Mechanical Engineers, Part J: Journal of Engineering Tribology, 227*(2), 126-140.

Azman, S. S. N., Zulkifli, N. W. M., Masjuki, H., Gulzar, M., & Zahid, R. (2016). Study of tribological properties of lubricating oil blend added with graphene nanoplatelets. *Journal of Materials Research, 31*(13), 1932-1938.

Bakunin, V., Suslov, A. Y., Kuzmina, G., & Parenago, O. (2005). Recent achievements in the synthesis and application of inorganic nanoparticles as lubricant components. *Lubrication Science, 17*(2), 127-145.

Bakunin, V., Suslov, A. Y., Kuzmina, G., Parenago, O., & Topchiev, A. (2004). Synthesis and application of inorganic nanoparticles as lubricant components–a review. *Journal of Nanoparticle Research, 6*(2), 273-284.

Barnwal, B., & Sharma, M. (2005). Prospects of biodiesel production from vegetable oils in India. *Renewable and Sustainable Energy Reviews, 9*(4), 363-378.

Bartz, W. J. (2000). *Synthetic hydraulic fluids for high performance applications.* Paper presented at the Proceedings of the national conference on fluid power.

Basu, S., Sengupta, S., & Ahuja, B. (2005). *Fundamentals of Tribology*: PHI Learning Pvt. Ltd.

Battersby, N., Pack, S., & Watkinson, R. (1992). A correlation between the biodegradability of oil products in the CEC L-33-T-82 and modified Sturm tests. *Chemosphere, 24*(12), 1989-2000.

Battez, H. A., Fernandez Rico, J. E., Navas Arias, A., Viesca Rodriguez, J. L., Chou Rodriguez, R., & Diaz Fernandez, J. M. (2006). The tribological behaviour of ZnO nanoparticles as an additive to PAO6. *Wear, 261*(3–4), 256-263.

Battez, H. A., González, R., Felgueroso, D., Fernández, J. E., del Rocío Fernández, M., García, M. A., & Peñuelas, I. (2007). Wear prevention behaviour of nanoparticle suspension under extreme pressure conditions. *Wear, 263*(7–12), 1568-1574.

Battez, H. A., González, R., Viesca, J. L., Fernández, J. E., Fernández, D. J. M., Machado, A., . . . Riba, J. (2008). CuO, ZrO_2 and ZnO nanoparticles as antiwear additive in oil lubricants. *Wear, 265*(3), 422-428.

Beitelman, A. (1998). Time for a change? Assessing environmentally acceptable lubricants. *HYDRO REVIEW, 17*, 46-61.

Birova, A., Pavlovičová, A., & Cvenroš, J. (2002). Lubricating oils based on chemically modified vegetable oils. *Journal of Synthetic Lubrication, 18*(4), 291-299.

Blau, P. J. (2002). A review of sub-scale test methods to evaluate the friction and wear of ring and liner materials for spark-and compression ignition engines. *ORNL Oak Ridge National Laboratory (US)*.

Brandenberger, S., Mohr, M., Grob, K., & Neukom, H. P. (2005). Contribution of unburned lubricating oil and diesel fuel to particulate emission from passenger cars. *Atmos Environ, 39*(37), 6985-6994.

Brownawell, D. W., Thaler, W. A., Bannister, E., & Ladwig, P. K. (1990). USA Patent No. US4906389 A.

Bukovnik, S., Dörr, N., Čaika, V., Bartz, W. J., & Loibnegger, B. (2006). Analysis of diverse simulation models for combustion engine journal bearings and the influence of oil condition. *Tribology International, 39*(8), 820-826.

Çakir, M., & Akçay, İ. H. (2014). Frictional behavior between piston ring and cylinder liner in engine condition with application of reciprocating test. *International Journal of Materials Engineering and Technology, 11*(1), 57-71.

Çelik, O. N., Ay, N., & Göncü, Y. (2013). Effect of nano hexagonal boron nitride lubricant additives on the friction and wear properties of AISI 4140 steel. *Particulate Science and Technology, 31*(5), 501-506.

Cesur, İ., Ayhan, V., Parlak, A., Savaş, Ö., & Aydin, Z. The effects of different fuels on wear between piston ring and cylinder. *Advances in Mechanical Engineering, 2014*, 8.

Chang, L., Zhang, Z., Breidt, C., & Friedrich, K. (2005). Tribological properties of epoxy nanocomposites: I. Enhancement of the wear resistance by nano-TiO_2 particles. *Wear, 258*(1–4), 141-148.

Chen, S., & Liu, W. (2006). Oleic acid capped PbS nanoparticles: Synthesis, characterization and tribological properties. *Materials Chemistry and Physics, 98*(1), 183-189.

Chiñas-Castillo, F., & Spikes, H. (2003). Mechanism of action of colloidal solid dispersions. *Journal of Tribology, 125*(3), 552-557.

Cho, Y., Park, J., Ku, B., Lee, J., Park, W.-G., Lee, J., & Kim, S. H. (2012). Synergistic effect of a coating and nano-oil lubricant on the tribological properties of friction surfaces. *International Journal of Precision Engineering and Manufacturing, 13*(1), 97-102.

Choi, Y., Lee, C., Hwang, Y., Park, M., Lee, J., Choi, C., & Jung, M. (2009). Tribological behavior of copper nanoparticles as additives in oil. *Current Applied Physics, 9*(2), e124-e127.

Chou, R., Battez, A. H., Cabello, J. J., Viesca, J. L., Osorio, A., & Sagastume, A. (2010). Tribological behavior of polyalphaolefin with the addition of nickel nanoparticles. *Tribology International, 43*(12), 2327-2332.

Daniels, C. C., & Braun, M. J. (2006). The friction behavior of individual components of a spark-ignition engine during warm-up. *Tribology Transactions, 49*(2), 166-173.

Das, S. K., Bedar, A., Kannan, A., & Jasuja, K. (2015). Aqueous dispersions of few-layer-thick chemically modified magnesium diboride nanosheets by ultrasonication assisted exfoliation. *Scientific Reports, 5*, 10522.

De Silva, P., Priest, M., Lee, P., Coy, R., & Taylor, R. (2011). Tribometer investigation of the frictional response of piston rings when lubricated with the separated phases of lubricant contaminated with the gasoline engine biofuel ethanol and water. *Tribology Letters, 43*(2), 107-120.

Demas, N. G., Timofeeva, E. V., Routbort, J. L., & Fenske, G. R. (2012). Tribological effects of BN and MoS_2 nanoparticles added to polyalphaolefin oil in piston skirt/cylinder liner tests. *Tribology Letters, 47*(1), 91-102.

Devlin, C. C., Passut, C., Campbell, R., & Jao, T.-C. (2008). Biodiesel fuel effect on diesel engine lubrication. *SAE Technical Paper, 2008-01-2375*.

Dwivedi, M., & Sapre, S. (2002). Total vegetable-oil based greases prepared from castor oil. *Journal of Synthetic Lubrication, 19*(3), 229-241.

EIA. *International energy statistics*. Retrieved from http://www.eia.gov/cfapps/ipdbproject/iedindex3.cfm?tid=79&pid=81&aid=2&cid=regions&syid=2008&eyid=2012&unit=TBPD.

Einstein, A. (1905). On the movement of small particles suspended in a stationary liquid demanded by the molecular-kinetic theory of heart. *Annalen der physik, 17*, 549-560.

Erhan, S., Adhvaryu, A., & Sharma, B. (2006). Chemically functionalized vegetable oils. *CHEMICAL INDUSTRIES-NEW YORK-MARCEL DEKKER-, 111*, 361.

Ettefaghi, E.-o.-l., Ahmadi, H., Rashidi, A., & Mohtasebi, S.-S. (2013). Investigation of the anti-wear properties of nano additives on sliding bearings of internal combustion engines. *International Journal of Precision Engineering and Manufacturing, 14*(5), 805-809.

Falvo, M. R., & Superfine, R. (2000). Mechanics and Friction at the Nanometer Scale. *Journal of Nanoparticle Research, 2*(3), 237-248.

Fan, W. T.-C. (2010). *Regeneration of used petroleum-based lubricants and biolubricants by a novel green and sustainable technology*: University of Southern California.

Fang, H. L., Whitacre, S. D., Yamaguchi, E. S., & Boons, M. (2007). Biodiesel impact on wear protection of engine oils. *SAE Technical Paper, 2007-01-4141*.

Fernandez, J. E., Viesca, J. L., & Battez, H. A. (2008). *Tribological behaviour of copper oxide nanoparticle suspension*. Paper presented at the Lubrication Management and Technology Conference & Exhibition, San Sebastian, Spain.

Fox, N., & Stachowiak, G. (2003). Boundary lubrication properties of oxidized sunflower oil. *Tribology & Lubrication Technology, 59*(2), 15.

Gao, C., Wang, Y., Hu, D., Pan, Z., & Xiang, L. (2013). Tribological properties of magnetite nanoparticles with various morphologies as lubricating additives. *Journal of Nanoparticle Research, 15*(3), 1-10.

Ghaednia, H. (2014). *An Analytical and Experimental Investigation of Nanoparticle Lubricants.* Auburn University.

Ginzburg, B., Shibaev, L., Kireenko, O., Shepelevskii, A., Baidakova, M., & Sitnikova, A. (2002). Antiwear Effect of Fullerene C 6 0 Additives to Lubricating Oils. *Russian journal of applied chemistry, 75*(8), 1330-1335.

Godfrey, D. (1987). Recognition and solution of some common wear problems related to lubricants and hydraulic fluids. *Lubricant Engineering, 43*, 111-114.

Greco, A., Mistry, K., Sista, V., Eryilmaz, O., & Erdemir, A. (2011). Friction and wear behaviour of boron based surface treatment and nano-particle lubricant additives for wind turbine gearbox applications. *Wear, 271*(9–10), 1754-1760.

Greenberg, R., Halperin, G., Etsion, I., & Tenne, R. (2004). The effect of WS_2 nanoparticles on friction reduction in various lubrication regimes. *Tribology Letters, 17*(2), 179-186.

Grushcow, J., & Smith, M. (2005). *Next generation feedstocks from new frontiers in oilseed engineering.* Paper presented at the World Tribology Congress III.

Gryglewicz, S., Piechocki, W., & Gryglewicz, G. (2003). Preparation of polyol esters based on vegetable and animal fats. *Bioresource Technology, 87*(1), 35-39.

Gullac, B., & Akalin, O. (2010). Frictional characteristics of IF-WS_2 nanoparticles in simulated engine conditions. *Tribology Transactions, 53*(6), 939-947.

Holmberg, K., Andersson, P., & Erdemir, A. (2012). Global energy consumption due to friction in passenger cars. *Tribology International, 47*, 221-234.

Honary, L. A. (1996). An investigation of the use of soybean oil in hydraulic systems. *Bioresource Technology, 56*(1), 41-47.

Hsu, S. M. (1997). Boundary lubrication: current understanding. *Tribology Letters, 3*(1), 1-11.

Hu, K. H., Huang, F., Hu, X. G., Xu, Y. F., & Zhou, Y. Q. (2011). Synergistic effect of Nano-MoS_2 and anatase Nano-TiO_2 on the lubrication properties of MoS_2/TiO_2 Nano-Clusters. *Tribology Letters, 43*(1), 77-87.

Hu, Z. S., Lai, R., Lou, F., Wang, L. G., Chen, Z. L., Chen, G. X., & Dong, J. X. (2002). Preparation and tribological properties of nanometer magnesium borate as lubricating oil additive. *Wear, 252*(5–6), 370-374.

Igartua, A., Fernández, X., Areitioaurtena, O., Luther, R., Seyfert, C., Rausch, J., . . . Woydt, M. (2009). Biolubricants and triboreactive materials for automotive applications. *Tribology International, 42*(4), 561-568.

Ingole, S., Charanpahari, A., Kakade, A., Umare, S., Bhatt, D., & Menghani, J. (2013). Tribological behavior of nano TiO_2 as an additive in base oil. *Wear, 301*(1), 776-785.

Isaksson, M., Frick, M., Gruvberger, B., Pontén, A., & Bruze, M. (2002). Occupational allergic contact dermatitis from the extreme pressure (EP) additive zinc, bis ((O, O′-di-2-ethylhexyl) dithiophosphate) in neat oils. *Contact dermatitis, 46*(4), 248-249.

Jaiswal, V., Rastogi, R. B., Kumar, R., Singh, L., & Mandal, K. D. (2014). Tribological studies of stearic acid-modified $CaCu_{2.9}Zn_{0.1}Ti4O_{12}$ nanoparticles as effective zero SAPS antiwear lubricant additives in paraffin oil. *Journal of Materials Chemistry A, 2*(2), 375-386.

Jatti, V. S., & Singh, T. P. (2015). Copper oxide nano-particles as friction-reduction and anti-wear additives in lubricating oil. *Journal of Mechanical Science and Technology, 29*(2), 793-798.

Jayadas, N., & Prabhakaran Nair, K. (2007). Tribological evaluation of coconut oil as an environment-friendly lubricant. *Tribology International, 40*(2), 350-354.

Jiang, Q., & Wang, S. (1998). Abrasive wear of locomotive diesel engines and contaminant control. *Tribology Transactions, 41*(4), 605-609.

Jiao, D., Zheng, S., Wang, Y., Guan, R., & Cao, B. (2011). The tribology properties of alumina/silica composite nanoparticles as lubricant additives. *Applied Surface Science, 257*(13), 5720-5725.

Johansson, S., Nilsson, P. H., Ohlsson, R., & Rosén, B.-G. (2011). Experimental friction evaluation of cylinder liner/piston ring contact. *Wear, 271*(3), 625-633.

Joly-Pottuz, L., Vacher, B., Ohmae, N., Martin, J. M., & Epicier, T. (2008). Anti-wear and friction reducing mechanisms of carbon nano-onions as lubricant additives. *Tribology Letters, 30*(1), 69-80.

Kalin, M., Kogovšek, J., & Remškar, M. (2012). Mechanisms and improvements in the friction and wear behavior using MoS_2 nanotubes as potential oil additives. *Wear, 280–281*(0), 36-45.

Kassfeldt, E., & Dave, G. (1997). Environmentally adapted hydraulic oils. *Wear, 207*(1), 41-45.

Kheireddin, B. A. (2013). *Tribological Properties of Nanopartice-Based Lubrication Systems.* Texas A&M University.

Kodali, D. R. (2002). High performance ester lubricants from natural oils. *Industrial Lubrication and Tribology, 54*(4), 165-170.

Kohashi, K.-i., Kimura, Y., Murakami, M., & Drouvin, Y. (2013). Analysis of piston friction in internal combustion engine. *SAE Int. J. Fuels Lubr., 6*(3), 589-593.

Kolodziejczyk, L., Martinez-Martinez, D., Rojas, T., Fernandez, A., & Sanchez-Lopez, J. (2007). Surface-modified Pd nanoparticles as a superior additive for lubrication. *Journal of Nanoparticle Research, 9*(4), 639-645.

Koshy, C. P., Rajendrakumar, P. K., & Thottackkad, M. V. (2015). Evaluation of the tribological and thermo-physical properties of coconut oil added with MoS_2 nanoparticles at elevated temperatures. *Wear, 330–331*, 288-308.

Laad, M., & Jatti, V. K. S. (2016). Titanium oxide nanoparticles as additives in engine oil. *Journal of King Saud University-Engineering Sciences*. doi:10.1016/j.jksues.2016.01.008

Labeckas, G., & Slavinskas, S. (2006). The effect of rapeseed oil methyl ester on direct injection Diesel engine performance and exhaust emissions. *Energy Conversion and Management, 47*(13–14), 1954-1967.

Lee, C.-G., Hwang, Y.-J., Choi, Y.-M., Lee, J.-K., Choi, C., & Oh, J.-M. (2009). A study on the tribological characteristics of graphite nano lubricants. *International Journal of Precision Engineering and Manufacturing, 10*(1), 85-90.

Lee, J., Cho, S., Hwang, Y., Cho, H.-J., Lee, C., Choi, Y., . . . Kim, D. (2009). Application of fullerene-added nano-oil for lubrication enhancement in friction surfaces. *Tribology International, 42*(3), 440-447.

Lee, K., Hwang, Y., Cheong, S., Choi, Y., Kwon, L., Lee, J., & Kim, S. H. (2009). Understanding the role of nanoparticles in nano-oil lubrication. *Tribology Letters, 35*(2), 127-131.

Lee, K., Hwang, Y., Cheong, S., Kwon, L., Kim, S., & Lee, J. (2009). Performance evaluation of nano-lubricants of fullerene nanoparticles in refrigeration mineral oil. *Current Applied Physics, 9*(2), e128-e131.

Lee, P., Priest, M., Stark, M., Wilkinson, J., Smith, L. J., Taylor, R., & Chung, S. (2006). Extraction and tribological investigation of top piston ring zone oil from a gasoline engine. *Proceedings of the Institution of Mechanical Engineers, Part J: Journal of Engineering Tribology, 220*(3), 171-180.

Li, B., Wang, X., Liu, W., & Xue, Q. (2006). Tribochemistry and antiwear mechanism of organic–inorganic nanoparticles as lubricant additives. *Tribology Letters, 22*(1), 79-84.

Li, W., Zheng, S., Cao, B., & Ma, S. (2011). Friction and wear properties of ZrO_2/SiO_2 composite nanoparticles. *Journal of Nanoparticle Research, 13*(5), 2129-2137.

Li, Z., Li, Y., Zhang, Y., Ren, T., & Zhao, Y. (2014). Tribological study of hydrolytically stable S-containing alkyl phenylboric esters as lubricant additives. *RSC Advances, 4*(48), 25118-25126.

Liu, G., Li, X., Lu, N., & Fan, R. (2005). Enhancing AW/EP property of lubricant oil by adding nano Al/Sn particles. *Tribology Letters, 18*(1), 85-90.

Liu, G., Li, X., Qin, B., Xing, D., Guo, Y., & Fan, R. (2004). Investigation of the mending effect and mechanism of copper nano-particles on a tribologically stressed surface. *Tribology Letters, 17*(4), 961-966.

Lockledge, S. P., & Brownawell, D. W. (2013a). Materials and processes for reducing combustion by-products in a lubrication system for an internal combustion engine. USA: Google Patents, US8607991 B2.

Lockledge, S. P., & Brownawell, D. W. (2013b). Oil filters containing strong base and methods of their use. USA: Google Patents, US20130068694 A1.

Lockledge, S. P., & Brownawell, D. W. (2014). USA Patent No. US8691096 B2.

Luo, T., Wei, X., Huang, X., Huang, L., & Yang, F. (2014). Tribological properties of Al_2O_3 nanoparticles as lubricating oil additives. *Ceramics International, 40*(5), 7143-7149.

Ma, S., Zheng, S., Cao, D., & Guo, H. (2010). Anti-wear and friction performance of ZrO_2 nanoparticles as lubricant additive. *Particuology, 8*(5), 468-472.

Mang, T., & Dresel, W. (2007). *Lubricants and lubrication*: John Wiley & Sons.

Mannekote, J. K., & Kailas, S. V. (2011). Experimental investigation of coconut and palm oils as lubricants in four-stroke engine. *Tribology Online, 6*(1), 76-82.

Martin, J. M., & Ohmae, N. (2008). *Nanolubricants* (Vol. 13): John Wiley & Sons.

Masjuki, H., & Maleque, M. (1997). Investigation of the anti-wear characteristics of palm oil methyl ester using a four-ball tribometer test. *Wear, 206*(1), 179-186.

Masjuki, H., Maleque, M., Kubo, A., & Nonaka, T. (1999). Palm oil and mineral oil based lubricants—their tribological and emission performance. *Tribol. Int., 32*(6), 305-314.

Meier, M. A., Metzger, J. O., & Schubert, U. S. (2007). Plant oil renewable resources as green alternatives in polymer science. *Chemical Society Reviews, 36*(11), 1788-1802.

Min, Y., Akbulut, M., Kristiansen, K., Golan, Y., & Israelachvili, J. (2008). The role of interparticle and external forces in nanoparticle assembly. *Nature materials, 7*(7), 527-538.

Mobarak, H. M., Niza Mohamad, E., Masjuki, H. H., Kalam, M. A., Al Mahmud, K. A. H., Habibullah, M., & Ashraful, A. M. (2014). The prospects of biolubricants as

alternatives in automotive applications. *Renewable and Sustainable Energy Reviews, 33*, 34-43.

Mofijur, M., Masjuki, H., Kalam, M., Hazrat, M., Liaquat, A., Shahabuddin, M., & Varman, M. (2012). Prospects of biodiesel from Jatropha in Malaysia. *Renewable and Sustainable Energy Reviews, 16*(7), 5007-5020.

Mohsin, R., Majid, Z. A., Shihnan, A. H., Nasri, N. S., & Sharer, Z. (2014). Effect of biodiesel blends on engine performance and exhaust emission for diesel dual fuel engine. *Energy Conversion and Management, 88*(0), 821-828.

Morina, A., Lee, P., Priest, M., & Neville, A. (2011). Challenges of simulating'fired engine'ring-liner oil additive/surface interactions in ring-liner bench tribometer. *Tribology-Materials, Surfaces & Interfaces, 5*(1), 25-33.

Mukesh, K. D., Jayashree, B., & SSV, R. (2013). PTFE based nano-lubricants. *Wear, 306*(1), 80-88.

Nagendramma, P., & Kaul, S. (2012). Development of ecofriendly/biodegradable lubricants: An overview. *Renewable and Sustainable Energy Reviews, 16*(1), 764-774.

Nakada, M. (1994). Trends in engine technology and tribology. *Tribology International, 27*(1), 3-8.

Nallasamy, P., Saravanakumar, N., Nagendran, S., Suriya, E., & Yashwant, D. (2014). Tribological investigations on MoS_2-based nanolubricant for machine tool slideways. *Proceedings of the Institution of Mechanical Engineers, Part J: Journal of Engineering Tribology, 229*(5), 559-567.

Nosonovsky, M., & Bhushan, B. (2012). *Green Tribology*: Springer.

Notay, R. B. R. S. (2013). *Evolution of lubricant degradation and lubricant behaviour in a piston assembly of a reciprocating gasoline engine.* (PhD), University of Leeds.

Ogunniyi, D. (2006). Castor oil: A vital industrial raw material. *Bioresource Technology, 97*(9), 1086-1091.

Ohmae, N., Martin, J. M., & Mori, S. (2005). *Micro and nanotribology*: ASME Press New York.

Okubo, H., Watanabe, S., Tadokoro, C., & Sasaki, S. (2016). Ultralow friction of a tetrahedral amorphous carbon film lubricated with an environmentally friendly ester-based oil. *Tribology Online, 11*(2), 102-113.

P. Andersson, J. Tamminen, & Sandstrom, C. E. (2002). Piston Ring Tribology; Literature Survey. *2178 de VTT Tiedotteita*.

Padgurskas, J., Rukuiza, R., Prosyčevas, I., & Kreivaitis, R. (2013). Tribological properties of lubricant additives of Fe, Cu and Co nanoparticles. *Tribology International, 60*(0), 224-232.

Peña-Parás, L., Taha-Tijerina, J., Garza, L., Maldonado-Cortés, D., Michalczewski, R., & Lapray, C. (2015). Effect of CuO and Al2O3 nanoparticle additives on the tribological behavior of fully formulated oils. *Wear, 332–333*, 1256-1261.

Peng, D. X., Chen, C. H., Kang, Y., Chang, Y. P., & Chang, S. Y. (2010). Size effects of SiO_2 nanoparticles as oil additives on tribology of lubricant. *Industrial Lubrication and Tribology, 62*(2), 111-120.

Peng, D. X., Kang, Y., Chen, S., Shu, F., & Chang, Y. (2010). Dispersion and tribological properties of liquid paraffin with added aluminum nanoparticles. *Industrial Lubrication and Tribology, 62*(6), 341-348.

Petraru, L., & Novotny-Farkas, F. (2012). Influence of biodiesel fuels on lubricity of passenger car diesel engine oils. *goriva i maziva, 51*(2), 157-165.

Priest, M., & Taylor, C. (2000). Automobile engine tribology—approaching the surface. *Wear, 241*(2), 193-203.

Quinchia, L., Delgado, M., Franco, J., Spikes, H., & Gallegos, C. (2012). Low-temperature flow behaviour of vegetable oil-based lubricants. *Industrial Crops and Products, 37*(1), 383-388.

Rabaso, P. (2014). *Nanoparticle-doped lubricants: potential of Inorganic Fullerene-like (IF-) molybdenum disulfide for automotive applications.* INSA de Lyon.

Rabaso, P., Ville, F., Dassenoy, F., Diaby, M., Afanasiev, P., Cavoret, J., . . . Le Mogne, T. (2014). Boundary lubrication: Influence of the size and structure of inorganic fullerene-like MoS_2 nanoparticles on friction and wear reduction. *Wear, 320*(1–2), 161-178.

Rakopoulos, C., Antonopoulos, K., Rakopoulos, D., Hountalas, D., & Giakoumis, E. (2006). Comparative performance and emissions study of a direct injection diesel engine using blends of diesel fuel with vegetable oils or bio-diesels of various origins. *Energy Conversion and Management, 47*(18), 3272-3287.

Ran, X., Yu, X., & Zou, Q. (2016). Effect of Particle Concentration on Tribological Properties of ZnO Nanofluids. *Tribology Transactions*, 1-17.

Randles, S. (1992). Environmentally considerate ester lubricants for the automotive and engineering industries. *Journal of Synthetic Lubrication, 9*(2), 145-161.

Rapoport, L., Bilik, Y., Feldman, Y., Homyonfer, M., Cohen, S., & Tenne, R. (1997). Hollow nanoparticles of WS_2 as potential solid-state lubricants. *Nature, 387*(6635), 791-793.

Rapoport, L., Leshchinsky, V., Lapsker, I., Volovik, Y., Nepomnyashchy, O., Lvovsky, M., . . . Tenne, R. (2003). Tribological properties of WS_2 nanoparticles under mixed lubrication. *Wear, 255*(7-12), 785-793.

Rapoport, L., Leshchinsky, V., Lvovsky, M., Nepomnyashchy, O., Volovik, Y., & Tenne, R. (2002). Mechanism of friction of fullerenes. *Industrial Lubrication and Tribology, 54*(4), 171-176.

Ratoi, M., Castle, R. C., Bovington, C. H., & Spikes, H. A. (2004). The influence of soot and dispersant on ZDDP film thickness and friction. *Lubrication Science, 17*(1), 25-43.

Reeves, C. J. (2013). *An experimental investigation characterizing the tribological performance of natural and synthetic biolubricants composed of carboxylic acids for energy conservation and sustainability*. The University of Wisconsin-Milwaukee.

Reeves, C. J., Menezes, P. L., Jen, T.-C., & Lovell, M. R. (2012). *Evaluating the tribological performance of green liquid lubricants and powder additive based green liquid lubricants.* Paper presented at the Proceedings of 2012 STLE Annual Meeting & Exhibition, STLE.

Rhee, I.-S., Velez, C., & Von Bernewitz, K. (1995). *Evaluation of Environmentally Acceptable Hydraulic Fluids*. Retrieved from http://www.dtic.mil/cgi-bin/GetTRDoc?Location=U2&doc=GetTRDoc.pdf&AD=ADA293037

Richardson, D. E. (2000). Review of power cylinder friction for diesel engines. *Journal of Engineering for Gas Turbines and Power-Transactions of the Asme, 122*(4), 506-519.

Rohrbach, R. P., Jones, G. W., Unger, P. D., & Bause, D. E. (2007). USA Patent No. WO2002096534 A1.

Rudnick, L. R. (2013). *Synthetics, mineral oils, and bio-based lubricants: chemistry and technology*: CRC press.

Sahoo, R. R., & Biswas, S. K. (2014). Effect of Layered MoS_2 Nanoparticles on the Frictional Behavior and Microstructure of Lubricating Greases. *Tribology Letters, 53*(1), 157-171.

Saidur, R., Kazi, S., Hossain, M., Rahman, M., & Mohammed, H. (2011). A review on the performance of nanoparticles suspended with refrigerants and lubricating oils in refrigeration systems. *Renewable and Sustainable Energy Reviews, 15*(1), 310-323.

Salimon, J., Salih, N., & Yousif, E. (2010). Biolubricants: Raw materials, chemical modifications and environmental benefits. *European Journal of Lipid Science and Technology, 112*(5), 519-530.

Salimon, J., Salih, N., & Yousif, E. (2012a). Improvement of pour point and oxidative stability of synthetic ester basestocks for biolubricant applications. *Arabian Journal of Chemistry, 5*(2), 193-200.

Salimon, J., Salih, N., & Yousif, E. (2012b). Triester derivatives of oleic acid: the effect of chemical structure on low temperature, thermo-oxidation and tribological properties. *Industrial Crops and Products, 38*, 107-114.

Schiøtz, J., & Jacobsen, K. W. (2003). A maximum in the strength of nanocrystalline copper. *Science, 301*(5638), 1357-1359.

Schneider, M. P. (2006). Plant-oil-based lubricants and hydraulic fluids. *Journal of the Science of Food and Agriculture, 86*(12), 1769-1780.

Scholz, V., & da Silva, J. N. (2008). Prospects and risks of the use of castor oil as a fuel. *Biomass and Bioenergy, 32*(2), 95-100.

Shayler, P., Leong, D., Pegg, I., & Murphy, M. (2009). Investigations of Piston Ring Pack and Skirt Contributions to Motored Engine Friction. *SAE international journal of engines, 1*(1), 723-734.

Singh, A. K. (2011). Castor oil-based lubricant reduces smoke emission in two-stroke engines. *Industrial Crops and Products, 33*(2), 287-295.

Singh, P. J., Khurma, J., & Singh, A. (2010). Preparation, characterisation, engine performance and emission characteristics of coconut oil based hybrid fuels. *Renewable energy, 35*(9), 2065-2070.

Singh, R. K., Kukrety, A., Thakre, G. D., Atray, N., & Ray, S. S. (2015). Development of new ecofriendly detergent/dispersant/antioxidant/antiwear additives from l-histidine for biolubricant applications. *RSC Advances, 5*(47), 37649-37656.

Smith, O., Priest, M., Taylor, R., Price, R., & Cantley, A. (2005). *In-cylinder fuel and lubricant effects on gasoline engine friction.* Paper presented at the World Tribology Congress III.

Socrates, G. (2004). *Infrared and Raman characteristic group frequencies: tables and charts*: John Wiley & Sons.

Song, X., Zheng, S., Zhang, J., Li, W., Chen, Q., & Cao, B. (2012). Synthesis of monodispersed $ZnAl_2O_4$ nanoparticles and their tribology properties as lubricant additives. *Materials Research Bulletin, 47*(12), 4305-4310.

Spikes, H. (2015). Friction Modifier Additives. *Tribology Letters, 60*(1), 1-26.

Stepien, Z., Urzedowska, W., Oleksiak, S., & Czerwinski, J. (2011). Research on Emissions and Engine Lube Oil Deterioration of Diesel Engines with BioFuels (RME). *SAE International Journal of Fuels and Lubricants, 4*(1), 125-138.

Su, Y., Gong, L., & Chen, D. (2015). An investigation on tribological properties and lubrication mechanism of graphite nanoparticles as vegetable based oil additive. *Journal of Nanomaterials, 16*(1).

Sugiyama, G., Maeda, A., & Nagai, K. (2007). Oxidation Degradation and Acid Generation in Diesel Fuel Containing 5% FAME. *SAE Technical Paper, 2007-01-2027*.

Sui, T., Song, B., Zhang, F., & Yang, Q. (2015). Effect of particle size and ligand on the tribological properties of amino functionalized hairy silica nanoparticles as an additive to polyalphaolefin. *Journal of Nanomaterials, 2015*, 1-9.

Sui, T., Song, B., Zhang, F., & Yang, Q. (2016). Effects of functional groups on the tribological properties of hairy silica nanoparticles as an additive to polyalphaolefin. *RSC Advances, 6*(1), 393-402.

Sunqing, Q., Junxiu, D., & Guoxu, C. (1999). Tribological properties of CeF 3 nanoparticles as additives in lubricating oils. *Wear, 230*(1), 35-38.

Tao, X., Jiazheng, Z., & Kang, X. (1996). The ball-bearing effect of diamond nanoparticles as an oil additive. *Journal of Physics D: Applied Physics, 29*(11), 2932.

Taylor, R., & Coy, R. (2000). Improved fuel efficiency by lubricant design: a review. *Proceedings of the Institution of Mechanical Engineers, Part J: Journal of Engineering Tribology, 214*(1), 1-15.

Thakur, M. R. N., Srinivas, D. V., & Jain, D. A. K. (2016). Anti-wear, anti-friction and extreme pressure properties of motor bike engine oil dispersed with molybdenum disulphide nano-particles. *Tribology Transactions*. doi:10.1080/10402004.2016.1142034

Thottackkad, M. V., Perikinalil, R. K., & Kumarapillai, P. N. (2012). Experimental evaluation on the tribological properties of coconut oil by the addition of CuO nanoparticles. *International Journal of Precision Engineering and Manufacturing, 13*(1), 111-116.

Truhan, J. J., Qu, J., & Blau, P. J. (2005a). The effect of lubricating oil condition on the friction and wear of piston ring and cylinder liner materials in a reciprocating bench test. *Wear, 259*(7), 1048-1055.

Truhan, J. J., Qu, J., & Blau, P. J. (2005b). A rig test to measure friction and wear of heavy duty diesel engine piston rings and cylinder liners using realistic lubricants. *Tribology International, 38*(3), 211-218.

Tung, S. C., & McMillan, M. L. (2004). Automotive tribology overview of current advances and challenges for the future. *Tribol. Int., 37*(7), 517-536.

Uosukainen, E., Linko, Y.-Y., Lämsä, M., Tervakangas, T., & Linko, P. (1998). Transesterification of trimethylolpropane and rapeseed oil methyl ester to environmentally acceptable lubricants. *Journal of the American Oil Chemists' Society, 75*(11), 1557-1563.

USDA Economics, S. a. M. I. S. (2016). *United States Department of Agriculture Economics, Statistics and Market Information System ESMIS*. Retrieved from https://www.library.cornell.edu/usda-economics-statistics-and-market-information-system

Usman, A., Cheema, T. A., & Park, C. W. (2015). Tribological performance evaluation and sensitivity analysis of piston ring lubricating film with deformed cylinder liner. *Proceedings of the Institution of Mechanical Engineers, Part J: Journal of Engineering Tribology, 229*(12), 1455-1468.

Verma, A., Jiang, W., Abu Safe, H. H., Brown, W. D., & Malshe, A. P. (2008). Tribological behavior of deagglomerated active inorganic nanoparticles for advanced lubrication. *Tribology Transactions, 51*(5), 673-678.

Viesca, J. L., Battez, A. H., González, R., Chou, R., & Cabello, J. J. (2011). Antiwear properties of carbon-coated copper nanoparticles used as an additive to a polyalphaolefin. *Tribology International, 44*(7–8), 829-833.

Waara, P., Norrby, T., & Prakash, B. (2004). Tribochemical Wear of Rail Steels Lubricated with Synthetic Ester-Based Model Lubricants. *Tribology Letters, 17*(3), 561-568.

Wan, Q., Jin, Y., Sun, P., & Ding, Y. (2014). Rheological and tribological behaviour of lubricating oils containing platelet MoS_2 nanoparticles. *Journal of Nanoparticle Research, 16*(5), 1-9.

Wang, X.-B., & Liu, W.-M. (2013). Nanoparticle-based lubricant additives *Encyclopedia of Tribology* (pp. 2369-2376): Springer.

Watson, S. A. (2010). *Lubricant-derived ash: in-engine sources and opportunities for reduction.* (PhD), Massachusetts Institute of Technology.

Watson, S. A., & Wong, V. W. (2008). *The Effects of Fuel Dilution with Biodiesel onLubricant Acidity, Oxidation and Corrosion –a Study with CJ-4 and CI-4 PLUS Lubricants.* Paper presented at the 2008 Diesel Engine-Efficiency and Emissions Research (DEER) Conference.

Watson, S. A., Wong, V. W., Brownawell, D., & Lockledge, S. P. (2009). *Controlling lubricant acidity with an oil conditioning filter.* Paper presented at the ASME 2009 Internal Combustion Engine Division Spring Technical Conference.

Watson, S. A., Wong, V. W., Brownawell, D., Lockledge, S. P., & Harold, S. (2009). Oil conditioning as a means to minimize lubricant ash requirements and extend oil drain interval. *SAE Technical Paper, 2009-01-1782*.

Weertman, J. (1993). Hall-Petch strengthening in nanocrystalline metals. *Materials Science and Engineering: A, 166*(1-2), 161-167.

Windom, B. C., Sawyer, W. G., & Hahn, D. W. (2011). A raman spectroscopic study of MoS_2 and MoO_3 :Applications to tribological systems. *Tribology Letters, 42*(3), 301-310.

Wong, V., Thomas, B., & Watson, S. (2007). Bridging macroscopic lubricant transport and surface tribochemical investigations in reciprocating engines. *Proceedings of the Institution of Mechanical Engineers, Part J: Journal of Engineering Tribology, 221*(3), 183-193.

Wu, X., Zhang, X., Yang, S., Chen, H., & Wang, D. (2000). The study of epoxidized rapeseed oil used as a potential biodegradable lubricant. *Journal of the American Oil Chemists' Society, 77*(5), 561-563.

Wu, Y. Y., Tsui, W. C., & Liu, T. C. (2007). Experimental analysis of tribological properties of lubricating oils with nanoparticle additives. *Wear, 262*(7-8), 819-825.

Xiaodong, Z., Xun, F., Huaqiang, S., & Zhengshui, H. (2007). Lubricating properties of Cyanex 302-modified MoS_2 microspheres in base oil 500SN. *Lubrication Science, 19*(1), 71-79.

Xie, H., Jiang, B., He, J., Xia, X., & Pan, F. (2015). Lubrication performance of MoS_2 and SiO_2 nanoparticles as lubricant additives in magnesium alloy-steel contacts. *Tribology International, 93*(A), 63-70.

Xu, H., Wang, W., & Zhu, W. (2006). Shape evolution and size-controllable synthesis of Cu_2O octahedra and their morphology-dependent photocatalytic properties. *The Journal of Physical Chemistry B, 110*(28), 13829-13834.

Xu, J., Ji, W., Shen, Z., Li, W., Tang, S., Ye, X., . . . Xin, X. (1999). Raman spectra of CuO nanocrystals. *Journal of Raman spectroscopy, 30*(5), 413-415.

Xu, Y. F., Yu, H. Q., Wei, X. Y., Cui, Z., Hu, X. G., Xue, T., & Zhang, D. Y. (2013). Friction and wear behaviors of a cylinder liner–piston ring with emulsified bio-oil as fuel. *Tribology Transactions, 56*(3), 359-365.

Yadgarov, L., Petrone, V., Rosentsveig, R., Feldman, Y., Tenne, R., & Senatore, A. (2013). Tribological studies of rhenium doped fullerene-like MoS_2 nanoparticles in boundary, mixed and elasto-hydrodynamic lubrication conditions. *Wear, 297*(1–2), 1103-1110.

Ye, W., Cheng, T., Ye, Q., Guo, X., Zhang, Z., & Dang, H. (2003). Preparation and tribological properties of tetrafluorobenzoic acid-modified TiO_2 nanoparticles as lubricant additives. *Materials Science and Engineering: A, 359*(1), 82-85.

Yu, H.-l., Xu, Y., Shi, P.-j., Xu, B.-s., Wang, X.-l., & Liu, Q. (2008). Tribological properties and lubricating mechanisms of Cu nanoparticles in lubricant. *Transactions of Nonferrous Metals Society of China, 18*(3), 636-641.

Yu, H. L., Xu, Y., Shi, P. J., Xu, B. S., Wang, X. L., Liu, Q., & Wang, H. M. (2008). Characterization and nano-mechanical properties of tribofilms using Cu nanoparticles as additives. *Surface and Coatings Technology, 203*(1–2), 28-34.

Yu, W., & Xie, H. (2012). A review on nanofluids: preparation, stability mechanisms, and applications. *Journal of Nanomaterials, 2012*, 1.

Yunus, R., Fakhru'I-Razi, A., Ooi, T., Biak, D., & Iyuke, S. (2004). Kinetics of transesterification of palm-based methyl esters with trimethylolpropane. *Journal of the American Oil Chemists' Society, 81*(5), 497-503.

Yunus, R., Fakhrul I-Razi, A., Ooi, T., Iyuke, S., & Idris, A. (2003). Preparation and characterization of trimethylolpropane esters from palm kernel oil methyl esters. *Journal of Oil Palm Research, 15*(2), 42-49.

Zainal, N., Zulkifli, N., Yusoff, M., Masjuki, H., & Yunus, R. (2015). *The feasibility study of $CaCO_3$ derived from cockleshell as nanoparticle in chemically modified lubricant.* Paper presented at the Proceedings of Malaysian International Tribology Conference 2015.

Zdrodowski, R., Gangopadhyay, A., Anderson, J. E., Ruona, W. C., Uy, D., & Simko, S. J. (2010). Effect of biodiesel (B20) on vehicle-aged engine oil properties. *SAE Technical Paper, 2010-01-2103*.

Zhang, Y., Xu, Y., Yang, Y., Zhang, S., Zhang, P., & Zhang, Z. (2015). Synthesis and tribological properties of oil-soluble copper nanoparticles as environmentally friendly lubricating oil additives. *Industrial Lubrication and Tribology, 67*(3), 227-232.

Zhao, Y., Zhang, Z., & Dang, H. (2004). Fabrication and tribological properties of Pb nanoparticles. *Journal of Nanoparticle Research, 6*(1), 47-51.

Zhou, J., Wu, Z., Zhang, Z., Liu, W., & Xue, Q. (2000). Tribological behavior and lubricating mechanism of Cu nanoparticles in oil. *Tribology Letters, 8*(4), 213-218.

Zhou, Y.-H., Harmelin, M., & Bigot, J. (1989). Sintering behaviour of ultra-fine Fe, Ni and Fe-25wt% Ni powders. *Scripta metallurgica, 23*(8), 1391-1396.

Zhu, D., Li, X., Wang, N., Wang, X., Gao, J., & Li, H. (2009). Dispersion behavior and thermal conductivity characteristics of Al_2O_3–H_2O nanofluids. *Current Applied Physics, 9*(1), 131-139.

Zhu, J., Bi, H., Wang, Y., Wang, X., Yang, X., & Lu, L. (2008). CuO nanocrystals with controllable shapes grown from solution without any surfactants. *Materials Chemistry and Physics, 109*(1), 34-38.

Zin, V., Agresti, F., Barison, S., Colla, L., & Fabrizio, M. (2015). Influence of Cu, TiO_2 nanoparticles and carbon nano-horns on tribological properties of engine oil. *Journal of Nanoscience and Nanotechnology, 15*(5), 3590-3598.

Zulkifli, N. W. M. (2014). *Lubricity and anti-wear characteristic of trimethylolpropane ester derived from edible and non-edible resources.* (PhD), University of Malaya, Malaysia. (TJ7 UMP 2014 Nurwmz)

Zulkifli, N. W. M., Azman, S., Kalam, M., Masjuki, H., Yunus, R., & Gulzar, M. (2016). Lubricity of bio-based lubricant derived from different chemically modified fatty acid methyl ester. *Tribology International, 93*, 555-562.

Zulkifli, N. W. M., Kalam, M. A., Masjuki, H. H., Al Mahmud, K. A. H., & Yunus, R. (2014). The Effect of Temperature on Tribological Properties of Chemically Modified Bio-Based Lubricant. *Tribology Transactions, 57*(3), 408-415.

Zulkifli, N. W. M., Kalam, M. A., Masjuki, H. H., Shahabuddin, M., & Yunus, R. (2013). Wear prevention characteristics of a palm oil-based TMP (trimethylolpropane) ester as an engine lubricant. *Energy, 54*, 167-173.

Zulkifli, N. W. M., Kalam, M. A., Masjuki, H. H., & Yunus, R. (2013). Experimental analysis of tribological properties of biolubricant with nanoparticle additive. *Procedia Engineering, 68*, 152-157.

LIST OF PUBLICATIONS AND PAPERS PRESENTED

ISI Indexed Journals:

1. **M. Gulzar**, Masjuki, H. H., Kalam, M. A., Varman, M., Zulkifli, N. W. M., Mufti, R. A., & Zahid, R. (2016). Tribological performance of nanoparticles as lubricating oil additives. ***Journal of Nanoparticle Research***, 18(8), 1-25.
2. **M. Gulzar**, Masjuki, H., Kalam, M., Varman, M., Zulkifli, N., Mufti, R., Zahid, R., Yunus, R. (2016). Dispersion stability and tribological characteristics of TiO_2/SiO_2 nanocomposites enriched bio-based lubricant. ***Tribology Transactions***. DOI: 10.1080/10402004.2016.1202366
3. **M. Gulzar**, Masjuki, H. H., Varman, M., Kalam, M. A., Mufti, R. A., Zulkifli, N. W. M., Zahid, R. (2015). Improving the AW/EP ability of chemically modified palm oil by adding CuO and MoS_2 nanoparticles. ***Tribology International***, 88(0), 271-279.
4. **M. Gulzar**, Masjuki, H. H., Varman, M., Kalam, M. A., Zulkifli, N. W. M., Mufti, R. A., Arslan, A. (2016). Effects of biodiesel blends on lubricating oil degradation and piston assembly energy losses. ***Energy***, 111, 713-721.
5. **M. Gulzar**, Masjuki, H. H., Kalam, M. A., Varman, M., & Rizwanul Fattah, I. M. (2015). Oil filter modification for biodiesel–fueled engine: A pathway to lubricant sustainability and exhaust emissions reduction. ***Energy Conversion and Management***, 91(0), 168-175.
6. **M. Gulzar**, H.H Masjuki, Abdullah Alabdulkarem, M.A Kalam, M. Varman, NWM Zulkifli (2017) Chemically Active Oil Filter to Develop Detergent Free Bio-based Lubrication for Diesel Engine, ***Energy***, 124, 413–422.

Papers Presented in International Conferences:

1. **M. Gulzar**, Zulkifli, N. W. M., Masjuki, H. H., Yunus, R. (2016). *Tribological characteristics of a surface-modified MoS_2 nanoparticles as an additive in bio-based lubricant*. Proceedings of Fifth International Conference Lubrication, Maintenance and Tribotechnology (lubmat), 7-8 June 2016, Spain.
2. **M. Gulzar**, H.H Masjuki., MA Kalam, M Varman, NWM Zulkifli (2017) *Antiwear Behavior of CuO Nanoparticles as Additive in Bio-Based Lubricant.* Proceedings of 2017 International Conference on Advanced Materials and Building Materials, 21-22 April 2017, Malaysia **(Best Paper Award).**
3. **M. Gulzar**, H.H Masjuki., MA Kalam, M Varman, RA Mufti, Rehan Zahid, R Yunus. (2015). *AW/EP behavior of WS_2 nanoparticles added to vegetable oil-based lubricant*. Proceedings of Malaysian International Tribology Conference, 16-17 November 2015, Malaysia.

Poster Presented:

1. **M. Gulzar**, Masjuki, H. H., Kalam, M. A., Varman, M., Zulkifli, N. W. M., & Zahid, R. (2016). *Chemically Active Oil Filter—A Pathway to Extended Oil Drain Interval and Wear Reduction in Diesel Engine*. Presented at MYTRIBOS Tribology Poster Competition, 1 June 2016, Malaysia.